



A University of Sussex DPhil thesis

Available online via Sussex Research Online:

<http://sro.sussex.ac.uk/>

This thesis is protected by copyright which belongs to the author.

This thesis cannot be reproduced or quoted extensively from without first obtaining permission in writing from the Author

The content must not be changed in any way or sold commercially in any format or medium without the formal permission of the Author

When referring to this work, full bibliographic details including the author, title, awarding institution and date of the thesis must be given

Please visit Sussex Research Online for more information and further details

**Palladium *N*-Heterocyclic Carbene
Complexes as Catalysts for
C-N, C-Si and C-S Bond Formations**

Deborah Elizabeth Roberts

Submitted for the degree of D.Phil

University of Sussex

January 2013

I hereby declare that this thesis has not been submitted, either in the same or different form, to this or any other university for a degree.

Signature:

Acknowledgements

I would like to thank Prof. Geoff Cloke for being such an extraordinarily understanding and supportive supervisor through my many problems.

Prof. Steve Caddick for his advice and support on the more organic side of the work.

Dr Nikos Tsoureas for his tremendous help with this thesis and with crystal structures and for being the only other person in the lab who knew anything about carbenes.

Dr. Alex Lewis for all her good ideas and for showing me some of the important laboratory techniques required in this work.

Dr. Oriana Esposito for welcoming me to the project and for her excellent work on which much of this thesis is based.

Dr. Robin Fulton for being kind and thorough in her analysis of my work.

Dr. Alastair Frey and Dr. Joy Farnaby for their help when I first joined Lab 14 and for their continuing advice and support throughout my time in the lab.

Dave, Zoe, Jess and Robin for being an excellent “Dark side”.

Steve, Chris, Ian, Ben and Dan for not minding having to be the “Light side”.

Dr. Ali Abdul Sada for his GCMS and MS analysis.

Dr. Martyn Cole and Dr. Peter Hitchcock for X-ray analysis.

Roger and Ken for their excellent glassblowing skills.

Jan Harrison, for all her support helping me find a way to get this thesis written. Angels bless you and so do I.

My brother, David Roberts, for being the brave man he is. Stay well.

My mother, Joan Roberts, for the strong example she set me and inspiring me to study chemistry.

Finally, I’d like to thank my father, Roy Roberts, for always believing in me, even when I don’t believe in myself.

***I dedicate this thesis to the memory of my grandmother,
“Daisy” Elizabeth Roberts.***

University of Sussex
Deborah Elizabeth Roberts
Submitted for the degree of D.Phil
Palladium *N*-Heterocyclic Carbene complexes as catalysts for
C-N, C-Si and C-S bond formations.

Abstract

This work is foremost a study of various palladium-bearing *N*-heterocyclic carbenes complexes and their catalytic potential to form C-N bonds. Both alkyl amination and aryl amination are considered. Further elucidation on the mechanism of such catalytic activity is investigated.

The viability of alkyl amination using palladium complexes bearing the ligands, ITMe, 1,2,3,4- tetramethylimidazol-2-ylidene, and ICy, 1,3- bis-cyclohexylimidazol-2-ylidene, as catalysts, is investigated. This includes the synthesis of [Pd(ITMe)(neopentyl)Cl]₂, [Pd(ITMe)₂(neopentyl)Cl], [Pd(ITMe)(neopentyl)(^tbutylamine)Cl], [Pd(ITMe)(neopentyl)(hexylamine)Cl], with successful elimination of the alkyl-amination reaction product in low yield from the latter complex. [Pd(ICy)(neopentyl)Cl]₂, [Pd(ICy)₂(neopentyl)Cl] are also isolated.

Unsuccessful attempts were made to vary the electronic properties of the complexes by replacing the amine with a hydrazine. Work was also done on indirect alkylation using ^tBuLi which led to a new method for synthesis of [Pd(I^tBu)₂] and novel complex, [Pd(I^tBu)Cl₃. I^tBuH] (I^tBu = 1,3- bis-*tert*butylimidazol-2-ylidene).

Aryl amination catalysed by complexes of palladium bearing the ligand, ITMe, is considered. This includes an improved synthesis of [Pd(ITMe)₂] and synthesis of [Pd(ITMe)₂(anisole)Cl]. Unsuccessful attempts at the elucidation of the mechanism of [Pd(ITMe)₂(anisole)] formation led to the unexpected formation of [Pd(ITMe)₂(SiMe₃)(Si(SiMe₃)₃)] and [Pd(ITMe)₂(SiMe₃)₂]. Aryl amination with using [Pd(ITMe)₂(SiMe₃)₂] led to two aryl amination products, 4-*ortho*-methoxyphenyl morpholine as well as the expected *para* isomer.

The use of complexes [Pd(I^tBu)₂] and [Pd(SIPr)₂] (SIPr = 1,3-bis(2,6-diisopropylphenyl)imidazol-2-ylidene) in C-S bond formation was explored.

Addition of mesityl magnesium bromide to $\text{Pd}(1,5\text{-COD})\text{Cl}_2$ led to addition of mesityl substrate across 1,5-COD double bond and the addition of ITMe formed the Heck cycle intermediate $[\text{Pd}(\eta^3\text{-8-mesityl-1,4,5-C}_8\text{H}_7\text{)}\text{X}_2]$ ($\text{X}=\text{Cl, Br}$). Addition of 4-tolyl magnesium chloride resulting in the formation of $\text{Pd}(\text{I}^t\text{Bu})_2(\text{tolyl})\text{Cl}$ *via* an indirect route.

Table of contents

Declaration	i
Acknowledgements.....	ii
Abstract	iii
Table of contents.....	v
Abbreviations	ix
Novel compound numbering	xi

Chapter 1: General Introduction

1.1. Carbenes	1
1.1.1. Carbene stability.....	1
1.1.2. Fischer and Schrock carbene complexes	5
1.1.3. Five membered <i>N</i> -Heterocyclic Carbenes	10
1.2. <i>NHCs</i> in transition metal catalysis	24
1.2.1. Ruthenium catalysts (Group 8)	25
1.2.2. Rhodium and iridium catalysts (Group 9)	27
1.2.3. Copper, silver and gold NHC complexes (Group 11)	31
1.2.4. Early to middle transition metal complexes (Groups 3-7)	33
1.2.5. Organocatalysis	35
1.2.6. Nickel and platinum catalysts (Group 10, part 1)	36
1.3. Palladium catalysts (Group 10, part 2).....	39
1.3.1. Mizoroki-Heck Reaction	41
1.3.2. The Hiyama reaction	43
1.3.3. The Kumada-Tamao-Corrui reaction	44
1.3.4. The Negishi reaction	45
1.3.5. The Stille reaction	46
1.3.6. The Sonogashira reaction	47
1.3.7. The Suzuki-Miyaura reaction	48
1.4. Carbon–Nitrogen bond formation using palladium catalysts	52
1.4.1. Buchwald-Hartwig Aryl Amination.....	53
1.4.2. Mechanism of Buchwald-Hartwig aryl amination	62
1.4.3. Palladium-based alkyl amination catalysis	71
1.5. References	74

Chapter Two:

Investigations into the development of a palladium-carbene catalyst for alkyl amination, specifically using 1, 2, 3, 4- tetramethylimidazol-2-ylidene and 1,3-cyclohexylimidazol-2-ylidene.

2.1. Introduction	81
2.2. Results and Discussion	88
2.2.1. Synthesis and decomposition of dimeric neopentyl <i>NHC</i> Pd complexes..	88
2.2.2. Synthesis of monomeric neopentyl Pd(II)- <i>NHC</i> complexes (<i>NHC</i> = ITMe, ICy).	94
2.2.3. Reactions of 2.1 and 2.2 with amines.....	98
2.2.4. Reductive elimination of C-N coupling product.....	102
2.2.5. Formation of the amido complexes	106
2.2.6. Aryl amination catalytic activity of 2.1	109
2.2.7. Attempts towards the preparation of alkyl palladium <i>NHC</i> complex in which the alkyl moiety has β -hydrogens.....	111
2.3. Conclusions	116
2.4. Experimental section	117
2.4.1. Synthesis of [Pd(ITMe)(neopentyl)(Cl)] ₂ , 2.1	117
2.4.2. Synthesis of cis-[Pd(ITMe) ₂ Cl ₂], 72	118
2.4.3. Synthesis of trans-[Pd(ICy)(neopentyl)(μ -Cl)] ₂ , 2.2	118
2.4.4. Synthesis of trans-[Pd(ICy) ₂ Cl ₂], 2.3	119
2.2.5. Synthesis of [Pd(ITMe) ₂ (neopentyl)(Cl)], 2.4	119
2.2.6. Synthesis of trans-[Pd(ICy) ₂ (neopentyl)(Cl)], 2.5	120
2.2.7. Synthesis of Pd(ITMe)(neopentyl)(hexylamine)chloride complex, 2.6 ..	120
2.2.8. Synthesis of Pd(ITMe)(neopentyl)(t-butylamine)chloride, 2.7	121
2.2.9. Synthesis of {[Pd(^t Bu)Cl ₃]- [^t BuH] ⁺ }, 2.9	121
General procedure for catalyst testing: NMR.....	122
General procedure for catalyst testing: GC-MS	122
2.5. References	124

Chapter Three:

Investigations into the use of the 1,2,3,4, tetramethylimidazol-2-ylidene NHC complexes of palladium as aryl amination catalysts.

Use of Pd(NHC)₂ complexes for Si-Si, C-Si bond cleavage and C-S bond formation.

3.1. Introduction	126
3.2. Results and Discussion	127
3.2.1. Synthesis of Pd(ITMe) ₂ , 71	128
3.2.2. Oxidative addition of aryl chlorides to Pd(ITMe) ₂	133
3.2.3. Unsuccessful kinetic studies on Pd(ITMe) ₂	134
3.2.4. Attempts towards isolation of the dimeric species	137
3.2.5. Silyl complexes of Pd-NHC complexes	143
3.2.6. Preliminary catalytic studies with and [Pd(ITMe) ₂ (anisole)Cl], 3.1 and [Pd(ITMe) ₂ (SiMe ₃) ₂], 3.6	145
3.2.7. C-Si bond cleavage	147
3.2.8. Use of Pd bis carbene complexes for aryl chloride-aryl thiol coupling... 149	
3.3. Conclusions	150
3.4. Experimental Section	150
3.4.1. Synthesis of Pd(ITMe) ₂ , 71	150
3.4.2. Synthesis of [Pd(ITMe) ₂ (CH ₃ O-4-C ₆ H ₄)Cl], 3.1	151
3.4.3. [Pd(ITMe)(CH ₃ O-4-C ₆ H ₄)Cl] ₂ , 3.3 :	151
3.4.4. Synthesis of [Pd(ITMe) ₂ (CH ₃ OOC-4-C ₆ H ₄))Cl], 3.4	151
3.4.5. [Pd(ITMe)(CH ₃ OOC-4-C ₆ H ₄)Cl] ₂ , 3.5 - observed by ¹ H NMR:	152
3.4.6. Synthesis of [Pd(ITMe) ₂ ((Si(SiMe ₃) ₃ (SiMe ₃) ₂), 3.2 :	152
3.4.7. Synthesis of [Pd(ITMe) ₂ (SiMe ₃) ₂], 3.6	153
3.4.8. General procedure for the catalytic amination of aryl halides ¹ H NMR.. 153	
3.4.9. General procedure for observation of the reaction of aryl chlorides and aryl/alkyl thiols with any of the pre-catalysts: GC-MS	153
3.5. References	154

Chapter Four:

Attempts to isolate of an aryl palladium chloride complex of 2,6-diisopropylimidazolin-2-ylidene using aryl Grignards and [Pd(1,5-COD)Cl]₂

4.1. Introduction	157
4.2. Results and Discussion.....	158
4.2.1. Revisiting the attempts to form aryl oxidative addition product directly.	158
4.2.2. Indirect formation of Pd <i>NHC</i> aryl halide complexes: Reactions using mesityl magnesium bromide.....	161
4.2.3. Reactions using 4-tolylmagnesium chloride.....	168
4.3. Conclusions	170
4.4. Experimental Section	171
4.4.1. Synthesis of Pd(SIPr) ₂ Cl ₂ ,	171
4.4.2. Synthesis of [Pd(8-mesityl, 1-η ¹ , 4, 5-η ² – C ₈ H ₁₂)X ₂] (X=Cl, Br), 4.1 ...	171
4.4.3. Synthesis of [Pd(ITMe)(8-mesityl, 1-η ¹ , 4, 5-η ² – C ₈ H ₁₂)Br], 4.2	172
4.4.4. [Pd(SIPr) (8-mesityl, 1- η ¹ , 4, 5-η ² – C ₈ H ₁₂)Br], 4.3	173
4.4.5. Synthesis of [Pd(1,5-COD)(tolyl)Cl], 4.4	173
4.5. References	174

Appendix I

General Experimental	A1-1
Instrumental Details	A1-2

Appendix II: Crystallographic Data

A2.1: Crystal data for <i>cis</i> -Pd(ITMe) ₂ (Cl) ₂	A2-2
A2.2: Crystal data for <i>trans</i> -Pd(ICy) ₂ (Cl) ₂	A2-7
A2.3 Crystal data for <i>trans</i> -Pd(ICy) ₂ (neopentyl)Cl.....	A2-13
A2.4 Crystal data for [Pd(^t Bu)Cl ₃]-[^t BuH] ⁺	A2-20
A2.5 Crystal data for <i>trans</i> -[Pd(ITMe) ₂ (p-anisole)(Cl)].....	A2-29
A2.6: Crystal data for <i>cis</i> -[Pd(ITMe) ₂ (SiMe ₃) ₂].....	A2-35
A2.7: Crystal data for <i>trans</i> -Pd(SIPr) ₂ Cl ₂	A2-42
A2.8: Crystal data for [Pd(ITMe)(8-mesityl (η ¹ (4, 5-η ²) – C ₈ H ₁₂)Br]	A2-48

Abbreviations

Anal.	Analysis
Atm.	Atmosphere
BARF	Tetrakis[3,5-bis(trifluoromethyl)phenyl]borate anion
BDE	Bond dissociation energy
BINAP	1,1'-binaphthylphenyl phosphine
ⁿ Bu	<i>normal</i> -butyl
^t Bu	<i>tertiary</i> -butyl
Bn	Benzyl
Calc'd	calculated
COD	Cyclooctadiene
Cy	Cyclohexyl
δ	Chemical shift
Db	Dibenzylidene acetone
dcpe	(1,4-(dicyclohexylphosphino)ethane)
Dppf	1,1'-bis-diphenylphosphino ferrocene
d	doublet
DCM	Dichloromethane
DMF	Dimethylformamide
Dvds	1,3-divinyl-1,1,3,3-tetramethyldisiloxane
EI	Electron Impact
Eq	Equation
Equiv.	Equivalents
Et	Ethyl
HMDS	Hexamethyldisilane or Bis(trimethyl)silane
Hr	hour(s)
Hz	Hertz
IBn	1,3-bis-benzyl-4,5-bis- <i>tert</i> -butylimidazolidin-2-ylidene
ICy	1,3-bis-cyclohexylimidazol-2-ylidene
l ^t BuHCl	1,3-bis-cyclohexylimidazol-2-ylidene hydrochloride
IPr	1,3-bis(2,6-diisopropylphenyl)imidazol-2-ylidene
IPrHCl	1,3-bis(2,6-diisopropylphenyl)imidazolium hydrochloride

IMes	1,3-bis(2,6-dimesityl)imidazol-2-ylidene
I ^t Bu	1,3- bis-tert-butylimidazol-2-ylidene
I ^t BuHCl	1,3-bis-tert-butylimidazolium hydrochloride
ITMe	1,2,3,4-tetramethylimidazol-2-ylidene
J	Spin-spin coupling constant, $^XJ_{YZ}$ – X bond coupling constant between nuclei Y and Z (Hz).
LHMDS	Lithium hexamethyldisilyl amide (or bis(trimethylsilyl)amide)
m	multiplet
Me	Methyl
MS	Mass Spectrometry
MVS	Metal Vapour Synthesis
NHC	<i>N</i> -Heterocyclic Carbene
NMR	Nuclear Magnetic Resonance
Np	Neopentyl
OA	Oxidative Addition
Ph	Phenyl
ⁱ Pr	<i>iso</i> -propyl
q	quartet
R	a general organic group
RE	Reductive Elimination
RT	Room Temperature (298K)
s	singlet
SIPr	1,3-bis(2,6-diisopropylphenyl)imidazolin-2-ylidene
SIMes	1,3-bis(2,6-dimesityl)imidazolin-2-ylidene
^t Bu	Tertiary butyl group
t	triplet
TBAF	Tetrabutylammonium fluoride, [N(<i>n</i> -Bu) ₄] ⁺ F ⁻
THF	Tetrahydrofuran
TM	Transmetallation
TMS	Trimethylsilyl
TON	Turn-over number

Novel compound numbering

2.1	$[\text{Pd}(\text{ITMe})(\text{CH}_2\text{C}(\text{CH}_3)_3)(\mu\text{-Cl})_2]$
2.2	$[\text{Pd}(\text{ICy})(\text{CH}_2\text{C}(\text{CH}_3)_3)(\mu\text{-Cl})_2]$
2.3	<i>Trans</i> - $[\text{Pd}(\text{ICy})_2\text{Cl}_2]$
2.4	$[\text{Pd}(\text{ITMe})_2(\text{CH}_2\text{C}(\text{CH}_3)_3)\text{Cl}]$
2.5	<i>Trans</i> - $[\text{Pd}(\text{ICy})_2(\text{CH}_2\text{C}(\text{CH}_3)_3)(\text{Cl})]$
2.6	$[\text{Pd}(\text{ITMe})(\text{CH}_2\text{C}(\text{CH}_3)_3)(\text{NH}_2(\text{CH}_2)_5\text{CH}_3)\text{Cl}]$
2.7	$\text{Pd}(\text{ITMe})(\text{CH}_2\text{C}(\text{CH}_3)_3)(\text{NH}_2\text{tBu})\text{Cl}]$
2.8	$[\text{Pd}(\text{ITMe})(\text{CH}_2\text{C}(\text{CH}_3)_3)(\text{NH}_2^t\text{Bu})\text{Cl}]$
2.9	$\{[\text{Pd}(\text{I}^t\text{Bu})\text{Cl}_3]^- [\text{I}^t\text{BuH}]^+\}$
3.1	<i>Trans</i> - $[\text{Pd}(\text{ITMe})_2(p\text{-CH}_3\text{OC}_6\text{H}_4)\text{Cl}]$
3.2	$[\text{Pd}(\text{ITMe})(\text{SiMe}_3)_3(\text{SiMe}_3)]$
3.3	$[\text{Pd}(\text{ITMe})(p\text{-CH}_3\text{OC}_6\text{H}_4)\text{Cl}]_2$
3.4	$[\text{Pd}(\text{ITMe})_2(p\text{-CH}_3\text{OOC}_6\text{H}_4)\text{Cl}]$
3.5	$[\text{Pd}(\text{ITMe})(p\text{-CH}_3\text{OOC}_6\text{H}_4)\text{Cl}]_2$
3.6	<i>Cis</i> - $[\text{Pd}(\text{ITMe})_2(\text{SiMe}_3)_2]$
4.1	$[\text{Pd}(\text{8-mesityl}, 1\text{-}\eta^1, 4,5\text{-}\eta^2\text{-C}_8\text{H}_{12})\text{X}_2] \text{ (X=Cl, Br)}$
4.2	$[\text{Pd}(\text{ITMe})(\text{8-mesityl}, 1\text{-}\eta^1, 4,5\text{-}\eta^2\text{-C}_8\text{H}_{12})\text{Br}]$
4.3	$[\text{Pd}(\text{SIPr})(\text{8-mesityl}, 1\text{-}\eta^1, 4,5\text{-}\eta^2\text{-C}_8\text{H}_{12})\text{Br}]$
4.4	$[\text{Pd}(1,5\text{-COD})(\text{tolyl})\text{Cl}]$

“I have not failed; I have just found 10,000 ways
that won’t work”

“Our greatest weakness lies in giving up.
The most certain way to succeed is always to try
just one more time”

Thomas A. Edison,
Inventor, b.1847- d.1931.

Chapter One

General Introduction

1.1 Carbenes

1.1.1 Carbene stability

A carbene is an uncharged species of the type :CXY (X, Y = NR₂ to SiR₃ to BR₂, CR₁R₂, halogen) where the carbon is divalent, with only 6 valence electrons. Two of the valence electrons are non-bonding and can occupy the carbene carbon atom's non-bonding orbitals in a number of electronic configurations. The three ground state stable configurations are shown in Figure 1.

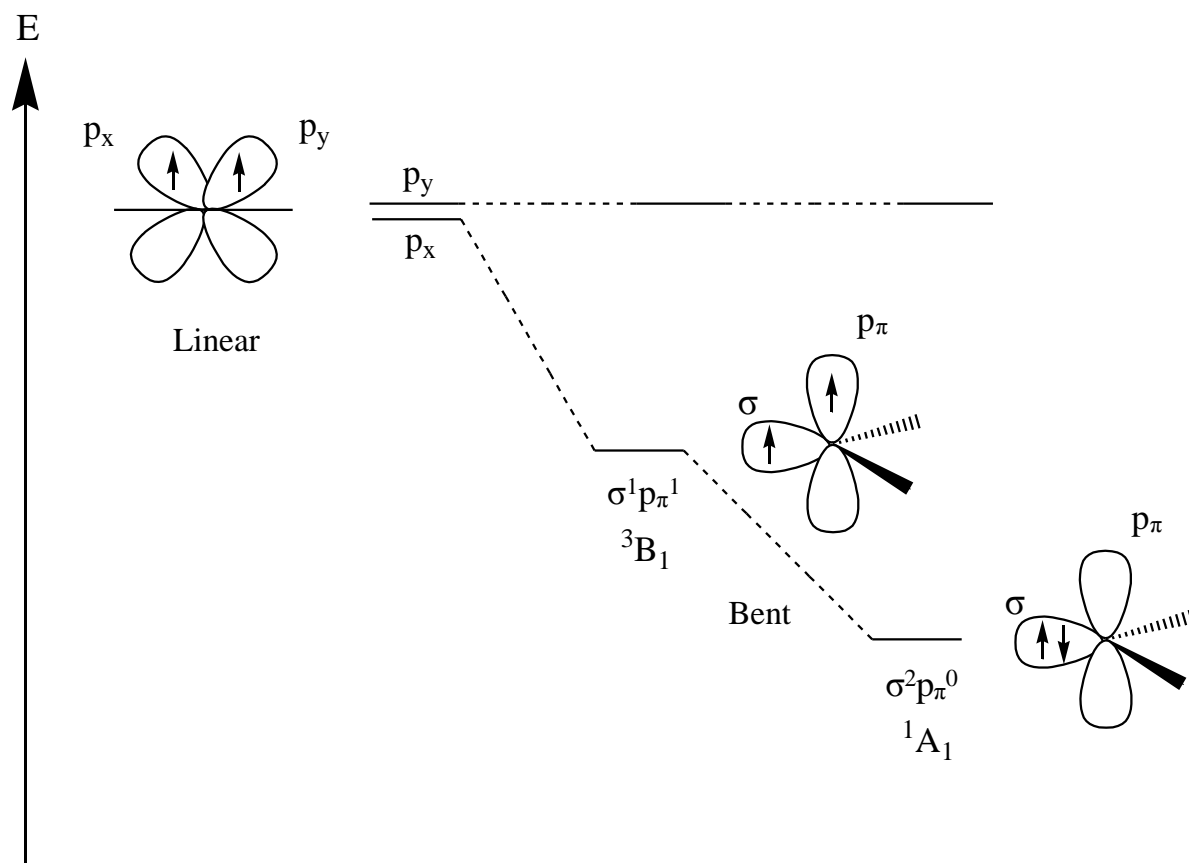


Figure 1: Frontier orbitals and possible electron configuration for carbene carbon atoms¹

The linear geometry is an idealised scenario that occurs when the carbon bonding orbitals are sp hybridised, thus the non-bonding orbitals are degenerate p-type. The

electronic degeneracy leads to a triplet state with non-bonding electrons in separate orbitals with parallel spins.

Bent geometry, common to most carbenes, arises when there is some degree of sp^2 hybridisation. This results in non-bonding orbitals, essentially one sp^2 orbital, the molecular σ orbital, and one orbital with essentially unchanged p character, the molecular p_π orbital. As can be seen from Figure 1, there are two configurations that are most likely for a carbene of bent geometry:

The triplet state, 3B_1 , where the energy difference between the σ and the p_π is less than 1.5eV ¹ results in electron occupation of both orbitals with parallel spins, essentially giving rise to a diradical. Triplet state carbenes tend to be very unstable (longest half-lives are minutes ^{Error! Reference source not found.}) due their radical nature.²

The singlet state, 1A_1 , occurs when the energy difference between the σ and the p_π is greater than approx. 2eV . In this case, the non-bonding electrons reside paired in the σ orbital, which should give rise to a species which is ambiphilic in nature.

So it is found that the multiplicity of the carbene's ground state is controlled by the energy difference between the σ and p_π orbitals. This variation in the energy gap is a direct result of electronic and steric effects of the carbene carbon's neighbouring substituents.

Inductive effects will influence the energy level of the σ orbital but have effectively zero effect on the p_π orbital hence more electropositive elements such as Li will donate electron density to carbon thus making the carbene carbon more negatively charged and increasing the σ orbital's energy level (Figure 2). These carbenes are therefore found in the triplet state. These species are high unstable diradicals; methylene, $:\text{CH}_2$ is one such species.

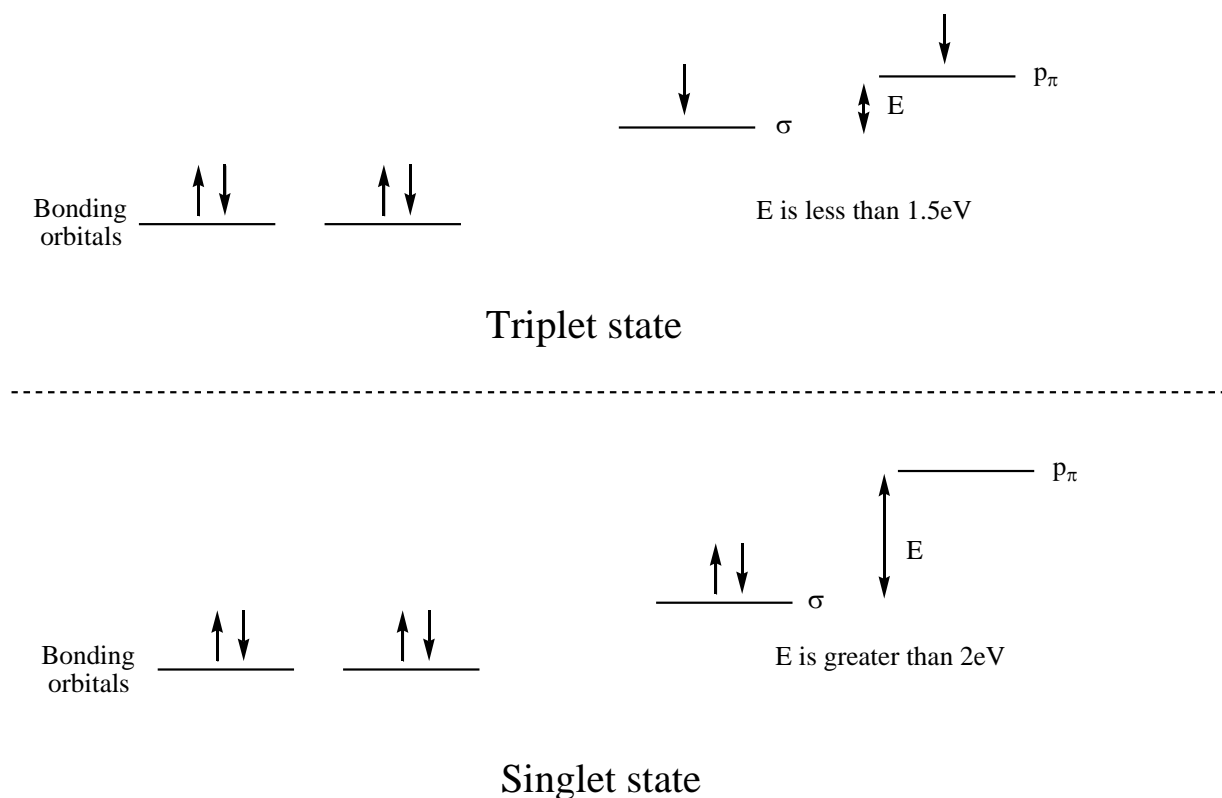


Figure 2: Inductive effects on the spin states of carbenes³

Electronegative atoms, such as F, will withdraw electrons from the carbene carbon which will lower the σ orbital energy and stabilise the singlet state,^{4,5} however the picture here is often complicated by mesomeric effects which are generally considered to be of more importance than inductive effects.^{6,7}

On the other hand when the carbene carbon is flanked by π electron donors, (*i.e.* :CXY; X, Y = NR₂, OR, SR, -Br, -I) it adopts a singlet state bent configuration due to the +M effect induced by the overlap of the $p_{\text{heteroatom}}-p_{\text{carbene}}$ orbitals (mesomeric effect). The electron density in the p_{π} orbital is raised by symmetrical overlap of the lone pair orbitals of X, causing an increase in the p_{π} energy thus stabilising the singlet state, ¹A₁. NHCs are an example of these carbenes, indeed they have added stability over acyclic diaminocarbenes because of the steric restrictions imposed by the heterocycle (*vide supra*) meaning NHCs are more bent (N-C-N angles of 100°-110°) than their acyclic counter parts (N-C-N angles of approx. 121°). These carbene carbons are nucleophilic, with a degree of zwitterionic nature (Figure 3) and some of the character of a 4-electron-3-atom centre delocalised π -electron system (*vide supra*, Figure 8). This results

in some double bond nature being ascribed to the C-N bonds. Other examples include dihalocarbenes and dimethoxycarbenes, both short-lived species.

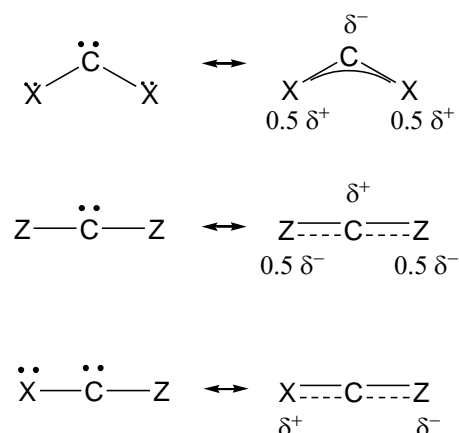


Figure 3: Charge distribution in carbenes

When electron-withdrawing groups such as -COR, -CN, CF₃, -BR₂, -SiR₃, -PR₃⁺ are attached to the carbene carbon, the resulting :CZ₂ carbene can be described as a 2 electron 3 atom centre delocalised π -electron system with a δ^+ charge on the carbon. The carbenes are linear thus the carbene carbon's non-bonding orbitals are the p orbitals, p_x and p_y. However, the degeneracy of these orbitals is lost because of p_y orbital overlap with the empty orbitals on the Z which lowers the energy of the p_y orbital enough to stabilise a singlet state. Examples of this carbene include boriranylideneboranes acting as masked diborylcarbenes, and transitory dicarbomethoxycarbenes.

A third type of carbene arises when one group attached to the carbene carbon is electron-withdrawing and one is electron-donating, :CXZ. These “push-pull” carbenes are linear as the empty p_y orbital overlaps with the lone pairs on the X group increasing its energy whilst the electrons in the p_x orbital interaction with the empty orbitals of Z. This results, not unexpectedly, with positive charge on the Z group and negative on the X and both the C-Z and C-X bonds have some double nature. Short lived halogenocarboethoxycarbenes are carbenes of this type as are the stable phosphinophosphoniocarbenes and phosphinosilylcarbenes (Figure 4).^{4,8}

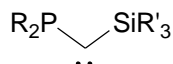


Figure 4: A (phosphino)-(silyl)carbene

Steric influences are generally secondary to electronic effects, however bulky X or Z groups will confer some kinetic stability. The bulkier substituents also widen the X-C-X bond angle and thus stabilise the triplet state by bringing the bond angle closer to the idealised triplet bond angle of 180° .

1.1.2 Fischer and Schrock carbene complexes

Attempted isolation of the simplest carbene, methylene, $:\text{CH}_2$, began as long ago as the 1830s when Dumas and Regnault reacted methanol with phosphorus pentoxide or concentrated sulphuric acid in an attempt to eliminate water³. In the 1890s, Nef famously announced that methylene would be available soon. At this point, it was still thought that methylene would be a stable compound as this was before carbon's tetravalent nature was confirmed.³ Shortly after in the 1910s, the Staudinger group did work which led to the understanding of carbenes as short-lived, intermediate diradicals. In the 1950s, Meerwein and Doering observed carbene insertion into carbon-hydrogen bonds which showed that most carbenes were not of a radical nature.⁵ The 1960s and 1970s was a time when many metal-carbene complexes were isolated including the two extreme types of metal-carbene complexes: the Fischer carbene complexes and the Schrock carbene complexes.

Fischer carbenes are singlet carbenes that have π electron donating substituents (OMe, NMe₂) attached, $:\text{CX}_2$; the complexes are formed with low oxidation state, late transition metals where the other ligands are π acceptors, such as CO, which back bond to the metal. The carbene carbon is then considered to have donated its two lone pair electrons, with this being more significant than any metal back bonding. Therefore it has a δ^+ charge and is electrophilic.^{3,9}

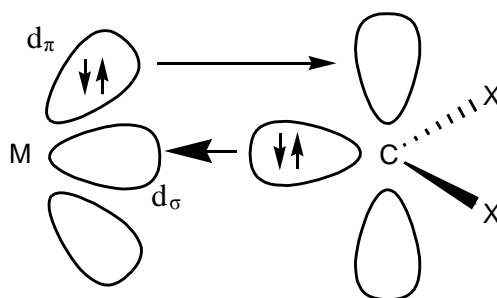
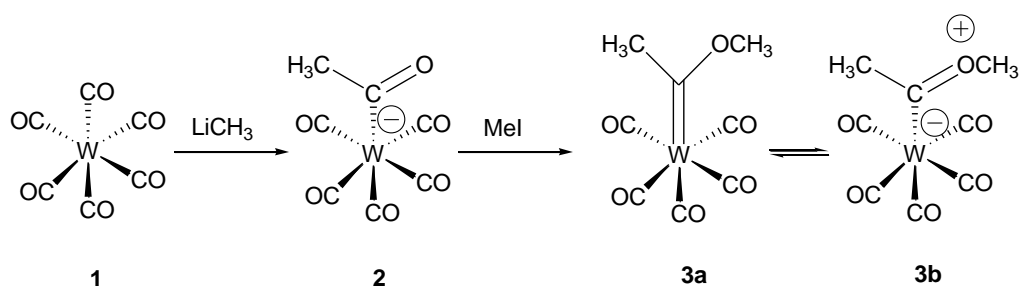


Figure 5: Electron transfer in a Fischer carbene⁹

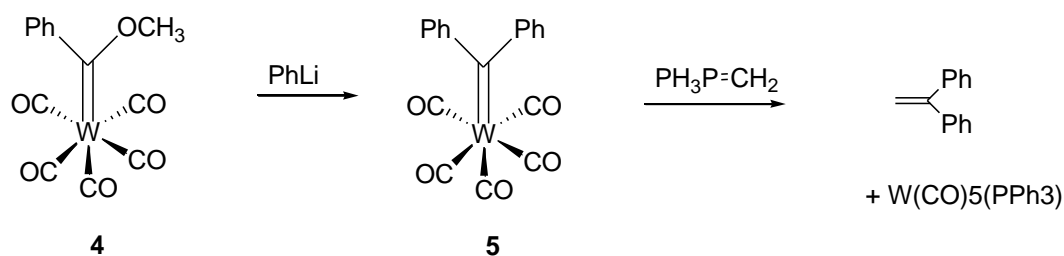
Fischer carbenes were synthesized by E. O. Fischer in 1964, by reaction of W(CO)_6 with MeLi , followed by addition of MeI (Scheme 1.01).¹⁰



Scheme 1.01: The reaction that formed the first Fischer carbene complex.¹⁰

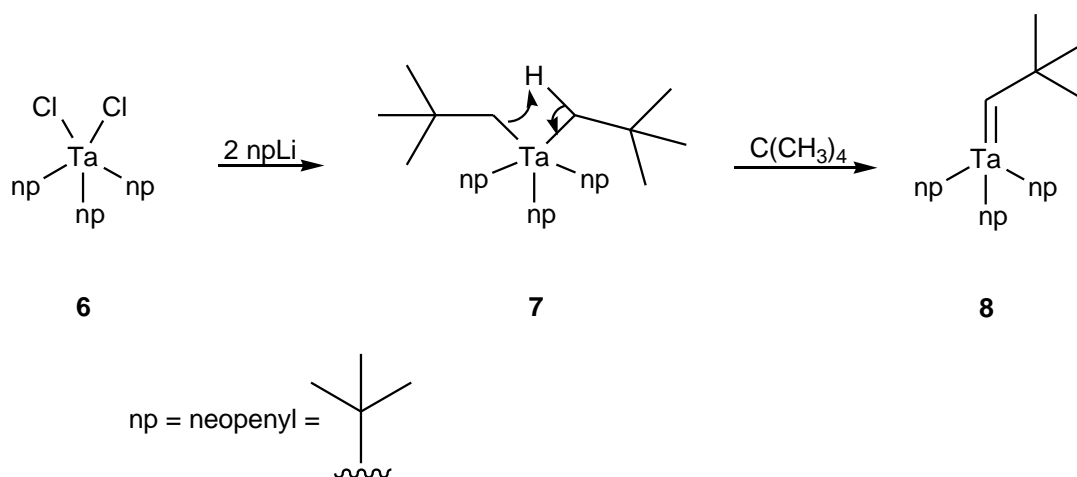
X-ray crystal diffraction studies show a long M-C bond (the bond order is much lower than 2, approaching 1.5) and a short C-O which means that **3b** is a more realistic representation than **3a**. The short C-O bond comes about through the donation of one of oxygen's lone pairs into the empty p_π of the carbene carbon. This bond therefore has some double bond character, and restricted rotation around the bond is often observed in NMR studies of Fischer carbenes.⁹

Fischer carbene complexes can be used as carbene transfer agents to other metal centres.⁹ They have also been used to make 4-methoxy-1-naphthols when reacted with certain alkynes; the former being intermediates in the synthesis of natural products such as vitamins E and K. They can also be reacted with nucleophiles such as amines and alkyl lithiums, to form other carbene complexes which can then undergo a form of Wittig reaction to increase carbon chain length.



Scheme 1.02: Use of Fischer complexes in a Wittig-type reaction.¹¹

Schrock carbenes¹² were discovered by R. R. Schrock in 1974, during an attempt to synthesise TaNP_5 . Schrock carbene complexes can be formed when metal alkyls undergo abstraction of a proton from an α carbon (Scheme 1.03). It is generally necessary in Schrock complex formation for the reactive intermediate to be sterically crowded to assist α -elimination.



Scheme 1.03: The reaction which produced the first Schrock carbene complex¹²

Schrock carbenes contain a triplet carbene where the carbene carbon is attached to other carbon groups or hydrogen; the complexes are formed with high oxidation state, early transition metals where the other ligands are poor π acceptors.

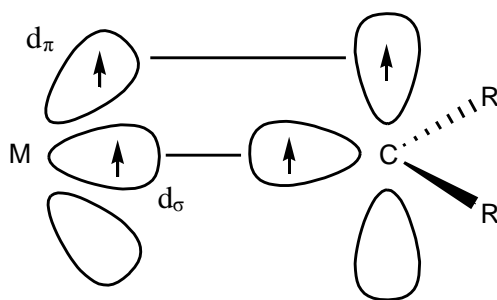
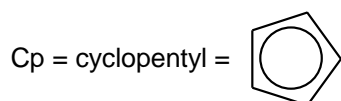
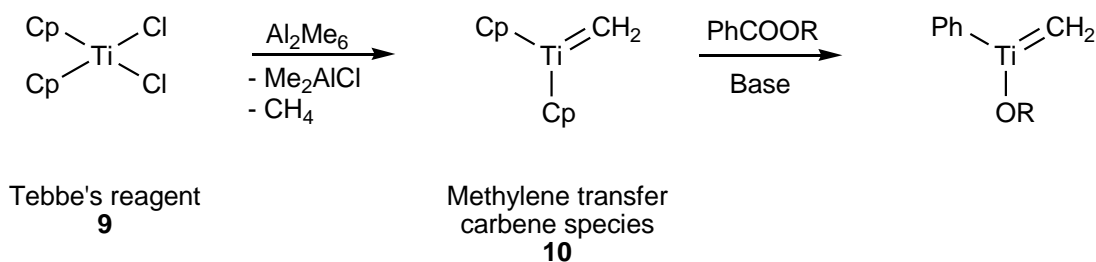


Figure 6: Electron transfer in a Schrock carbene metal complex

The absence of heteroatom neighbouring groups means π -back bonding between metal and carbene carbon occurs much more strongly than in the Fischer case, especially as the other ligands are non π acceptors. As can be seen in Figure 6, the M-C bond is more covalent in nature and as carbon is more electronegative than most metals, particularly high oxidation state, early transition metals, the bond is polar with δ^- on the carbene carbon. This leads to carbene carbon's nucleophilicity.

These complexes are more reactive than Fischer-type. When reacted with certain electrophiles such as aldehydes they can form alkenes. The Tebbe's reagent, **9** in Scheme 1.04, is a complex that is used to convert an ester to a vinyl ether.¹¹



Scheme 1.04: Use of Tebbe's reagent.¹¹

Other methods of indirect formation of carbene complexes during the 1960s to 1980s include: The reaction of carbonyl metallates and germinal dichlorides by Öfele in 1968¹³; Addition of an alcohol to isocyanide complexes by Chatt in 1969^{14b};

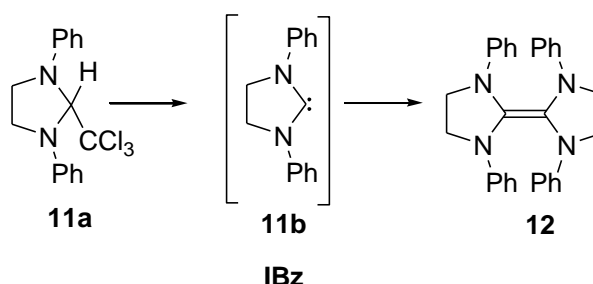
Interception of free carbenes, which are derived from CH_2N_2 by Herrmann in 1975^{14c},^{14d}; and dissociation of electron rich alkenes and insertion into metal carbonyls by Lappert in 1977¹⁵ (Scheme 1.6, *vide supra*)

Metal-carbene bonds are very strong as dissociation will be energetically unfavourable⁹, making these complexes a poor source of free carbene.

1.1.3 Five membered *N*-Heterocyclic Carbenes

It was Wanzlick¹⁶ in the 1960s who first showed interest in carbenes stabilised by nitrogen substituents, specifically phenyl groups. His method was the elimination of CHCl_3 from **11a** but this led to the electron rich alkene, **12**.

Wanzlick examined metathesis reactions between dimers with different *N* substituents in an attempt to establish whether equilibrium between the dimer and free carbene existed, and these experiments showed that this was not the case (Scheme 1.05).^{1, 9, 15}

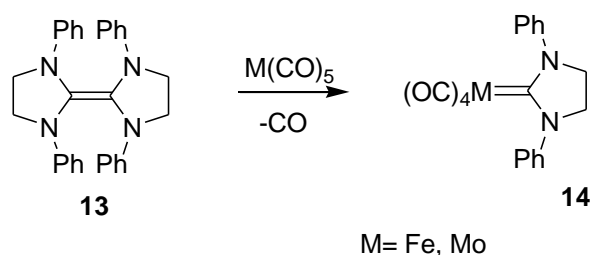


Scheme 1.05: Wanzlick's reaction to produce *NHCs*

This tendency to dimerise was a major stumbling block in achieving isolation of *NHCs*. Whilst Wanzlick's ideas that bulky substituents could prevent dimerization by kinetic stabilisation of the *NHC*, he was unlucky in his choice of saturated imidazolidinylienes (and choice of starting materials leading to electrophilic by-products)¹⁷ which meant he ended up with the dimer (Scheme 1.05).¹⁸ A further difference between the saturated and unsaturated carbene analogues is found in their hydrolysis. The imidazolidinyliene reacts rapidly to form acyclic aldehydes, whereas the imidazolyliene reacts much more slowly and, at low water concentrations only degrades as far as the imidazolium-hydroxide.¹⁹

Although the isolation of the free *NHC* carbene proved difficult, Wanzlick managed to capture it by the isolation of $\text{Hg}(\text{IBz})_2$ derived from the reaction of the parent 1,3-diphenylimidazolium salt to make $\text{Hg}(\text{OAc})_2$ and although he could not isolate free *NHCs*, he did capture them using this mercury (II) acetate reaction¹⁶.

Öfele also produced *NHC* complexes *via* the thermolysis of dimethylimidazolium hydridopentacarbonylchromate (II).¹³ And in the 1970s, Lappert¹⁵ used these *NHC* dimer alkenes to produce carbene complexes of Mo and Fe, the first complexes with saturated *NHCs* (Scheme 1.06).



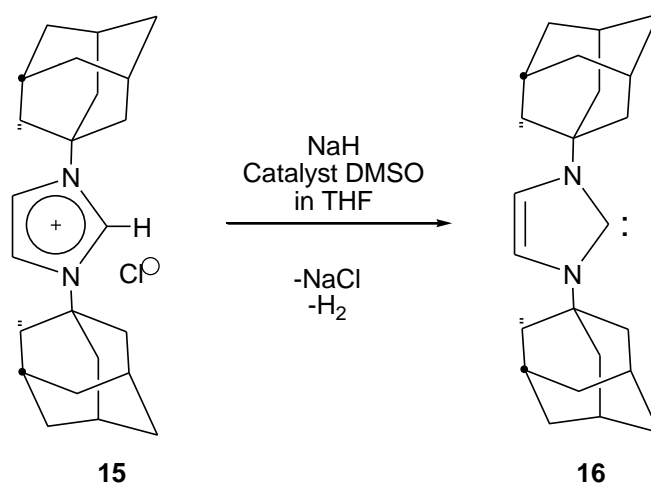
Scheme 1.06: Carbene insertion into metal carbonyls

Although Bertrand isolated the first carbene, a (phosphino)-(silyl)carbene, in the late 1980s,^{8, 20} the nature of Bertrand's compound was only definitively confirmed as an (phosphino)-(silyl)carbene by X-ray crystallography in 2000.

The use of carbenes as ancillary ligands did not really begin until Arduengo achieved isolation of the first *NHC*, IAd, **16**, in 1991 (Scheme 1.07).^{21, 22}

Arduengo was meticulous in gathering of characterisation data for **16**. X-ray crystallography showed the N-C-N bond angles to be around 100–102° which is smaller than in the imidazolium ion and the N-C(carbene) bond lengths are longer. This is indicative of imidazol-2-ylidenes. The ¹³C-NMR showed the imidazolium carbon had shifted significantly downfield in line with the de-shielded nature of a carbene carbon, C2, typically between 200-250 ppm whilst the signal of the C2 in imidazolium salts is between 130-160 ppm. Kunz *et al* later showed a correlation between the N-C-N bond angle and the ¹³C {¹H}-NMR shift; the smaller the angle the lower the carbene carbon's signal shifted downfield.²³ In the ¹H-NMR spectrum, the acidic proton on C2 of the imidazolium salt, found between 8-12 ppm depending on the salt, is no longer been observed.

Arduengo's initial synthetic route was by deprotonation of the sterically demanding *N*-*N'*-diadamantyl imidazolium salt, **15**, (Scheme 1.07).¹



Scheme 1.07: Synthesis of first stable *N*-heterocyclic carbene, *N,N*-1,3-diadamantylimadazolylidene, IAd, **16**

The adamantyl groups' steric bulk do add stability to the free carbene, however this first example, was quickly followed by the isolation of *N,N*-1,3-dimethylimidazolylidene, IMe, **17** in Figure 7, which, whilst not as stable as IAd, is still isolable in crystalline form.¹

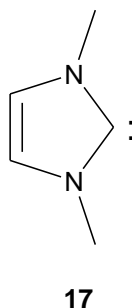


Figure 7: *N,N*-1,3-dimethylimidazolylidene, IMe.

Five membered *N*-heterocyclic carbenes, such as **16** and **17**, are strongly bent due not only to the interaction of the nitrogen π electron pairs with the p_{π} of the carbene carbon, but also to the cyclic nature of the compounds, which imposes a steric constraint. The σ - p_{π} energy gap is consequently large, which stabilises the singlet ground state and as previously stated, can be considered to have some of the character of a 4-electron-3-atom centre delocalised π -electron system (*vide infra*).¹

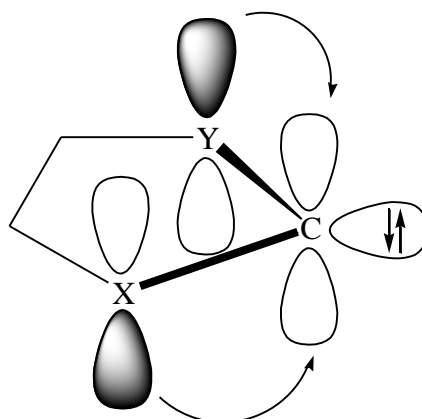


Figure 8: The 4-electron-3-atom centre delocalised π -electron system, N_2C :

The lone pair of electrons of the nitrogen atoms can partially occupy the carbene carbon's empty p_π orbitals, leading to the delocalisation of electrons and generating the resonance forms shown in Figure 9.

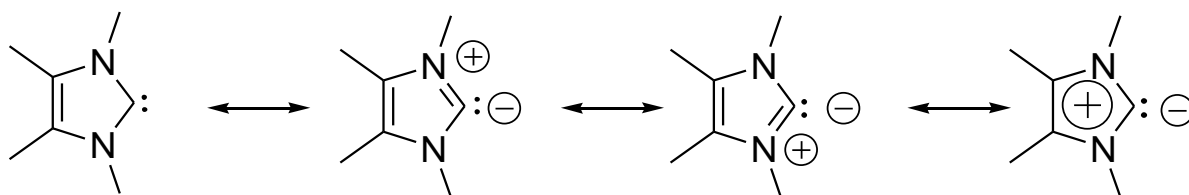


Figure 9: Resonance structures of 5 membered *N*-heterocyclic carbenes²⁴

The free *NHCs* are nucleophilic and highly basic and can be considered to be a new type of Lewis base.²⁵ In this respect, they are considered to behave more like P-, N- or O-donating ligands rather than classic Fischer- or Schrock type carbenes.^{26, 27}

Within metal complexes they have longer metal-carbon(carbene) bond than Fischer or Schrock carbene complexes but the bond is chemically and thermally more inert. In fact, the M-*NHC* bond has a high dissociation energy compared to many common ligands such as phosphines²⁸ so dissociation is not the primary cause of *NHC* catalyst degradation as the metal-*NHC* bond is very stable. This strong bond also means they are able to displace other ligands within a complex including highly basic phosphines. The thermal stability is an advantage over phosphine ligands, where cleavage of the P-C bond at high temperatures is often a problem; the most common degradation pathway for *NHC* catalysts being the reductive elimination to form the respective imidazolium

salt and this can be faster than the reductive elimination of the desired product in a catalytic cycle (*vide supra*).⁹

For a long while, *NHCs* were considered to be strong σ donors only with very little π back bonding from the metal taking place. More recently, it has been recognised that carbenes can take part in π -back bonding, accepting electron density from the metal d orbitals into the π^* orbital. It has also been found that with electron deficient metal centres, *NHCs* will take part in $\pi \rightarrow d$ electron donation so *NHCs* are also able to transfer electron density to the metal centre more readily than phosphines.

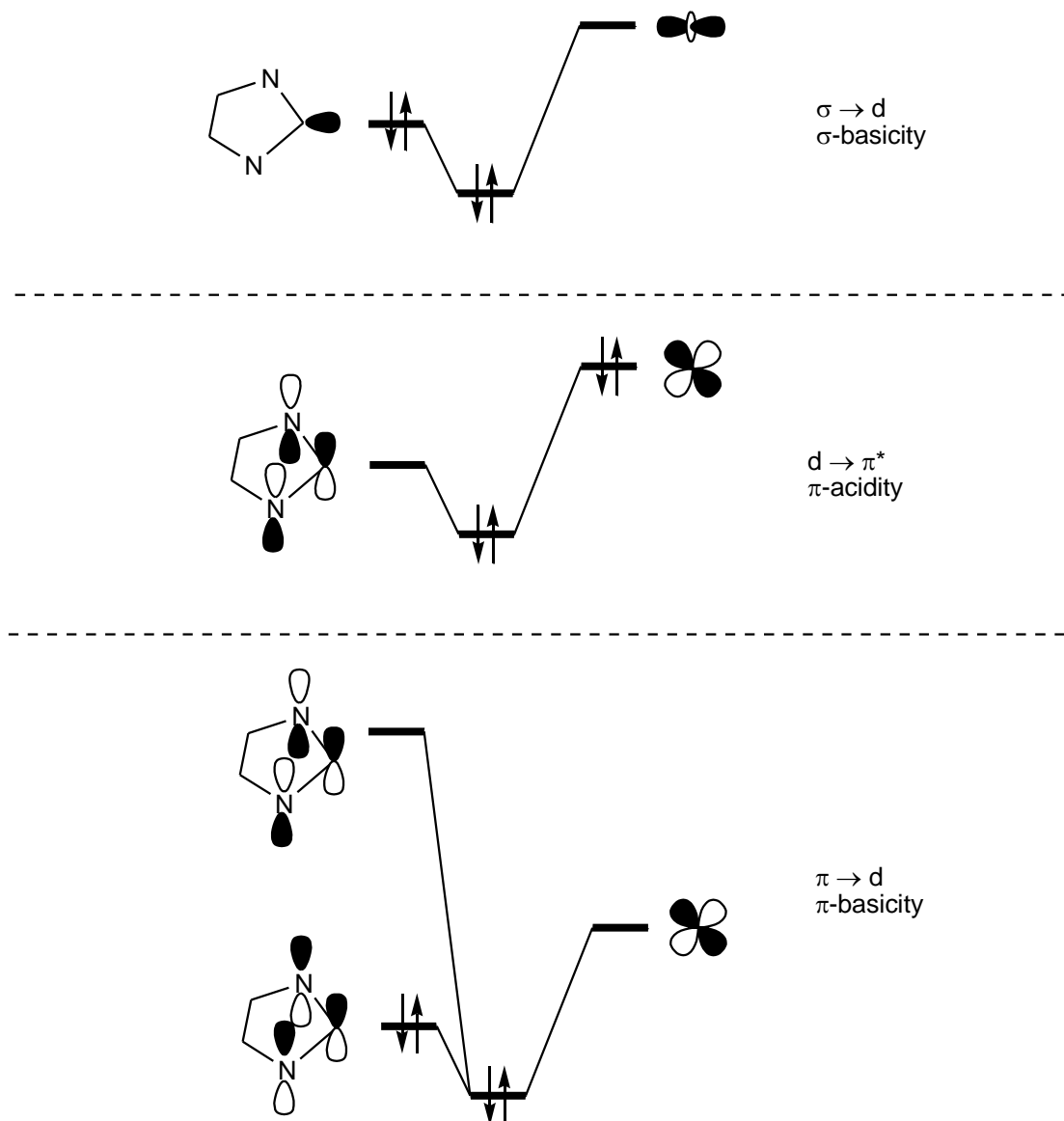


Figure 10: Bonding modes of *NHCs* with transition metals²⁹

Khramov *et al* investigated the π -acidity of various Rh complexes of the type $(NHC)Rh(COD)Cl$ (COD = 1,5 cyclooctadiene). He found that the π -acidity of *NHCs* was between the high π -acidity of CO and the π -acidity of alkenes.³⁰ He also found that back-bonding in *NHCs* is tunable. The steric and electronic properties of carbenes can be influenced by variation of substituents on the heterocycle nitrogens and the backbone carbons, C4 and C5, and by different bond saturation on the backbone. This offers the potential to subtly vary the catalyst's properties by fine tuning of the *NHC* ancillary ligand to find the optimal system for a process. Thus producing more highly specialised catalysts (target only specific reactions) which are more efficient (low catalyst loading and high TON).³¹

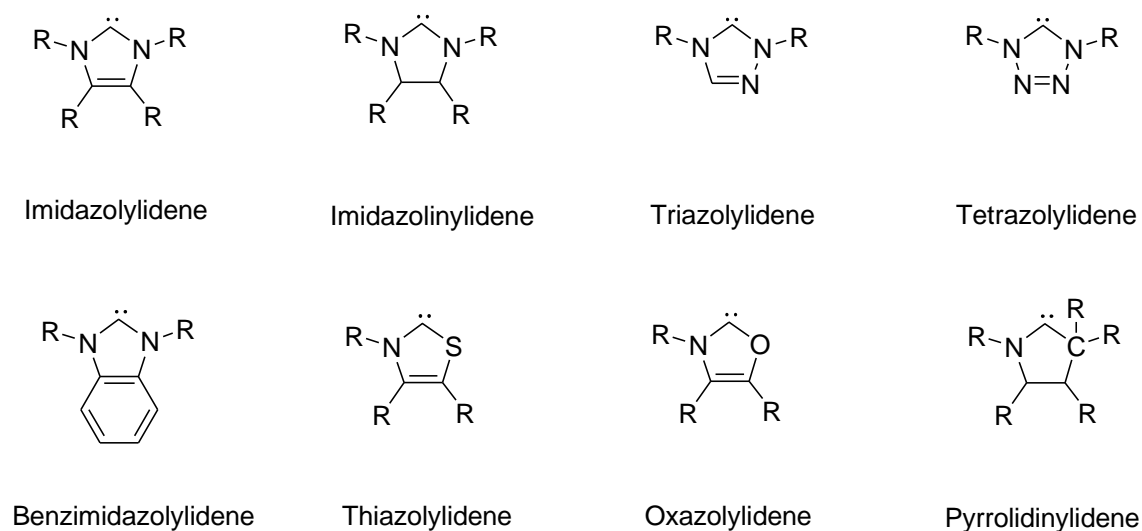


Figure 11: Eight common types of 5 membered heterocyclic carbenes³²

Five membered *NHCs* have been the most commonly researched types so far, in particular, imidazolylidenes and imidazolidinylidenes, but 3-, 4-, 6-, 7-, 8-membered carbenes as well as acyclic diaminocarbenes³³ have also been synthesised and used in transition metal complexes as ligands. There are also chiral and multi-dentate³⁴ *NHCs* which have been generated and used as ligands but this chapter will be concentrating on the symmetrical monodentate, 5-membered type of *NHC*.

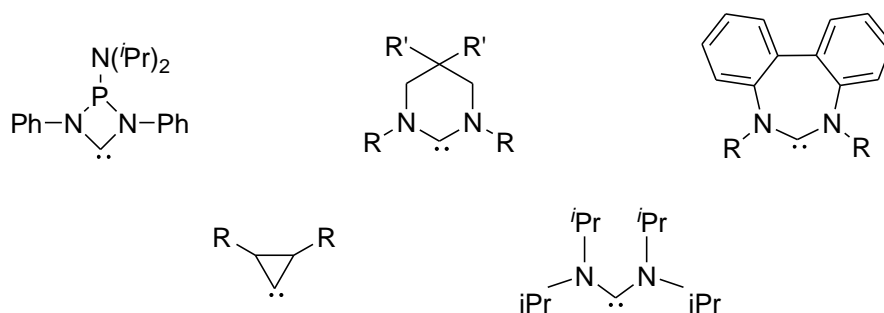
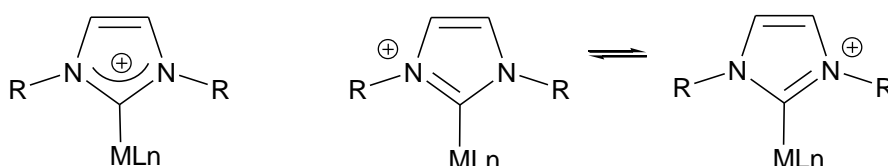


Figure 12: Examples of *NHCs* which are not five membered heterocycles

Coordination of 5-membered *NHCs* usually occurs via the C2 carbon, although there is a so-called “abnormal” coordination at the C4 carbon and a remote coordination when the carbene carbon is β to any nitrogen (Figure 13).



Accurate representation of the bonding between transition metals and normal *NHCs*

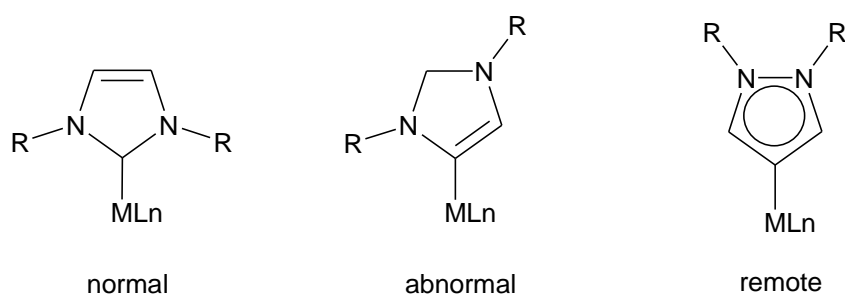


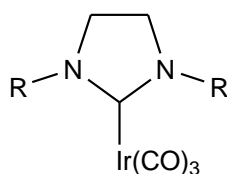
Figure 13: How *NHCs* coordinate to transition metals³¹

Surprisingly, experiments to determine BDE of the *NHC*-metal bond has found little difference in magnitude whether the backbone is of the imidazolylidene, imidazolidinylidene or benzimidazolylidene type.³² This suggests that the backbones are not important in varying the electronic properties and differences between saturated,

unsaturated and aromatic analogous carbene complexes may have more to do with sterics and the rigidity of the backbone.

Variation of the R groups on the backbone C4 and C5 carbons can have a more pronounced effect on the electronic properties. Electron-withdrawing groups such as Cl, NO₂, CN, on C4 and C5 have been found to increase the C-O bond stretching frequencies of carbon monoxide ligands in Rh and Ir complexes by between 5cm⁻¹ for Cl, up to 12cm⁻¹ for CN thus showing a decrease in M-*NHC* bond strength.³²

N-substituent change was initially considered the most promising way to vary *NHC* electronics. However, there is a small variation when changing from the electron donating alkyl groups to electron withdrawing aryl groups (Table 1). The most variation seems to occur by changing the group attached in the *para* position of an aryl R group.



<i>NHC</i>	SIPr	SIMes	SICy	SI ^t Bu	SIAd
V _{av} in cm ⁻¹	2023.9	2023.1	2023.0	2022.3	2021.6

Table 1: Change in CO stretching frequency by varying the *NHC* in Ir(0)(*NHC*)(CO)₃
(For *NHC* abbreviations, see Figure 16, page 22)

This is in contrast to the profound change seen when the R substituents on phosphines are varied (between PCy₃ and PPh₃ the CO stretching frequency increases by at least 20cm⁻¹). This difference is most likely due to the R groups being more remote on *NHCs*, not directly attached to the coordinating atom as with phosphines. So *NHCs* are more electron rich than all phosphines, although the variation in electron density is smaller. Interestingly, in abnormal *NHC* complexes, the CO stretching is much lower than for normal carbene complexes (approx. 2003cm⁻¹) making *NHCs* coordinated in this manner even more electron rich.³⁵

Sterically, *NHCs* differ from phosphines greatly, meaning that convention methods of describing phosphines' topology such as the Tolman cone angle³⁰ have been found to be ineffective when dealing with *NHCs*.

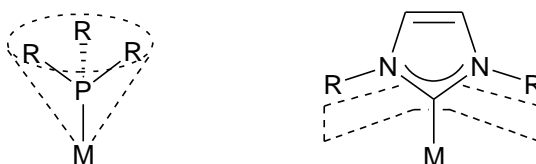


Figure 14: The differences in the shape of phosphines and *NHCs*³⁶

From Figure 14, it can be seen that the R groups on phosphorus in phosphines angle away from the metal centre whereas they angle towards the metal centre in a “fan-like” manner in *NHCs*³⁷, almost wrapping the metal centre in a pocket.³²

An early attempt to define the sterics of *NHCs* by measuring the length and height of the “fence” of the *NHC* around the metal did not properly describe the steric properties of even some common *NHCs*, in particular ICy.

The standard method now used was developed by Nolan *et al*^{38, 39}; it is described as the percentage buried volume and is the percentage of the carbene that is found within the first coordination sphere around the metal.³² This method is so general that it can also be used for phosphines enabling comparison with *NHCs*.

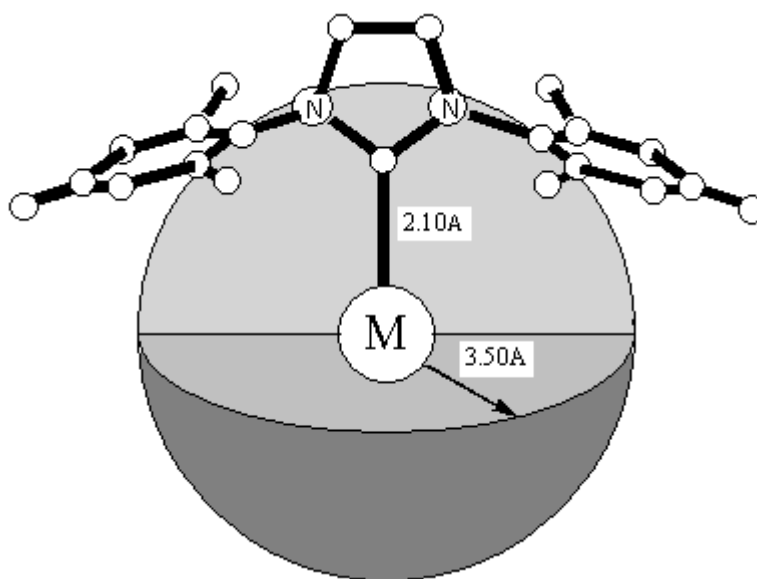


Figure 15: The first coordination sphere used to calculate % V_{Bur} ³²

The trend between the % V_{Bur} (percentage buried volume) and BDE (bond dissociation energy) has been found to be almost linear using data from both $[\text{RuClCp}^*(\text{NHC})]$ ⁴⁰ and $[\text{Ni}(\text{CO})_3(\text{NHC})]$ complexes⁴¹ where the BDE is found to be larger when the % V_{Bur} is smaller. Extended studies with $[\text{IrCl}(\text{CO})_2(\text{NHC})]$ (Table 2) show the difference in

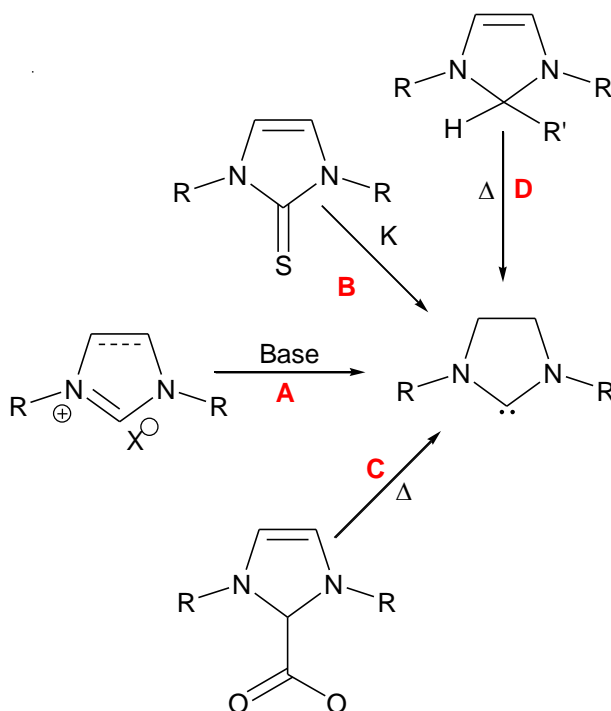
$\%V_{\text{Bur}}$ between saturated and unsaturated analogues, with the saturated version having the slightly greater $\%V_{\text{Bur}}$. This is due to the saturated backbone being less rigid so the N-C_{carbene}-N bond angle can be as much as 5° wider in the imidazolidinyldiene. Thus the nitrogen atoms are nearer the metal centre and their substituents are pushed further into the first coordination sphere. As the R groups attached to the C4 and C5 groups will also affect the positioning the N-substituents can take, alteration of the backbone substituents can be a very good way to vary the $\%V_{\text{Bur}}$. Further information can be obtained by measuring the dihedral angles of the N-substituent's bond to N atom. Measurements made by Diebolt *et al*⁴² and calculations by Ragone *et al*⁴³ show that for the same NHC, these angles can vary remarkably between different complexes. Thus the NHC shows steric adaptability conditional on the steric restraints found in in each unique complex.

L in [IrCl(CO) ₂ L]	$\%V_{\text{Bur}}$ of unsaturated NHC	$\%V_{\text{Bur}}$ of saturated NHC
Alkyl N-Substituent NHC		
H	118.8	19.0
Me	24.9	25.4
Et	26.0	25.9
CF ₃	31.1	31.8
^t Bu	35.5	36.2
Adamantyl	36.1	36.6
Aryl N-Substituent NHC		
Phenyl	30.5	31.6
Tolyl	30.5	32.4
1,3- difluorophenyl	31.3	32.3
Mesityl	31.6	32.7
1,3- diisopropylphenyl	33.6	35.7
Phosphine		
PPh ₃	30.5	
PCy ₃	35.3	

Table 2: $\%V_{\text{Bur}}$ calculated using [IrCl(CO)₂(L)] where L is an imidazolyldiene, imidazolidinyldiene or phosphine.³²

$\%V_{\text{Bur}}$ are also useful in rationalising why it is thermodynamically viable for saturated *NHCs* to dimerise but much less so for the unsaturated analogue.

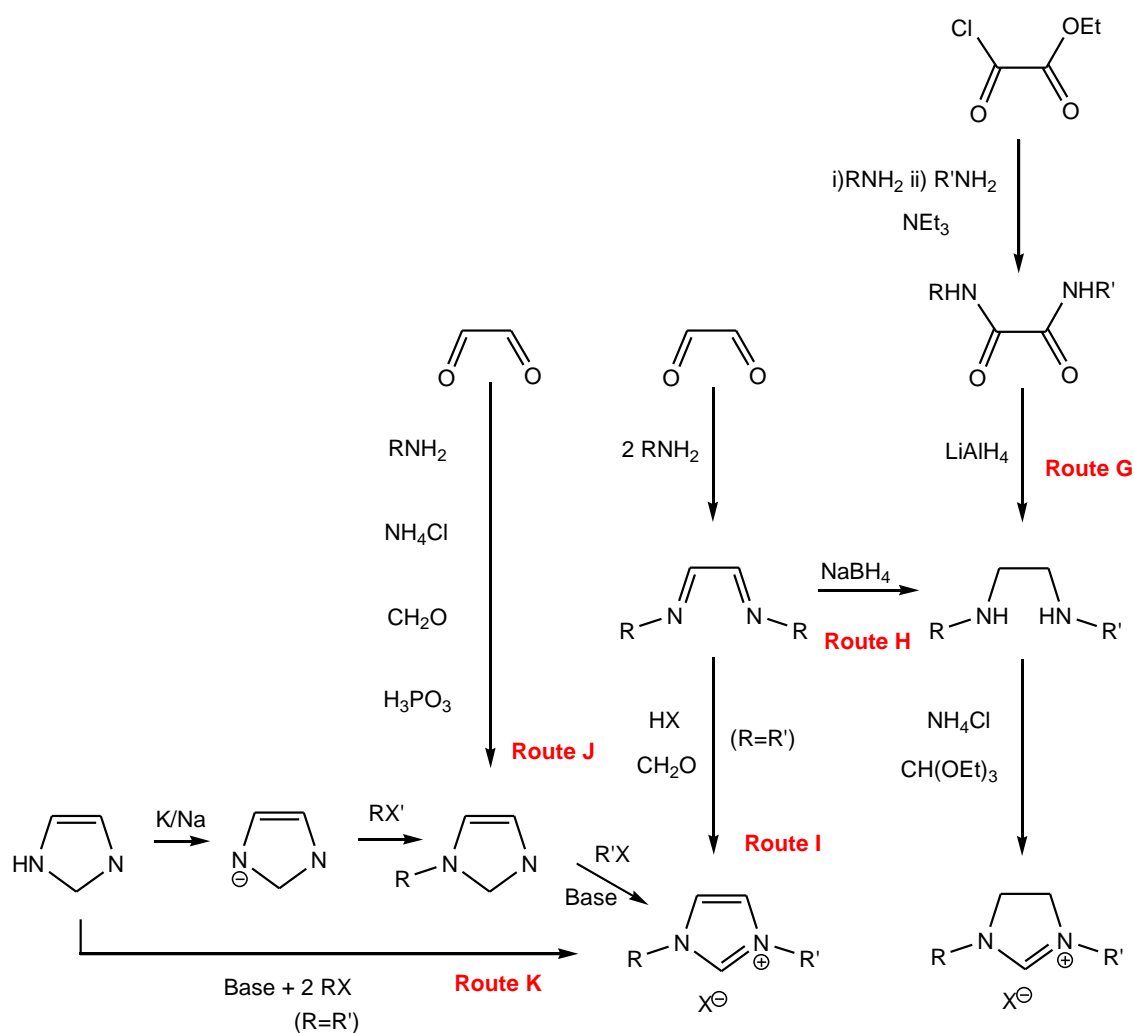
After Arguengo achieved *NHC* isolation in 1991, other synthetic pathways were developed, notably Kuhn *et al* in 1993⁴⁴ (pathway **B**, Figure 1.08) and Herrmann in 1996.⁴⁵ The synthetic strategies were developed as shown in Scheme 1.08.



Scheme 1.08: Synthetic pathways to free *NHCs*³²

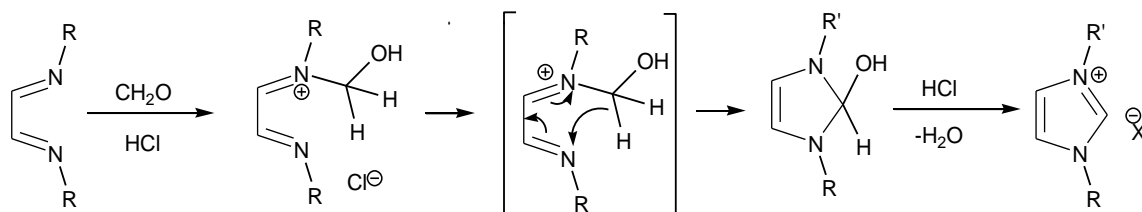
Pathway **A** is the most commonly used because there are several relatively easy pathways to the formation of the precursor imidazolium and imidazolidinium salts³² and a wide variation in base and solvent and temperature combinations that can be used (Scheme 1.09) (e.g. liquid ammonia as demonstrated by Herrmann *et al*). Kunz *et al*'s synthesis, pathway **B** in Scheme 1.09, is often used for *NHCs* with less sterically bulky *N*-substituents such as the 1, 2, 3, 4- tetramethylimidazole, ITMe, used extensively in the experimental work reported in this thesis.

The imidazolium salts which are precursors in pathway A can be formed in a number of ways as depicted in Scheme 1.09.



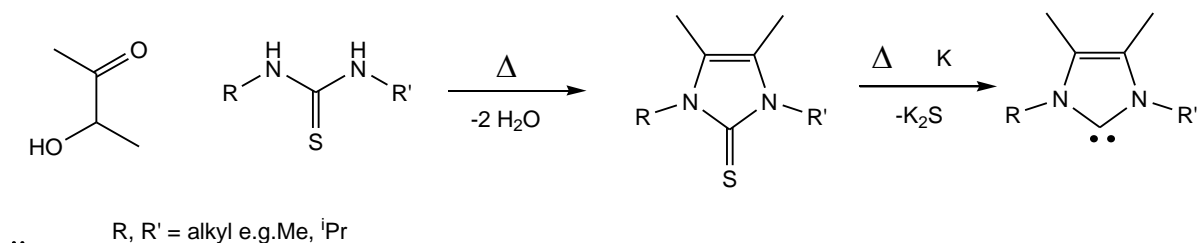
Scheme 1.09: Different methods for the formation of imidazolium and imidazolidinium salts^{32, 46}

Within this research, SIPr is formed using route G whilst ICy and I^tBu were formed by route I. The mechanism for the ring closure in route I is thought to be the one shown in scheme 1.10.⁴⁷



Scheme 1.10: Mechanism for the cyclisation step of Route I

The precursor in pathway B of Scheme 1.08 is an imidazole-2-thione. This pathway is generally used when methyl groups at C⁴ and C⁵ are required. The imidazole-2-thione synthesis is shown below in scheme 1.10.⁴⁷ It is the method used in this research to form the ITMe ligand.



Scheme 1.11: Synthetic route to imidazolylienes via imidazole-2-thione precursor⁴⁷

Commonly used *NHCs* are depicted in Figure 14. The four in the box, ITMe, ICy, ^tBu and SIPr, are the *NHCs* used in this research. The abbreviation used for imidazolylienes is derived as the I standing for imidazolylidene followed by the functional group on the *N*-substituent abbreviation. For imidazolidinylienes, the prefix is SI, standing for saturated imidazolylidene, is used, and (S)I to indicate both *NHC*.

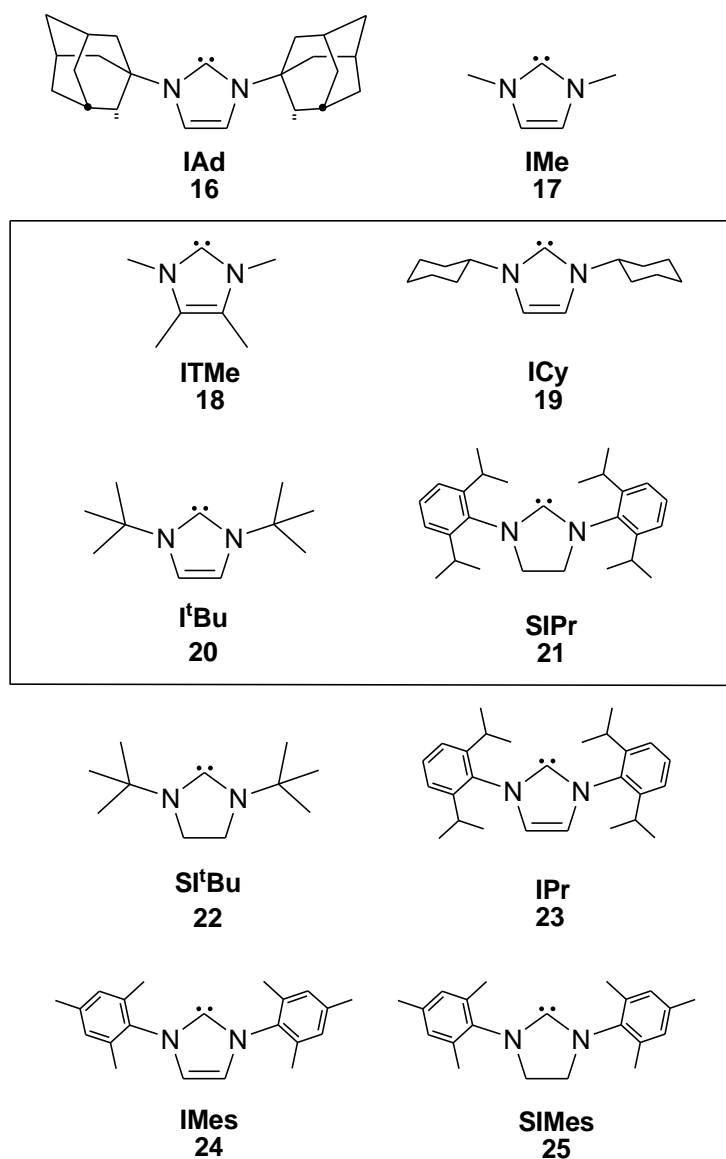
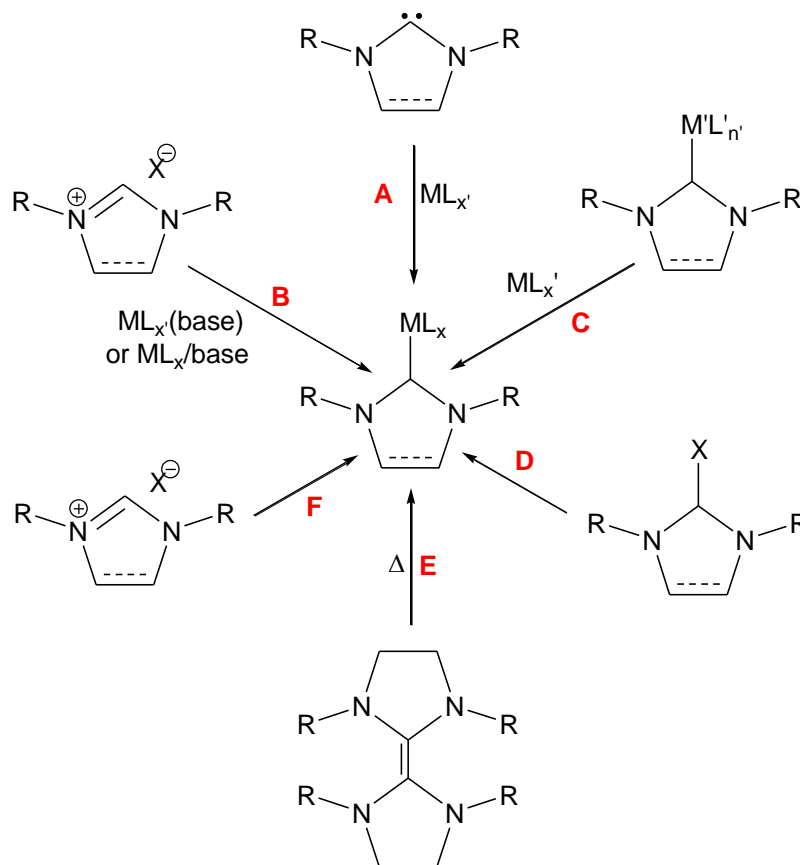


Figure 16: Commonly used *NHC*s, the four in the box are the ones used in this research

1.2 NHCs in transition metal catalysis

NHC complexes have been synthesised now using most of the transition metals as well as many of the lanthanides and even some actinides. The main synthetic methods to form a metal-*NHC* complex are summarized in Scheme 1.12.

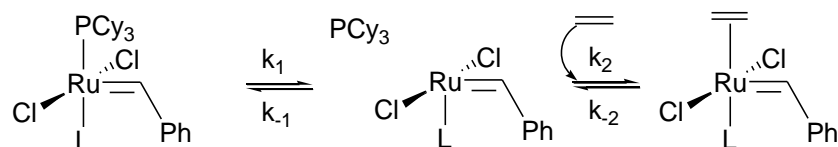


Scheme 1.12: Synthetic routes to metal-*NHC* complexes³²

Route E has already been discussed as it is the route pioneered by Lappert¹⁵. Route D and F involve the activation of a C-H or C-X bond. These three routes are less versatile than routes A-C. Route C occurs via transmetalation from a carbene transfer reagent, usually a silver complex. Route B is the indirect method where the *NHC* is formed *in-situ* by the action of the base ligand complexed to the metal or an external base and route A is where the free carbene is preformed. Both routes are completed by a ligand substitution reaction.

1.2.1 Ruthenium catalysts (Group 8)

Initially, *NHCs* were considered as “phosphine mimics” and thus research focused on synthesising *NHC* analogues of already known phosphine-based catalysts. Probably the best known example of this is olefin metathesis with ruthenium-based catalysts, so called Grubbs’ catalysts. Initially, Herrmann *et al* in 1998 replaced both phosphines with *NHCs*, however these catalyst were not a significant improvement on the so-called 1st generation Grubbs catalysts.⁴⁸ However, the replacement of only one phosphine in the 1st generation catalyst by a *NHC* improved the overall stability to high temperatures, air and moisture, most likely due to a decrease in the rate of phosphine dissociation in the 2nd generation catalysts. The rate of reaction with 2nd generation catalysts is increased as the active 14 electron species has a much greater affinity to olefins than to rebinding with the dissociated phosphine. So with *NHCs*, the difference between k_1 and k_2 (k_{-1} being smaller) is larger than for phosphines.³²



1st generation Grubbs catalyst, L = PCy₃
 2nd generation Grubbs catalyst, L = (S)IMes

Scheme 1.13 First two steps in the mechanism for olefin metathesis³²

The steric bulk of the *N*-substituents on the *NHC* appears to be a key factor in determining catalyst activity. Bulkier substituents increase the steric strain around the metal centre and facilitate phosphine dissociation and could protect the pre-catalyst from decomposition. However, if the *N*-substituents become too bulky as in the case of IPr, steric hindrance to the approaching olefin becomes an issue and the isopropyl groups may be close enough for C-H bond activation by ruthenium to occur.

Second generation Grubbs catalysts have greater diversity of application and can catalyse reactions such as ring-closing metathesis cross metathesis and polymerisation, which was not the case with the 1st generation catalysts.¹⁷

Ruthenium-*NHC* complexes have also shown activity in hydrogenation, olefin isomerisation, cycloisomerisation, polymerisation, alkylation of secondary alcohols and amide formation.⁴⁹

Osmium has been used with *NHCs* as an olefin metathesis catalyst. In this case, the bulkier IPr *NHC* is the ligand leading to a better catalyst rather than the IMes *NHC* predominately used with ruthenium metathesis catalysts.³⁵

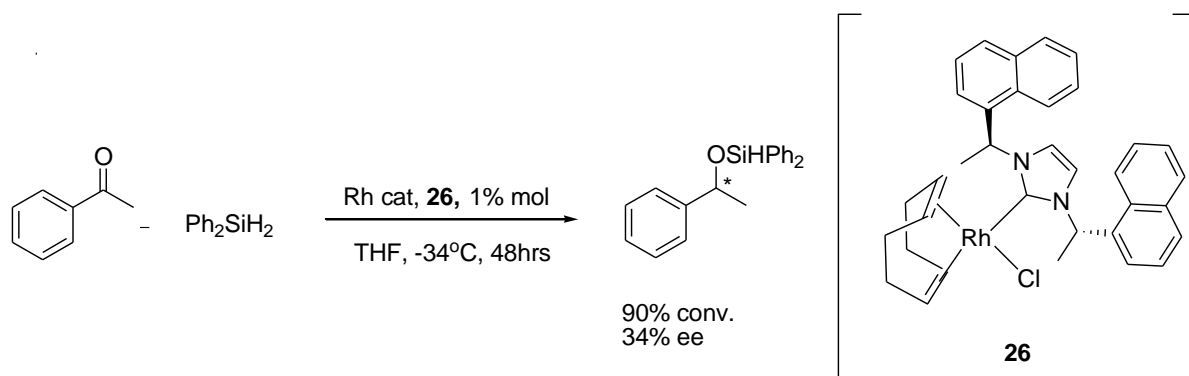
The development of iron-*NHC* systems is a growing field of interest. Research has been on the nature of some of the unusual complexes they form. Iron-*NHC* complexes have been investigated as polymerisation catalysts, cyclisation and some C-C bond formation⁴⁸ and their ability to stabilise some highly energetic, low coordinate Fe systems means they warrant further investigation.

1.2.2 Rhodium and iridium catalysts (Group 9)

Cobalt-*NHC* catalysts have been used in dehalogenation and cyclisation reactions, however, like iron, they have been under-developed as catalysts, though much work has been done on the types of complex they form with *NHCs*.

Rhodium-*NHC* complexes have been investigated for catalytic activity in hydrosilylation, hydrogenation and hydroformylation, again replacing phosphines in rhodium catalyst such as the Wilkinson catalyst.

Hydrosilylation of alkyne, alkene, carbonyl and imine groups using rhodium-*NHC* complexes have all been reported, including for asymmetric catalysis. Indeed, it was a chiral *NHC*-rhodium complex used for the hydrosilylation of acetophenone which demonstrated the potential of chiral *NHCs* in asymmetric catalysis.⁵⁰



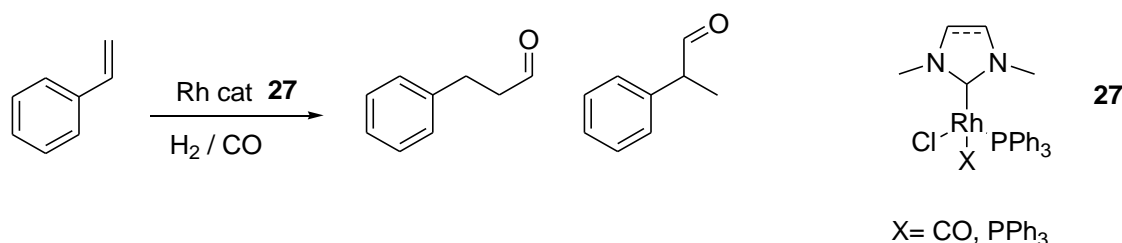
Scheme 1.14: Hydrosilylation using Rh-complex, **26**⁵⁰

It has been found that bis-*NHC* complexes give higher enantio-selectivity than monochelated ones and there is recent work using tetra-dentate *NHCs* which shows good ee results.^{49,51}

Hydrogenation using rhodium is less common than with iridium. Work by Herrmann *et al*⁵¹ showed that Rh(ICy)(L) catalysts ($\text{L} = \text{phosphine, COD, ICy}$) complexes were in fact comparable to Wilkinson catalysts already known. Future work would seem to be directed towards asymmetric transformations as with hydrosilylation. Arnanz *et al* produced rhodium, as well as gold and palladium-based, chiral bis-carbene catalyst, which have also shown activity for asymmetric hydrogenation.⁶

Hydroformylation is again an example of where *NHCs* have been used to replace phosphines.

Crudden *et al* used SIMes and IMes in mixed phosphine/*NHC* rhodium complexes (**27**) in the hydroformylation of styrene where these complexes showed better activity and selectivity for the branched product than older, phosphine-only catalysts. Herrmann *et al* has good results using a variety of *NHC*s starting with IMe for hydroformylation of aliphatic olefins. Problems arise when internal olefins are generated. This is more likely to occur when steric hindrance prevents the approach of the olefin reactant, or the Rh-*NHC* bond is not stable to the reducing conditions inherent in these reactions. The strong electron donating properties of *NHC*s also have to be finely balanced so that while H₂ activation is promoted, the hydrido complex formed is not still too electron rich to deter olefin coordination.⁵¹

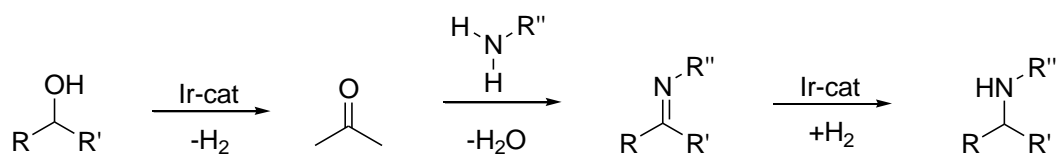


Scheme 1.15: Hydroformylation of styrene using mixed *NHC*/phosphine catalyst

Iridium catalysts have long been used in hydrogenation.⁵² Crabtree's catalyst, [Ir(COD)(PCy₃)(py)(PF₆)], is perhaps the best known iridium hydrogenation catalyst, which, while it has high activity, is known to degrade rapidly. Following the theme, when *NHC*s emerged as viable phosphine ligand alternatives, there was interest in using them in Crabtree's catalyst. Nolan *et al* replaced the PCy₃ with SIMes. At temperatures below 50°C, Crabtree's catalyst somewhat outperformed the *NHC* analogue but above that, the phosphine-based catalyst started to degrade whereas the new catalyst was stable. Replacement of the pyridine, instead of the phosphine, led to mixed *NHC*-phosphine complexes. However, although many were tested, the best one, [Ir(COD)(IMe)(P(*n*-Bu)₃)](PF₆), was still only comparable to the original Crabtree catalyst and indeed was also as unstable.³⁶ The breakthrough was made when the counter-ion was changed from PF₆ to a BARF (Tetrakis[3,5-bis(trifluoromethyl)phenyl]borate) anion, which can stabilise coordinatively unsaturated species in catalysis better than PF₆. The best catalyst found was then [Ir(COD)(IMe)(P(*n*-Bu)₃)](BARF), which, at 0.1% mol catalyst loading, can convert a

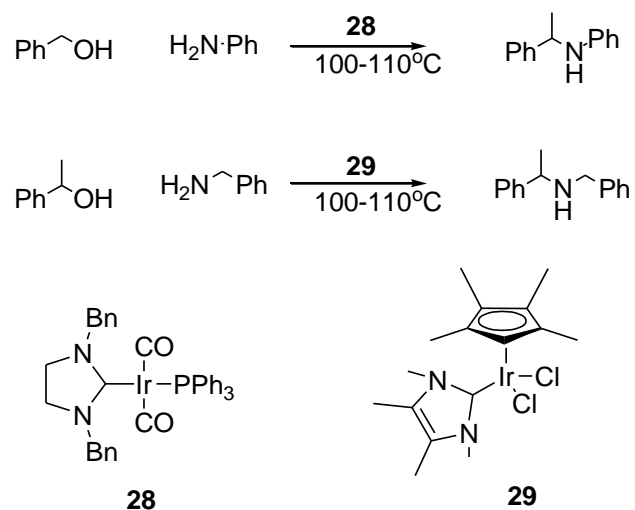
tetra substituted alkene in 100% yield whereas the Crabtree' catalyst had degraded at 49% conversion.³⁶

One transformation of Ir-*NHC* catalysts is of particular interest as pertains to this thesis is the transfer hydrogenation reaction. This is when the catalyst “borrows” hydrogen from an alcohol which leads to formation of an aldehyde or ketone which more readily react with certain other reactants to form an unsaturated compound which will then be saturated on the return of the “borrowed” hydrogen. Primary alcohols react with secondary alcohols in this way leading to C-C bond formation and, if the second reactant is an amine, C-N bond formation. This is then a method for alkyl amination using alcohol where the alkyl sython is an alcohol, not an alkyl halide.



Scheme 1.16: General reaction scheme for the alkylation of amines using alcohols and Ir-*NHC* catalysts

Chang *et al*⁵³ have used 1% mol of complex **28** to produce *N*-benzylaniline in 96% yield whilst Peris *et al*⁵⁴ have used a number of iridium catalysts including **29** which are activated by AgOTf with yields of up to 95%. This reaction has found use in converting biodiesel waste product, glycerol, to more useful amines.⁵⁵ These iridium catalysts can also be used for amine-amine coupling and, if the H₂ is not returned by the catalyst, the amide coupling product can be generated in an oxidative coupling.⁵⁶

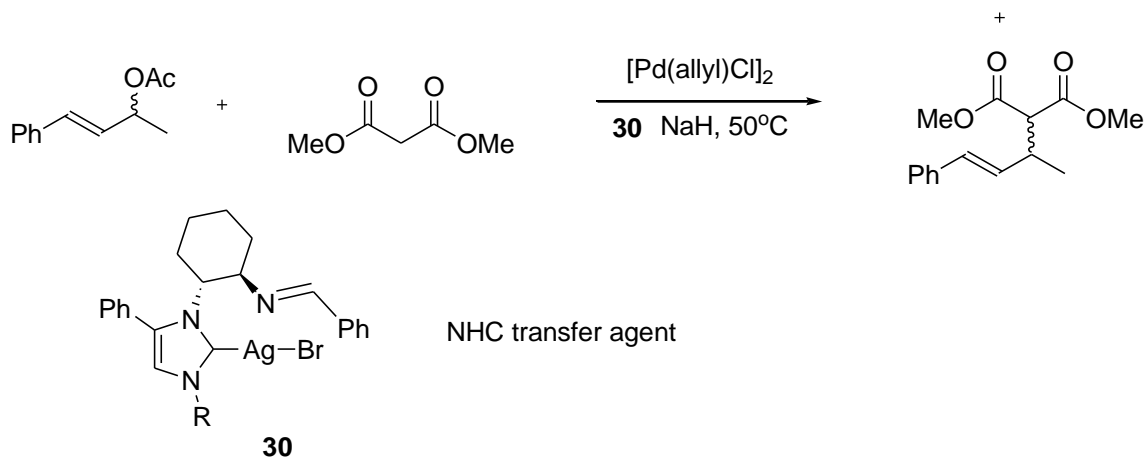


Scheme 1.17: Reactions of alcohols with amines catalysed by Iridium-*NHC* complexes³⁶

Recent work by Syska *et al* has developed water-soluble Rh, Ru and Ir complexes for hydrogenation using *N*-sulfoalkyl-substituted benzimidazolylidenes.⁵⁷

1.2.3 Copper, silver and gold *NHC* complexes (Group 11)

Silver *-NHC* complexes are the most commonly used *NHC*-transfer reagents. Silver-*NHC* complexes can be formed simply by reacting Ag_2O with the imidazolium salt and are most often air-stable.⁴⁷



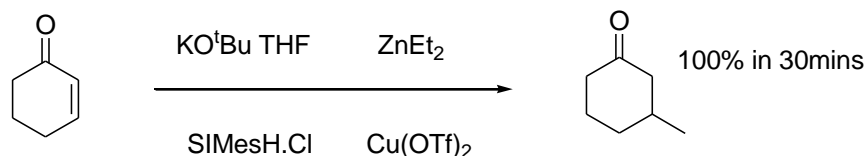
Scheme 1.18: Example of Ag-*NHC* transfer agent.³²

It has since been found that copper and gold *NHC* complexes can also be used as transmetallation reagents³⁶ and their complexes can be made from Cu_2O and Au_2O as with silver.⁵⁸ Silver-*NHC* complexes have been reported, to catalyse lactide polymerisation for instance, but the active catalyst turned out to be the free *NHC*.⁵⁹

Silver and gold *NHC* complexes have also found to be useful in pharmacology as they have anti-bacterial properties and gold-*NHC* complexes have been investigated for their anti-cancer properties and use in alleviating breathing difficulties for cystic fibrosis sufferers.⁶⁰ Gold catalysts where the *NHC* has replaced a phosphine within the complex has been an area where the phosphine analogues still out-perform the *NHC* versions. Examples include intramolecular cycloaddition reactions and other skeletal rearrangement reactions.³⁶ However, as gold was considered catalytically inert up until quite recently, there are fewer known gold catalysts so this is a field where use of *NHCs* can be explored without reference to phosphine analogues.⁴⁹

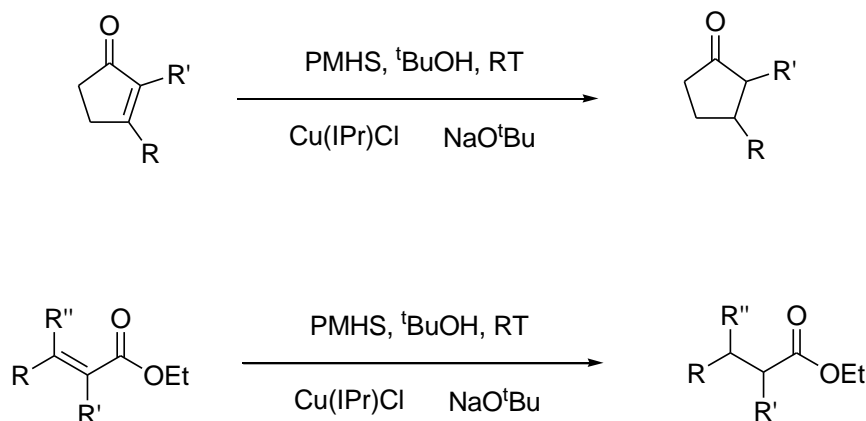
Copper-*NHC* complexes have been found to be active as catalysts for conjugate addition of dialkylzinc species to enones⁶¹ and allylic alkylations using Grignards and dialkylzinc.⁴⁹ All three of these transformations were previously known with other

ligands, notably phosphines, using copper so the main focus is now in the development of asymmetric protocols using chiral *NHCs*.



Scheme 1.19 Conjugate addition of diethyl zinc to cyclohexanone

The reduction of enone compounds is another area where copper catalysts have been used. Nolan *et al* found that when using $[\text{ICyCuCl}]$ as catalyst instead of the phosphine-copper version, the reactions were much more efficient. It has been suggested that this is due to the metal centre being made more open to the substrate interaction when the fan-like *NHC* is used over the cone-shaped phosphine.³⁶



Scheme 1.20: Reduction of cyclic and acyclic enone compounds by $\text{Cu}(\text{IPr})\text{Cl}$

1.2.4 Early to middle transition metal complexes (Groups 3-7)

Although many examples of early transition metals-*NHC* complexes have been synthesised⁶², they are not in widespread use as catalysts.

Polymerisation of lactide, the cyclic diester of lactic acid, by ring-opening polymerisation is one area where complexes of Mg, Zn, Ti and Y^{59, 63} have been investigated for catalytic activity. The product, PLA (poly (lactic acid)), is a biodegradable and recyclable commonly used plastic (Figure 17).

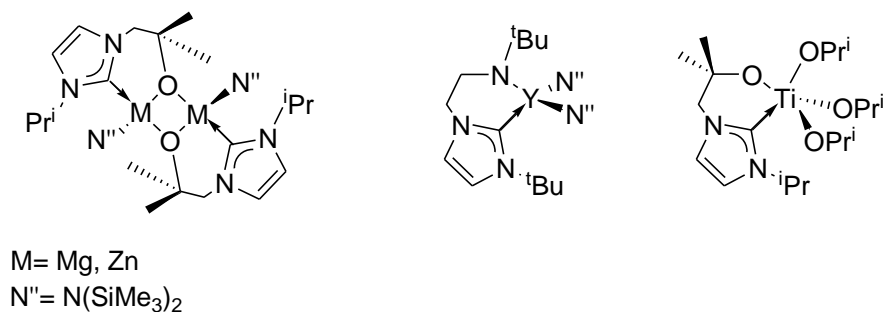
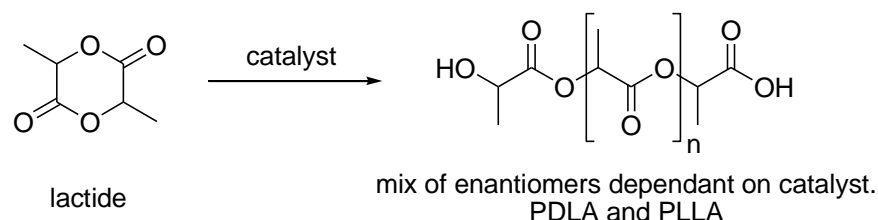
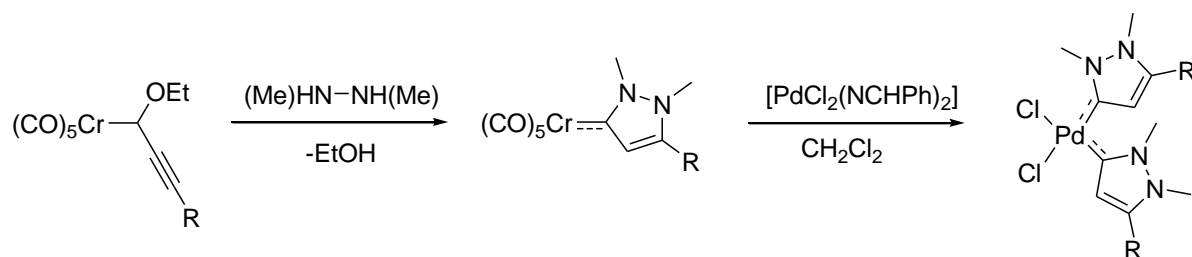


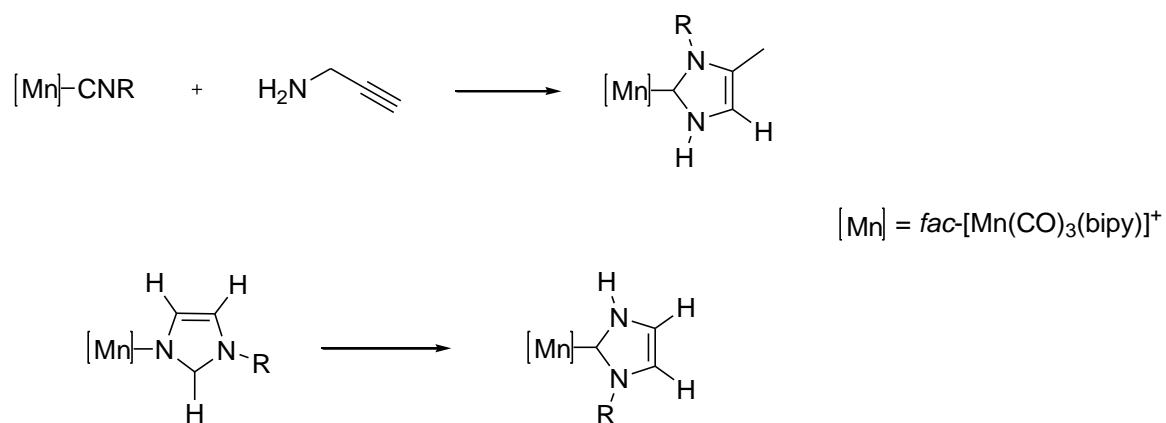
Figure 17: Examples of Mg, Zn, Ti and Y *NHC* complexes for lactide polymerisation catalysis

Chromium has been shown to be a good pyrazolin-3-ylidene carbene transfer agent to gold, palladium and, to a lesser extent, platinum. Although the resulting pyrazolin-3-ylidene late transition metal complexes are only moderately good catalysts in Suzuki-Miyaura reactions, they were found to be superior to analogous imidazolylidene catalysts for Heck reactions.⁶⁴



Scheme 1.21: Chromium catalyst as pyrazolin-3-ylidene transfer agent

Manganese *NHC* complexes show activity as *NHC* transfer agents to gold. The synthesis of the Mn-*NHC* takes place by the reaction of a manganese-isocyanide complex with propargylamine or by the tautomerisation of an imidazole-Mn complex.⁶⁵



Scheme 1.22: Formation of manganese-*NHC* transfer agents

1.2.5 Organocatalysis

Recently, interest has been directed towards the use of *NHCs* as catalysts on their own and not within a metal complex.

The *NHC* forms four types of synthon; acyl anions (d^1) generated by the reaction of *NHCs* with an aldehyde; enolate (d^2) from *NHC* reaction with enals; homoenolate (d^3) also from reaction with enals; and acylazolium (a^1) in the transesterification of esters and oxazolyl carbonates with primary and secondary alcohols.³²

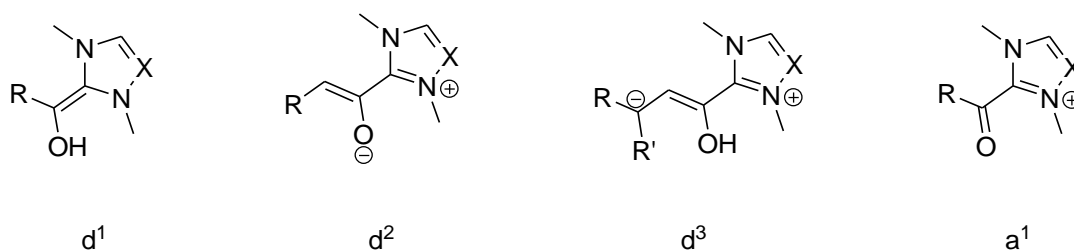


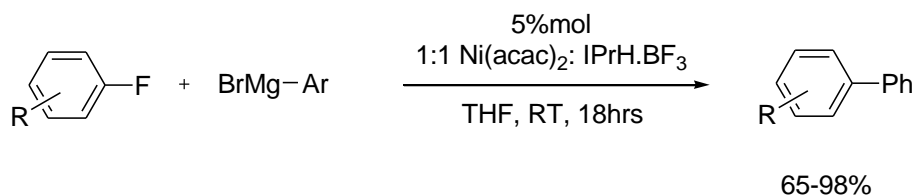
Figure 18: Synthons generated using *NHCs*

As this is primarily a review of *NHC*-metal catalysis, no further discussion of *NHCs* used in this manner will be had at this time.

1.2.6 Nickel and platinum catalysts (Group 10, part 1)

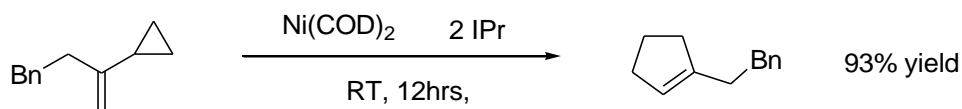
The use of nickel as an alternative to other transition metals is a desirable end, mainly because of nickel's relative abundance and therefore its lower cost. Nickel catalysts have been investigated for use in many of the same cross coupling reactions such as Suzuki-Miyaura, Heck and Buchwald-Hartwig amination, for which palladium catalysts are used (*vide supra*).

The use of $\text{Ni}(\text{NHC})_x$ ($x = 1, 2$) species as catalysts in the Kumada reaction is one characteristic example.⁶⁶ Bohm *et al* first showed how the *in-situ* formation of a monomeric Ni-IPr active species was successful in this reaction with both electron poor and electron rich aryl fluorides.⁶⁷ The mechanism is thought to proceed via oxidative addition of the aryl halide to the Ni-NHC complex. Further studies have shown activity with aryl chlorides and bromides^{66, 68} using bidentate NHCs.



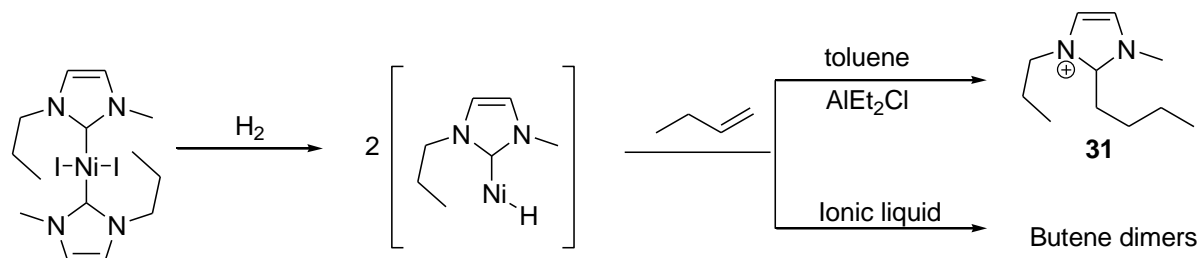
Scheme 1.23: Kumada reaction performed by Bohm *et al*⁶⁷

Nickel-NHC complexes have also shown catalytic activity in rearrangement reactions with vinyl cyclopropanes (Scheme 1.24) where they replaced phosphines in previously known catalysts. The bulky IPr and SIPr used led to catalysts with significantly improved activity. The phosphine-based catalysts needed high temperatures, which led to catalyst degradation, whereas the NHC analogues were stable at these temperatures.³²



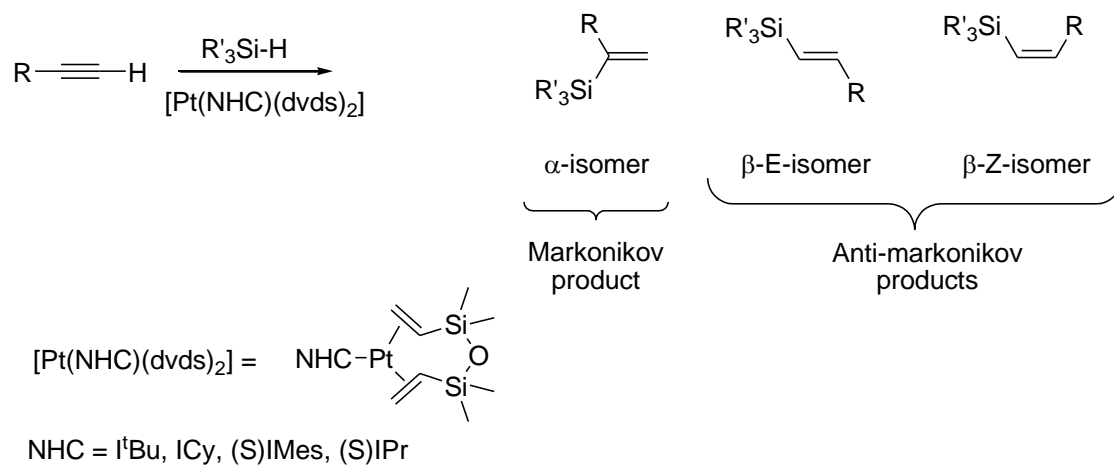
Scheme 1.24: Vinyl rearrangement using Ni-IPr catalyst generated *in situ*⁶⁹

Interesting results have been obtained for Ni-*NHC* catalysts in olefin metathesis. As with Pd, Nickel-*NHC* systems complexed to alkyl, acyl or aryl groups (R) can degrade by reductive elimination of the R-imidazolium salt. McGuinness *et al*⁷⁰ found that this side reaction can be suppressed when using an ionic liquid (e.g. 1-butyl-3-methylimidazolium chloride, AlCl₃, *N*-methylpyrrole) instead of classic organic solvents, such as toluene, and in this instance butene was cleanly converted to its dimers (Scheme 1.25).



Scheme 1.25: How solvent affects Ni-*NHC* catalysed olefin metathesis

Cycloaddition reactions are another area where Ni-*NHC* catalysts are used to good effect. They have been employed in reactions for the synthesis of both oxygen- and nitrogen- containing heterocycles and Ni-*NHC* catalysts have been investigated for insertion, polymerisation and hydrogenation reactions.³² C-S, S-H and S-S bond cleavage has recently been investigated with Ni-*NHC* catalysts and shown good results. Platinum catalysts are often used for hydrosilylation reactions of alkynes and alkenes. There are often side-products formed besides the desired Anti-Markonikov alkyl- or alkenyl- silanes thought to be formed because the two prevailing catalysts, Speier's system (H₂PtCl₆/^{*i*}PrOH) and Karstedt's complex, [Pt₂(divinyl-disiloxane)₃], are not very stable under the reaction conditions. Pt-*NHC* complexes with their strong Pt-*NHC* bond would likely be more stable and therefore inhibit side-product formation. Systems based on Karstedt's complex show improved selectivity although the activity is only comparable to the Karstedt's complex and then only with *N*-aryl substituted *NHC*s (Scheme 1.26).³²

Scheme 1.26: Hydrosilylation with Pt-*NHC*-(dvds)₂ complexes

[Pt(*NHC*)(dvds)₂] complexes have also been found to active for hydroboration and diboration reactions whilst a 5% mol loading of [Pt(IPr)(methallyl)Cl] has shown good activity for the reductive cyclisation of diynes and enynes with SnCl₂ as co-catalyst and at 5 atm of H₂.⁵⁶

1.3. Palladium catalysts (Group 10, part 2)

The focus here will be the cross-coupling reactions with Pd *NHC* catalysts but they also catalyse many other types of reaction. These include C-H activation reactions such as oxidation of methane to methanol using bis-chelating *NHCs*^{32,35}; direct arylation reactions including ortho-arylation of aldehydes⁴³; hydroarylation of alkynes³⁶; hydration of alkynes and nitriles³²; hydrogenation of alkenes and alkynes³²; diboration of alkenes³⁶; hydroamination of alkenes and alkynes³⁶; allylic alkylations³⁶; cyclization of dienes^{71a}; oxidation of alcohols^{71b}; oxidation of terminal olefins to methyl ketones (Wacker oxidation)³⁵; oxidative esterification of alcohols^{71c} and aldehydes^{71d} using phenols; dioxygenation^{71e} of alkenes; copolymerisation of ethene and carbon monoxide^{71f, 45}; homocoupling of terminal alkynes^{71g}; telomerisation with alcohols and amines^{71h, 71i, 35}; the polymerisation of functionalised norbornenes^{71k}; and arylation of carbonyls^{71j} and dehalogenation of aryl halides. Although the last have often been observed as side reactions in cross-couplings involving aryl halides, they are now being investigated.⁴⁴

Palladium cross-coupling reactions are now commonly used in organic synthesis. This was recognised when the 2010 Nobel Prize in Chemistry was awarded jointly to Richard F. Heck, Ei-ichi Negishi, and Akira Suzuki for “palladium-catalysed cross-couplings in organic synthesis”.⁷²

Many new catalysts have been produced which efficiently perform in reactions necessary to a target molecule synthesis. One of the reasons for the arrival of many new catalysts is that there has been a significant increase in the number of ligands available, of which *NHCs* make up a significant part. These ligands are used to synthesise Pd complexes which can then be assessed for catalytic ability. So it should not be surprising that using Pd-*NHC* complexes for cross-coupling transformations is possibly the most highly researched area of *NHC* catalysis, rivalled only by Ru/Rh-*NHC* metathesis reactions.

If a catalyst is to be industrially viable, there are issues which have to be addressed. Firstly, the catalyst's efficiency must be high (high TON) so that the expense of the catalyst is minimised, particularly when using an expensive metal such as palladium. It is also necessary that the metal content in the desired product be well below any toxicity

level especially in pharmaceuticals and agrochemicals. High catalyst loadings make this a more difficult proposition, so loadings should ideally be below 0.1 ppm.⁷³

Pd-*NHC* complexes have been found to show excellent catalytic activity in many carbon-carbon cross-coupling reactions such as Heck, Hiyama, Kumada, Negishi, Sonogashira, Stille, and Suzuki-Miyaura and the carbon-nitrogen bond forming Buchwald-Hartwig amination.

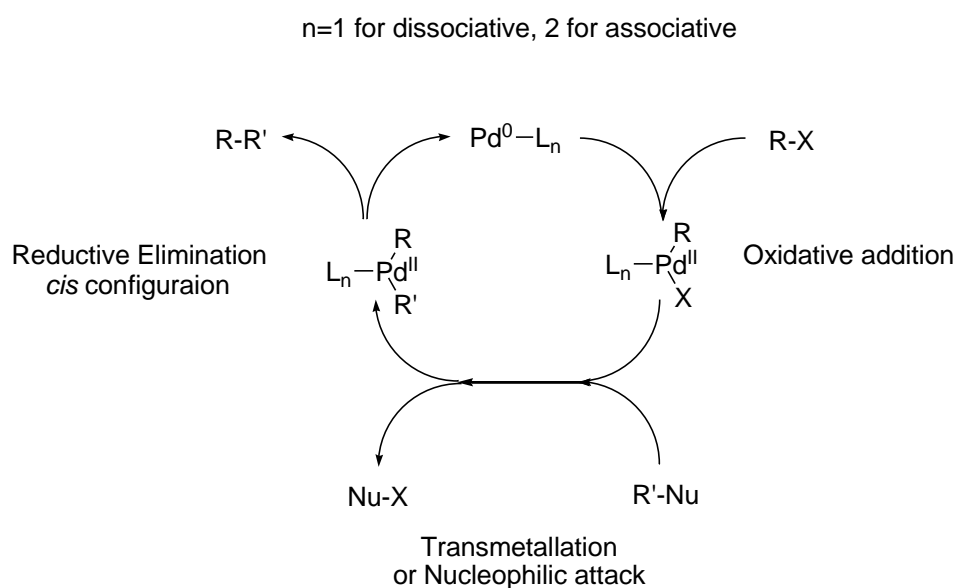


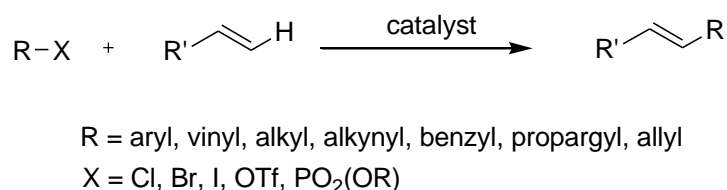
Figure 19: A generalised catalytic cycle for Pd-cross-coupling reactions³²

For most of these couplings, one of the substrates is an aryl halide and, in the first step of the catalytic cycle (Figure 19) the aryl-halide bond undergoes oxidative addition to the metal centre. *NHCs* have the advantage over phosphines in this step by virtue of their stronger σ donor abilities which increases the electron density on the metal making oxidative addition easier. This means that aryl chlorides, with their stronger aryl-halide bond, can often be used in place of the bromide, iodide, or triflate equivalents which are generally less available or more expensive.⁷⁴ In the case of Pd-phosphine catalysts, it has been established that the oxidative addition step is usually the rate-limiting one, however, with Pd-*NHC* it is much less clear (*vide supra*).

The complex synthesised is often a pre-catalyst, the actual active catalytic species being too reactive to isolate. In many cases, this will be a Pd(II) complex as they are more stable and therefore easier to prepare and handle. However, an induction time will then

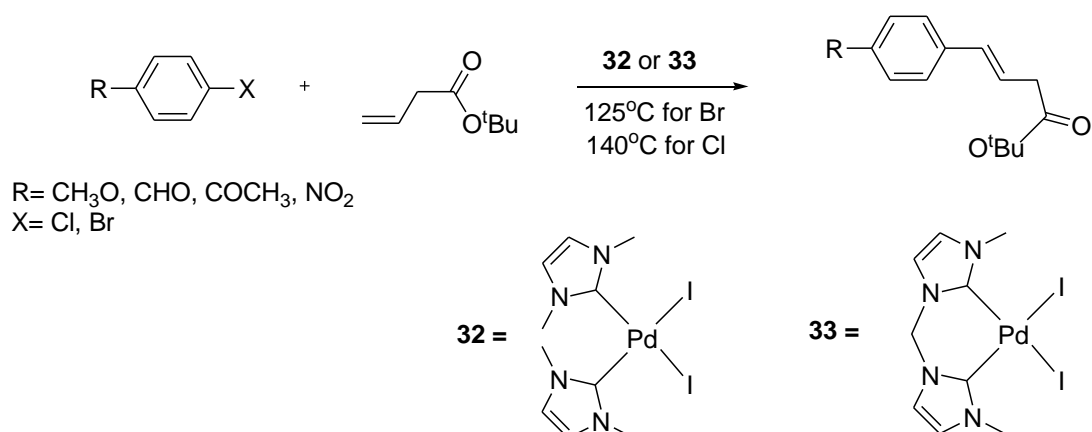
be necessary during which the Pd(0) active species is generated by reduction of the pre-catalyst. When starting from Pd(0) pre-catalyst, no induction time is observed. However whether the actual catalytic species is mono-ligated or bis-ligated with respect to the *NHC* is something determined by whether the reaction mechanism proceeds *via* a dissociative mechanism (Pd(0)L) or an associative mechanism (Pd(0)L₂). Mono-ligated pre-catalysts are often desirable for reactions which proceed *via* a dissociative mechanism as, once reduced to Pd(0), they will be in the PdL form without any actual dissociation occurring, which means that no free ligand is in the reaction mixture which could retard the reaction rate.

1.3.1 Mizoroki-Heck Reaction



Scheme 1.27: General reaction scheme for the Mizoroki-Heck reaction³²

The reports of Heck coupling by Pd-*NHC* are substantial, as this reaction and the Suzuki-Miyaura reaction, are generally how new Pd *NHC* complexes are tested for catalytic activity.³² In the case of the Heck reaction, this is firstly a case of historical precedence as it was the first example of a cross-coupling transformation achieved using Pd *NHC* catalysts; and also because the harsh reaction conditions necessary, test any new catalyst's stability as well as its catalytic ability.³⁵



Scheme 1.28: Herrmann's Pd-*NHC* catalysed Heck reaction in 1995²³

Systems tested for Heck activity include *in situ* preparations of common *NHC*s, Pd(II) salt, and base, palladacycles, bis-*NHC* chelating ligands, bidentate *NHC*-phosphine ligands but most show poor catalytic activity towards aryl chlorides. However, Beller has developed a system which takes place in an ionic liquid using **34**, a Pd-*NHC* naphthquinone complex, which shows good activity with aryl chlorides.

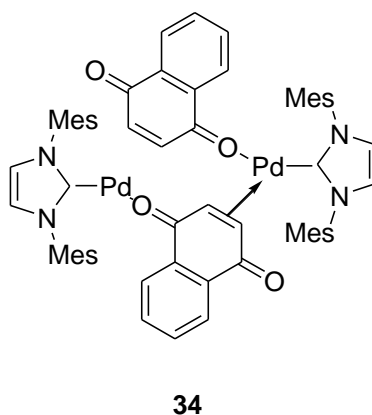
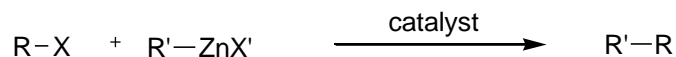


Figure 20: Beller's catalyst³⁵

1.3.2 The Hiyama reaction



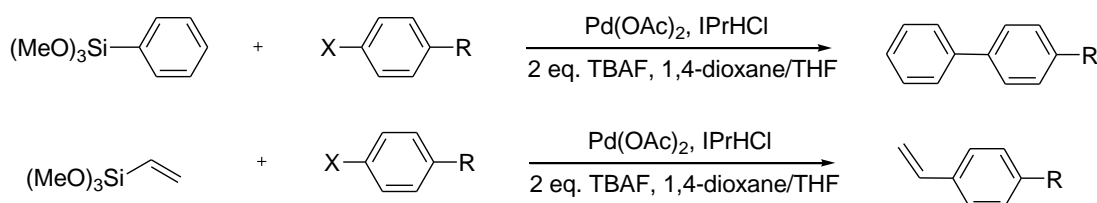
R = aryl, vinyl, alkyl, alkynyl, benzyl, propargyl, allyl

X = Cl, Br, I, OTf, PO₂(OR)

Scheme 1.29: General reaction protocol for the Hiyama reaction

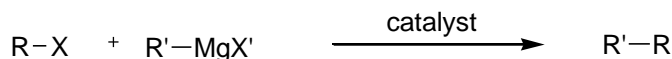
The use of silyl species in reactions is desirable as they are widely available, cheaply synthesised and stable. Another advantage is that their by-products are biodegrade, thus reducing detrimental environmental impact.

So far, there has only been one example of a Pd-*NHC* system for this type of coupling reaction. In general, the C-Si bond needs to be activated using a source of fluoride anion, unless there is an electronegative substituent in the aryl/vinyl-siloxane. In the Pd-*NHC* system reported⁷⁵, the aryl bromides and chlorides used were activated by [N(*n*-Bu)₄]⁺F⁻ (TBAF).



Scheme 1.30 The Hiyama reaction as catalysed by an *in-situ* generated Pd-*NHC* complex.

1.3.3 The Kumada-Tamao-Corrui reaction



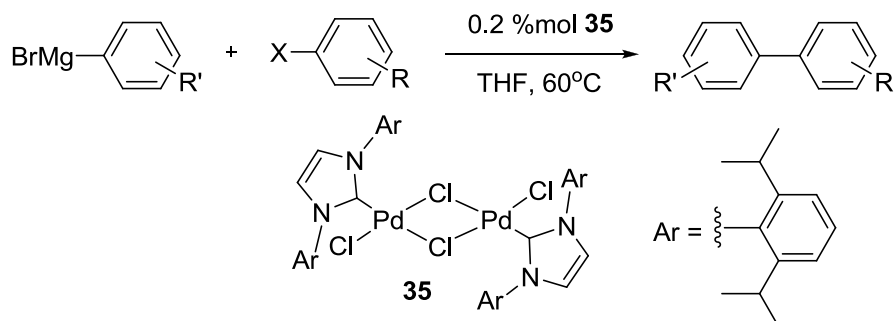
R = aryl, vinyl, alkyl, alkynyl, benzyl, propargyl, allyl

X = Cl, Br, I, OTf, PO₂(OR)

Scheme 1.31: General reaction scheme for the Kumada reaction.

Usually, Grignards cannot be coupled directly to aryl halides as this would mean an aromatic nucleophilic substitution which usually follows the trend of F>Cl>Br>I.

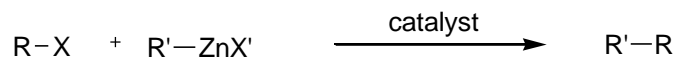
There is often the further complication of functional group intolerance or because of the homocoupling of the Grignard³². Unactivated aryl chlorides are coupled with arylmagnesium bromides by the dimer [Pd(μ-Cl)(IPr)Cl]₂ (**35**) which can catalyse this type of coupling between sterically hindered reagents²⁸. This reaction can also be utilised for alkyl chlorides using Beller's catalyst, **34**.⁷⁶



Scheme 1.32: Kumada reaction

Recently, complexes of the type (η⁵-Cp)Pd(*NHC*)Cl were found to catalyse ability this reaction with excellent results. Interestingly complex (η⁵-Cp)Pd(IMes)Cl outperforms the corresponding complex with the bulkier IPr *NHC*, possibly due to the shorter distance from the Pd to the Cp plane in the less bulky IMes complex.⁷⁷

1.3.4 The Negishi reaction



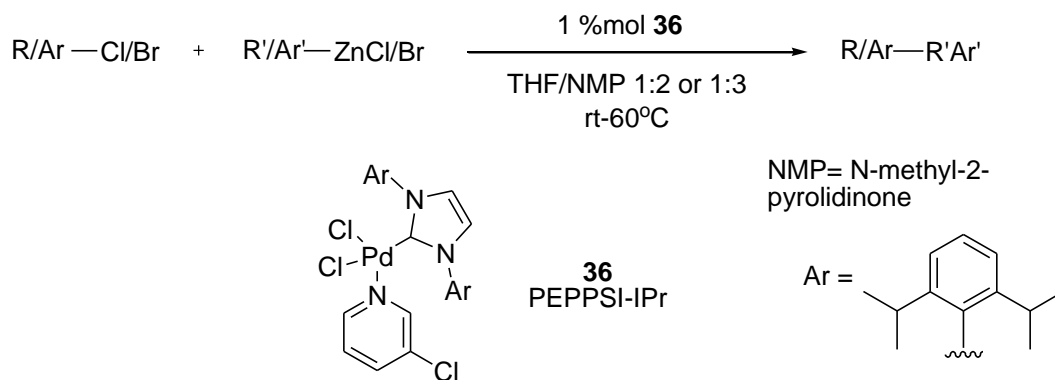
R = aryl, vinyl, alkyl, alkynyl, benzyl, propargyl, allyl

X = Cl, Br, I, OTf, PO₂(OR)

Scheme 1.33: General reaction scheme for the Negishi reaction

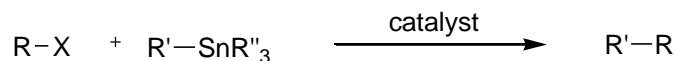
The organozinc compounds used in the Negishi reaction, whilst they have the drawback that they are sensitive to air and water, are more tolerant to functional groups than the Grignards used in the Kumada reaction.

As with the Kumada reaction, this reaction can be applied to alkyl as well as aryl organic electrophiles. Indeed, the first Pd-*NHC* system for this reaction was applied to an alkyl-alkyl coupling.³² The use of the PEPPSI-*NHC* (Scheme 1.30) catalyst by the Organ group has led to a versatile procedure for this cross-coupling.



Scheme 1.34: The Negishi reaction using PEPPSI-IPr

1.3.5 The Stille reaction



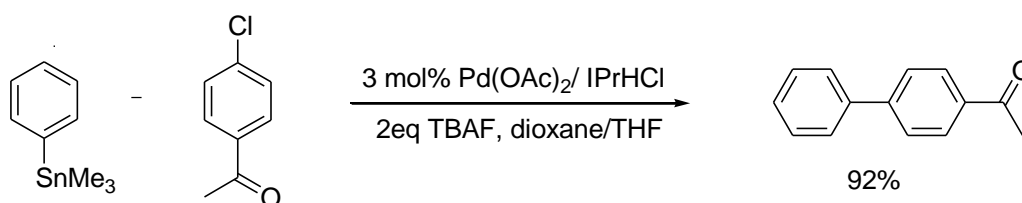
R = aryl, vinyl, alkyl, alkynyl, benzyl, propargyl, allyl

X = Cl, Br, I, OTf, PO₂(OR)

R'' = alkyl

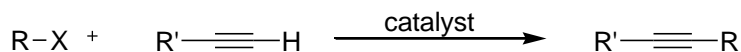
Scheme 1.35: General reaction scheme for the Stille reaction³²

Pd-phosphine catalysts are used for this reaction which would generally mean Pd-*NHC* catalysts would also have been tested or devised. However, the reaction has fallen out of favour recently, mainly because of its use of organostannanes, which whilst air and moisture stable and having excellent functional group tolerance, are often extremely toxic. The first example was a phosphine-*NHC*-Pd complex which was not active for aryl chlorides. The addition of a fluorine anion source, TBAF (tetrabutylammonium fluoride), to an *in situ* catalyst mixture, gave improved results in the coupling of aryl chlorides to vinyl and arylstannanes. The fluoride is thought to coordinate to tin in order to facilitate the transmetallation step.³²



Scheme 1.36: An example of the Stille reaction using TBAF³²

1.3.6 The Sonogashira reaction

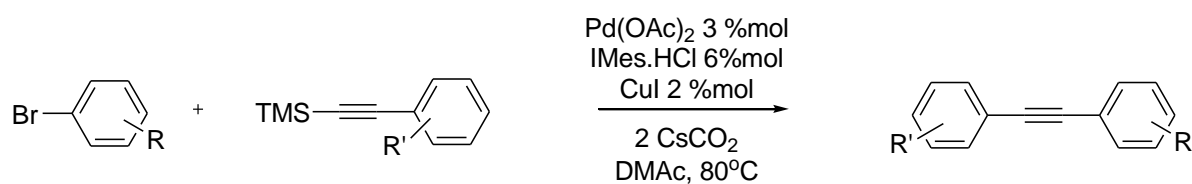


R = aryl, vinyl, alkyl, alkynyl, benzyl, propargyl, allyl

X = Cl, Br, I, OTf, PO₂(OR)

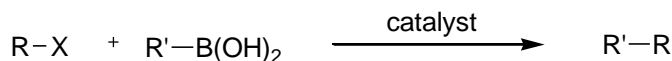
Scheme 1.37: General reaction scheme for the Sonogashira reaction³²

When using a Pd-*NHC* catalyst, this reaction was initially confined to aryl bromides or alkenyl bromides and alkynylsilanes as the steric bulk of the trimethylsilane group prevented any dimerization of the alkyne. A Pd(OAc)₂/IMesHCl/Cs₂CO₃/CuI system gave good to excellent yields for aryl bromides whilst the zero valent bis carbene complex, Pd(I^tBu)₂, was found to give excellent yields in coupling with alkenyl bromides.⁴⁰ When the bulkier *NHC*, IAd, was employed, the necessity for the TMS group was removed. The use of a Cu co-catalyst is usually required but the Pd-IMes system in Scheme 1.32 was found to give good yields without it. Indeed, recent studies have found that this reaction can be carried out in air and water and as the copper-acetylide intermediate is known to be water sensitive, it may be the Pd-acetylide intermediate is not formed by transmetallation.³² So far, these reactions have not been successful using aryl chlorides.³²



Scheme 1.38: The Sonogashira reaction with TMS-protected alkynes

1.3.7 The Suzuki-Miyaura reaction



R = aryl, vinyl, alkyl, alkynyl, benzyl, propargyl, allyl

X = Cl, Br, I, OTf, PO₂(OR)

Scheme 1.39 :General reaction scheme for the Suzuki-Miyaura reaction³²

The boron sources used in this reaction to couple to aryl halides or pseudohalides are air and moisture tolerant, are not toxic, are tolerant to a large number of functional groups and they are readily available. This makes the Suzuki reactions one of the most commonly used protocols for carbon-carbon bond formation. Mostly, the boron source will be boronic acid but there are examples of other sources such as Ar-B⁺F₃K⁺, or Ar-B(O-O) (O-O = pinacol).⁹

The initial *NHC* utilised by Herrmann *et al* for this protocol was **33** (Scheme 28) , a bis-chelating *NHC* based on IMe whereas IMes and IPr were used by Nolan *et al*. Nolan found the choice of base had an impact on the reaction rate, where Cs₂CO₃ and K₃PO₄ gave the best results. For aryl chlorides, the use of a preformed zero valent Pd(*NHC*)₂ complex gives much reduced rates than in situ generation of *NHC* with equimolar amounts of imidazolium salt and base and a Pd(II) source.⁷⁸ This is indicative of a mono-ligated active catalyst, Pd(0)L with the oxidative addition of the aryl chloride being the rate-limiting step.⁴²

This means that Pd-*NHC* dimers such as **35**, preformed mixed monoligated *NHC* Pd complexes (**37-39**), palladacycles (**40**) and functionalised-*NHC* Pd complexes (**41**) generally show catalytic activity for this reaction.

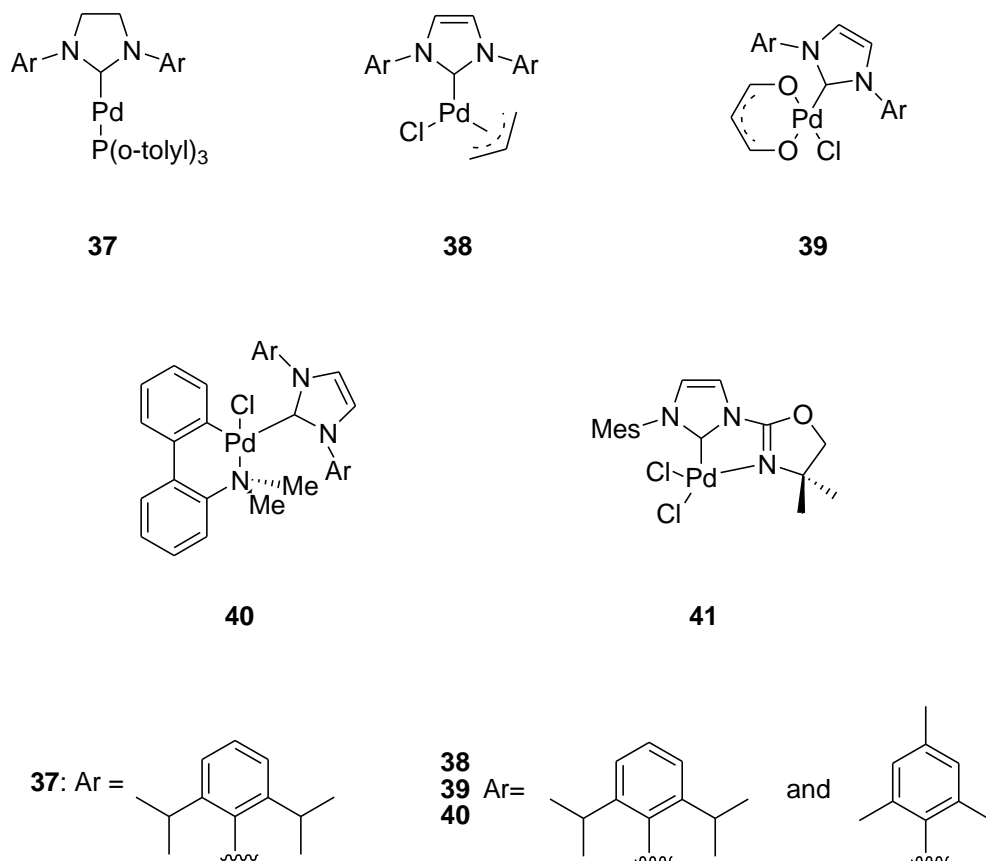
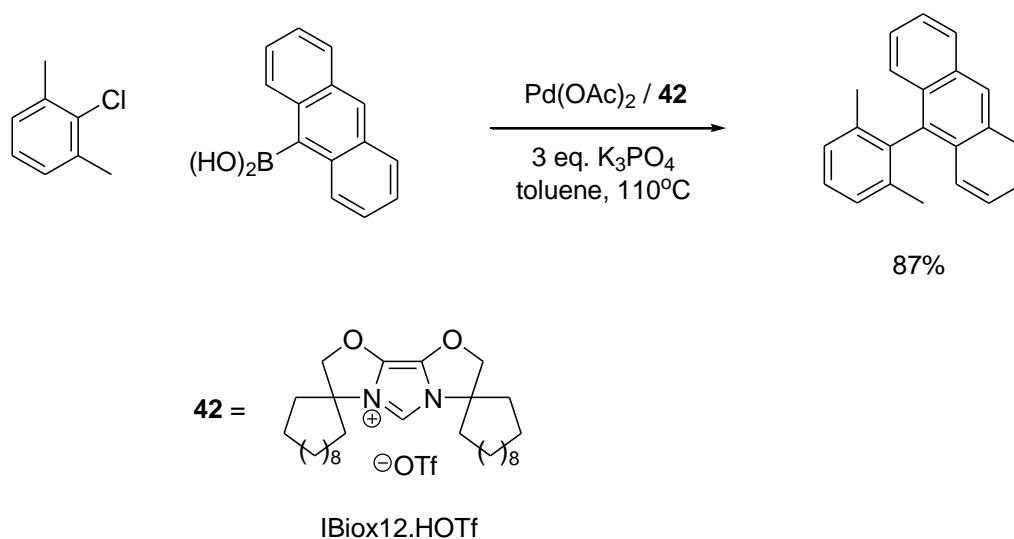


Figure 21: Examples of Pd-NHC complexes used for cross-coupling catalysis⁷⁹

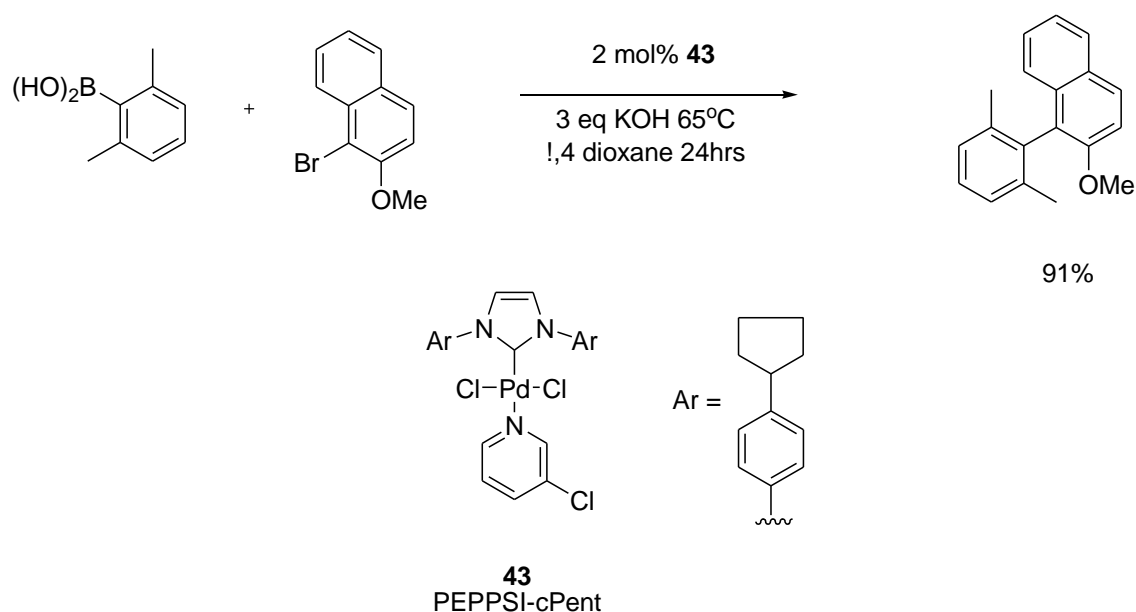
(**37** = Caddick and Cloke⁸⁰, **38-40** = Nolan *et al.*, **41** = Cesar, Bellemin-Laponnaz, and Gade⁸¹)

Bulky substituents on the *NHC* have been found to increase reaction rate when they have conformational flexibility. Steric adjustment within the complex can promote the formation of a catalytically active species by accommodation of hemilabile interactions whilst being able to stabilise low coordinate catalytic intermediates. The bulky $Pd(IAd)_2$ was found to give excellent results by Herrmann *et al.*⁸² For use with very bulky aryl substrates, Glorius *et al.* found that the extremely bulky IBiox *NHCs* do not catalyse the reaction when in the bis-*NHC* complex because of the competitive side reaction of proto-deboronation of substrate. However, excellent results are obtained if the catalyst is formed *in situ* from 1eq of IBiox, 5-12, triflate salt, and 1 eq. $Pd(OAc)_2$ and 1 eq. base. IBiox-12 (**42**), the bulkiest of these ligands, gave the best results (Scheme 1.33) whereas, under the same conditions, IAd and IMes did not catalyse the reaction.



Scheme 1.40: Example of an IBiox12 Pd catalysed Suzuki-Miyaura reaction⁷⁹

Recently, Organ *et al* have reported that use of the Pd-PEPPSI-cPent complex(**43**) can give yields of 91% for reactions with some very sterically demanding substituted bromobiaryls, such as tetra-*ortho* substituted ones, at the relatively low temperature of 65°C.⁷⁹ (Scheme 1.40)



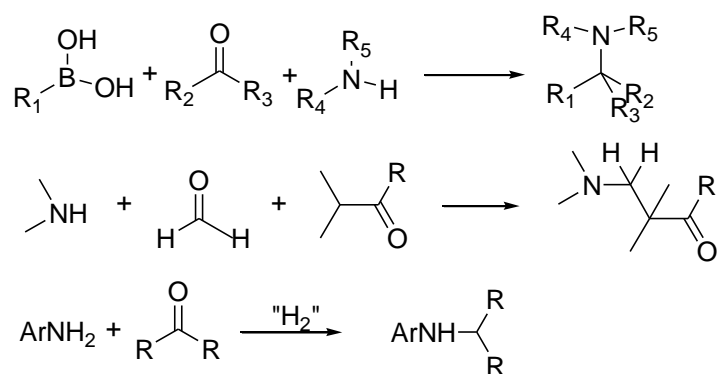
Scheme 1.40: The reaction on PEPPSI-cPent with bulky tetra-*ortho* substrates⁸¹

The ability to perform reactions in water is often desirable due to economic and environmental considerations and as boronic acids are water tolerant, this reaction can be attempted in an aqueous medium. However, often the organic aryl halide are not soluble pure water and so phase transfer catalysts are used or some percentage of alcohol is added to the water. The IBiox system described above (Scheme 1.40) is able to perform Suzuki couplings in water. Other examples of aqueous systems have been described using *NHC*-Pd complexes which are water tolerant such as caffeine-derived *NHC*s⁸³ and *NHC* ligands or complexes containing sulfonate functionalities.^{84, 85}

1.4 Carbon–Nitrogen bond formation using palladium catalysts

Carbon-nitrogen bond formation is common within a large number chemical synthesis in most areas of industrial chemistry, particularly in pharmaceuticals, agrochemicals, synthesis of natural products and nitrogen-containing synthetic polymers.⁸⁶ In fact, it is estimated that 80% of all drugs synthesised have either a C(aryl)-N bond or a C (heteroaryl)- N bond within their chemical structure.⁷¹

There are a number of different reactions used to access C-N bonds. Direct combination of aryl halides with amines requires very harsh conditions with temperatures of 300°C and high pressure. For both aryl and alkyl amination there is the reaction of aldehydes or ketones with ammonia, primary or secondary aryl/alkyl amines in presence of different reducing agents. A third method is the reduction of nitrogen-containing functional groups such as nitro, cyano, azide, and carboxamide derivatives. Other methods include copper-mediated chemistry at high temperature and addition to benzyne intermediates. Whilst the traditional method for alkyl amination is alkylation of ammonia, primary or secondary amines, achieved via S_N2 substitution of alkyl halides and reductive amination.

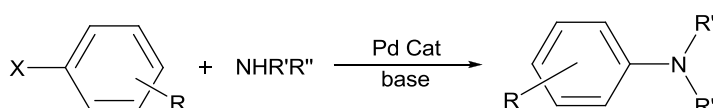


Scheme 1.41: Classic synthetic routes for alkyl/aryl amination

These classical synthetic protocols for amination are atom intensive and inefficient due to the large number of steps and of the generation of waste by-products. With alkylation, the reactions have low selectivity and generate polyalkylation side-products.⁸⁷ Thus there has been a great deal of interest in using catalysts to improve these reactions. As stated above, catalysts suited for industrial use need to have certain

properties such as ease of handling, use with a wide variety of functional groups but regio- and stereo-specific, mild reaction conditions, low catalyst loading and very low metallic residue found in the product (especially in pharmaceuticals). The catalyst system must also scale-up well without intolerable loss of yield.⁸⁸

1.4.1 Buchwald-Hartwig Aryl Amination



Scheme 1.42: General scheme for palladium-catalysed aryl amination

These aryl amination reactions have become commonly known as Buchwald-Hartwig aminations due to the extensive work that has been conducted by Buchwald *et al*^{73, 89, 90} and Hartwig *et al*^{74, 92, 93, 94} into developing the catalysis of this type of reaction.

Initially, tin amides were employed with a palladium catalyst, $\text{PdCl}_2[(\text{P}(o\text{-tolyl})_3)_2]$ with aryl bromides. Hartwig *et al* determined that oxidative addition to $\text{PdCl}_2[(\text{P}(o\text{-tolyl})_3)_2]$ of the aryl bromides was the first step in the mechanism.⁹⁵ The tin amides then reacted with the dimeric oxidative addition product resulting in the reductive elimination of the desired aryl amine.³²

In 1995, both Hartwig's and Buchwald's groups reported palladium catalysed amination of aryl bromides without the use of a tin amide.^{96, 97} Buchwald has investigated the coupling of numerous amines with aryl bromides using the bis-chelating phosphine ligand BINAP (2,2'-bis(diphenylphosphino)-1,1'-binaphthyl) with $\text{Pd}(\text{OAc})_2$ as well as the coupling of aryl triflates with amines using BINAP with $\text{Pd}(\text{dba})_2$. Hartwig concentrated on ferrocene-based phosphine, dppf (1,1-bis(diphenylphosphino)ferrocene) Pd systems after initially using trialkylphosphine $\text{Pd}/\text{P}(o\text{-tolyl})_3$ Pd systems for work on aryl bromides (Figure 22).

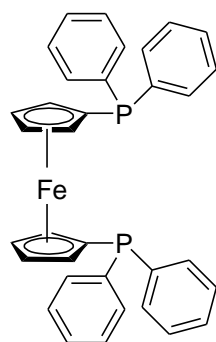
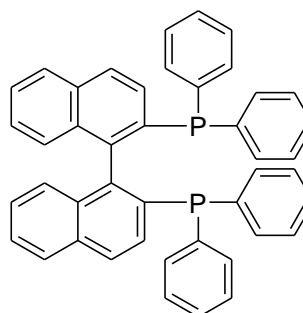
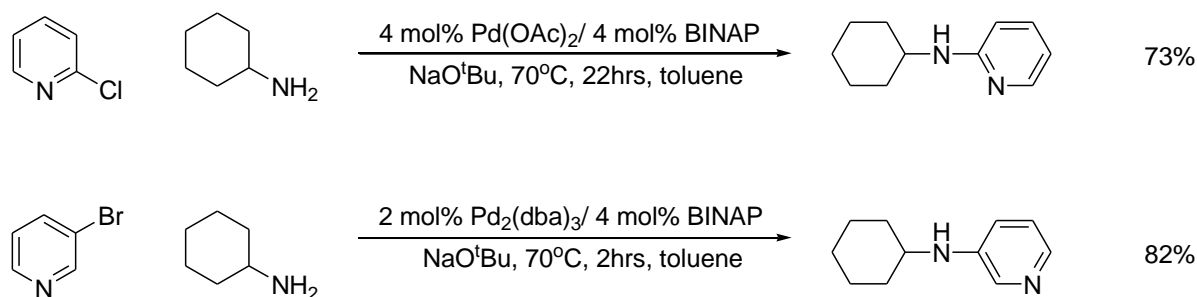
DPPF, **44***rac*-BINAP, **45**

Figure 22: Two of the first ligands used for aryl aminations with Pd catalyst and base.

Aryl chlorides are much more widely available and cheaper than bromides or iodides so they would be the arylating reagent of choice, however the Ar-Cl bond (96 kJ mol^{-1}) is stronger than the Ar-Br bond (81 kJ mol^{-1}) which in turn is stronger than the Ar-I bond (65 kJ mol^{-1}).⁷⁴ The first example of a coupling of a heteroaryl chloride with an amine (cyclohexylamine) was reported in 1996 by Buchwald and Wagaw (Scheme 1.43).⁹⁸ In this instance, the palladium catalyst was generated in situ from $\text{Pd}(\text{OAc})_2$ and *rac*-BINAP.

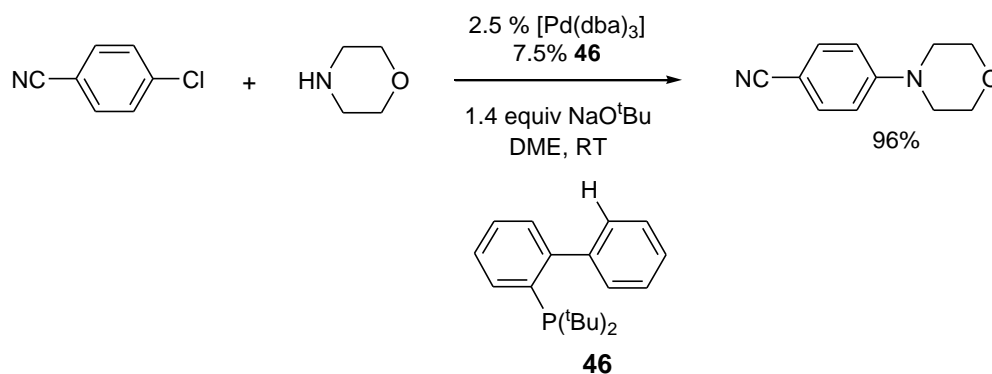


Scheme 1.43: First coupling of heteroaryl chloride with a similar bromide reaction to illustrate the difference in reactivities⁹⁸

Palladium catalysed aminations of chloroquinolines, heteroarylimidoyl chlorides, chloropurines, chlorothiophenes, chlorobenzothiazoles, chlorobenzooxazoles, and other chloropyridines have been achieved using BINAP or DPPF as the ligand.⁷⁴

The amination of unactivated aryl chlorides was first reported by Reddy and Tenka in 1997⁷⁴ using the complex *trans*-PdCl₂(PCy₃)₂ as catalyst. The Pd(II) chloride complex using P^{*i*}Pr₃ as ligand was also found to give good yields of the coupling products, but the BINAP and DPPF complexes gave poor results. The trialkyl phosphine PCy₃ was subsequently found to be excellent for promoting the oxidative addition step but less well adapted for promoting reductive elimination over the β-hydride elimination step. Tosoh Company reported that P(*t*-Bu)₃ was a resilient catalyst for the formation of arylpiperazines at 120°C.

The first room temperature C-N couplings were demonstrated by Buchwald in 1997 using a ligand system of electron-rich monophosphines with the most effective being phosphanyl-substituted biphenyl ligand, **46**, in Scheme 1.44. For some amine/aryl chloride combinations, catalyst loadings as low as 0.05% Pd were reported. The weaker base K₃PO₄ was used when either reactant had a sensitive functional group.⁸⁹



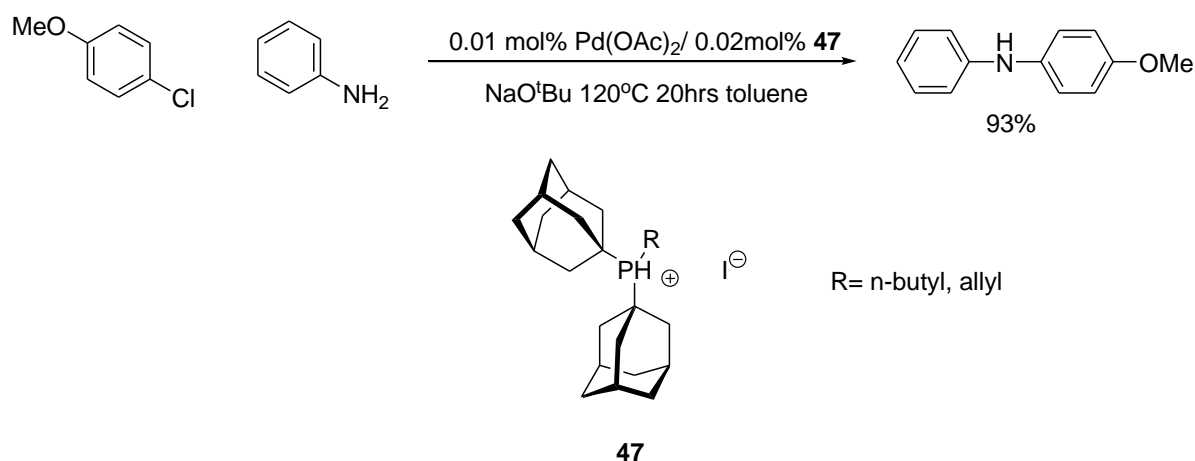
Scheme 1.44: C-N coupling using Pd/ dialkylarylphosphane

N-heterocyclic carbene catalysts for amination were first used by Nolan *et al* in 1999 who generated their catalyst *in-situ* using Pd(II)/IPrH⁺ and achieved good yields, even at room temperature.³² Caddick, Cloke, and co-workers have worked with pre-formed, discrete palladium bis-carbene complexes and found these to be excellent amination catalysts at temperatures above 80°C when using bulky aryl *NHCs* such as SIPr and IPr.⁴⁰

These ligands, bulky electron rich trialkylphosphines, biaryldialkylphosphines, bidentate diphosphines, and *NHCs*, along with a few variations⁹⁹, have been expanded upon since and many second and third and even fourth generation ligands have been

found. These can be active at room temperature or with a softer base or lower catalyst loadings with higher TON or with unactivated aryl chlorides.

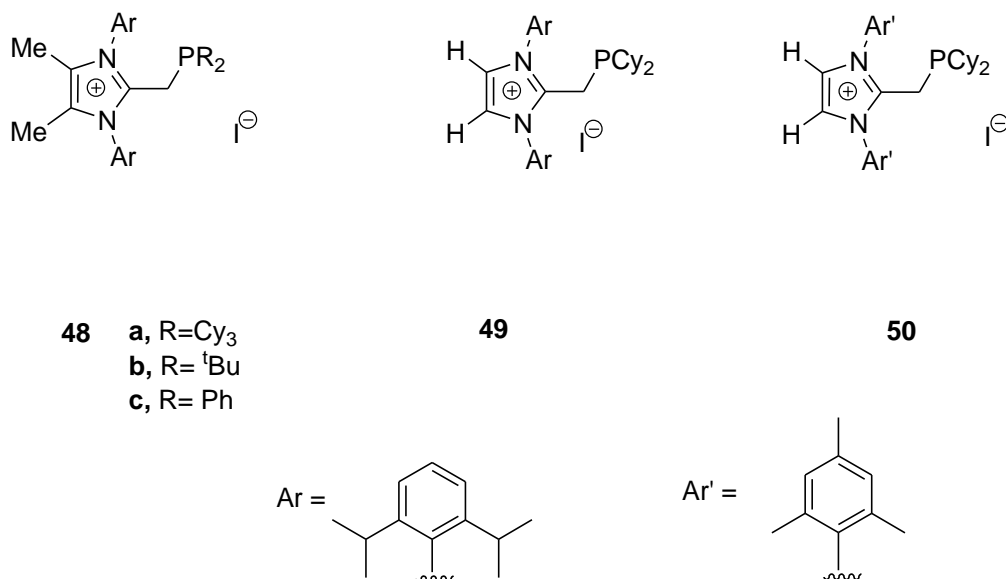
Beller's group developed trialkyl phosphines with sterically demanding 1-adamantyl (known as cata-CXium A ligands), both forming catalysts for amination reactions of aryl chlorides. They also developed the use of the phosphonium salts of these ligands **47** as more stable precursors for in situ ligand and catalyst formation⁸⁸ and have high TONs of 8900-9400 at catalyst loadings of 0.01 mol % (Scheme 1.45).



Scheme 1.45: Aryl amination reaction using cat-CXium A phosphonium ions as catalyst

Recently, Dumrath *et al* developed novel cationic imidazolium-based phosphane ligands and showed their potential as a long-lived catalyst in a batch process. The aryl amine coupling product was precipitated out using HCl to form the salt and the catalyst stayed in solution with the yields staying at between 89-99% of the original for three consecutive runs.¹⁰⁰

Work has so far shown very good yields for diarenes with 1 mol% $\text{Pd}(\text{OAc})_2$ /**48a** (Figure 23) at 120°C for 20 hrs in dioxane with NaO^tBu as base.

Figure 23: Imidazolium-based phosphine ligands¹⁰¹

Buchwald's group continued to investigate the biphenyl monophosphines based on XPhos (**51**). Some recent variations are BrettPhos (**52**) and RuPhos (**53**) shown in Figure 24.

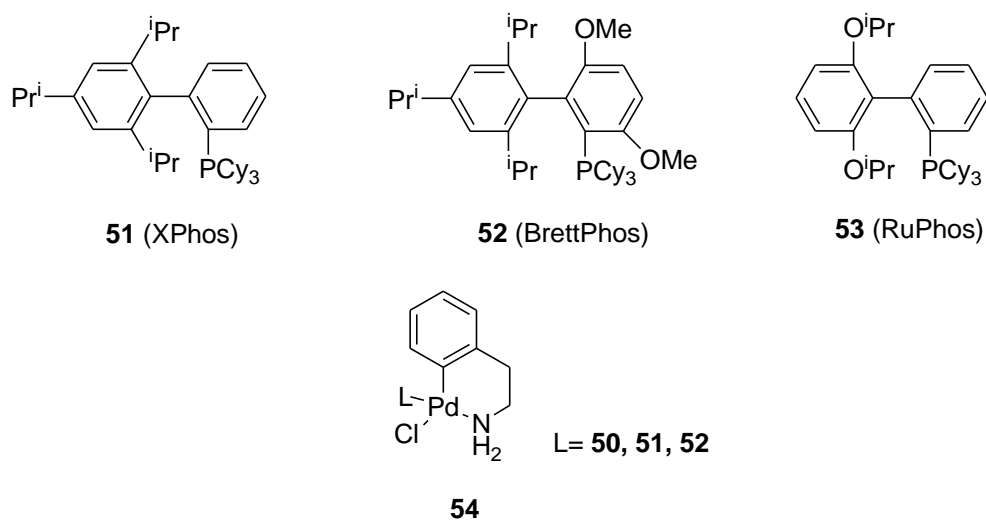
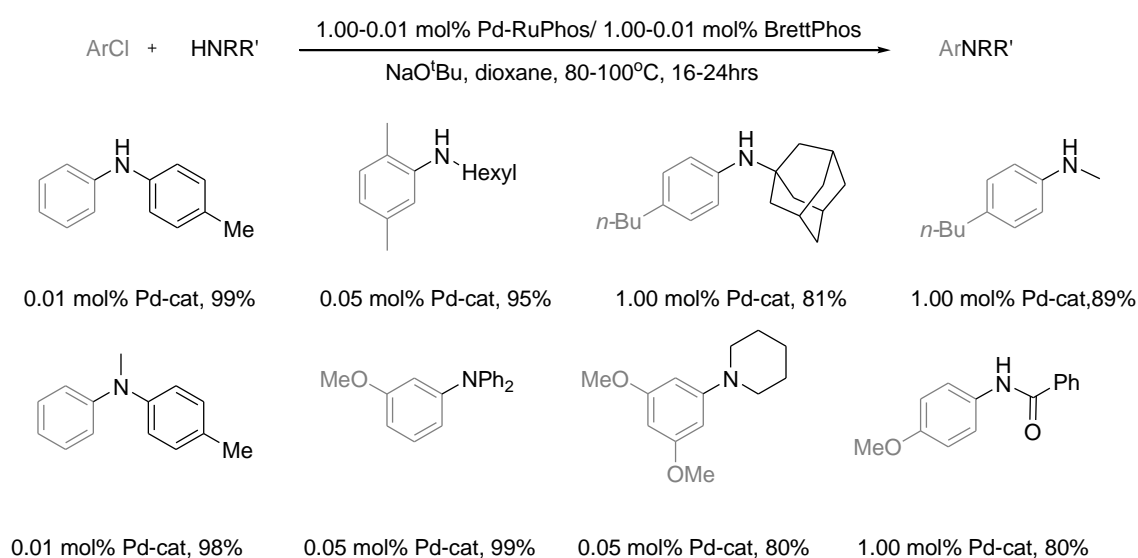


Figure 24: Examples of Buchwald's ligands and the pre-formed palladium catalyst they are used in, **54**.

This has culminated in a multi-ligand system of the latter two, where BrettPhos's poor ability to couple with secondary amines and RuPhos's poor ability with primary amines meant they were complimentary to each other within the catalyst system.¹⁰¹

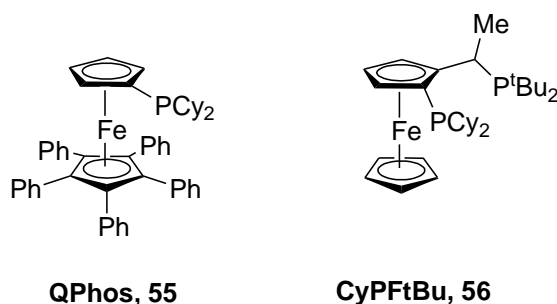
The preformed catalyst **54** with ligand RuPhos as L and free BrettPhos in the reaction mixture gives an almost identical result as the vice versus situation (Scheme 1.46).

These ligands work well with weak nitrogen nucleophiles such as amides and electron-poor arylamines. The use of Cs₂CO₃ as base in 2-methyl propan-2-ol meant that the catalyst system could be used with substrates containing sensitive functional groups like nitro groups, esters, thiofurans and pyridines.¹⁰¹

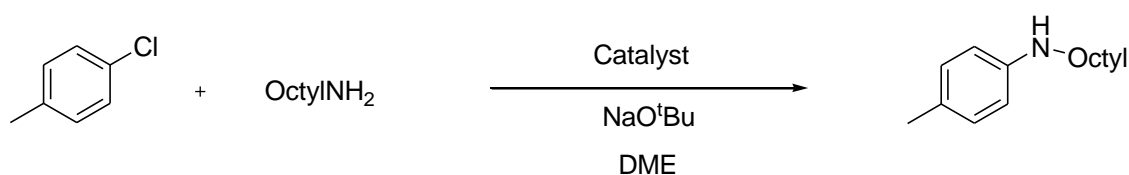


Scheme 1.46: The multiligand system exemplified by Buchwald and co-workers to increase catalyst scope to both primary and secondary amines

The development of Josiphos ligands in palladium arylation catalysis has been continued by Hartwig and co-workers. The Q-phos ligand (**55**, Figure 25) produced catalysts which were good for secondary amines with haloarenes but less so for primary amines.¹⁰² The use of the bisphosphine Josiphos ligand meant that the ligand was bis-chelating which was considered important to help stabilise these catalysts towards dissociation of one ancillary ligand and thus help amine coordination.¹⁰² The current ligand used by this group is CyPF^tBu (**56**, Figure 25).

Figure 25: Josiphos ligand, Q-Phos and CyPF^tBu,

In situ formation of the catalyst with Pd(OAc)₂ gives excellent yields but the catalyst loading is less when the preformed complex *cis*-[(CyPF^tBu)PdCl₂] is used¹⁰², in some instances as low as 50 ppm. Scheme 1.41 shows a comparison of the two systems for a comparable reaction and conditions. This highlights the fact that 10 times as much palladium salt is needed when the catalyst is generated *in situ* than when the preformed catalyst is used shown in the table in Scheme 1.47. Functional group tolerance is in this instance increased by using LHMDS (lithium hexamethyldisilane) as base.



Catalyst	Pd(OAc) ₂ / CyFP ^t Bu	[(CyFP ^t Bu)PdCl ₂]
Loading/ mol %	0.01	0.001
Temperature	100°C	110°C
Reaction time	48hrs	36hrs
Yield	100% conversion	98% conversion

Scheme 1.47: Coupling of chlorotoluene and the primary amine, octylamine, using a preformed Josiphos Pd catalyst or one formed *in situ*

Other phosphines that have been used are *N*-phenylpyrrole/indole-substituted (cata-CXium P, **57**, Figure 26) and the more sterically demanding imidazole-based phosphines (**58**, Figure 26).¹⁰³

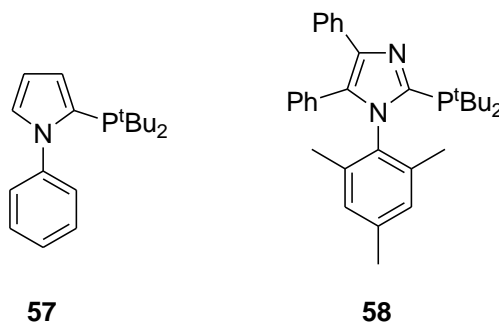


Figure 26: Examples of other phosphines used in Pd aryl amination

In situ generation of the catalysts using a Pd source and imidazolium salts or free *NHC* is highly effective in aryl amination, particularly with a ratio of Pd source to *NHC* of 1:1. Never the less, many air and moisture stable *NHC* Pd(II) preformed catalysts have been developed. Much like for the Suzuki-Miyaura reaction, the emphasis has been on the more bulky, but flexible, aryl *NHC*s used in mono-ligated *NHC* with ancillary ligand complexes or bis-chelated *NHC* complexes. In fact, many of the same complexes used in Suzuki-Miyaura coupling are good amination catalyst, too e.g. **34-43** (Scheme 1.29-1.34). Nolan has developed the allyl-*NHC* Pd complexes, $[\text{Pd}(\eta^3\text{-C}_3\text{H}_5)((\text{NHC})\text{Cl})]$, with SIPr, **38**. Recently, this allyl-IPr Pd complex was used to in the synthesis of polytriarylamines using anilines and dibromobiphenyl where lower catalyst loading was required than for $\text{P}(\text{tBu})_3$.¹⁰⁴ Substituting at one of the terminus positions means that the allyl species is more readily lost from the complex thus reducing the catalyst's induction time³². The complex $[\text{Pd}(\text{IPr}^*)(\text{acac})\text{Cl}]$ ($\text{IPr}^* = \text{N,N}'\text{-bis}(2,6\text{-bis}(\text{diphenylmethyl})\text{-4-methylphenyl})\text{-imidazol-2-ylidene}$, **62**) gave good conversions at room temperature for unactivated aryl chlorides with 72% conversion after 24hrs in 1,4-dioxane with 4-chloroanisole and morpholine.¹⁰⁵ Other auxiliary ligands used in mono-*NHC* Pd(II) precatalyst include triethyl amine $[\text{Pd}(\text{NHC})(\text{Et}_3\text{N})\text{Cl}_2]$, **60**, and imidazoles $[\text{Pd}(\text{NHC})(\text{Im})\text{Cl}_2]$, **61** in Figure 27 as well as palladacycles with N,C biaryl species, $[\text{Pd}(\text{NHC})\text{-(dmba)Cl}]$, **59** and **40**.¹⁰⁵

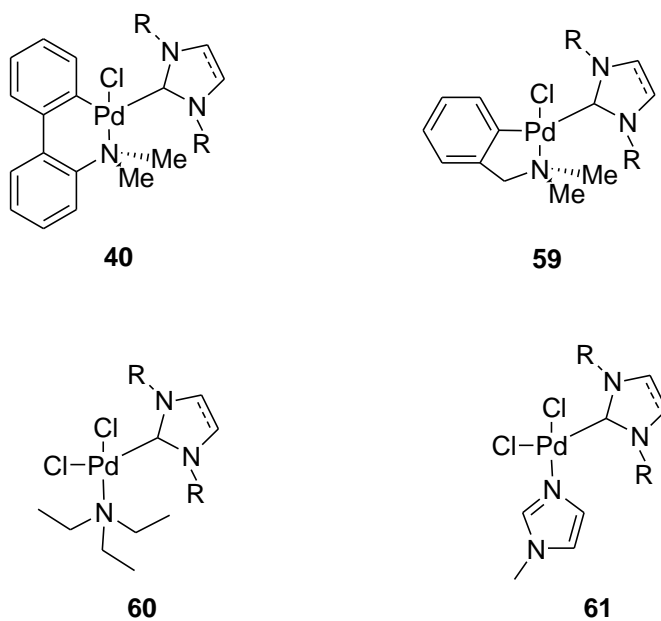


Figure 27: Examples of palladacycles and mono-*NHC*-ligated complexes used in aryl amination

IPr* has also been used in the PEPPSI type complex, *trans*-[Pd(IPr*)(3-Cl-pyridinyl)Cl₂], to excellent effect.¹⁰⁴

Cheng and Trudell used a similar system with the carbene DiPr, **63** (Figure 28). In this system, aryl chlorides react preferentially to aryl bromides and iodides.

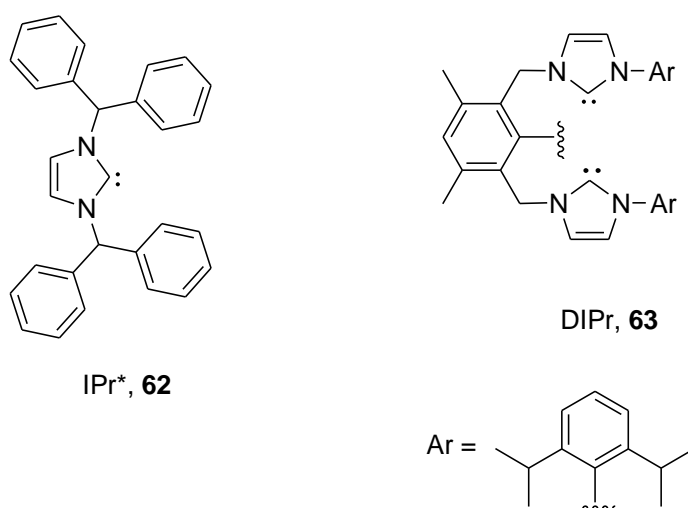


Figure 28: Very bulky *NHC*s used in amination

Oxidative addition complexes and, latterly the Pd-amido/transmetallation complexes, found in the mechanistic studies are often found to be good catalysts in aryl amination. These complexes will be discussed further in the next section and the chapters within this work.

1.4.2 Mechanism of Buchwald-Hartwig aryl amination

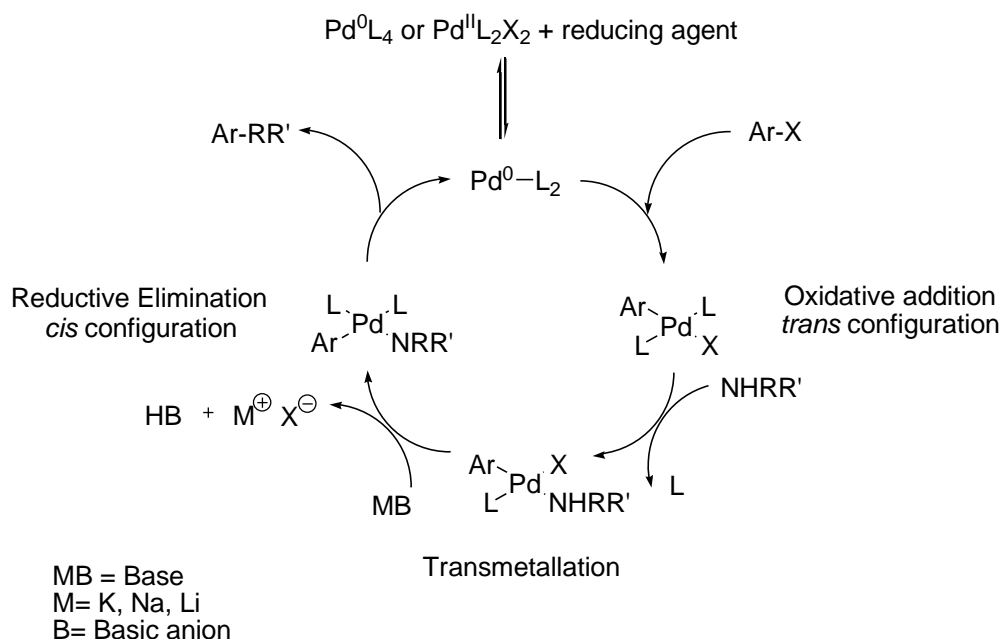


Figure 29: Classic catalytic cycle for Pd cross-coupling¹⁰⁶

Numerous mechanistic studies into aryl amination have been conducted over the years. Studies by Amatore *et al* in the early 1990s on the oxidative addition of aryl halides to palladium phosphine complexes showed that the active catalytic species for zero valent $\text{Pd}(\text{PPh}_3)_4$ was low-ligated zero valent $\text{Pd}(\text{PPh}_3)_2$, which is solvent-ligated in its resting state. In the early 1990s, Amatore and co-workers undertook electrochemical and $^{31}\text{P}\{^1\text{H}\}$ -NMR studies on *rac*- $\text{Pd}^{\text{II}}\text{Cl}_2(\text{PPh}_3)_2$. They postulated an anionic catalytic cycle where the $\text{Pd}^0(\text{PPh}_3)_2$ was not the active species but $[\text{Pd}^0(\text{PPh}_3)\text{X}]^-$ and the aryl halide adds to form a pentacoordinated Pd(II) anion with two halide dative ligands, $[\text{Pd}(\text{PPh}_3)_2(\text{Ar})\text{Cl}_2]^-$. The halide ligands rapidly interchange with the solvent and loss of one solvent ligand from $[\text{Pd}(\text{PPh}_3)_2(\text{Ar})\text{Cl}(\text{solvent})]^-$ can generate the *trans*-

$[\text{Pd}(\text{PPh}_3)_2(\text{Ar})\text{Cl}]$ oxidative addition species, which is more thermodynamically stable than the *cis* isomer. If a halide is replaced by a nucleophile reactant instead, $[\text{Pd}(\text{PPh}_3)_2(\text{Ar})\text{Cl}(\text{Nu})]^-$ can be generated which upon loss of one PPh_3 can form either the *cis* or *trans* isomer which are in equilibrium. The *cis* isomer will eliminate the coupling product, and the *cis/trans* equilibrium will shift further to the *cis* isomer.¹⁰⁴ This mechanism was thought to run concurrent with the classic cycle becoming the faster pathway when there was excess halide salt in solution. The role of the cation is to stabilise the anionic species. In the absence of cations, protons are formed in the solvent which means that when base is added the reaction rate will be slowed by the reaction with these protons. This mechanism is not thought to be very active in aryl amination but may be of more significance in Heck reactions using $\text{Pd}(\text{OAc})_2$ and phosphines for in situ catalyst generation.¹⁰⁶

Kinetic studies using ^1H and ^{31}P $\{^1\text{H}\}$ NMR were undertaken by Hartwig and co-workers to propose the neutral catalytic cycle in Figure 30. Ligand dissociation occurs first, then the oxidative addition step before generation of a chloride bridged dimer, $[\text{Pd}(\mu\text{-Cl})(\text{P}(\text{o-tolyl})_3)(\text{Ar})]_2$ which was shown to be a resting state for the oxidative addition species.¹⁰⁷

Another study by Hartwig *et al* using $\text{Pd}(\text{P}^t\text{Bu}_3)_2$ found the aryl amination reaction rate to be first order with respect to the aryl chloride (chlorotoluene), zero order with respect to the amine (*N*-methylbenzylamine), and inverse first order with respect to added excess ligand (P^tBu_3) and zero order with respect to base ($\text{NaOC}(\text{Et})_3$). These results mean that oxidative addition is the rate-limiting step and irreversible. The retardation caused by added ligand means disruption of the equilibrium between $\text{PdL} + \text{L} = \text{PdL}_2$. Excess ligand means more $\text{Pd}(\text{P}^t\text{Bu}_3)_2$ and less $\text{Pd}(\text{P}^t\text{Bu}_3)$ in solution and as this is slowing the rate it means the oxidative addition is to the 12 electron PdL species i.e. dissociative mechanism for oxidative addition. Interestingly, when a relatively unhindered base such as NaO^tBu or a softer base (2,4,6-*trtert*-butylphenoxide) was used, the reaction was first order with respect to the base. It was hypothesised that an anionic reaction mechanism ran concurrent to the dissociative mechanism as illustrated in Figure 29.¹⁰⁸ The mechanism adopted by a system would depend on the base used as well as the ligand with bases that have a higher binding ability to $\text{Pd}(\text{P}^t\text{Bu}_3)_2$, such as unhindered and softer bases, promoting the anionic pathway.

Studies were done with the bis-ligated palladium complexes of bidentate phosphines such BINAP (2,2'-bis(diphenylphosphino)-1,1'-binaphthyl) and dppf (1,1'-bis(diphenylphosphanyl) ferrocene), $\text{Pd}(\text{BINAP})_2$ and $\text{Pd}(\text{dppf})_2$. It was determined that generation of a 14 electron $\text{Pd}(\text{L})$ species from the dissociation of one bidentate ligand was rate-limiting for reactions involving aryl tosylates, ArBr and for ArI when present concentrations levels considered appropriate for most reaction. Reactions undertaken with ArI at higher concentrations revealed that the mechanism requires only one coordination site to be vacated so only dissociation of one of the chelating arms of the one of the bidentate ligands is required. This results in a 16 electron Pd species, $[\text{Pd}(\text{L}-\text{L})(\text{L}-\text{L})]$ to which ArI can coordinate. That the iodide is able to coordinate to this low valence metal centre is a result of its electron donating abilities being superior to other halides and tosylate.¹⁰⁹

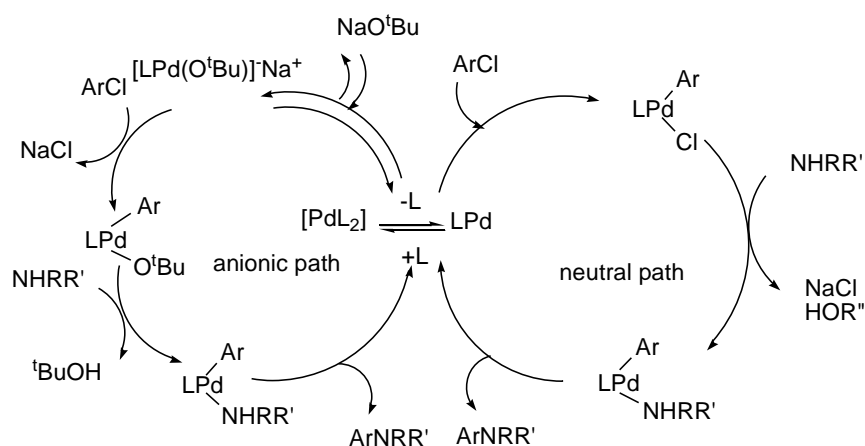


Figure 30: Proposed concurrent neutral and an anionic mechanism for aryl-amination catalysed by $\text{Pd}[\text{P}(\text{tBu})_3]_2$

In 2002, a study by Blackmond *et al* on a $\text{Pd}_2(\text{dba})_3/\text{BINAP}$ system gave results which were not in agreement with either of these mechanisms. The kinetic data showed that the reaction was 1st order with respect to the amine and aryl chloride and zero order with respect to the base. The mechanism suggested by their data was one in which the amine coordinated to the monoligated Pd first, followed by oxidative addition to this $\text{Pd}(\text{NR}_2)(\text{BINAP})$ species. This mechanism has little corroborating evidence from further studies and the results may well be the result of slow in situ formation of the active catalyst. A subsequent study in 2006 by Blackmond, Buchwald, Hartwig and co-

workers using the same system did in fact disprove this mechanism. A new mechanism was proposed where the initial dissociation of the ligand from $\text{Pd}(\text{BINAP})_2$ is placed outside of the cycle and oxidative addition then occurs at the $\text{Pd}(\text{BINAP})$ species.

In 2005, Barrios-Landeros and Hartwig conducted a detailed study of the oxidative addition step of the catalytic cycle with aryl iodides, bromides and chlorides using bidentate (Q-phos, **55** in Figure 25) in $\text{Pd}(\text{Q-phos})_2$ as catalyst. Their findings are shown in Figure 31.

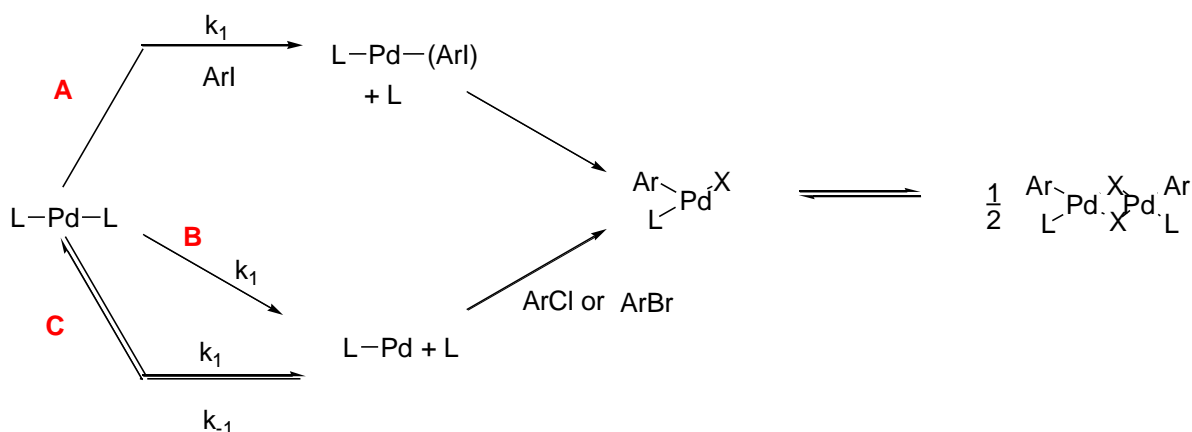


Figure 31: The different pathways taken by ArI , ArBr and ArCl for oxidative addition

The conclusions were that for the aryl iodide, oxidative addition occurs *via* a fast associative mechanism to the PdL_2 species. The aryl bromide addition proceeds *via* a dissociative mechanism in which the rate-determining step is the ligand dissociation from PdL_2 . Aryl chloride also occurs *via* dissociative mechanism, however the rate-determining step is oxidative addition of aryl chloride to the PdL species.

Work by Lewis, Caddick, Cloke and co-workers into Pd/NHC systems have also found evidence to support this mechanism. Using the zero valent, bis carbene complex $\text{Pd}(\text{I}^t\text{Bu})_2$ (**64**), ^1H NMR kinetic studies were undertaken into the oxidative addition step of the aryl chloride to the $\text{Pd}(\text{I}^t\text{Bu})_2$. The results show that the rate is retarded by the addition of excess I^tBu , confirming a dissociative mechanism. However, the dissociation of I^tBu from $\text{Pd}(\text{I}^t\text{Bu})_2$ was found to be rate-limiting, not the oxidative addition of the aryl chloride to the 12 electron $\text{Pd}(\text{I}^t\text{Bu})$ species. The I^tBu ligand in solution then coordinates to the $\text{Pd}(\text{I}^t\text{Bu})\text{ArCl}$ three-coordinate species to form the stable resting state complex $\text{Pd}(\text{I}^t\text{Bu})_2\text{ArCl}$. A subsequent study showed that the oxidative

addition step was the rate-determining step for the whole catalytic cycle. The study also showed that electron withdrawing groups on the aryl chloride increase the rate of reaction over electron donating substituents such that $\text{COOMe} > \text{CH}_3 > \text{OMe}$. This can be seen by the resonance structures in Figure 32.¹¹⁰

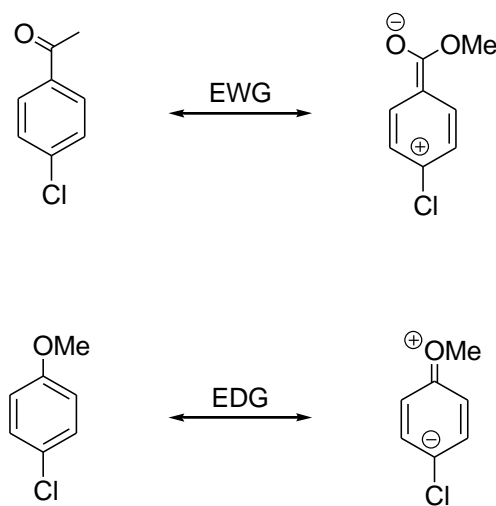


Figure 32: Resonance structures of EWG and EDG aryl chlorides.

Decomposition of the oxidative addition products of aryl iodides where the aryl imidazolium salt and Pd black form was observed by McGuinness *et al.*¹¹¹ This reductive elimination from $\text{Pd}(\text{NHC})_2(\text{Ar})\text{X}$ competes with amine coordination. For a *NHC*-Pd catalyst to be useful, the rate of reductive elimination must be considerably slower than amine coordination. Solvent effects contribute to the rate of this reductive elimination, with solvents stabilizing the formation of polar transition species promoting the reductive elimination. Therefore polar solvents such as DCM increase the rate over non-polar solvents such as benzene.¹¹² It is also thought that iodide complexes are more susceptible to this reaction over chloride complexes, most likely due to the increased electron density imparted by the iodine weakens the Pd-NHC bond. This decomposition step is similar to how phosphine complexes decompose by loss of the aryl group to one of the phosphine ligands to form $[\text{ArPR}_3]^+ \text{X}^-$ but then reacts further with the Pd species. There will be further discussion on these steps in Chapter 3.

Based on the work described above, the general consensus is that oxidative addition occurs first and is generally rate-limiting. The next stage in the catalytic cycle is the

dative coordination of the amine to form the transmetallation complex, $\text{Pd(L)(Ar)(NHR}^{\prime})$, where the primary or secondary amines have yet to lose the acidic proton on the nitrogen.

Formation of Pd amido complexes has previously been achieved by reaction of a Pd complex with amide salt. However, isolation of neutral transmetallation complexes proved more difficult and has only recently been reported where two groups isolated complexes of this type; Buchwald and Biscoe¹¹³, using the SPhos ligand, and Caddick and Cloke¹¹⁴, using the $\text{I}^t\text{Bu NHC}$. Direct addition of amine to oxidative addition product, $\text{Pd(I}^t\text{Bu)}_2\text{ArCl}$ leads to coupling products as the free I^tBu which dissociates from the complex is a good enough base to deprotonate the amine once it had coordinated to the complex. Formation of a dimeric oxidative addition species would eliminate free I^tBu , this is undertaken by taking advantage of the reductive elimination of aryl imidazolium salts in protic solvents (*vide infra*). The second I^tBu was removed harmlessly by precipitation as $\text{I}^t\text{BuH}^+\text{Cl}^-$ generated when the complex was heated gently in CHCl_3 . The dimer then coordinates the amine but there is no base available to deprotonate it so the aryl amine complex can be isolated. These complexes were isolated as the *cis*-isomers and shown to be a species in the catalytic cycle by addition of base and subsequent generation of aryl amine coupling product.¹¹⁴

Buchwald and Biscoe evaluated amine binding constants and acidity of the amines' C-H bond to gain insight into how these affect the C-N coupling. By putting a series of different amines with aniline by into reaction with the $[\text{Pd(SPhos)(Ph)(}\mu\text{-Cl)}]_2$ dimer and then evaluating amount of the C-N product each amine produced as a ratio to aniline coupling product, they were able to evaluate the selectivity of the catalyst. It was found that, for isosteric aliphatic amines, the acidity of the amine was the determined which coupling product formed. So a more acidic amine, which will have a lower binding constant, will form coupling product in preference to a less acidic amine, with a better binding ability (Curtin-Hammett control).¹¹³ For aromatic amines, this trend was reversed and binding ability is the stronger influence on C-N product formation than the subsequent enhancement of acidic proton by coordination to the $[\text{Pd(SPhos)(Ph)(}\mu\text{-Cl)}]_2$ dimer. The overall trend is that alkyl amines are faster than aryl amine, and in general the more basic the nitrogen the faster the reductive elimination of the coupling product. The explanation for this appears to be that either more basic nitrogen will more readily

form a bond with the ipso carbon or that a more basic amine will have a less polar bond with the palladium metal centre which decreases the Pd-N bond strength.¹⁰²

Once the nitrogen's acid proton is lost, an amide complex is formed. These have been generated by indirect methods using alkali metal amides since the 1980s, long before the monoligated amine complexes were isolated. Both monomeric and dimeric amido complexes have been isolated. Kinetic studies on the rate of reductive elimination of C-N coupling product by Driver and Hartwig¹¹⁵ showed that from the monomeric species *trans*-[Pd(L)₂(Ar)(NHR)], two different mechanisms can occur. At low concentration of ligand, the reaction proceeds through a 14-electron three-coordinate species, [Pd(L)(Ar)(NHR)], where one of the ligands has dissociated (pathway A₁ + A₂, Figure 33). This is corroborated by the fact that reductive elimination is known to be facilitated by bulky ligand substituents.¹⁰³ At high ligand concentration, the reaction pathway involves *trans-cis* isomerization and then elimination from the bis-ligated four-coordinate species, *cis*-[Pd(L)₂(Ar)(NHR)] (Pathway B₁ + B₂ in Figure 33). This would be the pathway of a bidentate complex such as DPPF would follow, as these complexes overwhelmingly favour formation of *cis* complexes.⁹ The dimer was found to fully dissociate into the [Pd(L)(Ar)(NHR)] species following pathway A₃ + A₂.

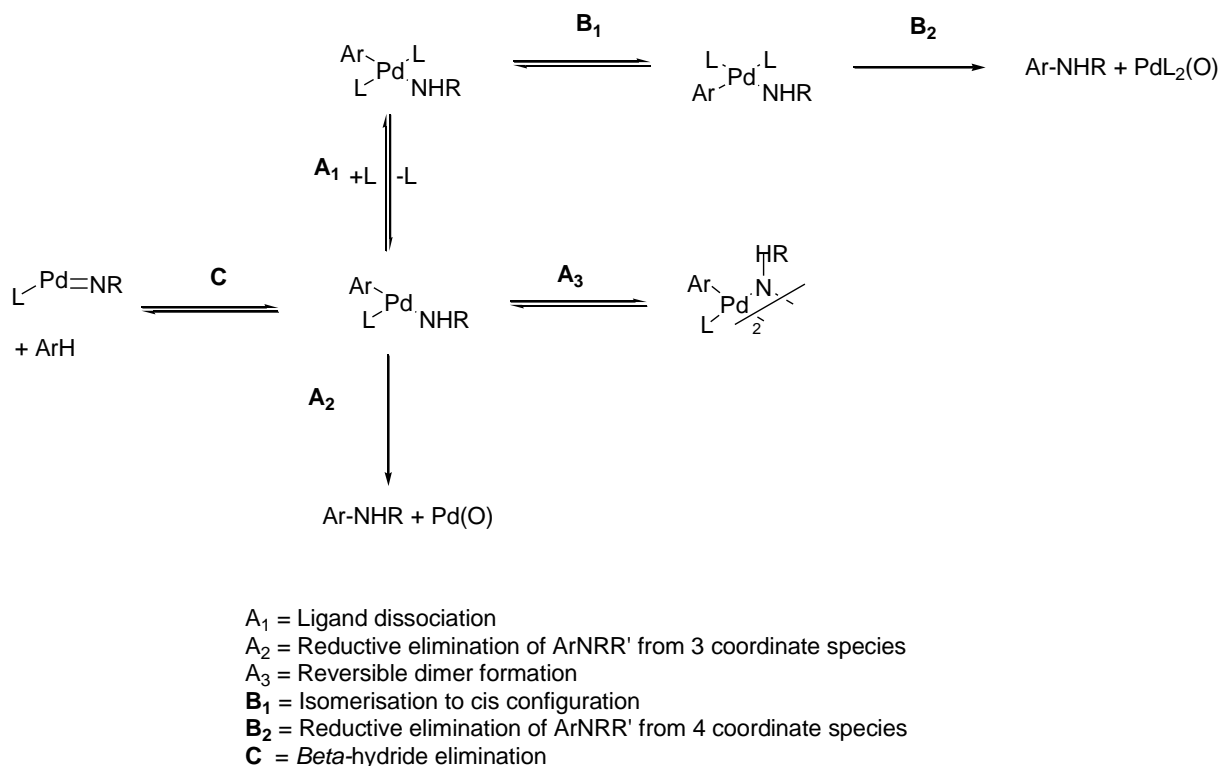


Figure 33: Reductive elimination pathways for aryl amination.

Pathway A+C is the competing β -hydride elimination of arene. Surprisingly, for aryl amination, this pathway is much slower than the reductive elimination pathway but suppression of this pathway is enhanced by more electron-withdrawing groups on the aryl chloride, more electron-donating groups on the amine and bulky groups on the ligand.¹¹⁶

The conclusions drawn are summarized in Figure 34, a modified catalytic cycle and in Figure 34, a summary of the influences of the reactants and substrates on the rate of reaction.

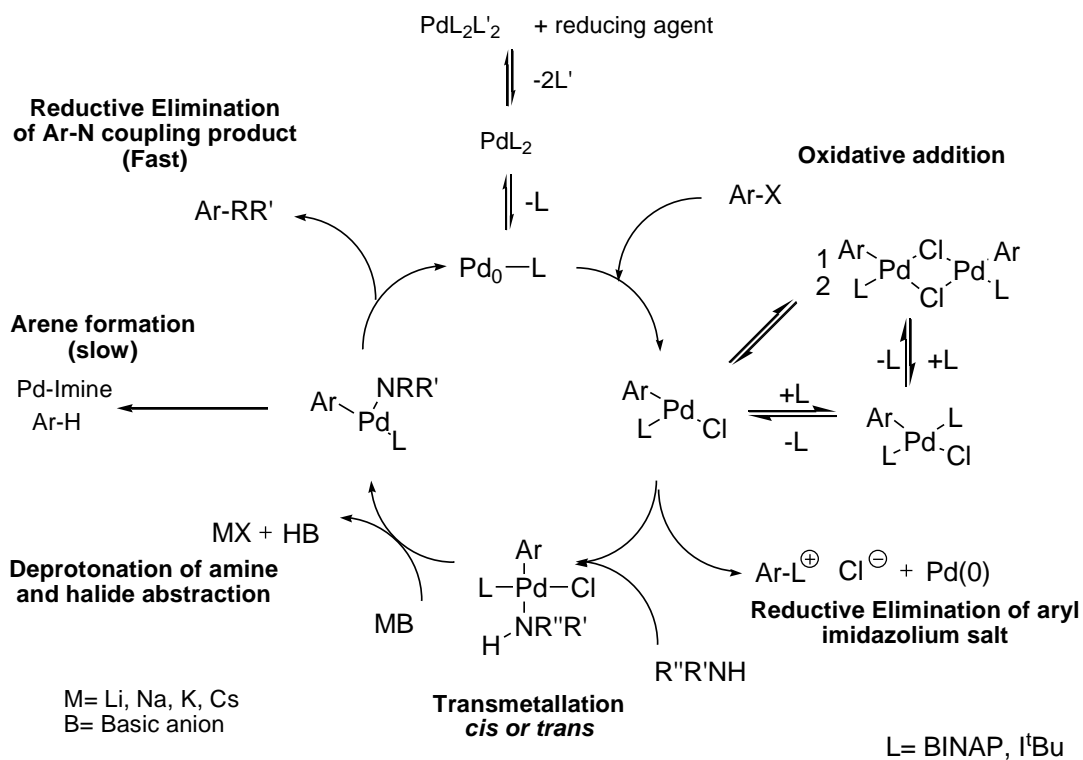
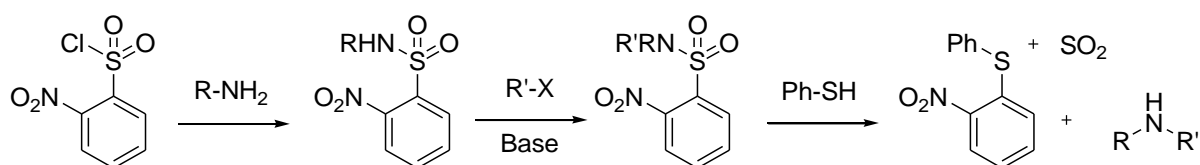


Figure 34: General amination catalytic cycle applicable to $\text{Pd}(\text{BINAP})_2$ and $\text{Pd}(\text{I}^t\text{Bu})_2$ with aryl chlorides.¹¹⁷

1.4.3 Palladium-based alkyl amination catalysis

Alkyl amination is traditionally achieved via S_N2 reaction with alkyl halides or *via* reductive amination.¹¹⁸ Reductive protocols with aldehydes and ketones suffer from the problem of over-alkylation and other syntheses depend on multi-step protection and de-protection (Scheme 1.48).¹¹⁸

There have been recent studies into Iridium-catalysed alkylation of amines using alcohols as the sythons rather than alkyl halides (*vide infra*, Scheme 1.16, page 28).³²



Scheme 1.48: Deprotection of nosyl amides

Figure 35 has been proposed as the catalytic cycle for palladium-based alkyl amination. It is based on theoretical viability studies of palladium-based alkyl amination by Green *et al.*¹¹⁹ The study was calculated with $t\text{Bu}$ as ligand and chloromethane as the alkyl chloride. The transition state to oxidative addition of alkyl chloride was calculated to be higher in energy than oxidative addition of aryl chloride (45.9 KJmol^{-1} *versus* 30 KJmol^{-1}). This was thought due to poor solvation of alkyl complexes compared with aryl complexes.

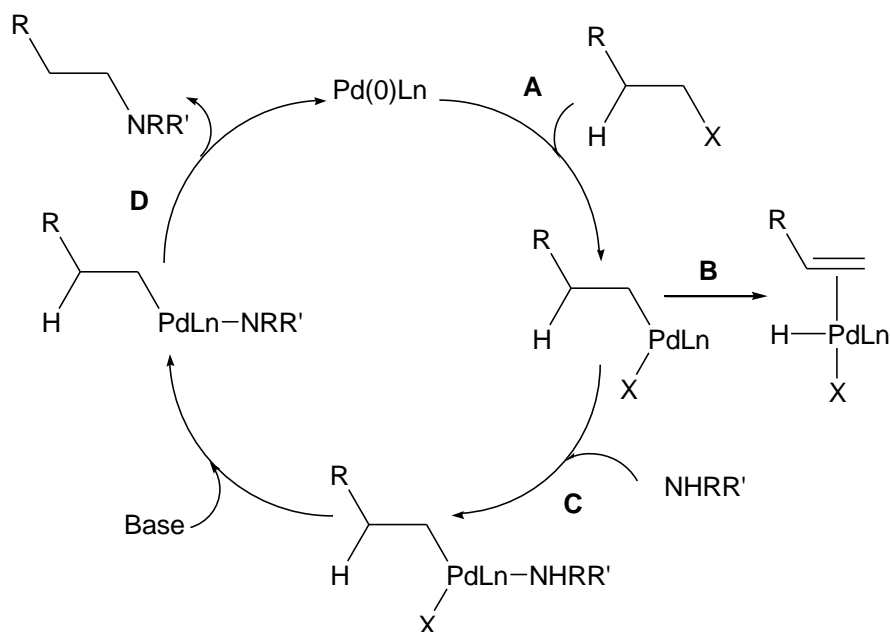


Figure 35: Proposed catalytic cycle for alkyl amination¹¹⁹

Fu *et al*¹²⁰ reported the formation of palladium catalyst alkyl oxidative addition product in their work into the Suzuki cross couplings with alkyl bromides. They found that unactivated alkyl halides were reluctant to oxidative add to the $\text{Pd}(0)\text{L}_2$ (L = trialkylphosphine). They did however manage to observe $\text{Pd}(\text{P}(\text{t-Bu})_2\text{Me})_2(\text{CH}_3\text{CH}_2\text{CH}_2)\text{Br}$ at 0°C , which they attributed to the extreme reactivity of $\text{Pd}(\text{P}(\text{t-Bu})_2\text{Me})_2$. β -hydride elimination was not significant and this was attributed to the mild conditions (0°C , diethyl ether).

β -hydride elimination can be avoided by use of an alkyl halide devoid of β -hydrogen such as methyl or neopentyl halides. Experimental work carried by Esposito *et al*¹²¹ in the amination of alkyl halides without β -hydrogens, including chloromethane, has found that direct alkyl oxidative addition to a monoligated $\text{Pd}(\text{I}^t\text{Bu})$ species does not occur for alkyl chlorides and indirect methods must be used to generate their alkyl *NHC*-Pd oxidative addition products. Interestingly, there was no appreciable generation of the alkylimidazolium salt reductive elimination which has been an issue for Cavell and McGuiness in their work with cationic alkyl *NHC* palladium (II) species. They did find, however, that for the neutral species, $[\text{Pd}(\text{ITMe})_2(\text{Me})(\text{I})]$, this decomposition did not occur until 120°C .¹²² This experimental work is the foundation of alkyl amination studies reported in Chapter 2 where this will be discussed further.

Recently, Buchwald's group achieved CH_2 alkyl amination by the means of an intramolecular C-H activation followed by C-N bond formation, instead of C-halide activation.¹²³

Very recently, Hartwig's group did achieve an alkyl amination product using *NHCs*. The alkyl species was the bridged norbornyl species and the *NHC* was IPr. The elimination occurred from a tri-coordinate amido complex, prepared from the corresponding chloride complex and potassium amide. Simple warming to 90°C generated the C-N coupling product. The authors ascribed this to the bulky nature of IPr.¹²⁴ More discussion will be had on this in Chapter 2.

1.5 References

- ¹ Hahn, F. E.; Jahnke, M. C.; *Angew. Chem. Int. Ed.*, **2008**, 47, 3122.
- ² Russo, N., Sicilia, E., Toscano, M., *J. Chem. Phys.*, **1992**, 97, 5031.
- ³ Kirmse, W., '*Carbene Chemistry*', Academic Press, London, **1964**, and references therein.
- ⁴ Bourissou, D., Guerret, O., Gabbaï, F.P., Bertrand, G., *Chem. Rev.*, **2000**, 100, 39.
- ⁵ Irikura, K. I.; Goddard, W. A., III; Beauchamp, J. L. *J. Am. Chem. Soc.* **1992**, 114, 48.
- ⁶ Hoffmann, R.; Zeiss, G. D.; Van Dine, G. W.; *J. Am. Chem. Soc.*, **1968**, 90, 1485.
- ⁷ Baird, N., C.; Taylor, K. F.; *J. Am. Chem. Soc.* **1978**, 100, 1333.
- ⁸ Guy Bertrand, Taylor & Francis. Kindle Edition. **2002**, and references therein
- ⁹ Crabtree, R., H., Wiley, Hoboken, New Jersey, **2009**, and references therein.
- ¹⁰ Fischer, E. O.; Maasbol, A.; *Angew. Chem. Int. Ed.*, **1964**, 3, 580.
- ¹¹ Elschenbroich, C., Salzer, A., VCH, New York, **1992**, and references therein.
- ¹² a) Schrock, R. R.; *J. Am. Chem. Soc.*, **1974**, 96, 6796; b) Schrock, R. R., Fellmann, J. D., *J. Am. Chem. Soc.*, **1978**, 100, 3359.
- ¹³ a) Öfele, K., *Angew. Chem. Int. Ed. Engl.*, **1968**, 7, 950; b) Öfele, K. *J. Organomet Chem.*, **1968**, 12, 42.
- ¹⁴ a) Badley, E. M., J. Chatt, R. L. Richards, and G. A. Sim., **1969**, *J. Chem. Soc. D* 22 1322. b) Herrmann, W. A., *Angew. Chem. Int. Ed. Engl.*, **1974**, 13, 599. c) Clark, G. R., Hoskins, S.V., Jones, T.C., Roper, W. R., *J. Chem. Soc., Chem. Commun.*, **1983**, 719.
- ¹⁵ Lappert, M. F., Pye, P. L., **1977**, *J. Chem. Soc., Dalton Trans.*, 2172.
- ¹⁶ Wanzlick, H. W.; *Angew. Chem. Int. Ed.*, **1962**, 1, 75.
- ¹⁷ Kirmse, W., *Angew. Chem. Int. Ed.*, **2010**, 49, 8798.
- ¹⁸ R. W. Alder, M. E. Blake, L. Chaker, J. N. Harvey, F. Paolini, J. Schutz, *Angew. Chem. Int. Ed.*, **2004**, 43, 5896.
- ¹⁹ Holloczki, O., Terleczky, P., Szieberth, D., Mourgas, G., Gudat, D., Nyulaszi, L., *J. Am. Chem. Soc.*, **2011**, 133, 780.
- ²⁰ Moss, R.A., *Acc. Chem. Res.*, **1980**, 13, 58.
- ²¹ Arduengo, A. J., Krafczyk, R., Schmutzler, R., *Tetrahedron* **1999**, 55, 14523.
- ²² Arduengo A. J., Dias, H. V. R., Harlow, R. L., Kline, M., *J. Am. Chem. Soc.*, **1992**, 114, 5530.

-
- ²³ Herrmann, W.A., Elison, M., Fischer, J., Kocher, C., Artus, G.R.J., *Angew. Chem. Int. Ed. Engl.*, **1995**, *34*, 2371.
- ²⁴ Regitz, M. *Angew. Chem. Int. Ed. Engl.* **1996**, *35*, 725.
- ²⁵ Berding, J., Kooijman, H., Spek, A. L., Bouwman, E., *Organomet.*, **2009**, *28*, 1845.
- ²⁶ Westkamp, T.; Volkler, P.; Bohm, P. W.; Herrmann, W. A., *J. Organomet. Chem.*, **2000** *600* 12.
- ²⁷ McGuinness, D. S.; Cavell, K. J.; *Organometallics*, **1999**, *18*, 1596.
- ²⁸ Schwarz, J.; Bohn, P. W.; Gardiner, M. G.; Grosche, M.; Herrmann, W. A.; Hieringer, W.; Raudaschl-Sieber, G.; *Chem. Eur. J.*, **2000**, *6*, 1773.
- ²⁹ Jacobsen, H., Correa, A., Poater, A., Costabile, C., Cavallo, L., *Coord. Chem. Rev.*, **2009**, *253*, 687.
- ³⁰ Khramov, D. M., Lynch, V. M., Bielawski, C. W., *Organometallics* **2007**, *26*, 6042.
- ³¹ Schlummer, B.; Scholz, U.; *Adv. Synth. Catat.*, **2004**, *346*, 1599.
- ³² Cazin, C. S. J., ed, Springer, London, **2010** and references therein.
- ³³ Herrmann, W. A., Reisinger, C-P., Spiegler, M., *J. Organomet. Chem.*, **1998**, *557*, 93.
- ³⁴ Denk, K., Sirsch, P., Herrmann, W. A., *J. Organomet.Chem.*, **2002**, *649*, 219.
- ³⁵ Glorius, F., ed., Springer, Berlin, **2007**, and references therein.
- ³⁶ Nolan, S. P., ed., Wiley-VCH, Weinheim, 2006, and references therein.
- ³⁷ Zhang, C., Huang, J., Trudell, M.L., Nolan, S.P., *J. Org. Chem.*, **1999**, *64*, 3804.
- ³⁸ Clavier, H., Nolan, S.P., *Chem. Commun.*, **2010**, *46*, 841.
- ³⁹ Poater, A., Ragone, F., Giudice, S., Costabile, C., Dorta, R., Nolan, S.P., Cavallo, L., *Organometallics*, **2008**, *27*, 2679.
- ⁴⁰ Caddick, S., Cloke, F.G.N., Clentsmith, G.K.B., Hitchcock, P.B., McKerrecher, D., Titcomb, L.R., Williams, M.R.V., *J. Organomet. Chem.* **2001** *617–618* 635.
- ⁴¹ Dorta, R.; Stevens, E. D.; Scott, N. M.; Costabile, C.; Cavallo, L.; Hoff, C. D., Nolan, S. P. *J. Am. Chem. Soc.* **2005**, *127*, 2485.
- ⁴² Hillier, A. C., Grasa, G. A., Viciu, M. S., Lee, H. M., Yang, C., Nolan, S.P., *J. Organomet. Chem.*, **2002**, *653*, 69.
- ⁴³ Ragone, F, Poater, A., Cavallo, L., *J. Am. Chem. Soc.*, **2010**, *132*, 4249.
- ⁴⁴ Kuhn, N., Kratzer, T., *Synthesis* 1993, 561.
- ⁴⁵ Herrmann, W. A., Elison, M., Fischer, J., Kocher, C., Artus, G. R. J., *Chem. Eur. J.*, **1996**, *2*, 772.

-
- ⁴⁶ Benhamou, L., Chardon, E., Lavigne, G., Bellemin-Laponnaz, S., Cesar, V., *Chem. Rev.* **2011**, *111*, 2705.
- ⁴⁷ De Frémonta, P., Marionb, N., Nolan, S. P., *Coord. Chem. Rev.*, **2009**, *253*, 862.
- ⁴⁸ Herrmann, W. A., *Angew. Chem. Int. Ed.*, **2002**, *41*, 1290.
- ⁴⁹ Diez-Gonzalez, S., Marion, N., Nolan, S.P., *Chem. Rev.* **2009**, *109*, 3612.
- ⁵⁰ Herrmann, W. A., Goossen, L. J., Kocher, C., Artus, G. R. J., *Angew. Chem. Int. Ed. End.*, **1996**, *35*, 23.
- ⁵¹ Herrmann, W. A., Frey, G.D., Herdtweck, E., Steinbecka, M., *Adv. Synth. Catal.*, **2007**, *349*, 1677.
- ⁵² a) Arnanz, A., González-Arellano, C., Juan, A., Villaverde, G., Corma, A., Iglesias, M., Sánchez, F., *Chem. Commun.*, 2010, *46*, 3001. b) Prinz, M.; Grosche, M.; Herdtweck, E.; Herrmann, W. A. *Organometallics*, **2000**, *19*, 1692.
- ⁵³ Chang, Y-H., Fu, C-F., Liu, Y-H., Peng, S-M., Chen, J-T., Liu, S-T., *Dalton Trans.*, **2009**, 861.
- ⁵⁴ Prades, A., Corberán, R., Poyatos, M. and Peris, E., *Chem. Eur. J.*, **2008**, *14*, 11474.
- ⁵⁵ Liu, S., Rebros, M., Stephens, G., Marr, A.C., *Chem. Commun.*, **2009**, 2308.
- ⁵⁶ Dobereiner, G. E., Crabtree, R. H. *Chem. Rev.*, **2010**, *110*, 681.
- ⁵⁷ Syska, H., Herrmann, W.A., Kühn, F. E., *Journal of Organometallic Chemistry*, **2012**, *703*, 56.
- ⁵⁸ Alcarazo, M., Stork, T., Anoop, A., Thiel, W. and Fürstner, A., *Angew. Chem. Int. Ed.*, **2010**, *49*, 2542.
- ⁵⁹ Patel, D., Liddle, S. T., Mungur, S. A., Rodden, M., Blake, A. J., Arnold, P. L., *Chem. Commun.*, **2006**, 1124.
- ⁶⁰ Gil, W., Trzeciak, A. M., *Coord. Chem. Rev.*, **2011**, *255*, 473.
- ⁶¹ Panzner, M. J., Hindi, K. M., Wright, B. D., Taylor, J. B., Han, D. S., Youngs, W. J., Cannon, C. L., *Dalton Trans.*, **2009**, *35*, 7308.
- ⁶² Lorber, C., Vandier, L., *Dalton Trans.*, **2009**, *35*, 6972.
- ⁶³ Arnold, P. L., Casely, I. J., Turner, Z. R., Bellabarba, R., Tooze, R. B., *Dalton Trans.*, **2009**, *35*, 7236.
- ⁶⁴ Kessler, F., Szesni, N., Maaß, C., Hohberger, C., Weibert, B., Fischer, H., J. *Organomet. Chem.*, **2007**, *692*, 3005.
- ⁶⁵ Ruiz, J., Berros, A., Perandones, B. F., Vivanco, M., *Dalton Trans.*, **2009**, *35*, 6999.

-
- ⁶⁶ Berding, J., Kooijman, H., Spek, A. L., Bouwman, E., *Organomet.*, **2009**, 28, 1845.
- ⁶⁷ Böhm, V. P. W., Weskamp, T., Gstötmayr, C. W. K. and Herrmann, W. A., *Angew. Chem. Int. Ed.*, **2000**, 39, 1602.
- ⁶⁸ Zhou, Y., Xi, Z., Chen, W., Wang, D., *Organomet.*, **2008**, 27, 5911.
- ⁶⁹ Wang, S. C., Troast, D. M., Conda-Sheridan, M., Zuo, G., LaGarde, D., Louie, J., Tantillo, D. J., *J. Org. Chem.*, **2009**, 74, 7822.
- ⁷⁰ McGuinness, D. S., Mueller, W., Wasserscheid, P., Cavell, K. J., Skelton, B. S., White, A. H., Englert, U., *Organomet*, **2002**, 21, 175.
- ⁷¹ Song, Y-J., Jung, I. J., Lee, H., Lee, Y. T., Chung, Y. K., Jang, H-Y., *Tetrahedron Lett.*, **2007**, 48, 6142. b). Nielsen, R.J., Goddard, W.A., *J. Am. Chem. Soc.*, **2006**, 128, 9651. c). Luo, F., Pan, C., Cheng, J., Chen, F., *Tetrahedron*, **2011**, 67, 5878. d). Zhang, M., Zhang, S., Zhang, G., Chen, F., Cheng, J., *Tetrahedron Lett.*, **2011**, 52, 2480. e). Wang, W., Wang, F., Shi, M., *Organometallics*, **2010**, 29, 928. f). Gardiner, M.G., Herrmann, W.A., Reisinger, C-P., Schwarz, J., Spiegler, M., *J. Organomet. Chem*, **1999**, 572, 239. g). Mesnager, J., Lammel, P., Jeanneau, E., Pinel, C., *App. Catal. A-Gen.*, **2009**, 368, 22. h) Jackstell, R., Gomez Andreu, M., Frisch, A., Selvakumar, K., Zapf, A., Klein, H., Spannenberg, A., Rttger, D., Briel, O., Karch, R., Beller, M., *Angew. Chem. Int. Ed.*, **2002**, 41, 986. i) Kuriyama, M., Ishiyama, N., Shimazawa, R., Onomura, O., *Tetrahedron*, **2010**, 66, 6814. j) I.G. Jung, J. Seo, Y.K. Chung, D.M. Shin, S.-H. Chun, S.U. Son, *J. Polym. Sci. A: Polym. Chem.*, **2007**, 45, 3042. k) Gurbuz, N., Demir, S., Ozdemir, I., Cetinkaya, B., *Tetrahedron Lett.*, **2005**, 46, 2273.
- ⁷² "The Nobel Prize in Chemistry 2010 - Presentation Speech". *Nobelprize.org*. 23 Nov 2012 http://www.nobelprize.org/nobel_prizes/chemistry/laureates/2010/presentation-speech.html.
- ⁷³ Shen, Q.; Ogata, T.; Hartwig, J. F.; *J. Am. Chem. Soc.*, **2008**, 130, 6586.
- ⁷⁴ Littke, A. F, Fu, G. C., *Angew. Chem. Int. Ed.*, **2002**, 41, 4176.
- ⁷⁵ Lee, H.M., Nolan, S. P., *Org Lett.*, **2000**, 2, 2053.
- ⁷⁶ Frisch A. C., Rataboul, F., Zapf, A., Beller, M., *J. Organomet. Chem.*, **2003**, 687, 403.
- ⁷⁷ Jin, Z., Gu, X-P., Qiu, L-L., Wu, G-P., Song, H-B., Fang, J-X., *J. Organomet. Chem.*, **2011**, 696, 859.
- ⁷⁸ Arentsen, K., Caddick, S., Cloke, F.G.N., *Tetrahedron* **2005** 61 9710.

-
- ⁷⁹ Wurtz, S., Glorius, F., *Acc. Chem. Res.*, **2008**, *41*, 1523.
- ⁸⁰ Titcomb, L.R., Caddick, S., Cloke, F.G.N., Wilson, D.J., McKerrecher, D., *Chem. Commun.*, **2001**, 138.
- ⁸¹ Organ, M. G., Çalimsiz, S., Sayah, M., Hoi, K. and Lough, A. J, *Angew. Chem. Int. Ed.* **2009**, *48*, 2383.
- ⁸² Christmann, U. and Vilar, R, *Angew. Chem. Int. Ed.* 2005, *44*, 366.
- ⁸³ Luo, F-T., Lo, H-K., *J. Organomet. Chem.*, **2011**, *696*, 262.
- ⁸⁴ Godoy, F., Segarra, C., Poyatos, M., Peris, E., *Organometallics*, **2011**, *30*, 684.
- ⁸⁵ Türkmen, H., Pelit, L., Cetinkaya, B., *J. Mol. Catal. A: Chem.*, **2011**, *348*, 88
- ⁸⁶ Nador, F., Moglie, Y., Ciolino, A., Pierini, A., Dorn, V., Yus, M., Alonso, F., Radivo, G., *Tetrahedron Lett.*, **2012**, *53*, 3156.
- ⁸⁷ Balcells, D., Nova, A., Clot, E., Gnanamgari, D., Crabtree, R. H.; Eisenstein, O., *Organometallics*, **2008**, *27*, 2529.
- ⁸⁸ Tewari, A., Hein, M., Zapf, A., Beller, M., *Tetrahedron*, **2005**, *61*, 9705.
- Singh, U. K., Strieter, E. R., Blackmond, D. G., Buchwald, S. L., *J. Am. Chem. Soc.*, **2002**, *124*, 14104.
- ⁸⁹ Biscoe, M. R., Barder, T. E., Buchwald, S. L., *Angew. Chem. Int. Ed.*, **2007**, *46*, 1.
- ⁹⁰ Buchwald, S. L., Mauger, C., Scholz, M., *Adv. Synth. Catat.*, **2006**, *348*, 23.
- ⁹¹ Barder, T.E., Buchwald, S.L., *J. Am. Chem. Soc.*, **2007**, *129*, 12003.
- ⁹² Shen, Q., Ogata, T., Hartwig, J. F., *J. Am. Chem. Soc.*, **2008**, *130*, 6586.
- ⁹³ Shen, Q., Hartwig, J. F., *J. Am. Chem. Soc.*, **2006**, *128*, 1002.
- ⁹⁴ Stambuli, J. P., Buhl, M., Hartwig, J. F., *J. Am. Chem. Soc.*, **2002**, *124*, 9346.
- ⁹⁵ Paul, F., Patt, J., Hartwig, J. F., *J. Am. Chem. Soc.*, **1994**, *116*, 5969.
- ⁹⁶ Guram, A. S., Rennels, R. A., Buchwald, S. L., *Angew. Chem. Int. Ed. Engl.*, 1995, *34*, 1348.
- ⁹⁷ Louie, J., Hartwig, J. F., *Tetrahedron Lett.*, **1995**, *36*, 3609
- ⁹⁸ Wagaw, S., Buchwald, S. L., *J. Org. Chem.*, **1996**, *61*, 7240.
- ⁹⁹ Chartoire, A., Lesieur, M., Slawin, A. M. Z., Nolan, S. P., Cazin, C. S. J., *Organometallics*, **2011**, *30*, 4432.
- ¹⁰⁰ Dumrath, A., Lübbe, C., Neumann, H., Jackstell, R., Beller, M., *Chem. Eur. J.*, **2011**, *17*, 9599.

-
- ¹⁰¹ Fors, B., Buchwald, S., *J. Am. Chem. Soc.* **2010**, *132*, 15914.
- ¹⁰² a).Hartwig, J. F., *Acc. Chem. Res.*, **2008**, *41*, 1534. , b).Shen, Q., Hartwig, J. F., *Org. Lett.*, **2008**, *10*, 4109.
- ¹⁰³ Schulz, T., Torborg, C., Enthaler, S., Schäffner, B., Spannenberg, A., Neumann, H., Börner, A., Beller, M., *Chem. Eur. J.* **2009**, *15*, 4528; and references therein.
- ¹⁰⁴ Chartoire, A., Frogneux, X., Boreux, A., Slawin, A. M. Z., Nolan, S. P., *Organometallics* **2012**, *31*, 6947.
- ¹⁰⁵ Meiries, S., Chartoire, A., Slawin, A. M. Z., Nolan, S. P., *Organometallics*, **2012**, *31*, 3402.
- ¹⁰⁶ a) Amatore, C., Jutand, A., Khalil, F., M'Barki, M.A., Mottier, L., *Organometallics* **1993**, *12*, 3168. b) Amatore, C., Jutland, A., *Acc. Chem. Res.*, **2000**, *33*, 314.
c) Amatore, C., Jutand, A., Suarez, A., *J. Am. Chem. Soc.*, **1993**, *115*, 9531.
- ¹⁰⁷ a) Hartwig, J. F., Richards, S., Baranano, D., Paul, F., *J. Am. Chem. Soc.*, **1996**, *118*, 3626. b) Hartwig, J. F., Paul, F., *J. Am. Chem. Soc.*, **1995**, *117*, 537. c) Louie, J., Hartwig, J. *Tetrahedron Lett.*, **1995**, 3609.
- ¹⁰⁸ Alcazar-Roman, L.M., Hartwig, J.F., *J. Am. Chem. Soc.* **2001**, *123*, 12905.
- ¹⁰⁹ a) Alcazar-Roman, L.M., Hartwig, J.F., Rheingold, A.L., Liabe-Sands, L.M., Guzei, I.A., *J. Am. Chem. Soc.* **2000**, *122*, 4618. b) Portnoy, M., Milstein, D., *Organometallics*, **1993**, *12*, 1665.
- ¹¹⁰ Lewis, A. K. de K.; Caddick, S.; Cloke, F. G. N.; Billingham, N. C.; Hitchcock, P. B., Leonard, J. *J. Am. Chem. Soc.* **2003**, *125*, 10066.
- ¹¹¹ McGuinness D. S.; Green, M. J.; Cavell, K. J.; Skelton, B. W.; White, A. H.; *J. Organomet. Chem.*, **1998**, *565*, 165.
- ¹¹² Marshall, W. J., Grushin, V. V., *Organometallics*, **2003**, *22*, 1591. Grushin, V. V., *Organometallics*, **2000**, *19*, 1888.
- ¹¹³ Biscoe, M.R., Barder, T.E., Buchwald, S.L., *Angew. Chem. Int. Ed.*, **2007**, *46*, 7232.
- ¹¹⁴ a) Lewis, A.K.de K., Caddick, S., Esposito, O., Cloke, F.G.N., Hitchcock, P.B., *Dalton Trans.*, **2009**, *35*, 7094. b) Esposito, O.; University of Sussex, Brighton, DPhil Thesis, **2008**.
- ¹¹⁵ Driver, M. S., Hartwig, J. F., *J. Am. Chem. Soc.*, **1997**, *119*, 8232.
- ¹¹⁶ Hartwig, J. F., Richards, S., Baranano, D., Paul, F., *J. Am. Chem. Soc.*, **1996**, *118*, 3626.

-
- ¹¹⁷ Surry, D. S., Buchwald, S. L., *Chem. Sci.*, 2011, 2, 27.
- ¹¹⁸ a) Cavello, L., Correa, A., Costabile, C., Jacobsen, H., *J. Organomet. Chem.*, **2005**, 690, 5407., b) Kovavcic, P., Lowery, M. K., *J Org. Chem.*, **1968**, 34, 911.
- ¹¹⁹ Green, J. C., Benjamin, J. H., Lonsdale, R., *J. Organomet. Chem.*, **2005**, 690, 6054.
- ¹²⁰ Kirchhoff, H.; Netherton, M.R.; Hills, I.D.; Fu G.C. *J. Am. Chem. Soc.* **2002**, 124, 13662.
- ¹²¹ Esposito, O., Lewis A. K. de K., Hitchcock, P. B., Caddick, S., Cloke, F. G. N., *Chem. Commun.*, **2007**, 1157.
- ¹²² Green, M. J.; Cavell, K. J.; Skelton, B. W.; White, A. H.; *J. Organomet. Chem.* **1998**, 554, 175.
- ¹²³ Pan, J., Su, M., Buchwald, S. L., *Angew. Chem. Int. Ed.*, **2011**, 50, 8647.
- ¹²⁴ Hanley, P. S., Marquard, S. L., Cundari, T. R., Hartwig, J. F., *J. Am. Chem. Soc.* **2012**, 134, 15281

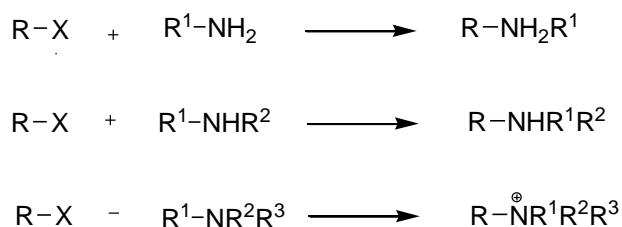
Chapter Two:

Investigations into the development of a palladium-carbene catalyst for alkyl amination, specifically using 1,2,3,4- tetramethylimidazol-2-ylidene and 1,3- cyclohexylimidazol-2-ylidene.

2.1 Introduction

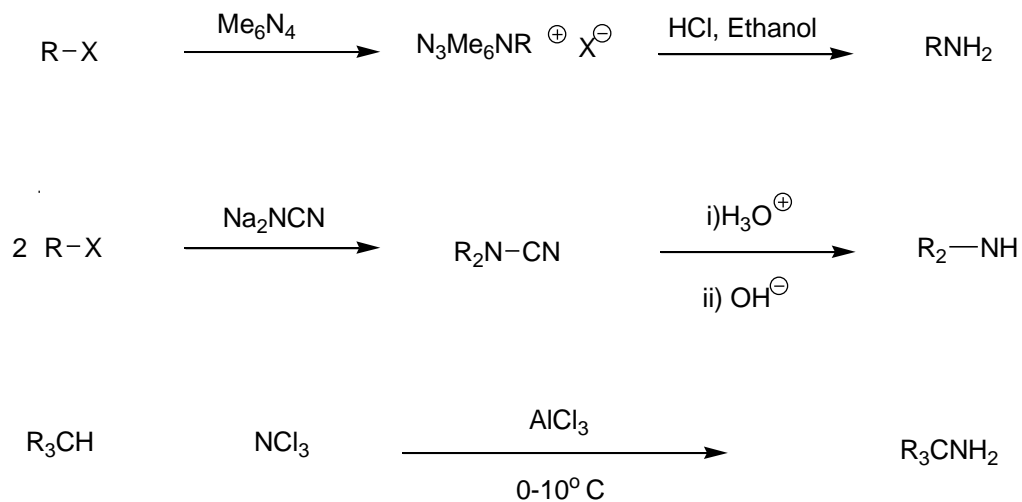
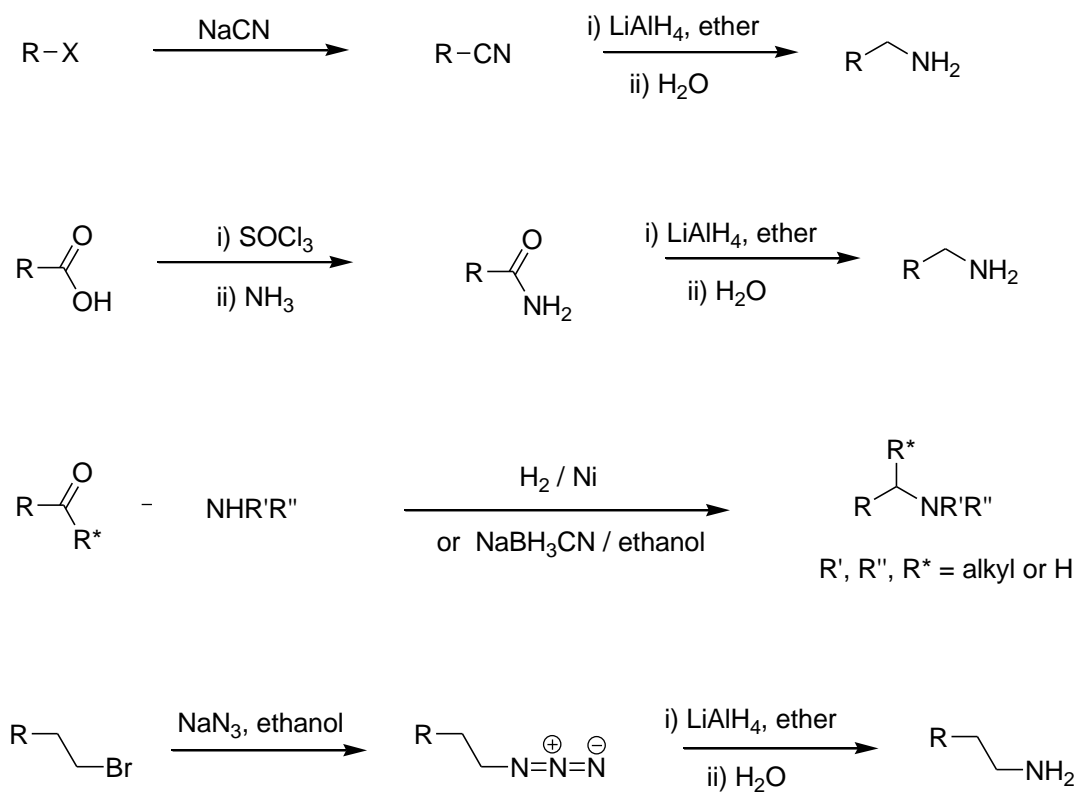
The arylation of primary and secondary amines by palladium catalysis has been widely investigated, whilst their alkylation remains relatively unexplored¹.

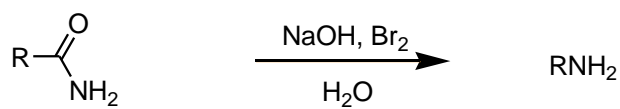
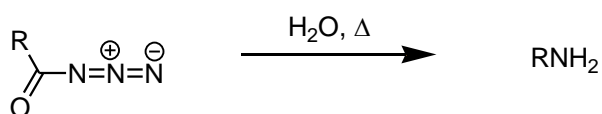
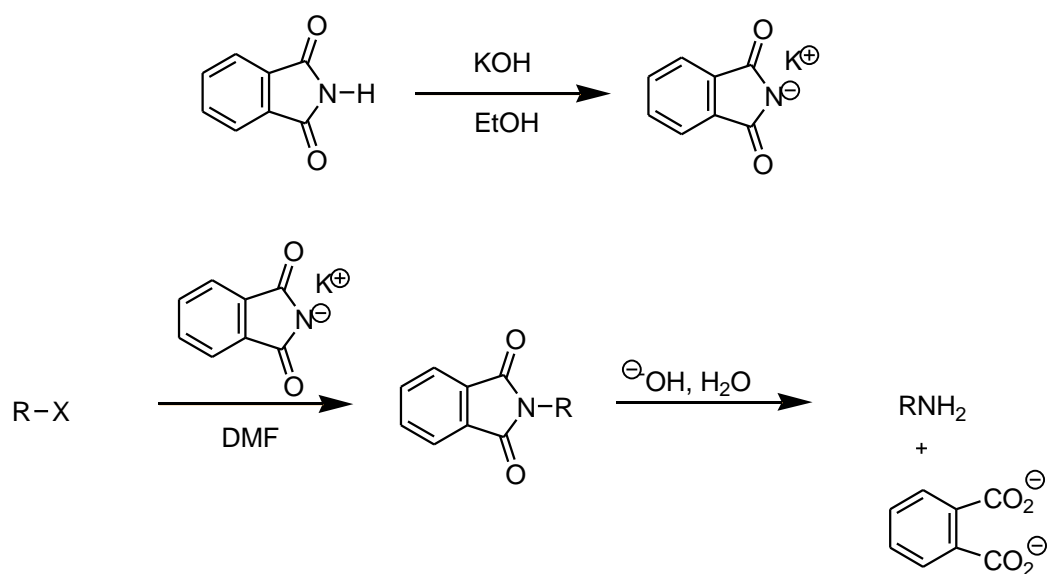
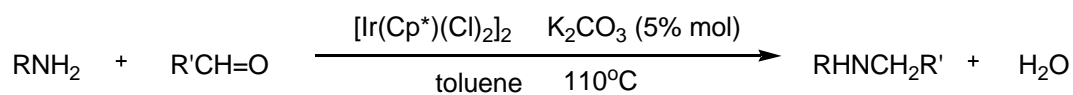
Alkyl amination is currently achieved mainly *via* the S_N2 reaction of alkyl halides with ammonia and primary amines². This process is limited by the fact that the more substituted amine product is a better nucleophile than the reactant amine and thus polyalkylation occurs as depicted in Scheme 2.1. The yield can be improved by employing an excess of amine but even then the yields tend to be low and the reaction produces a considerable amount of waste products and is energetically costly³.



Scheme 2.1: S_N2 polyalkylation of amines³

There are other methods to achieve alkyl amination which are shown in Scheme 2.2; many of these are based on the reduction of the appropriate nitrogen containing starting material to the amine^{2,3} (Scheme 2.2). There are also transition metal catalysed reactions such as the iridium catalysed transformation of aliphatic alcohols to amines discussed in Chapter One⁴(Scheme 2.2).

Substitution ReactionsReduction Reactions

Hofmann RearrangementCurtius RearrangementGabriel SynthesisIridium-based protocol with alcoholsScheme 2.2: Methods of Alkyl Amination^{2, 3, 4.}

None of the protocols shown in Scheme 2.2 can be applied in a general synthetic protocol since they are each limited to certain types of amine. A method which can be applied more generally is therefore a desirable aim. Palladium-*NHC* complexes have proven to be very successful catalysts for aryl amination and C-C coupling reactions⁵ and therefore theoretical⁶ and experimental^{7,8} work has been undertaken to establish whether these systems can be adapted for use in alkyl amination.

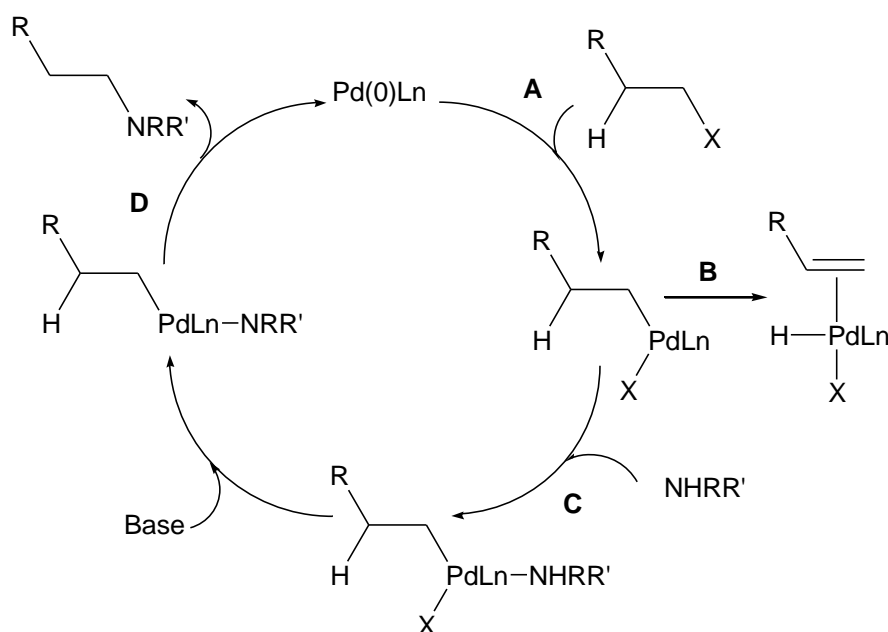
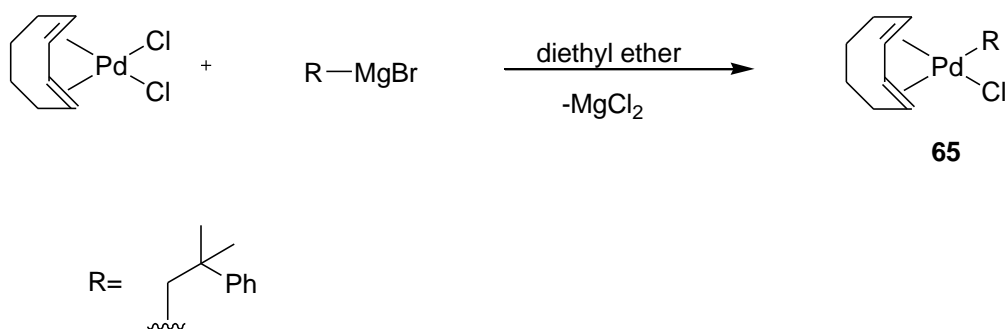


Figure 36: Proposed catalytic cycle for alkyl amination⁶

The conceptual catalytic cycle proposed in Figure 36 is based on the general palladium cross-coupling catalytic cycle discussed in Chapter One. The cycle shows the oxidative addition as step A, followed by the transamination in step C, with base abstraction of the hydrido ligand and reductive elimination and regeneration of catalyst in step D. Step B is β -hydrogen elimination of alkene, an alternative pathway to step C which has a lower activation energy in alkyl palladium complexes than in aryl counterparts and so the viability of this pathway for an alkyl Pd species needs consideration.

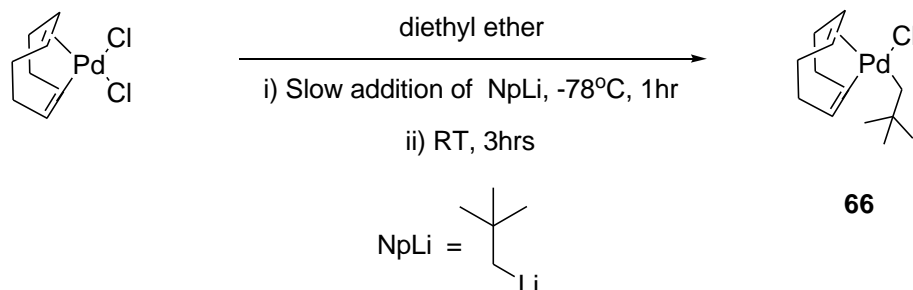
Therefore, study of this proposed catalytic cycle is simplified by the use of non- β -hydrogen-containing alkyl halides in order to attempt the isolation of the complexes formed in the catalytic cycle.

Theoretical analysis on $\text{Pd}(\text{I}^t\text{Bu})_2$, **64**, has found that direct oxidative addition of non- β hydrogen-containing alkyl chlorides is not as thermodynamically favourable as the oxidative addition of aryl chlorides. In fact, unlike the oxidative addition of phenyl chloride, the transition state for the methyl chloride addition is higher in energy than dissociation of I^tBu from **64**⁶. Experiments within our group have verified that direct alkylation to **64** with the non- β hydrogen- containing alkyl chloride, neopentyl chloride, did not occur⁷. Direct methylation of Pd-NHC complexes had previously been attempted by Cavell *et al*, but was also unsuccessful which led them to devise an indirect method to form a methyl- Pd-NHC complexes using $[\text{Pd}(1,5\text{-COD})\text{MeCl}]$ ⁹ (COD= cyclooctadiene). Gutierrez *et al* also produced Pd alkyl complexes by reaction of PMe_3 with $\text{Pd}(1, 4\text{-COD})\text{Cl}_2$ followed by alkylation with an alkyl Grignard¹⁰ (Scheme 2.3).



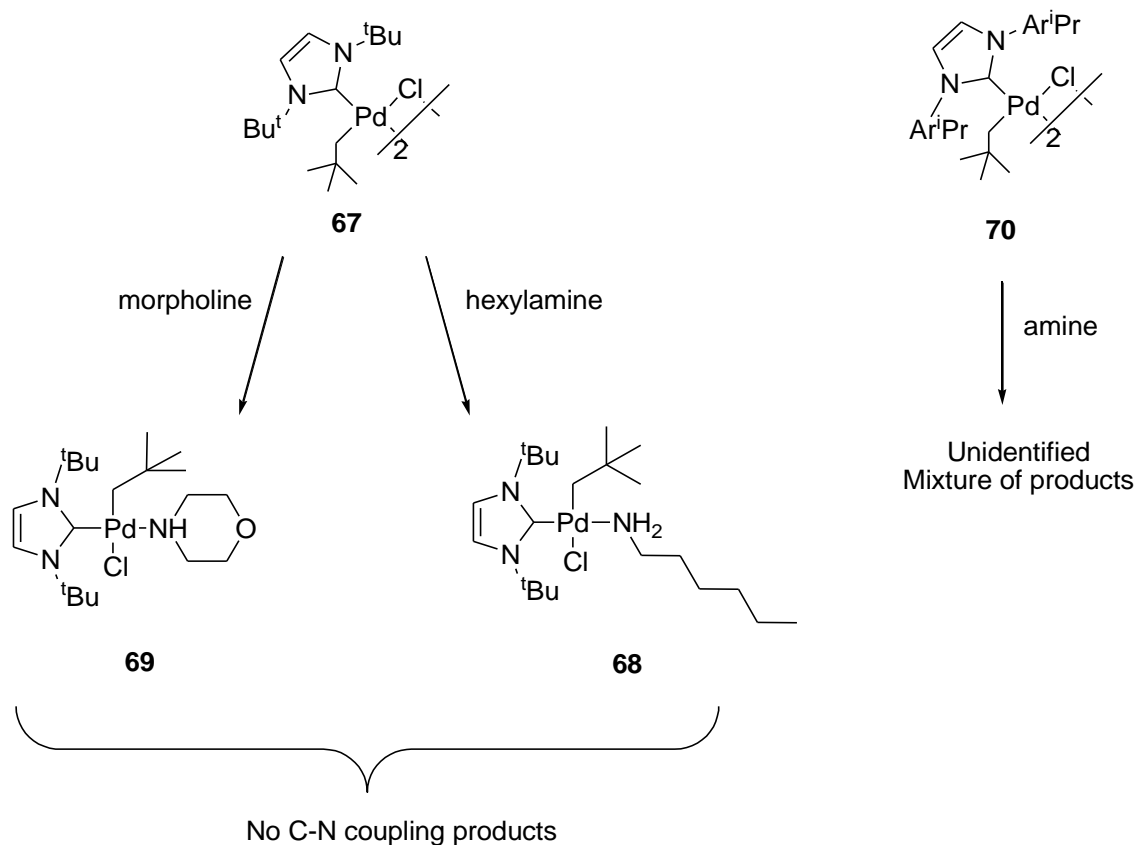
Scheme 2.3: Formation synthesis of $\text{Pd}(\text{CH}_2\text{CMe}_2\text{Ph})(1, 4\text{-COD})\text{Cl}$, **65**.¹⁰

The novel alkyl Pd complex, $\text{Pd}(1,5 \text{ COD})(\text{neopentyl})\text{Cl}$, **66**, was synthesized by the reaction depicted Scheme 2.4.



Scheme 2.4 :Reaction of $\text{Pd}(1,5 \text{ COD})\text{Cl}_2$ and alkyl lithium to form **66**.⁷

Our group successfully utilised $[\text{Pd}(1,5\text{-COD})(\text{neopentyl})\text{Cl}]$, **66** to prepare novel $\text{Pd}(\text{II})\text{-NHC}$ alkyl complexes **67** and **70** by ligand exchange of *NHC* with 1,5-COD. These complexes can be reacted with aliphatic amines to synthesise complexes, **68** and **69** (Scheme 2.4).⁷



Scheme 2.5: Previous alkyl palladium complexes produced by our group⁷

However, attempts to eliminate the C-N coupling products from the *t*Bu complexes, **68** and **69**, were not successful. It was thought that the strong σ -electron donating properties of both *t*Bu and the alkyl adduct may have increased the electron density on the palladium metal centre to such a degree that the lone pair of electrons on the amine nitrogen interact only weakly with the metal and thus the amine's acidic proton is still too strongly bound to be removed by standard bases.⁷

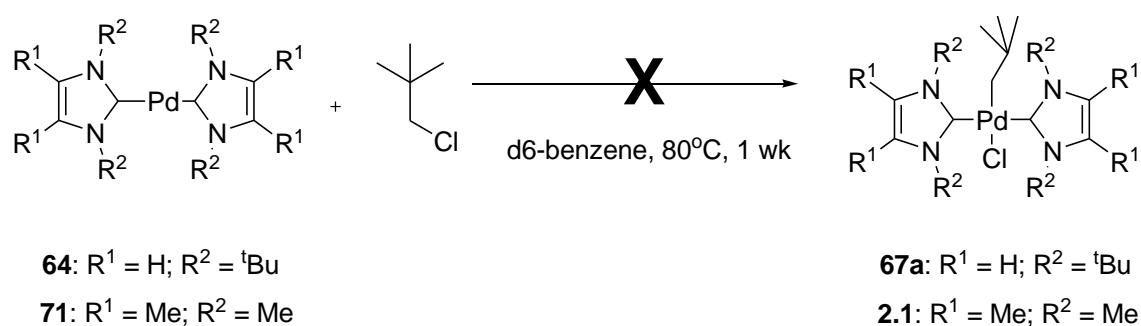
It was therefore envisaged that other *NHC*s might provide a subtle change in the electronic influences on the metal centre, generating a transamination complex with a *pK*_a lowered enough to allow deprotonation of the amine and thus promote C-N coupling. The choice of ITMe and ICy was motivated by the generally accepted view that they are less σ -donating *NHC*s than *t*Bu but more electron-donating than *i*Pr.⁵ It

has also been found that Pd ITMe alkyl complexes are more resistant to decomposition.^{11, 12}

2.2 Results and Discussion

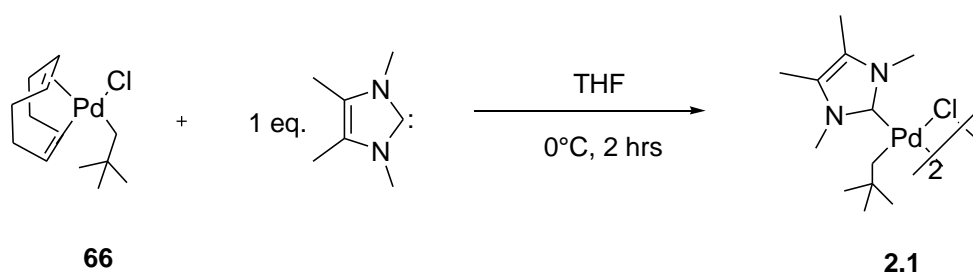
2.2.1 Synthesis and decomposition of dimeric neopentyl NHC Pd complexes (*NHC* = ITMe and ICy)

The reaction of [Pd(ITMe)₂], **71**, with neopentyl chloride did not yield the desired oxidative addition product (Scheme 2.6) just as [Pd(I^tBu)₂] (**64**) did not.⁷



Scheme 2.6: Unsuccessful direct attempt at oxidative addition of neopentyl chloride to Pd(*NHC*)₂. (*NHC* = ITMe, I^tBu)⁷

The method used previously to generate **67** and **70** by an indirect route was employed with the *NHC*, ITMe (Scheme 2.7). This led to the isolation of dimer [Pd(ITMe)(np)(μ-Cl)]₂, **2.1**.



Scheme 2.7: Synthesis of Pd(ITMe)(neopentyl)(μ-Cl) dimer, **2.1**

Complex [Pd(ITMe)(neopentyl)(μ-Cl)]₂, **2.1**, is insoluble in most common solvents, with the exception of THF and DCM. It is tolerably air stable as a solid, however palladium black is observed to deposit from its solutions, particularly in the case where dichloromethane (DCM) is used as a solvent. The identity of **2.1** was confirmed by

spectroscopic and analytical methods. Characteristic ITMe methyl peaks were found at 2.96 ppm and 2.14 ppm in ^1H NMR with the neopentyl peaks at 0.87 ppm for the CH_3 group and 0.68 ppm for the CH_2 group and ^{13}C NMR showed the *NHC* peak at 153.46 ppm and neopentyl methyl peaks at 35.26 ($\text{C}(\text{CH}_3)$), 34.02 ($\text{C}(\text{CH}_3)$), and 33.89 ($\text{CH}_2\text{C}(\text{CH}_3)$). The MS (EI) gave $[\text{M} - 2\text{CH}_3]^+$ of m/z 657. The elemental analysis agreed with calculated values.

However, a THF solution of **2.1** furnished crystals suitable for a single crystal X-ray diffraction experiment after standing for 2 months at room temperature. The identity of these crystals was found to be *cis*- $[\text{Pd}(\text{ITMe})_2(\text{Cl})_2]$,

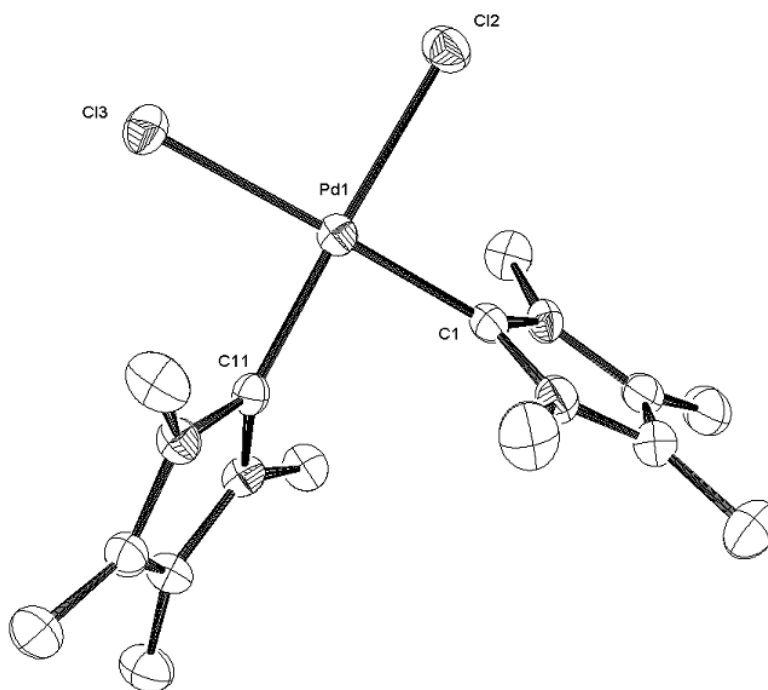


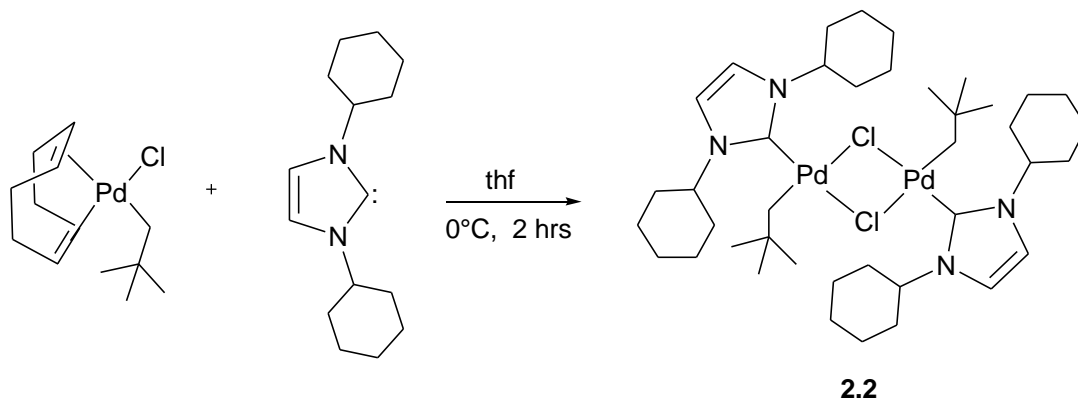
Figure 37: Molecular structure of **72**. Selected bond lengths (Å) and angles(°):

Pd(1)-C(1) 1.978(4); Pd(1)-C(11) 1.989(4); Pd(1)-Cl(2) 2.3714(11); Pd(1)-Cl(3) 2.3855(11); C(1)-Pd(1)-C(11) 89.25(16); C(1)-Pd(1)-Cl(2) 88.79(12); C(11)-Pd(1)-Cl(2) 178.00(12); C(1)-Pd(1)-Cl(3) 176.20(12); C(11)-Pd(1)-Cl(3) 89.71(11); Cl(2)-Pd(1)-Cl(3) 92.27(4).

The complex **72** has been found in the *cis* geometry whereas $\text{Pd}(\text{ITMe})_2\text{I}_2$ ¹³ and *trans*- $\text{Pd}(\text{ITMe})_2\text{Br}_2$ (Chapter 4) are found in the *trans* geometry but this is most likely due to the smaller size of the chlorine atom compared to bromine and iodine.

It is interesting to note that palladium black had been deposited and analysis of the mother liquor of these crystals by GC-MS showed that it contained fragments associated with 2,2,5,5-tetramethylhexane. Pd(ITMe)₂, **71**, was not observed in the ¹H NMR spectrum.

The analogous complex [Pd(ICy)(neopentyl)(μ-Cl)]₂, **2.2**, has also been synthesised in a manner analogous to **2.1** (Scheme 2.8).



Scheme 2.8: Synthesis of [Pd(ICy)(neopentyl)(μ-Cl)]₂ dimer.

The identity of complex **2.2** was confirmed by spectroscopic and analytical methods. The ¹H-NMR spectrum shows peaks at 1.24 ppm (s, 18H, CH₃ (neopentyl)), 0.69 ppm (s, 4H, CH₂ (neopentyl)); 6.40 ppm (s, 4H, CH (NHC C=C)), 5.52 ppm (m: 4H, CH, (NHC CH(cy))), 2.25 ppm (s, 4H) and the mass spectrum produced peaks at 642 *m/z* [M - ICy - CH₃]⁺, 631 *m/z* [M - ICy - (CH₃)₂]⁺ and 601 *m/z* [M - ICy - CH(CH₃)₃]. The identity of **2.2** was further established by a single crystal X-ray diffraction study (Figure 38) which confirmed the molecular structure depicted in Scheme 2.7. Unfortunately in this case as well, the collected dataset was not of sufficient quality to provide reliable bond lengths and angles.

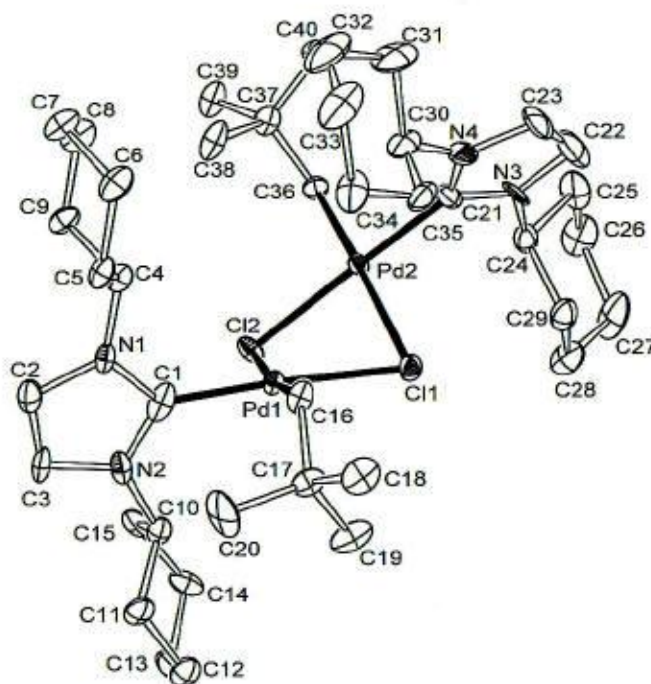


Figure 38: Molecular structure of **2.2**, *trans*-[Pd(ICy)(neopentyl)Cl]₂.

In an attempt to improve the quality of the crystals obtained (Figure 38), the reaction was repeated and after workup involving extraction in a) Et₂O and b) *n*-pentane, a second crop of thin needles was obtained by layering the *n*-pentane extract with Et₂O and storing at 4 °C. A single crystal X-ray diffraction study revealed that they were *trans*-Pd(ICy)₂(Cl)₂, **2.3**.

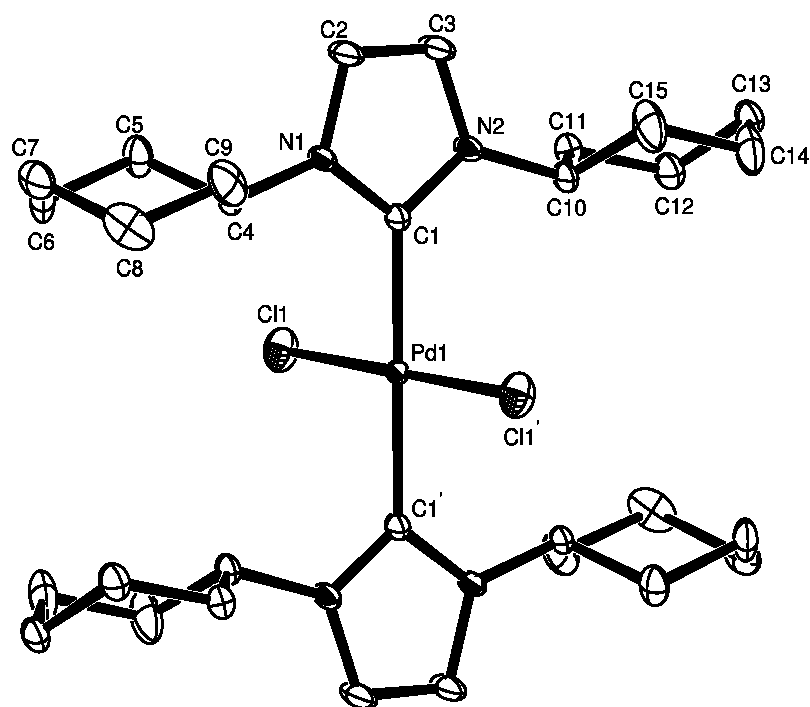


Figure 39: Ortep diagram of the mmolecular structure of *trans*-Pd(ICy)₂Cl₂, (**2.3**) showing 50% thermal ellipsoids. Selected bond lengths (Å) and angles(°): Pd(1)-C(1) 2.019(3); Pd(2)-C(16) 2.0273(3) ; Pd(1)-Cl(1) 2.3084(7); Pd(2)-Cl(2) 2.3125(7) ; C(1)-Pd(1)-C(1)' 180.0 ; C(1)-Pd(1)-Cl(1) 88.97(9); C(1)'-Pd(1)-Cl(1) 91.03(9); C(1)-Pd(1)-Cl(1)' 91.03(9); C(1)'-Pd(1)-Cl(1)' 88.97(9); Cl(1)-Pd(1)-Cl(1)' 180.00 (5).

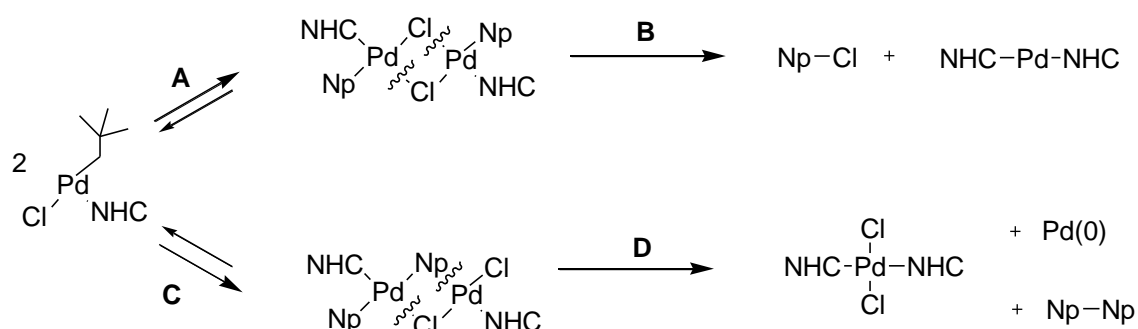
The crystallographic data found compares well with data from previously isolated dichloro bis-*NHC* palladium (II) complexes, accepting for the expected changes due to differences in steric bulk.

Again, 2,2,5,5- tetramethylhexane was found in the mother liquor *via* GC-MS.

Both **67** and **70** were found to decompose to the zero valent Pd(*NHC*)₂ complex and reductively eliminate neopentyl chloride. The mechanism in Scheme 2.9 is proposed to account for these observations. There has been no evidence that ITMe and ICy follow the pathway A + B which is the pathway the analogous reactions with I^tBu and IPr¹⁴ follow (Scheme 2.9). The reason for this is most probably steric effects. ITMe and ICy are less bulky than either I^tBu or IPr¹⁴ so the Pd(*NHC*)(Np)(μ -Cl)(μ -Np) dimer may be more readily formed. In the case of ITMe, solubility issues may be the key to why the Pd(ITMe)₂ complex does not form; poor solvation of the Pd(ITMe) species may mean

that there is little preventing this high energy species disintegrating to Pd black¹⁴. There is the possibility that a Pd(IV) intermediate could be formed but, whilst this would explain the presence of Pd(*NHC*)₂Cl₂, Pd(0) and 2,2,5,5- tetramethylhexane, the fact that the corresponding 2-alkyl-imidazolium salts are not observed as decomposition products, means that such a pathway is unlikely.¹⁷

It is interesting that **2.2** should have been found as a *trans* isomer whereas **70** has been found as both the *cis* and the *trans* isomers. Both of these complexes decompose more rapidly than **2.1** and **67**. Complex **67** has only been found in the *trans* configuration whilst the ¹H-NMR for **2.1** shows a broadening and the start of the separation of the *NHC* methyl peak into two peaks which suggests that, like **70**, both the *cis* and *trans* isomers are present. For **2.2**, ¹H NMR is more difficult to interpret and no conclusive evidence of either dimer configurations has been seen.

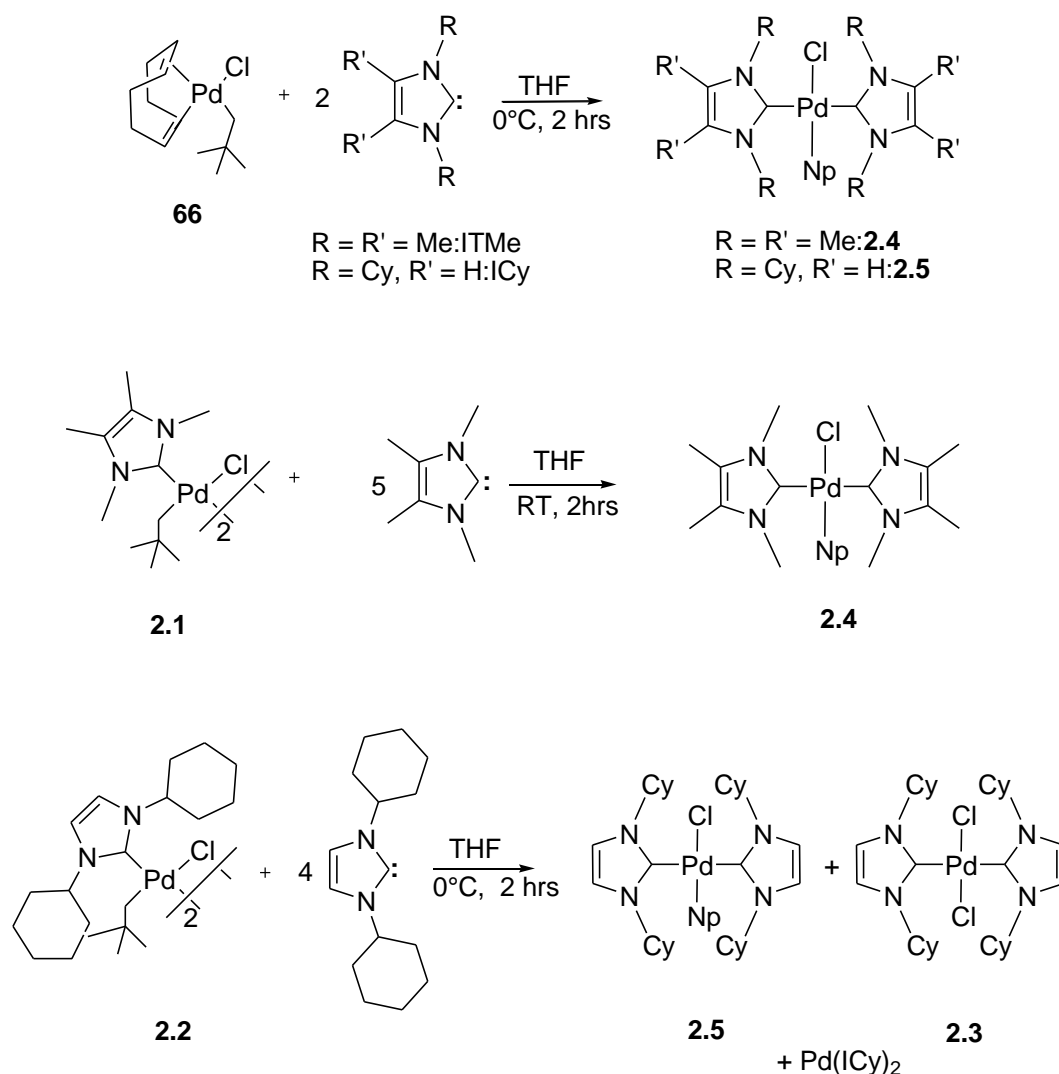


For pathway A+B, NHC = ITMe, ICy
 For pathway C+D, NHC = IPr, I^tBu

Scheme 2.9: Proposed intermolecular exchange mechanism for the formation of *trans*-Pd(ICy)₂Cl₂, **2.3** and *cis*-Pd(ITMe)₂Cl₂, **72**.

2.2.2 Synthesis of monomeric neopentyl Pd(II)-NHC complexes (NHC = ITMe, ICy).

Addition of an excess of ITMe or ICy (2 mol eq) to Pd(1,5-COD)(Np)Cl (**66**) led to the isolation of monomeric complexes **2.4** and **2.5** respectively (Scheme 2.10). Alternatively, **2.4** and **2.5** be prepared by addition of an excess of the corresponding free carbene to the dimeric complexes [Pd(NHC)(neopentyl)(μ -Cl)]₂ (NHC = ITMe:**2.1**; NHC = ICy:**2.2**) respectively (Scheme 2.10).



Scheme 2.10: Preparative methods for the Synthesis of monomeric species, **2.4** and **2.5**

It is interesting to note that when the latter preparative method was used to access complex **2.5**, the reaction mixture also contained some unreacted starting material, *trans*-Pd(ICy)₂Cl₂ and Pd(ICy)₂

Fortunately the desired product **2.5** could be isolated by crystallization from Et₂O at 4 °C (Figure 40). The integration of the ¹H NMR peaks for this complex were in agreement with a neopentyl:cyclohexyl NCH ratio of 9:4 with the peaks occurring at 5.55- 5.49 ppm for the cyclohexyl NCH peak and 1.24 ppm for the neopentyl. The mass spectrum (EI) showed peaks at *m/z* 651[M – 2CH₃], *m/z* 642 [M-Cl]⁺ and *m/z* 605 [M-CH₂C(CH₃)₃]⁺, which is similar to the fragmentation pattern seen for **2.4**, where loss of neopentyl occurs from the molecular ion can occur whilst the halide is still coordinated. In this complex, the [M-Cl]⁺ peak and the neopentyl-ICy peak are observed whereas the analogous peaks do not occur in the mass spectrum (EI) for **2.4**. **2.4** could not be characterised crystallographically but the integration of the ITMe methyl peaks and the neopentyl peak in the ¹H NMR were in the ratio 12:9.

Selected bond lengths (Å) and angles(°):

Cl(1) Pd(1) 2.4397(18); C(028) Pd(1) 2.075(6); C(1) Pd(1) 2.029(6); C(2) Pd(1)

[illegible]

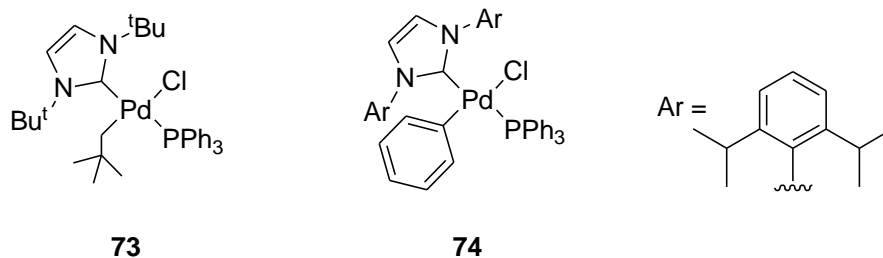
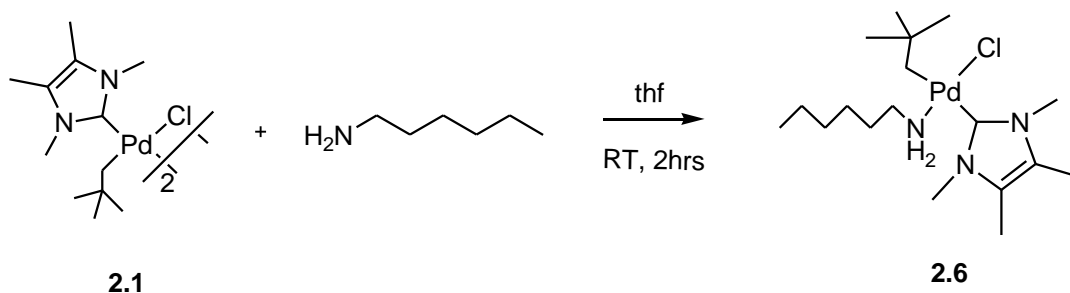


Figure 41: *Trans*-(I^tBu)(Pd)(PPh₃)(neopentyl)Cl, **73**¹⁵, and *trans*-(IPr)(Pd)(PPh₃)(phenyl)Cl, **74**¹⁴.

Comparison with the heterolytic complex, *trans*-(I^tBu)(Pd)(PPh₃)(neopentyl)Cl, **73**, isolated by our group⁵ shows that the Pd-Cl (2.4554(7) in **73** and 2.4397(18) in **2.5**) and Pd-C(neopentyl) bond lengths (2.090(3) in **73** and 2.075(5) in **2.5**) are comparable and show the expected shortening of the Pd-C(carbene) bond due to the smaller steric bulk of ICy

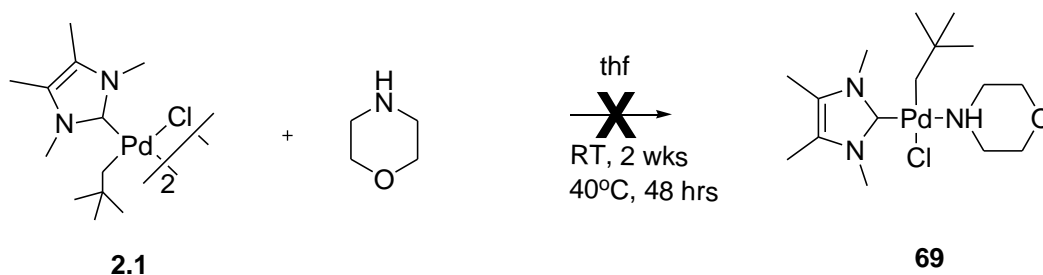
It was previously thought that the long I^tBu bond in **73** (longer than the IPr bond in *trans*-(IPr)(Pd)(PPh₃)(phenyl)Cl, **74**, synthesised by Grushin¹⁴) was due to the difference in σ-donation between the aryl and the neopentyl groups¹⁵. However, when comparing **2.3** and **2.5**, it can be seen in Table 2.1 that the Pd-ICy bond length has increased only a very small amount. Thus the difference in Pd-carbene bond lengths is most likely due to the smaller % buried volume of ICy and IPr compared to I^tBu with the longer phosphine bond in **73** a necessity induced by the I^tBu's bulk.

2.2.3 Reactions of **2.1** and **2.2** with amines.



Scheme 2.11: Synthesis of Pd(ITMe)(Neopentyl)(hexylamine) monomer, **2.6**

Reaction of dimer **2.1** with hexylamine formed the transmetallation complex, [Pd(ITMe)(neopentyl)(hexylamine)Cl], (**2.6**). This is shown in Scheme 2.11.

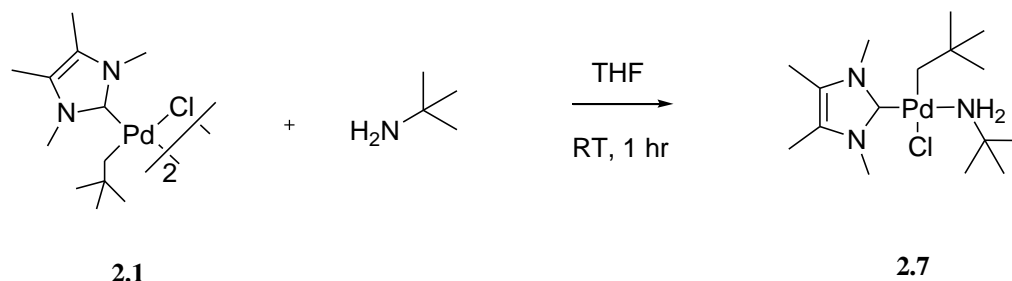


Scheme 2.12: Unsuccessful reaction of **2.1** with morpholine

It was found that **2.1** did not react with morpholine. After 48 hours at 25°C, the ^1H NMR data revealed only [Pd(ITMe)(neopentyl)($\mu\text{-Cl}$)]₂, **2.1** and free morpholine. Increasing the temperature to 40°C did not yield the desired product. Complex **70** [Pd(IPr)(neopentyl)Cl]₂ and **2.2** also did not react with morpholine. [Pd($t^t\text{Bu}$)(neopentyl)Cl]₂, **67**, however, did form the morpholide complex, [Pd($t^t\text{Bu}$)(neopentyl)(morpholine)Cl], **69**.

Morpholine is considered to have a lower binding affinity to Pd complexes than hexylamine¹⁶ so this could suggest that with these complexes, the stability of the Pd-amine complex is more strongly influenced by the amine binding affinity than by the resulting decrease in pKa afforded by complexation.¹⁷ It is unclear what accounts for the

apparent inability of the less electron rich complexes, **70**, **2.1** and **2.2** to coordinate morpholine whilst **67** is able to do so.

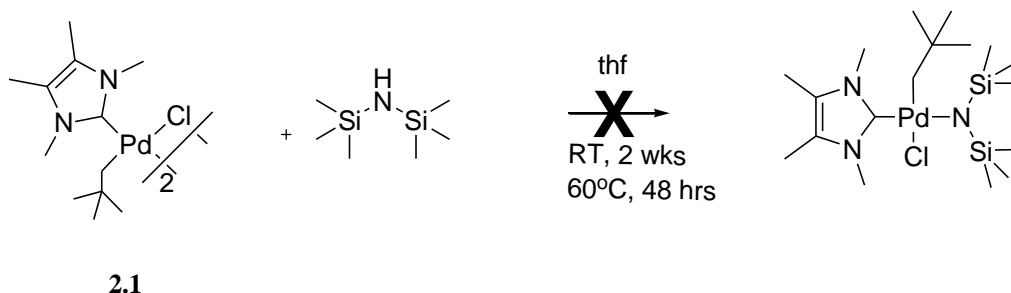


Scheme 2.13: Synthesis of Pd(ITMe)(neopentyl)(t-butylamine)Cl monomer, **2.7**

Transamination of *t*-butylamine to **2.1** was attempted (Scheme 2.13). This amine was chosen in order to produce a complex with fewer peaks in the ^1H -NMR data to facilitate monitoring of the reaction by ^1H NMR and direct comparison with the amido complex, **2.8**, would be possible (*vide supra*, Scheme 2.20, page 104).

It was unclear whether complex **2.7** was generated. Unfortunately, the product of Scheme 2.13 was more insoluble in THF than **2.6** and the ^1H NMR data acquired from a d_6 -benzene sample at RT showed possible generation of neopentyl 1,2,3,4-tetramethylimidazolium. The mass spectrum (EI) showed a peak at m/z 391 $[\text{M} - \text{CH}_3]^+$, and a peak at m/z 196 $[\text{ITMe}-\text{CH}_2(\text{CH}_3)_3]^+$. McGuinness and Cavell have also found some ITMe complexes extremely insoluble, e.g. $[\text{Pd}(\text{ITMe})_2(\text{tetracyanoethylene})]^7$ and decomposition to the alkyl imidazolium salt.

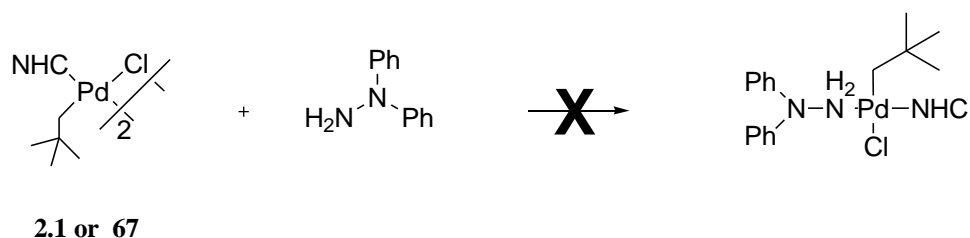
In an attempt to form an amine complex with a more electron donating amine, bis(trimethylsilyl) amine was reacted with **2.1**. However, no reaction was seen to occur before **2.1** began to degrade to unknown *NHC* fragments.



Scheme 2.14: Unsuccessful Reaction of **2.1** with bis(trimethylsilyl)amine

Numerous attempts have been made to form a hydrazine transmetallation complex with both **2.1** and **67** using 1,1-diphenylhydrazine. It was thought that the more acidic NH of the hydrazine might ease the elimination of a C-N coupling product.

However, no reaction has occurred between this hydrazine and either dimer. It is likely that the electron withdrawing nature of the NPh_2 attached to the NH_2 group has made the lone pair electrons on the NH_2 nitrogen less available for donation so the hydrazine does not form a dative bond to the palladium. Even with its more electron rich metal centre **67**, which is able to form a complex with morpholine unlike **2.1**, **2.3** and **68**, is unable to coordinate with the strongly electron deficient hydrazine.

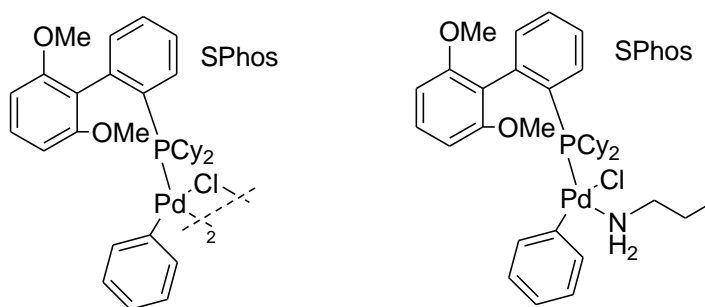


Scheme 2.15: Unsuccessful reaction of **2.1** with 1,1-diphenylhydrazine

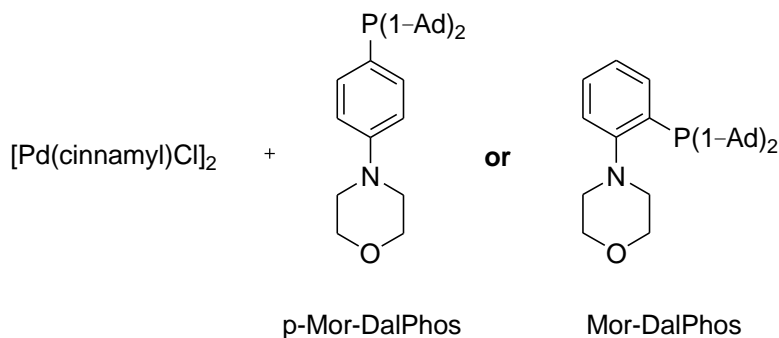
Reaction conditions: 1) **2.1**, THF, RT, 3 hrs. 2) **2.1**, THF, 60°C, 3 days 3) **67**, toluene, RT, 3 hrs 4) **67**, toluene, RT, 3 days, 5) **67**, toluene, 60°, 3 days.

This seems to be a limitation of this catalyst system. Only amines with sufficiently high binding affinities (a function of the amine's basicity and sterics) can successfully form a transamination complex. The one amine which formed a stable dative bond with the 3-membered $\text{Pd}(\text{ITMe})(\text{neopentyl})\text{Cl}$ active species was a stronger base/better nucleophile than morpholine and 1,1-diphenylhydrazine and unhindered sterically compared to all four other reactants and therefore it has a higher binding affinity.¹⁸ Thus

transmetallation complexes of this system form most readily with strong, unhindered nucleophiles.¹⁹ This parallels the findings of Tardiff *et al* when they performed competition reactions between amines using a Pd(cinnamyl)Cl/ Mor-DalPhos system (Figure 41) for aryl amination. Biscoe and Buchwald, using SPhos/Pd systems, in Figure 41, found with their particular system, competition reactions between amines were under Curtin-Hammett control, not directed by relative amine binding abilities, and thus the more acidic complex was formed.¹⁷



Biscoe and Buchwald's catalysts



Tardiff *et al*'s catalytic system

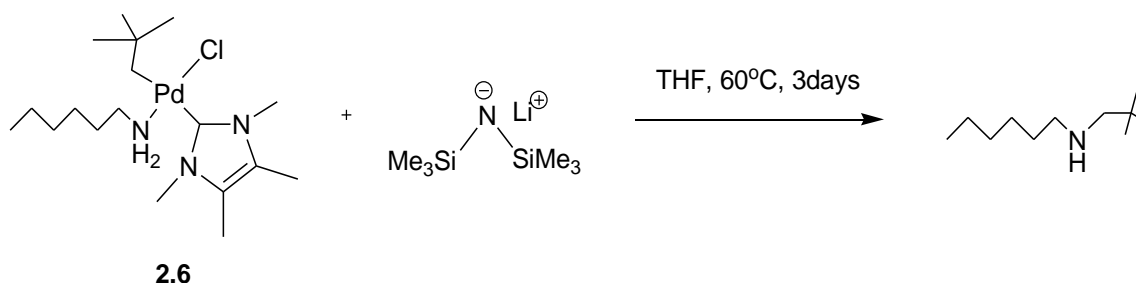
Figure 41: Catalysts used in investigating the competitive reactivity of amines for formation of aryl amination TM complexes.

This preliminary work suggests that the formation of transamination complexes in the alkyl Pd ITMe system is controlled by amine binding affinity, not the TM complexes' lowered pKa, and with reactivity of hexylamine > t-butylamine >> bis(trimethylsilyl)amine, morpholine, 1,1- diphenylhydrazine.

2.2.4 Reductive elimination of C-N coupling product

Extensive studies have been carried to achieve the elimination of the C-N coupling product from **2.6**.

The reaction was initially undertaken using alkoxy bases such as KO^tBu and sodium malonate but these brought about the decomposition of the dimer. NMR reactions were then undertaken using LHMDS in d₆-benzene. The solubility of the complex is sufficient that these could be monitored by ¹H NMR but the reaction data at 40C, 50C, and 60C were complex and no clear evidence of C-N coupling was observable. The reaction was then attempted at these same temperatures in THF and followed by GC-MS. No evidence of coupling was observed at 40 °C and 50 °C, however after 3 days at 60 °C the C-N coupling product was observed (Scheme 2.16) and its presence confirmed by accurate mass determination by HRes-ESI⁺. However, analysis run on days 4 and 5 showed the disappearance of this secondary amine and instead the presence of neopentyl 1,2,3,4- tetramethylimidazolium salt was prominent. A control reaction was performed to determine whether the C-N coupling occurred at 60 °C without base present; the alkyl amination coupling product was not observed.



Scheme 2.16: Reductive elimination of alkyl amine product from **2.6**

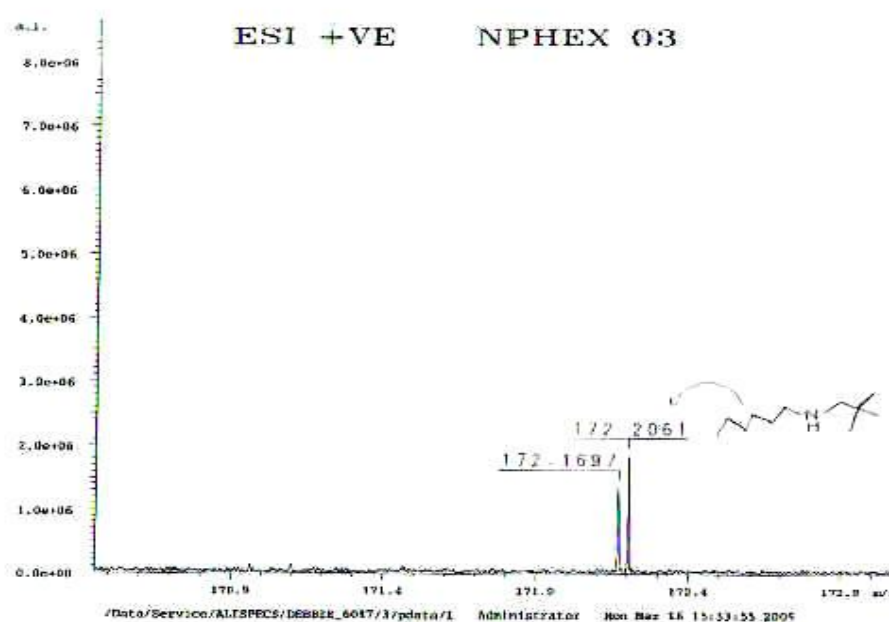


Figure 42: HRes-ESI⁺ confirming the presence of the alkyl amine product

In further attempts to make this elimination more reliable, the base AgBF_4 was used in an effort to abstract the Cl, forming AgCl , in order to facilitate the C-N coupling by forming an empty coordination site. There were solubility issues here so the initial ^1H NMR reaction was performed in d_6 -benzene with a small amount of d_8 -THF added. The ^1H NMR again showed that numerous products had formed. The most prominent product again appeared to be the alkyl-imidazolium salt. This is analogous to the results reported by Cavell and co-workers, when methyl 1,2,3,4- tetramethylimidazolium was eliminated from the complex $\text{Pd}(\text{ITMe})_2(\text{Me})\text{Cl}$, **65**.¹¹

A series of reactions were undertaken using base AgBPh_4 in THF and base LHMDs (lithium hexamethyldisilane) in both DCM and THF with reaction temperatures of 60°C . After analysis of the results, evidence of the coupling product was again seen after 3 days in the reaction run with LHMDs and THF at 60°C . The reactions with AgBPh_4 were complicated by what appeared to be phenyl-alkyl coupling products. The detection of the amine was complicated by the fragmentation patterns of secondary and tertiary amines in EI mass spectrometry where the amine peak is rarely, if ever, observed.¹⁷ Secondary amines with long alkyl chains often give mass spectrum patterns where at least one of any long straight chain alkyl substrates is commonly reduced to a methyl substrate within the amine mass spectrum fragment.²⁰ This may explain why the secondary amine coupling product molecular ion peak seemed to disappear on day 4 in

the initial study. The ESI+ technique was only to be performed after the molecular ion had been detected by MS-EI.

Another complication was the formation of the tertiary amine (Figure 42).

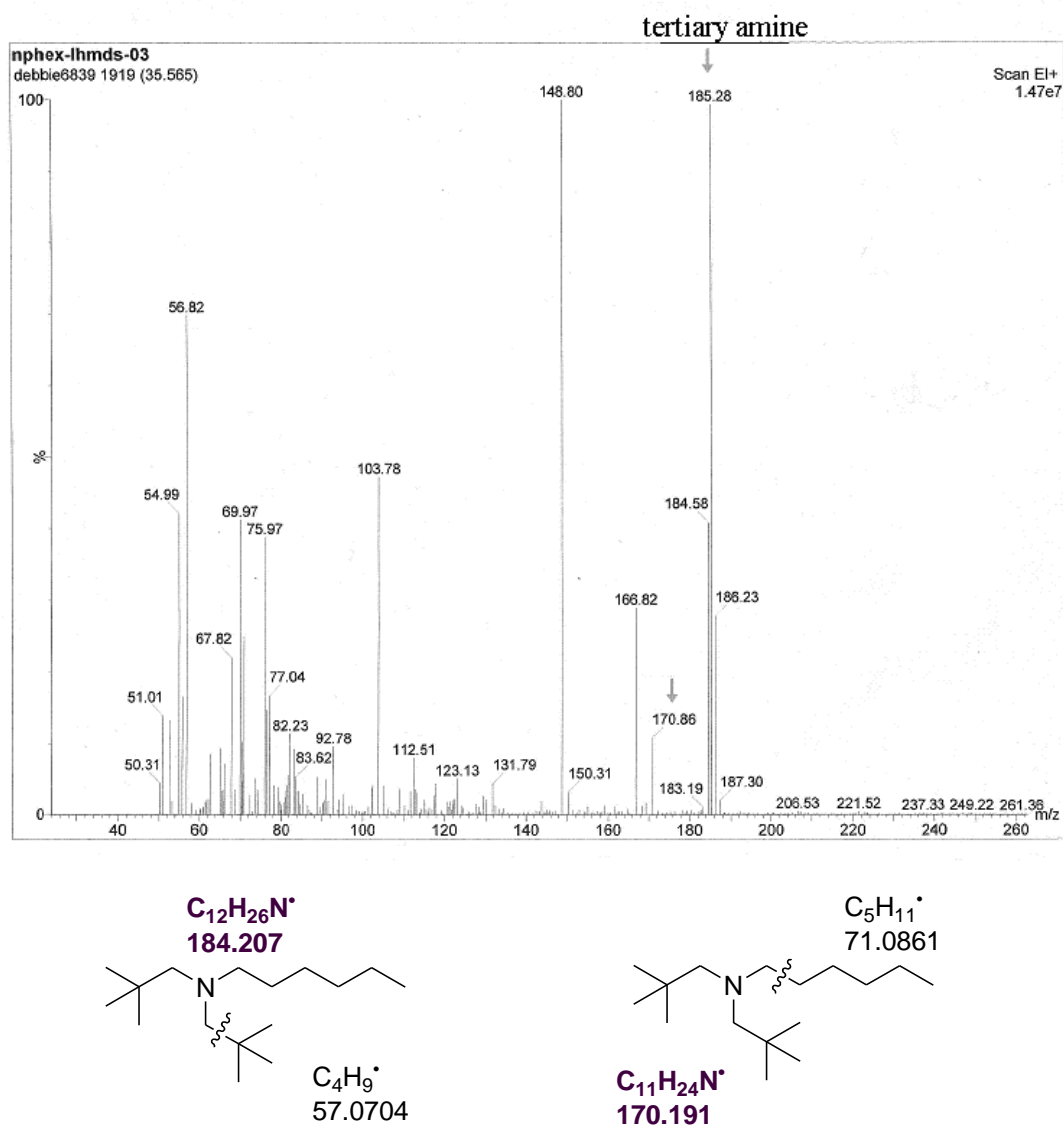
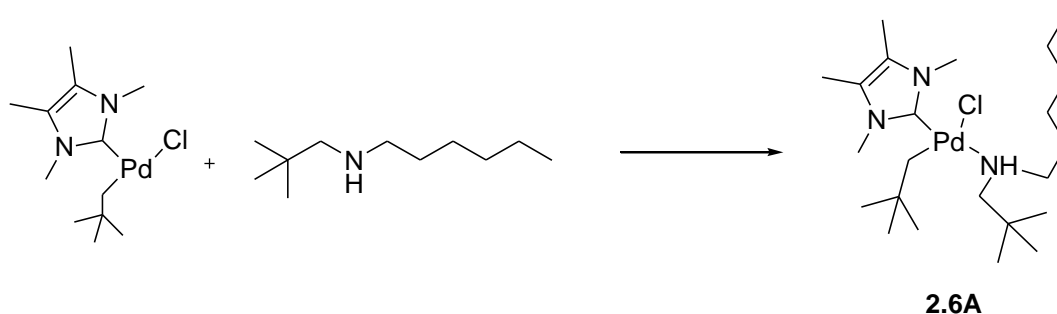


Figure 43: Mass Spectrum showing the presence of tertiary amine, *N, N*-(2-dimethylpropyl)hexylamine



Scheme 2.17: Formation of a TM complex with *N*-(2-dimethylpropyl) hexylamine, the C-N coupling product of **2.6A**

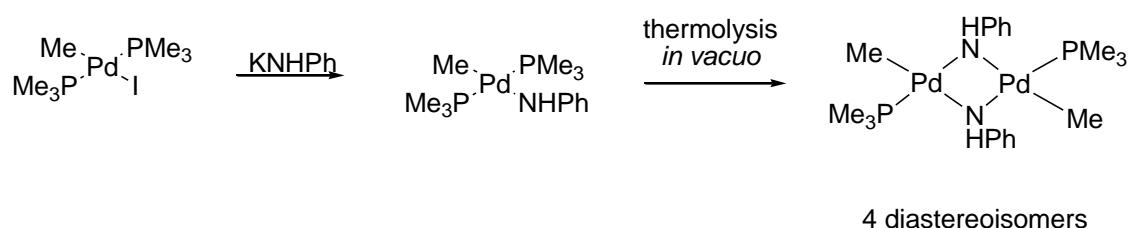
The formation of the complex **2.6A** (Scheme 2.17) has been inferred by the presence of *N*, *N*-(2,2- dimethylpropyl)hexylamine and a peak of 732 *m/z*, which would correspond to molecular ion of **2.6A**, recorded in the GC-MS data. It may be possible to prevent or at least reduce the formation of tertiary amines by the use of a larger *NHC* in order to hinder the re-coordination of the secondary amine to the catalyst. No evidence of the tetra ammonium salt was seen.

Theoretical calculations by Ryan and Caddick²¹ based on **69**, Pd(^tBu)(neopentyl)(morpholide)Cl show that there is an additional pathway which is lower in energy than reductive elimination of neopentyl morpholide; that of morpholine-assisted elimination 1,1-dimethyl cyclopropane. It is interesting that this system using hexylamine does not promote C-H bond activation of the neopentyl moiety. They calculated that the distorted T-shape of a 3 coordinate species of **69**, [(Pd(^tBu)(neopentyl)(morpholide))] meant the neopentyl group had to rotate 90° to achieve the necessary alignment with the nitrogen to facilitate C-N bond formation but, in **69**, this rotation was hindered by the ^tBu groups. The *tert*-butyl group on ^tBu has 9 coordination sites available for C-H bond activation which further increases the likelihood of C-H activation occurring as there is only one site available for C-N bond activation. Of course, the ITMe methyls would be much less likely clash sterically with the neopentyl group and so the energy required to attain a similar distorted T-shape complex, Pd(ITMe)(neopentyl)(hexylamine) should be lower.

2.2.5 Formation of the amido complexes

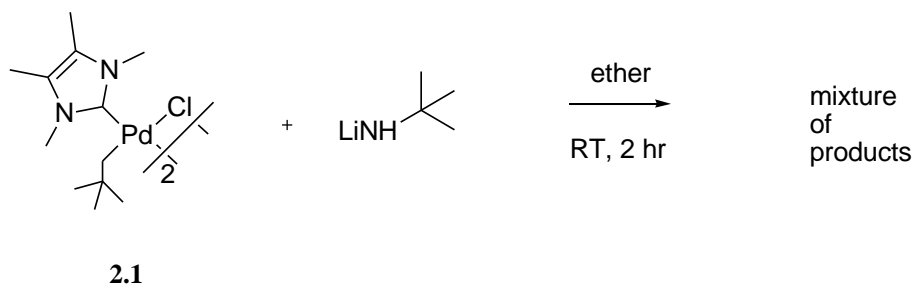
It can be seen that direct addition of an amine to an alkyl palladium complex results in stable alkyl amine complexes which, when they do form, cannot readily be deprotonated and indeed could suffer from the same problems experienced in the direct S_N2 reaction *i.e.* polyalkylation.

Indirect formation of the deprotonated alkyl amido complex can be achieved by reaction of Pd(II) species with alkali metal amide salts.^{22,23} This is a well-known protocol with aryl Pd(II) species^{24, 25, 26}. Scheme 2.18 shows an example of this synthesis with a Pd(II) alkyl complex



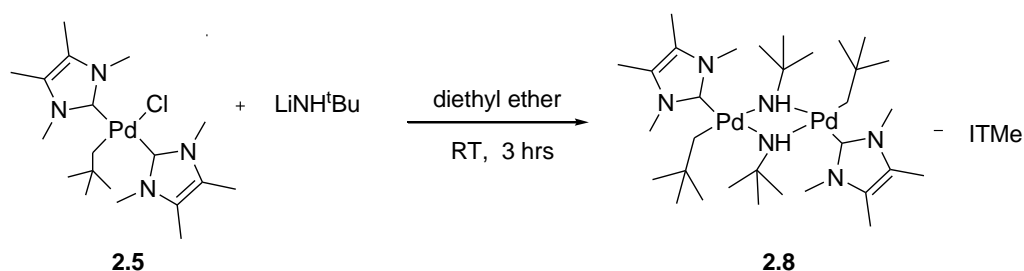
Scheme 2.18: A Pd alkyl amido complex and corresponding dimer by Villanueva *et al*²⁴

It was thought that an alkyl amido complex could be formed by this procedure. To this end, the reaction in Scheme 2.19 was attempted and the products analysed by ^1H -NMR spectroscopy. The products were numerous and it was not possible to clearly identify them.



Scheme 2.19: A mixture of products is formed by the reaction of **2.1** with lithium *tert*-butyl amide

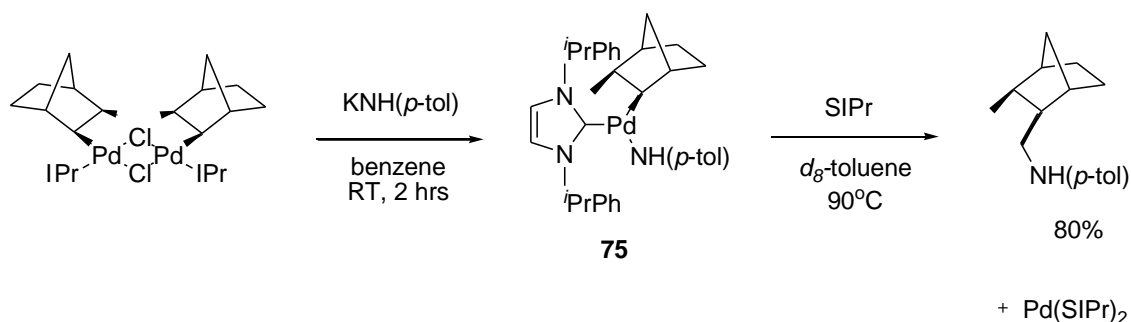
The reaction was then attempted with the more soluble $\text{Pd}(\text{ITMe})_2(\text{neopentyl})\text{Cl}$, **2.5**, and lithium *tert*-butyl amide (Scheme 2.20). The reaction products were identified by ^1H -NMR and were found to be the amido dimer, **2.8**, indicated by integration of peaks and the presence of a peak, corresponding to the one amide hydrogen, at -0.06 ppm (Scheme 2.20) and free ITMe.



Scheme 2.20: Formation of $[\text{Pd}(\text{ITMe})(\text{neopentyl})(\mu\text{-}^t\text{BuNH})]_2$, **2.8**, which was not isolated.

It proved difficult to separate the dimer and the ITMe and so the two species were heated together to induce reductive elimination. Unfortunately, heating to 70 °C resulted in no elimination before the complex started to degrade to palladium black. When the reaction was attempted using lithium morpholide, no amido complex was formed.

Hartwig and co-workers have recently achieved reductive elimination of an alkyl amine from a similar complex, **75**, $[(\text{IPr})\text{Pd}(\text{2-CH}_3\text{-norbornyl})(\text{NHAr})]$ depicted in Scheme 2.20.²⁷

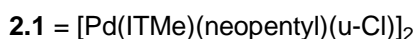
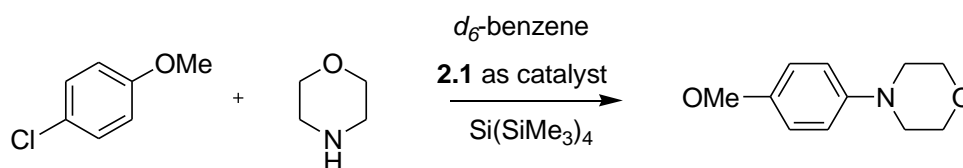


Scheme 2.21: Formation of and reductive elimination from **75**, $[(\text{IPr})\text{Pd}(\text{2-CH}_3\text{-norbornyl})(\text{NHAr})]$ ²⁷

The significant difference between **2.8**, [Pd(ITMe)(neopentyl)(μ -NH^tBu)] (Scheme 2.20), and **75** is one of size. Each alternative substrate in **75** is much bulkier than in **2.8**, so much so that **75** exists quite stably as a 3 co-ordinate complex and is so crowded that it does not adopt the T shaped geometry which is typical of a 3 co-ordinate complex of this nature²⁷. Hence, **75** is better primed to reductively eliminate than the smaller dimeric species, **2.8**, which would find it more energetically unfavourable to form a 3 co-ordinate complex.²¹

However, this result does inform on why reductive elimination from **2.6** [(Pd(ITMe)(neopentyl)(hexylamine)Cl)] can occur. Whilst the amido dimer may not readily form the 3 coordinate species, once **2.6** is de-protonated, it is likely that the neopentyl group will still provide sufficient steric bulk to induce reductive elimination and indeed, the theoretical calculations of Caddick and Ryan suggest that reductive elimination of alkyl amine coupling product will be exothermic, giving an calculated figure of -102.9 KJmol⁻¹ for the elimination of neopentyl morpholide from [Pd(^tBu)(neopentyl)(morpholide)Cl] species²¹.

2.2.6 Aryl amination catalytic activity of **2.1**.



Scheme 2.22: Catalytic coupling of 4-chloroanisole and morpholine

Scheme 2.22 depicts the reaction conducted on an NMR scale in *d*₆-benzene using NaOCEt₃ as base at 5% mol catalyst, **2.1** and Si(SiMe₃)₄ as the internal standard for integration. No coupling was seen after 18 hours, however, new peaks were seen at 7.29-7.31 ppm, 6.86-6.84 ppm, 6.60 ppm, 3.39 ppm and 3.33 ppm.

Indeed, there are new peaks at 0.16 ppm and 0.11 ppm and smaller peaks to -0.04 ppm upfield from the Si(SiMe₃)₄ peak. This raises the possibility that the NMR standard, Si(SiMe₃)₄, has had a non-innocent interaction with **2.1**. Pd(ITMe)₂, **71**, has been found to react with this internal standard and the product affect isomerisation of 4-chloroanisole to 3-chloroanisole. This would therefore suggest that 4-chloroanisole has been partly isomerised to 3-chloroanisole (see Chapter 3).

The isomerisation was more than 90% complete after 6 hours 20 mins with the ratio of p-isomer: m-isomer of 55:45. This isomerisation strongly suggests an aryne or radical mechanism. In Chapter 3, this behaviour of Pd-ITMe systems is discussed in further detail.

GC-MS experiments were conducted using dodecane as the standard. In the absence of the Si(SiMe₃)₄ species, the results are tabulated in Table 2.2 and show complete conversion to p-anisole morpholide after 13 days at 60°C in THF by the complex **2.1**; catalytic activity that, whilst poorer than analogous SIPr and I^tBu alkyl complexes⁷, **67** and **70**, is considerably better than Pd(ITMe)₂.

Complex	Solvent	Base	Temperature	Time	Yield
70 (IPr)	THF	LHMDS	40° C	1 hr	99% ⁵
67 (I^tBu)	Toluene	NaOCEt ₃	90°C	1.5 hrs	37% ⁵
2.1 (ITMe)	THF	NaOCEt ₃	60° C	13 days	> 95%
71 (ITMe)	<i>d</i> ₆ -benzene	NaOCEt ₃	80° C	42 days	>5%

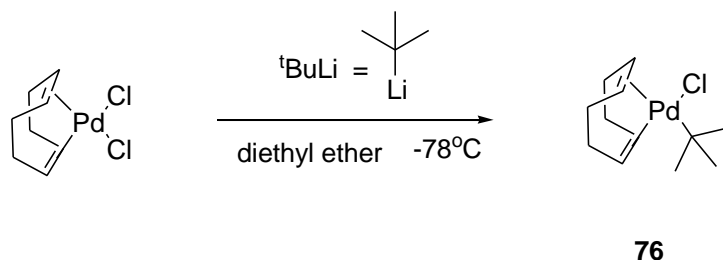
Table 2.2: Selected examples of Pd(*NHC*) complexes as pre-catalysts for the reaction in Scheme 2.22⁷

Table 2.2 shows comparison of catalysts containing IPr, I^tBu and ITMe. ITMe complex, **71**, is a bis-*NHC* complex whilst **2.1** is a monoligated *NHC* complex.

This is a clear example of the steric bulk of the *NHC* influencing the catalytic activity and that a monochelated *NHC* complex performs better than a bis-ligated one.

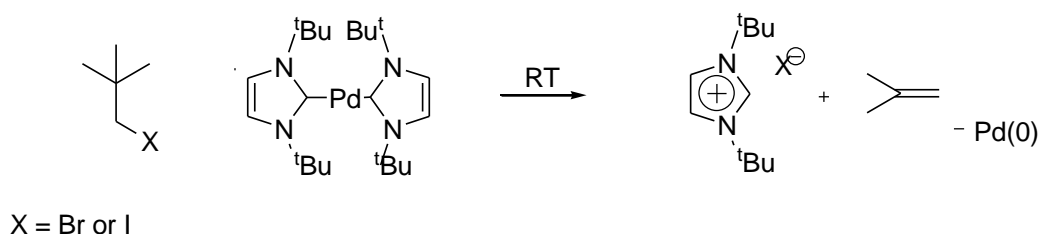
2.2.7 Attempts towards the preparation of alkyl palladium *NHC* complex in which the alkyl moiety has β -hydrogens.

We thought that the indirect method described in Scheme 2.3 should be attempted with a β hydrogen-containing alkyl species to see what would occur with regards to β hydrogen elimination. Scheme 2.23 shows the desired result.



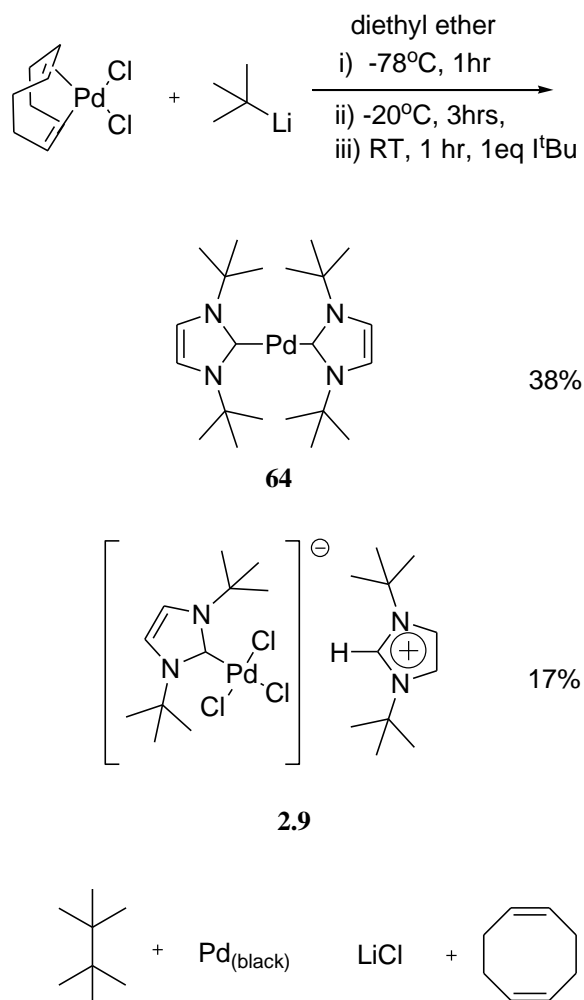
Scheme 2.23: Desired reaction; Formation of species **76**

Theoretical calculations show that β hydrogen elimination is energetically favoured²⁷ and previous attempts to isolate a stable *NHC* β -hydrogen-containing alkyl palladium by oxidative addition of *t*-butyl bromide or iodide at $\text{Pd}(\text{tBu})_2$ (**64**) were unsuccessful as β -hydrogen elimination produce the imidazolium salt and isobutene (Scheme 2.24)¹⁵.



Scheme 2.24: Reaction of **64** with *tert*-butyl bromide/ iodide

It was decided best not to try to isolate $[\text{Pd}(\text{1,5 COD})(2,2\text{-dimethylpropane})\text{Cl}]$, **76** (Scheme 2.23) as prevention of β -hydride elimination before ligand exchange might prove difficult. It was to be generated *in situ*. Scheme 2.25 depicts the reaction undertaken and its products.



Yields are approximate and based on NMR ratios and crude product weight

Scheme 2.25: Reaction of $\text{Pd}(1,5\text{ COD})\text{Cl}_2$ with $^t\text{BuLi}$ and 1^tBu

Crystals of **64** were grown in hexane at -20°C after 2 days. The crystals of the trichloropalladate imidazolium salt, **2.9**, were grown at RT in an NMR tube of the crude product of d_6 -benzene after 2 weeks.

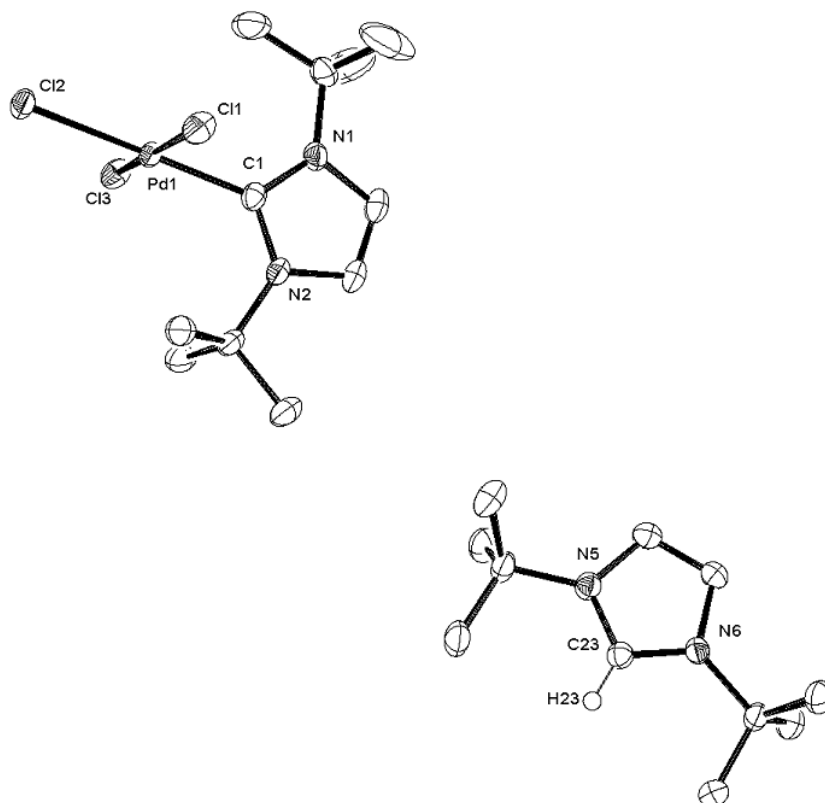


Figure 44: Ortep diagram of the molecular structure of $[\text{Pd}(\text{I}^t\text{Bu})\text{Cl}_3]^- [\text{I}^t\text{BuH}]^+$, **2.9** showing 50% thermal ellipsoids.

Hydrogens omitted for clarity, excepting imidazolium hydrogen on C23.

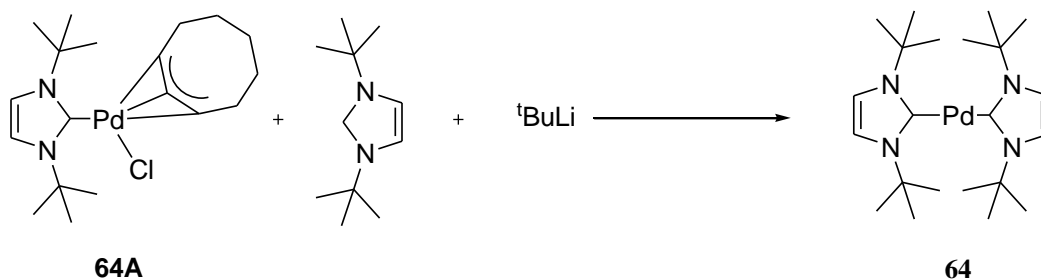
Selected bond lengths (Å) and angles(°):

Pd1–Cl1, 2.3258(6); Pd1–Cl3 2.3362(6); Pd1–Cl2 2.3696(6); C1–Pd 1.967(2);

C1–Pd1–Cl3 88.96(7); Cl1–Pd1–Cl2 91.77(2); Cl3–Pd1–Cl2 91.92(2);

N1–C1–Pd1–Cl1 –86.4(2); N1–C1–N2 105.6(2); N5–C23–N6 109.3(2).

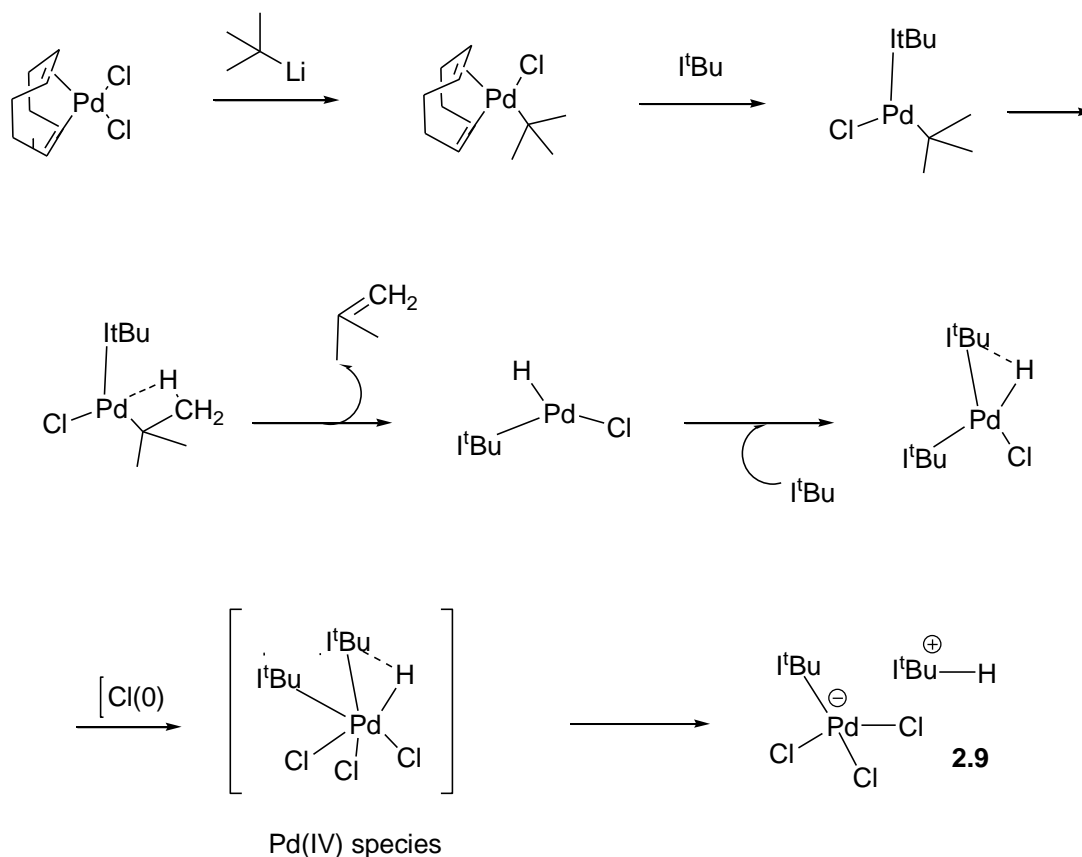
The mechanism for the formation of **64** in this reaction is based upon the general method used within our group to produce $\text{Pd}(\text{NHC})_2$ complexes²⁸ and the isomerisation of 1,5 COD by UV light to 1,3, COD²⁹. The reaction vessel is lagged with aluminium foil during the time it is kept at -78°C but this is not vigorously adhered to and after removal from the dry ice bath, the lagging is generally removed. The reaction is shown in Scheme 2.25; in the instance the $^t\text{BuLi}$ is acting as a reducing agent and not an alkylating agent The ^1H -NMR data shows small peaks which can be attributed to **64A** (Scheme 2.25).



Scheme 2.25: Reaction to form **64** from Pd(1,5 COD)Cl_2 and I^tBu with tBuLi as base

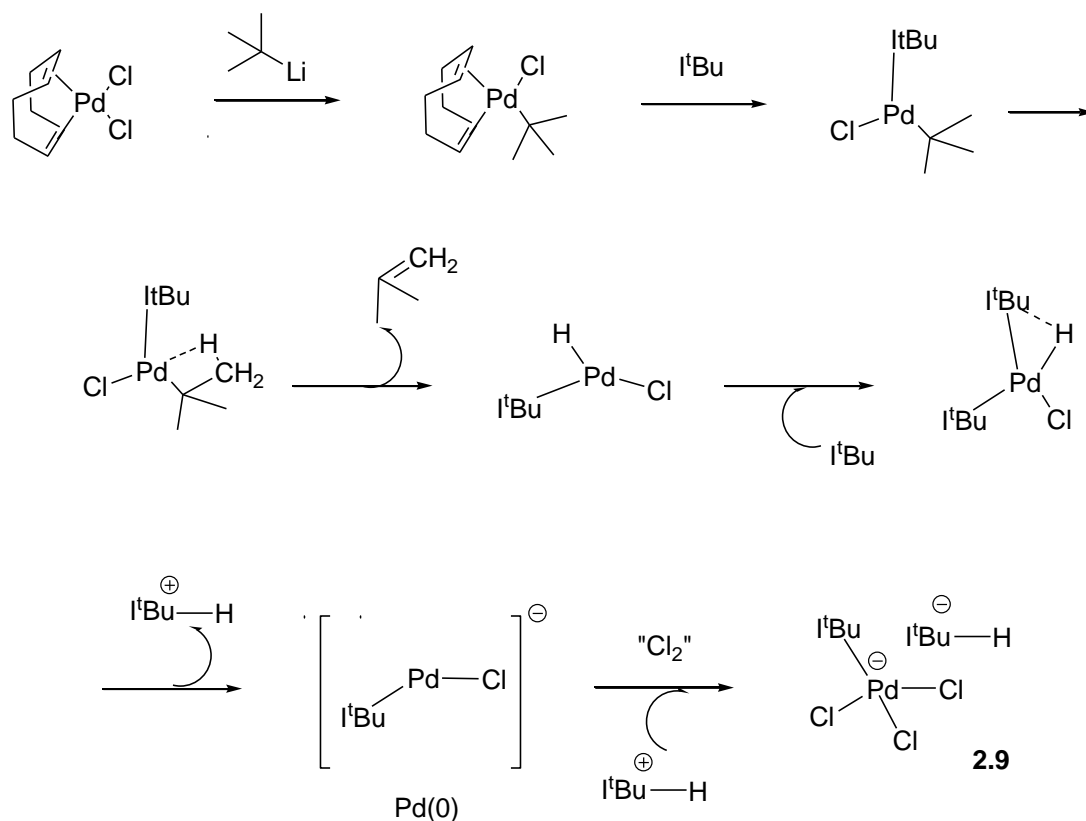
The formation of **2.9** could be attributed to β hydride elimination from $[\text{Pd}(\text{I}^t\text{Bu})(2,2\text{-dimethylpropane})\text{Cl}]$ of 1,1- dimethylpropene followed by chlorination of the hydrido complex (Schemes 2.26 and 2.27).

Danopoulos *et al* saw a similar reaction using the bis-chelating mixed phosphine-*NHC*, 3-(2,6-diisopropylphenyl)-1-(β -(diphenylphosphino)ethyl)imidazolydene³⁰. In their case the bis-chelating ligand meant that the proposed mechanism involved a Pd(IV) complex. Scheme 2.26 shows the proposed mechanism based on this work.



Scheme 2.26: Mechanism for the formation of **2.9** involving a Pd(IV) intermediate

Work by de Vries *et al*³¹ suggested a different mechanism. They have been working with palladium nanoparticles for ligand-free cross coupling reactions. The system they use is $\text{PdCl}_2/\text{NaCl}$ without any ligands. Scheme 2.27 is based on their proposed catalytic cycle where they observe PdCl_3^-



Scheme 2.27 Mechanism for the formation of **2.9** based on a $\text{Pd}(0)$ intermediate.

In both cases, oxidation of Cl^- occurs to form Cl_2 but the oxidising agent is unknown³¹ unless it is a disproportionation with the formation of **64**, where the identity of the reducing agent is unclear.

This reaction is a new method by which to make $\text{Pd}(\text{I}^t\text{Bu})_2$ and possibly other $\text{Pd}(\text{NHC})_2$ complexes that prove difficult to achieve using the original method. However, whilst it may be less wasteful with regards to NHC consumption, it does not have good atom economy.

2.3 Conclusions

Reductive elimination of a secondary alkyl amine has been achieved from [Pd(ITMe)(neopentyl)(hexylamine)Cl], though the reaction is not yet optimised and can be complicated by side-reactions. Use of bulky *NHCs* in alkyl amination may be detrimental to this procedure, encouraging secondary pathways of complex disintegration, however the use of ITMe in the complexes led to poor solubility of the complexes which limited the conditions which could be investigated. Use of the ICy ligand led to difficulty in separating the various co-products formed. It is considered that the next *NHC* used in these investigations should be an aryl with no substitution at the ortho position or an ethyl or isopropyl *NHC* with ethyl groups on the C4-C5 unsaturated backbone to improve solubility³².

[Pd(ITMe)(neopentyl)Cl]₂ as an aryl amination catalyst has higher activity than Pd(ITMe)₂, though both are poor and require days at elevated temperatures to achieve coupling. There was also evidence of a non-innocent interaction with Si(SiMe₃)₄, and isomerisation of *p* isomer to *m* isomer which mirrors a similar result in Chapter 3, where it shall be discussed further.

Indirect attempts to form an analogous complex to the neopentyl one with *t*-butyl were undermined by the *t*-butyl lithium being a superior reducing agent to neopentyl lithium and the expected β-hydrogen elimination. However, this led to a new method for the production of Pd(I^{*t*}Bu)₂.

2.4 Experimental Section

For general experimental, see Appendix I; X-ray crystallography data, see Appendix II. PdCl₂ was prepared from K₂PdCl₄, supplied by Aldrich, using Amberlite IR120 cation exchange resin in the H⁺ form³³. K₂PdCl₄ is dissolved in water and passed through the resin. The H₂PdCl₄ eluent had the solvent removed by rotor vaporator to leave the solid PdCl₂. Pd(1,5-COD)(neopentyl)Cl, ITMe, ICy and I^tBu were synthesised according to literature procedures³⁴. 1,5-cyclooctadiene, morpholine, ^tbutylamine, *n*-hexylamine, trimethylsilyl amine, 1,1-diphenylhydrazine hydrochloride were purchased from Aldrich and dried over activated 3Å molecular sieves, degassed and vacuum transferred into ampoules equipped with greaseless stopcocks. Solid ^tbutyl lithium was purchased from Aldrich and kept at 4°C in a dry glove box.

1,1-diphenylhydrazine³⁵ and neopentyl lithium³⁶ were prepared from literature procedures.

2.4.1. Synthesis of [Pd(ITMe)(neopentyl)(Cl)]₂, 2.1.

Pd(1,5-COD)(neopentyl)Cl (0.492 g; 1.5 mmol) was placed in a Schlenk tube, dissolved in 20 mL of THF at RT. ITMe (0.19 g, 1 equiv.) was weighed in a dry box, dissolved in 5 mL of THF and transferred into the (neopentyl)Pd(Cl)(1,5-COD) solution *via* cannula. The reaction was stirred for 1 hour, during which time the dimer product precipitated. It was left to settle then the mother-liquor was decanted from the product *via* a thin cannula. The product was washed with pentane (2 x 10 mL) and Et₂O (15 mL) yielding the desired complex as a chalky white powder.

The product was obtained in 48% yield

¹H NMR(*d*₈-THF): 3.96 ppm (s, 12H, NCH₃ (*NHC*)), 2.14 ppm (s, 12H CH₃ (*NHC* C=C)), 0.87 ppm (s, 18H, CH₃ (neopentyl)), 0.68 ppm (s, 4H, CH₂ (neopentyl)), ¹³C{¹H} NMR(*d*₈-THF): 153.46 (Pd-C(*carbene*)), 122.69 (NC=CN), , 9.26 CH₃C=C(CH₃),) **MS (ES):** *m/z* 657 [M⁺ - 2CH₃]⁺, 615 [M - CH₂C(CH₃)₃]⁺ **Elemental analysis:** Anal. Calc'd. for C₁₂H₂₃N₂ClPd: C: 42.77, H: 6.99, N: 8.17. Found: C: 42.79, H: 6.90, N: 8.19.

Attempts to grow crystals have been made using THF, DCM as well as THF layered with toluene, and vapour deposition of diethyl ether towards a THF solution, saturated with **2.1**. No crystals found.

2.4.2. Synthesis of *cis*-[Pd(ITMe)₂Cl₂], 72.

The Pd(1,5-COD)(neopentyl)Cl (0.492 g; 1.5 mmol) was placed in a Schlenk tube, dissolved in 20 mL of THF at RT. ITMe (0.19 g, 1 equiv.) was weighed in a dry box, dissolved in 5 mL of THF and transferred into the (neopentyl)Pd(Cl)(1,5-COD) solution *via* cannula. The reaction was stirred for 1 hour, during which time the dimer product precipitated. It was left to settle then the liquor was decanted from the product via a thin cannula. The product was washed with pentane (2 x 10 mL) and with Et₂O (15 mL) yielding a chalky white powder. After 2 months dissolved in THF, small needle crystals of **72** had formed.

¹H NMR: agreed with literature reference¹³

MS (ES): 230 *m/z* (Pd(ITMe)⁺)

Crystals suitable for X-ray analysis grown in THF.

2.4.3. Synthesis of *trans*-[Pd(ICy)(neopentyl)(μ-Cl)]₂, 2.2.

[Pd(1,5-COD)(neopentyl)Cl] (0.492 g; 1.5 mmol) was placed in a Schlenk tube, dissolved in 20 mL of THF at RT. ICy (0.19 g, 1 equiv.) was weighed in a dry box, dissolved in 5 mL of THF and transferred into the [Pd(1,5-COD)(neopentyl)Cl] solution *via* cannula. The dark yellow reaction was stirred for 2 hours, during which time the reaction solution darkened to brown. The THF solvent was removed *in vacuo*, washed in cold pentane (2 x 5 ml) and the pale brown product was re-dissolved in Et₂O. The solution was filtered through cannula and the product crystallized after 3 days at -20 °C. The product was obtained in 22% yield.

¹H NMR(*d*₆-benzene): 6.40 ppm (s, 4H, CH (_{NHC} C=C)), 5.52 ppm (m: 4H, CH, (_{NHC} CH(cy))), 2.25 ppm (s, 4H), 1.91-0.90 ppm (m, 80H, CH₂ (_{NHC} cyclohexyl)), 1.24 ppm (s, 18H, CH₃ (neopentyl)), 0.69 ppm (s, 4H, CH₂ (neopentyl)) ¹³C{¹H} NMR: not resolved MS (ES): 642 [M - ICy - CH₃]⁺, 631 [M - ICy - (CH₃)₂]⁺, 601 [M - ICy - CH(CH₃)₃]⁺

Crystals unsuitable for X-ray analysis grown in diethyl ether at -20°C after 3 days.

2.4.4. Synthesis of *trans*-[Pd(ICy)₂Cl₂], 2.3.

Pd(1,5-COD)(neopentyl)Cl (0.492 g; 1.5 mmol) was placed in a Schlenk tube, dissolved in 20 mL of THF at 0°C. ICy (0.19 g, 1 equiv.) was weighed in a dry box, dissolved in 5 mL of THF and transferred into the Pd(1,5-COD)(neopentyl)Cl solution *via* cannula

whereupon the solution darkened. The dark yellow solution was stirred for 2 hours, during which time the reaction solution further darkened to brown. The THF solvent was removed *in vacuo* and the brownish-white product was washed with 2 x 10 mL of pentane. Crystals suitable for X-ray diffraction were grown after 6 days at 4°C. The product was obtained in 22% yield.

^1H NMR(d_6 -benzene): 6.53 ppm (m, H, CH ($\text{NHC C}=\text{C}$)), 2.97-3.00 ppm (m, 4H, CH, ($\text{NHC CH}(\text{cy})$)), 1.91-0.90 ppm (m, 40H, CH₂ (NHC cyclohexyl)) **$^{13}\text{C}\{^1\text{H}\}$ NMR**: could not be assigned
MS (ES): 642 [M]⁺, 606 ([M - Cl]⁺), 569 [M - 2Cl]⁺ Crystals suitable for X-ray analysis grown in pentane.

2.2.5. Synthesis of [Pd(ITMe)₂(neopentyl)(Cl)], 2.4.

1) The Pd(1,5-COD)(neopentyl)Cl (0.29 g; 0.9 mmol) was placed in a Schlenk tube, dissolved in 20 mL of THF at RT. ITMe (0.23 g, 2 equiv.) was weighed in a dry box, dissolved in 5 mL of THF and transferred into the Pd(1,5-COD)(neopentyl)Cl solution via cannula. The reaction was stirred for 1 hour then the THF was removed *in vacuo*. The product was washed with pentane (2 x 10 mL) and with Et₂O (15 mL) yielding the desired complex as a chalky white powder. The product was obtained in 70% yield.

2) Alternatively, two Schlenk tubes were prepared in the dry glove box, one with 0.04 g (5.93 x 10⁻⁵ mol) of [Pd(ITMe)(neopentyl)Cl]₂ and one with 0.31 g of ITMe (2.49 x 10⁻⁴ mol, 5 eq.). The two Schlenk tubes were cycled onto the Schlenk line, then 5 mL of THF was added to the ITMe and 10 mL to the [Pd(ITMe)(neopentyl)Cl]₂. The ITMe solution was transferred via cannula to the [Pd(ITMe)(neopentyl)Cl]₂ suspension. The cloudy solution initially turned a clear pale yellow before a white precipitate reappeared within a minute. After 2 hours at RT, the THF was removed *in vacuo* and the chalky white powder remaining was washed in 2 x 5 mL pentane and 5 mL cold THF.

^1H NMR(d_8 -THF): 3.87 ppm (s, 12H, (s, 6H, NCH₃ (NHC)), 1.64 ppm (s, 2H, CH₂ (neopentyl)), 1.43 ppm (s, 12H CH₃ ($\text{NHC C}=\text{C}$)), 1.09 ppm (s, 9H, CH₃ (neopentyl)) **$^{13}\text{C}\{^1\text{H}\}$ NMR** (d_6 -benzene): 164.4 (Pd-C(carbene)), 124.3 (NC=CN), 83.28 (N(CH₃), 35.73 (C(CH₃)), 34.02 (C(C(CH₃)), 32.72 (C(carbene)(C(CH₃)), 29.53 (CH₂C(CH₃)) **MS (ES)**: m/z 425 (M⁺), 391 (M⁺ - Cl - CH₃) **Elemental analysis**: Not found

2.2.6. Synthesis of *trans*-[Pd(ICy)₂(neopentyl)(Cl)], 2.5.

The Pd(1,5-COD)(neopentyl)Cl (0.212 g, 1.5 mmol) was placed in a Schlenk tube, dissolved in 20 mL of THF at RT. ICy (0.77 g, 5 equiv.) was weighed in a dry box, dissolved in 5 mL of THF and transferred into the (neopentyl)Pd(Cl)(1,5-COD) solution *via* cannula technique. The dark yellow reaction was stirred for 2 hours, during which time the reaction solution darkened to brown. The THF solvent was removed in vacuo and the browny-white product was re-dissolved in Et₂O. The solution was filter cannulaed into a Schlenk tube and the product recrystallized out of solution after 3 days at -20°C. The product was obtained in 17% yield.

¹H NMR(*d*₆-benzene): 6.40 ppm (s, br, 4H, CH (*NHC* C=C)), 5.55- 5.49 ppm (m: 4H, CH, (*NHC* CH(cy))), 2.35 ppm (s, 4H), 1.72-1.51 ppm (m, 16H, CH₂ (*NHC* cyclohexyl)), 1.44-1.21 ppm (m, 18H, CH₂ (*NHC* cyclohexyl)), 1.15- 0.96 ppm (m, 8H, CH₂ (*NHC* cyclohexyl)), 1.24 ppm (s, 9H, CH₃ (neopentyl)), 1.03 ppm (s, 2H, CH₂ (neopentyl)) ¹³C NMR(*d*₆-benzene): Could not be resolved MS (EI): *m/z* 651[M – 2CH₃]⁺, 642 [M-Cl]⁺, 605 [M-CH₂C(CH₃)₃]⁺, 337 [ICy- CH₂C(CH₃)₃] Elemental analysis: Not found

Crystals suitable for X-ray diffraction were grown from diethyl ether.

2.2.7. Synthesis of Pd(ITMe)(neopentyl)(hexylamine)chloride complex, 2.6

An ampoule was taken into the dry glove box and charged with [Pd(ITMe)(neopentyl)(μ-Cl)]₂ (0.043 g; 0.063 mmol). Once the ampoule was cycled onto the Schlenk Line, 10ml of THF was added. The hexylamine: (3 eq., 0.025ml) was injected into the ampoule *via* syringe, and the reaction solution stirred at RT for two hours. After that time, the solvent and the excess of amine were removed under reduced pressure. A white solid was recovered. This was re-dissolved in ether and the solution was filter using a filter cannula. The ether was removed in vacuo and the resulting white solid was washed with 2 x 10ml of pentane. Crystal growth was unsuccessfully attempted from diethyl ether at -20°C. Yield= 78%

¹H NMR (*d*₆-benzene): 3.76 ppm (s, 6H, NCH₃ (*NHC*)), 2.84-2.82 ppm (broad q, 2H, NH₂, J_(H-H)= 7 Hz), 2.23-2.22 ppm (br, s, 2H, CH₂ (hexylamine)), 1.95 ppm (s, 6H, CH₃ (*NHC* C=C)), 1.54-1.51 ppm (m, 2H, CH₂ (hexylamine)), 1.30-1.17 ppm (m, 4H, CH₂ (hexylamine)), 1.25- 1.19 ppm (m, CH₂ (hexylamine)), 1.24 ppm (s, 2H, CH₂ (neopentyl)), 0.80-0.78 ppm (t,

3H, CH₃ (hexylamine), $J_{(H-H)} = 6.90$ Hz), 0.72 ppm (s, 9H, CH₃ (neopentyl)) ¹³C{¹H} NMR: sample too dilute **MS (ES):** m/z 425 ($M^+ - CH_3$), 391 ($M^+ - Cl - CH_3$) **Elemental analysis:** Anal. Calc'd. for C₁₈H₃₆N₃PdCl: C: 49.61, H: 8.32, N: 9.58. Found C: 49.62, H: 8.36, N: 9.58.

2.2.8. Synthesis of Pd(ITMe)(neopentyl)(*t*-butylamine)chloride, 2.7.

An ampoule was taken into the dry glove box and charged with [Pd(ITMe)(neopentyl)(μ-Cl)]₂ (0.043 g; 0.063 mmol). Once the ampoule was cycled onto the Schlenk Line, 10ml of THF was added. The *t*-butylamine: (6 eq., 39 ml) was injected into the ampoule *via* syringe, and the reaction solution stirred at RT for two hours. After that time, the solvent and the excess of amine were removed under reduced pressure. A white solid was recovered. This was washed with 2x10ml pentane then re-dissolved in THF. The white solid which was insoluble in THF was collected by removal of the solvent by filter cannula. Yield= 62%

¹H NMR (*d*₆-benzene): 3.88 ppm (s, 6H, NCH₃ (*NHC*)), 3.04 ppm (broad q, 2H, NH₂, $J_{(H-H)} = 7$ Hz), 2.08 ppm (s, 6H, (*NHC* C=C)), 0.85 ppm (s, 9H, CH₃ (*t*-butylamine)), 0.67 ppm (s, 9H, CH₃ (neopentyl)) ¹³C{¹H} NMR: sample decomposed in solution **MS (ES):** m/z 391 [$M - CH_3$]⁺, 196 [ITMe-CH₂(CH₃)₃]⁺ **Elemental analysis:** Not found. Compound decomposed readily in solution.

2.2.9. Synthesis of {[Pd(I^{*t*}Bu)Cl₃]⁻ [I^{*t*}BuH]⁺}, 2.9.

The [Pd(1,5-COD)Cl₂] (0.334 g; 1.17 mmol) was placed in a ampoule and suspended in 50 ml of diethyl ether, then stirred and cooled to -78°C. 0.0824g of solid ^{*t*}BuLi (1.29 mmol, 1.1 eq) was placed in another ampoule in the dry glove box. This ampoule was cycled onto the Schlenk line and dissolved in 20 mL of cold diethyl ether (-78°C) and stirred. This solution of ^{*t*}BuLi was added very slowly drop-wise to the [Pd(1,5-COD)Cl₂] diethyl ether suspension which had been lagged with cotton wool and aluminium foil. After an hour the reaction was transferred to an IMS/dry ice bath and kept at -20°C for 3 hours. The black solution/suspension was filtered via filter cannula then I^{*t*}Bu (1 eq., 0.2109g, 1.17mmol) was added to the resulting dark yellow solution and the solution is stirred for an hour at RT. The diethyl ether is then removed in vacuo, the resulting dark yellow solid is washed with 2x10ml of cold pentane (0°C) and then

dissolved in petroleum ether/ hexane and left at -30C for 5 days. Dark yellow crystals of $[\text{Pd}(\text{I}^t\text{Bu})\text{Cl}_3]^- [\text{I}^t\text{BuH}]^+$ co-crystallise out of solution with $\text{Pd}(\text{I}^t\text{Bu})_2$.

^1H NMR: (d_6 -benzene): 6.96 ppm (s, 2H, CH ($\text{NHC C}=\text{C}$)), 6.61 ppm s, 2H, CH ($\text{NHC C}=\text{C}$)), 1.48 ppm (s, 12H), CH_3 (NHC t-butyl) imidazolium H peak not observed **$^{13}\text{C}\{^1\text{H}\}$ NMR:** could not be resolved **MS (ES):** m/z 285 $[\text{M} - 3\text{Cl}]^+$, 179 $[\text{I}^t\text{Bu}]^+$ **Elemental analysis:** Not found. Crystals suitable for X-ray crystallography grown in d_6 -benzene after 3 weeks.

General procedure for catalyst testing: NMR

An NMR tube with a Young's tap, 2 syringes, 3 glass weighing boats and a 5ml beaker are taken into the dry glove box. The base, the internal standard and the catalyst are weighed out. 0.6ml of NMR solvent is pipetted into the 5ml beaker and the required quantity of morpholine and 4-chloroanisole are transferred by syringe into the solvent. The NMR internal standard is added, then the catalyst, and the solution is stirred. Finally, the base is added and the reaction solution is transferred *via* pipette to the NMR tube then gently agitated. An initial NMR scan is taken. The NMR tube is then placed in a heating block at the designated reaction temperature and NMR scans are taken at appropriate times during the reaction length.

General procedure for catalyst testing: GC-MS

A 100ml ampoule with a Young's tap with a magnetic stirrer bar and a glass weighing boat are taken into the dry glove box. The catalyst is weighed out and put into the ampoule, which is sealed. The ampoule is cycled 3 times onto the Schlenk vacuum line. A suba-seal is placed on the ampoule's opening and dry, deoxygenated solvent is added *via* cannula. The solution is stirred using a magnetic stirrer. A syringe is flushed with argon and the prescribed quantity of 4-chloroanisole taken up and then injected into the reaction ampoule. The procedure is repeated for morpholine and for the GC-MS internal standard (dodecane). After 5 minutes stirring, the first sample is taken by a long-needled syringe (first having been flushed 3 times with argon) into a GC-MS vial. The reaction vessel is placed in an oil bath preheated to the reaction temperature and stirred. Periodically, the reaction vessel is cycled back onto the Schlenk vacuum line and further

samples are taken once the reaction has cooled and any suspended matter has settled out.

2.5 References

- ¹ a) Seligson, A. L., Troglor, W. C., *Organometallics*, **1993**, *12*, 744, b) Balcells, D., Nova, A., Clot, E., Gnanamgari, D., Crabtree, R.H. Eisenstein, O., *Organometallics* **2008**, *27*, 2529; c) Kovacic, P., Lowery, M. K., *J. Org. Chem.*, **1969**, *34*, 911.
- ² March, J. "Advanced Organic Chemistry", 4th ed, John Wiley and Sons, Inc., New York, **1992**.
- ³ McMurray, J., "Organic Chemistry- International Student Edition", 6th ed., Brooks/Cole, New York, **2004**.
- ⁴ Balcells, D., Nova, A., Clot, E., Gnanamgari, D., Crabtree, R.H. Eisenstein, O., *Organometallics* **2008**, *27*, 2529.
- ⁵ Cazin, C. S. J., ed, Springer, London, **2010** and references therein.
- ⁶ Green, J. C., Benjamin, J. H., Lonsdale, R., *J. Organomet. Chem.*, **2005**, *690*, 6054.
- ⁷ a) Esposito, O.; Lewis A. K. de K; Hitchcock, P. B.; Caddick, S.; Cloke, F. G. N.; *Chem. Commun.*, **2007**, 1157
- ⁸ Esposito, O., Hitchcock, P.B., Lewis, A.K.de K., Caddick, S., Cloke, F.G.N., *Organometallics*, **2008**, *27*, 6411
- ⁹ Green, M. J.; Cavell, K. J.; Skelton, B. W.; White, A. H.; *J. Organomet. Chem.* **1998**, *554*, 175.
- ¹⁰ Gutierrez, E., Nicasio, M.C., Paneque, M., Ruiz, C., Salazar, V., *J. Organomet. Chem.*, **1997**, *549*, 167.
- ¹¹ McGuinness, D.S., Saendig, N., Yates, B. F., Cavell, K.J., *J. Am. Chem. Soc.*, **2001**, *123*, 4029.
- ¹² McGuinness, D.S., Cavell, K.J., *Organometallics*, **2000**, *19*, 4918.
- ¹³ Titcomb, L., DPhil Thesis, University of Sussex, 2001 and references therein.
- ¹⁴ Marshall, W.J.; Grushin, V.V. *Organometallics*, **2003**, *22*, 1591.
- ¹⁵ Esposito, O., D.Phil. Thesis, University of Sussex, November **2007**
- ¹⁶ Widenhoefer, R.A., Buchwald, S.L., *Organometallics*, **1996**, *15*, 2755.
- ¹⁷ Hartwig, J. F., Richards, S., Baranano, D., Paul, F., *J. Am. Chem. Soc.*, **1996**, *118*, 3626.
- ¹⁸ Tardiff, B. J., McDonald, R., Ferguson, M. J., Stradiotto, M., *J. Org. Chem.* **2012**, *77*, 1056.
- ¹⁹ Hartwig, J. F., Driver, M.S., *J. Am. Chem. Soc.*, **1997**, *119*, 8232.

-
- ²⁰ Data from NIST Standard Reference Database 69: *NIST Chemistry WebBook*. Accessed 29/12/12.
- ²¹ Ryan, C., Lewis, A., K. de K., Caddick, S., Kaltsoyannis, N., *Theor Chem Acc*, **2011**, *129*, 303
- ²² Pan, J., Su, M., Buchwald, S. L., *Angew. Chem. Int. Ed.*, **2011**, *50*, 8647 and references therein
- ²³ Hanley, P. S., Marquard, S. L., Cundari, T. R., Hartwig, J. F., *J. Am. Chem. Soc.* **2012**, *134*, 15281
- ²⁴ Villanueva, L. A., Abboud, K. A., Boncella, J. A., *Organometallics*, **1994**, *13*, 3921;
- ²⁵ Hartwig, J. F., Richards, S., Baranano, D., Paul, F., *J. Am. Chem. Soc.*, **1996**, *118*, 3626.
- ²⁶ Shen, Q., Hartwig, J. F., *J. Am. Chem. Soc.*, **2007**, *129*, 7734.
- ²⁷ See 23
- ²⁸ Caddick, S., Cloke, F.G.N., Clentsmith, G.K.B., Hitchcock, P.B., McKerrecher, D., Titcomb, L.R., Williams, M.R.V., *J. Organomet. Chem.* **2001** 617–618 635
- ²⁹ Gleiter, R.; Sander, W.; *Angew. Chem. Int. Ed. Engl.*, **1985**, *24*, 566.
- ³⁰ Tsoureas, N., Danopoulos, A.A., Tulloch, A.A.D., Light, M.E., *Organometallics*, **2003**, *22*, 4750.
- ³¹ de Vries, J.G., *Dalton Trans.*, **2006**, 421.
- ³² Urban, S., Tursky, M., Frolich, R., Glorius, F., *Dalton Trans.*, **2009**, *35*, 6934.
- ³³ Arduengo A. J.; Dias, H. V. R.; Harlow, R. L.; Kline, M.; *J. Am. Chem. Soc.*, **1992**, *114*, 5530
- ³⁴ a) Arduengo III, A.J., Krafczyk, R., Schmutzler, R., *Tetrahedron*, **1999**, *55*, 14523.
b) Herrmann, W. A., Elison, M., Fischer, J., Kocher, C., Artus, G. R. J., *Chem. Eur. J.*, **1996**, *2*, 772. c) Dorta, R., Stevens, E. D., Scott, N. M., Costabile, C., Cavallo, L., Hoff, C. D., Nolan, S. P., *J. Am. Chem. Soc.*, **2005**, *127*, 2485.
- ³⁵ Leung, S. K-Y., Huang, J-S., Zhu, N., Che, C-M., *Inorg. Chem.* **2003**, *42*, 7266.
- ³⁶ Diversi, P., Fasce, D., Santini, R., *J. Organomet. Chem.*, **1984**, 269, 285.

Chapter 3:

Investigations into the use of the 1,2,3,4, tetramethylimidazol-2-ylidene

NHC complexes of palladium as aryl amination catalysts.

Use of Pd(*NHC*)₂ complexes for Si-Si, C-Si bond cleavage and C-S bond formation.

3.1 Introduction

When *NHCs* first began to be used in organometallic complexes¹⁶¹ shortly after Arduengo isolated them¹⁶², ITMe, and the dihydro version, IMe, were often used to investigate the properties of *NHC* complexes.^{163,164,165,166,167} As the field matured, the importance of steric bulk on *N*-substituents became clearer^{168,169,170,171}, and more sophisticated synthetic led to functionalised^{172, 173} and multi-dentate *NHCs*^{13, 174}, these smaller, simple *NHCs* were less frequently utilised.

It was initially thought that the ITMe complexes would prove to be good catalysts

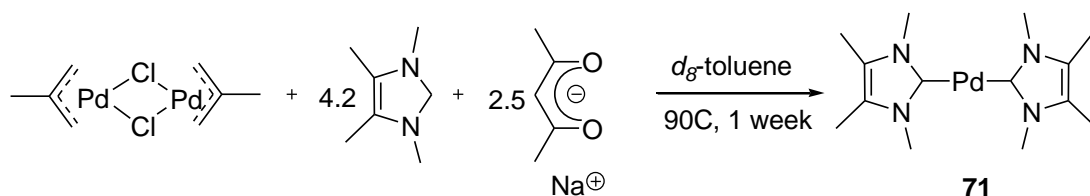
When our group started to investigate bis-*NHC* palladium(0) complexes for their catalytic ability in Heck, Suzuki-Miyaura and Buchwald-Hartwig reactions, the electron-donating methyl substituents on the nitrogens and on the vinyl carbons of the backbone were thought to be able to render this *NHC* a strong σ donor towards the palladium centre. Initial catalytic tests, however, showed that Pd(ITMe)₂ was inactive for Buchwald-Hartwig amination reactions¹⁷⁵. Other bis-carbene palladium complexes range in ability; Pd(IPr)₂ is an excellent catalyst for Buchwald-Hartwig amination¹⁵ whilst Pd(I^tBu)₂ shows moderate activity due to a slow kinetic profile.¹⁷⁶ This proved to be advantageous when it came to isolating intermediates of the catalytic cycle and performing kinetic studies.^{177, 178}

Recently, we have used ITMe in our work on alkyl amination¹⁷⁹ and it was thought that there was some merit in looking again at the activity of Pd(ITMe)₂ for Buchwald Hartwig aryl amination. Possibly, the very inability to catalyse this transformation could shed further light on the mechanism for this particular cross-coupling protocol.

3.2 Results and Discussion

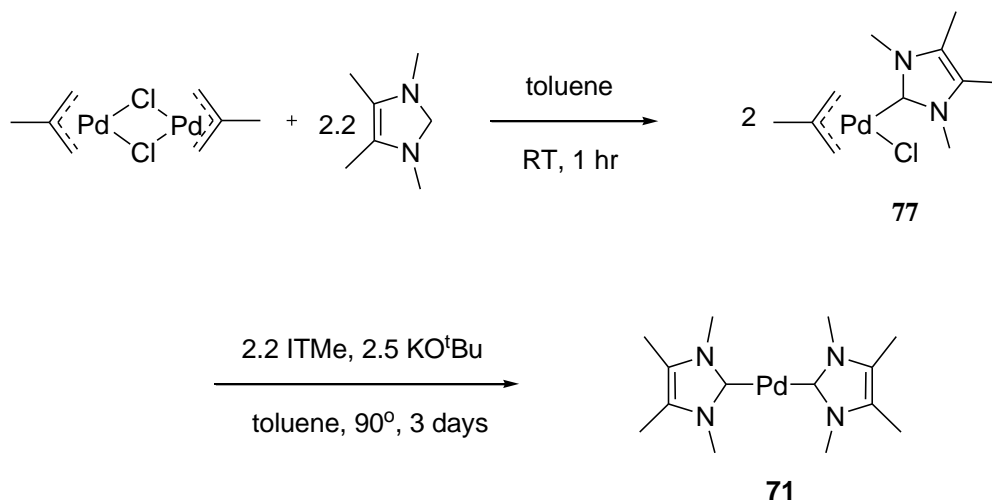
3.2.1 Synthesis of Pd(ITMe)₂, **71**.

Pd(ITMe)₂, **71**, was previously synthesised within our group using MVS (metal vapour synthesis)¹⁵ but there has been no previous recorded attempt to make it via the one pot synthesis¹⁵⁻²¹ that our group has used to prepare Pd(IPr)₂, Pd(SIPr)₂, Pd(I^tBu)₂ and Pd(SI^tBu)₂¹⁸⁰ (Scheme 3.01). The one pot synthesis was attempted on an NMR scale but no evidence of the formation of Pd(ITMe)₂ was found.



Scheme 3.01: 1st Attempt at 1 pot synthesis of Pd(ITMe)₂, **71**.

An improved synthesis for Pd(IPr)₂ has recently been developed¹⁸¹ by our group whereby [Pd(NHC)₂(η³-methallyl)Cl]₂ is isolated first then reacted with a base to promote the reduction to Pd(0) and a further equivalent of *NHC* to trap it. Stronger bases can be used in this protocol as one *NHC* is already co-ordinated to the Pd centre. This method proved successful for the synthesis of **71** as depicted in Scheme 3.02.



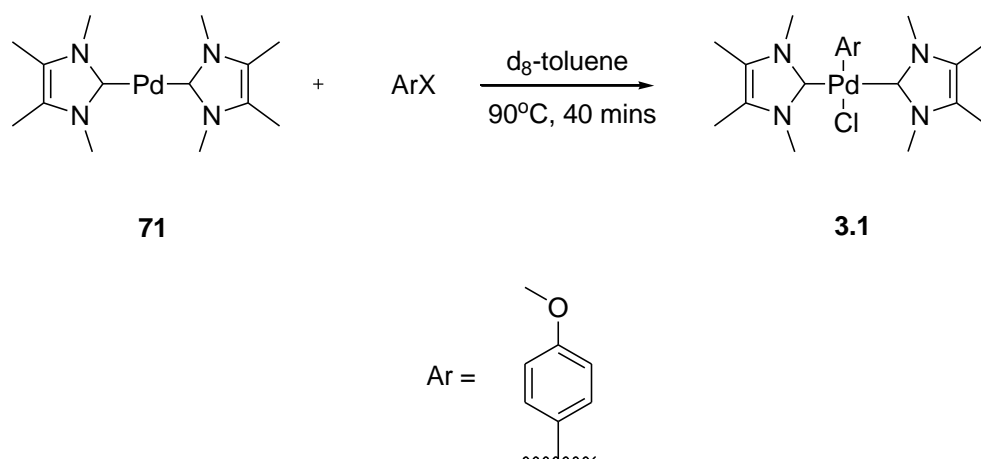
Scheme 3.02: Successful two step synthesis of Pd(ITMe)₂

Eventually when undertaking the reaction, isolation of **71** was found not to be necessary and when the amount of base used was reduced to 2 equivalents, the one pot method proved reliable (66% yield)..

As complex **71** had previously been evaluated as an aryl amination catalyst and found to have no activity.¹⁵ Indeed, when it was tested again in ¹H-NMR studies, the complex was found to catalyse aryl amination reactions, but with an extremely poor activity of 5% conversion after 42 days at 90°C.

That there was any activity at all, whilst very poor indeed, meant that further investigation into the reasons behind this catalytic inability were considered to be of interest.

3.2.2. Oxidative addition of aryl chlorides to Pd(ITMe)₂, **71**.



Scheme 3.03: ¹H NMR Reaction of Pd(ITMe)₂ and 4-chloroanisole

Scheme 3.03 shows the reaction of Pd(ITMe)₂ with 4-chloroanisole. The oxidative addition product, [Pd(ITMe)₂(anisole)Cl], **3.1**, is formed rapidly on a time scale and with an experimental yield comparable to the reaction of Pd(I^tBu)₂ with 4-chloroanisole. (40°C, 120hrs benzene: 66% yield for *trans*-[Pd(I^tBu)₂(anisole)(Cl)], **78**; 69% yield of **3.1**).

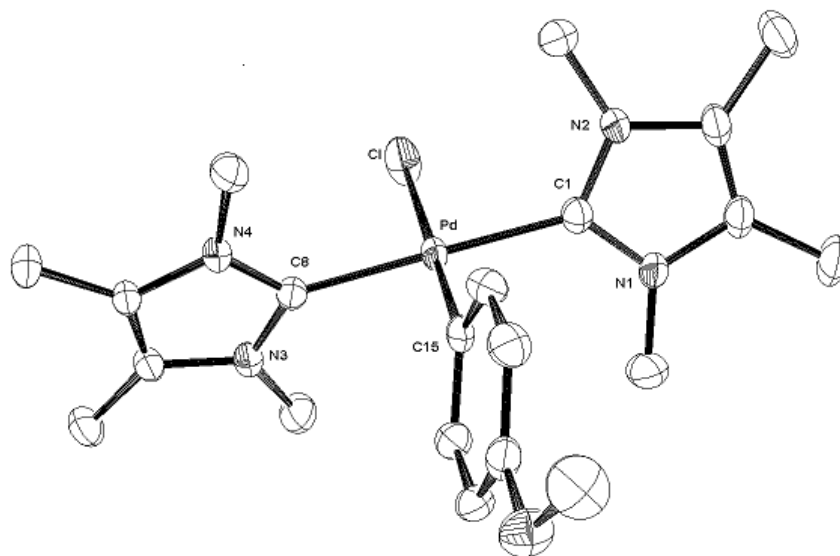


Figure 45: Ortep diagram of the molecular structure of $[\text{Pd}(\text{ITMe})_2(\text{anisole})\text{Cl}]$, **3.1**, showing 50% thermal ellipsoids. Hydrogens omitted for clarity.

Selected bond lengths (Å) and angles (°):

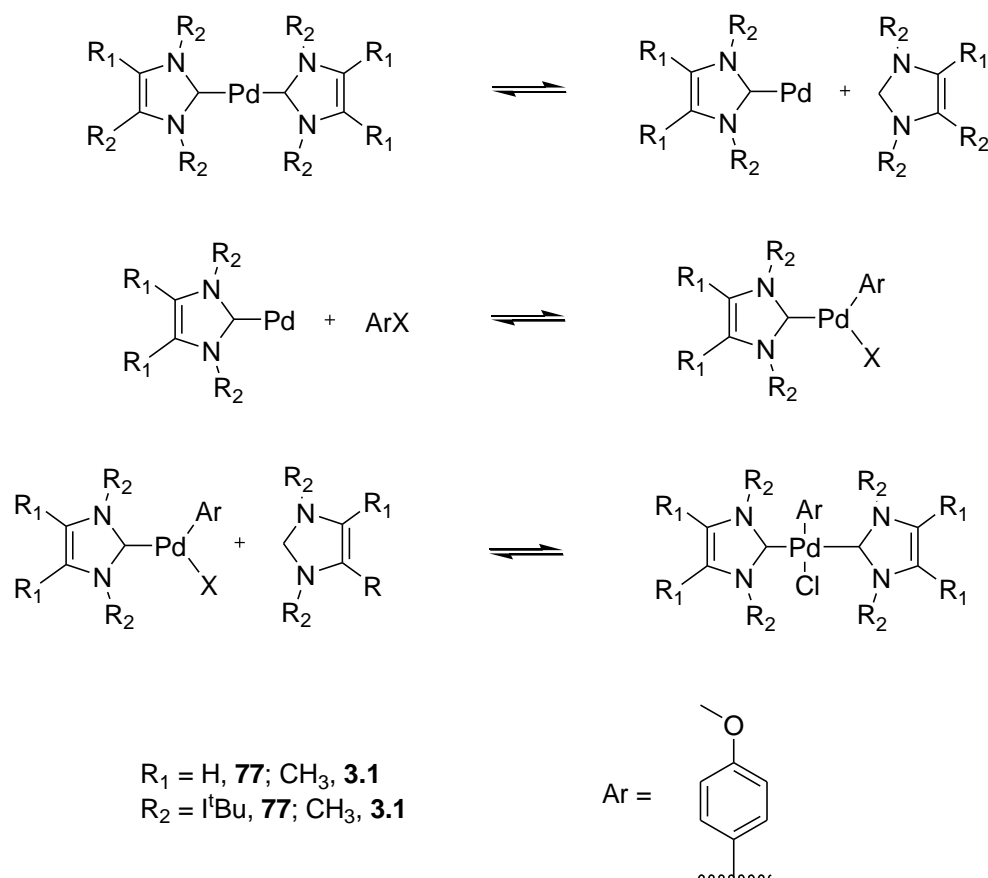
Pd-C(15), 2.007(3); Pd-C(8), 2.033(3); Pd-C(1), 2.040(3); Pd-Cl, 2.4078(8);
C(15)-Pd-C(8), 88.99(11); C(15)-Pd-C(1), 88.87(11); C(8)-Pd-Cl, 90.53(8); C(1)-Pd-Cl,
91.57(9); C(8)-Pd-C(1); 177.70(12) C(15)-Pd-Cl; 177.51(9)

Bond or angle	78¹⁷	3.1
Pd-NHC(1)	2.097(3)	2.033(3)
Pd-NHC-(2)	2.094(3)	2.040(3)
Pd-C(anisole)	2.063(3)	2.007(3)
Pd-Cl	2.4456(7)	2.4078(8)
NHC-Pd-Cl	87.39(7); 90.64(8)	90.53(8); 91.57(9)
NHC-Pd-C(anisole)	91.80(10); 90.16(11)	88.99(11); 88.87(11)
NHC-Pd-NHC	178.01(10)	177.70(12)
Cl-Pd-C(anisole)	179.18(8)	177.51(9)

Table 3.1: Selected bond lengths and angles of **78** and **3.1**

The crystals of **3.1** were grown in toluene after 2 days at -50°C . Table 3.1 shows selected bonds and angles of **3.1** and **78**. When comparison between **78**¹⁷ and **3.1** is made, the bonds lengths are longer in **78** (Pd-*NHC* bond is 2.033(3) in **3.1** and 2.097(3) in **78**) and distortion from idealised square planer geometry more pronounced in **3.1** (Cl-Pd-C(anisole) is $179.18(8)^{\circ}$ in **78** and $177.51(9)^{\circ}$ in **3.1**). This is to be expected given larger steric bulk of $\text{I}^{\text{t}}\text{Bu}$ will constrain the geometry of **78**.

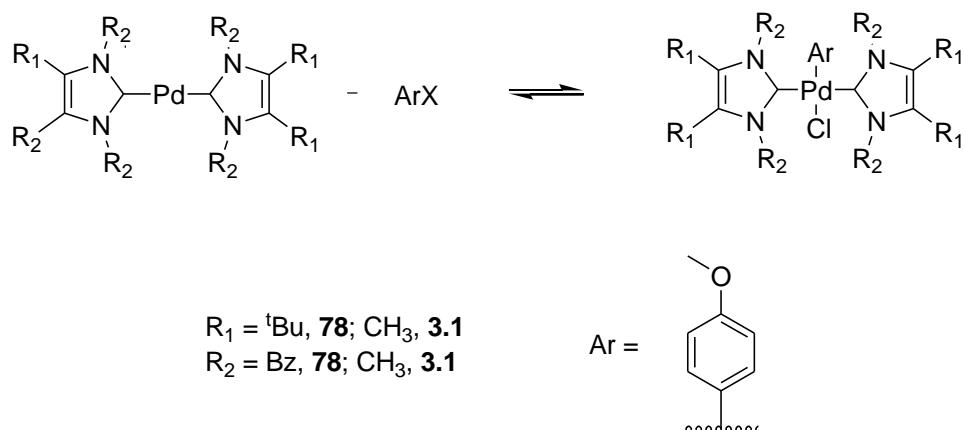
It has been suggested that the lack of steric bulk in ITMe means the formation of monoligated Pd(ITMe) species such as shown in Scheme 3.04 is energetically unfavourable and one of the reasons for the poor performance of Pd-ITMe complexes as catalysts.^{15, 182, 183} Extensive work within this group using the $\text{I}^{\text{t}}\text{Bu}$ ligand system has found that the formation of the $\text{I}^{\text{t}}\text{Bu}$ oxidative addition product proceeds *via* a dissociative mechanism.^{18,184} If the mechanism for oxidative addition is dissociative for Pd(ITMe)₂ (Scheme 3.04)¹⁷, then the comparable rate of formation of the oxidative addition complexes for $\text{I}^{\text{t}}\text{Bu}$ and ITMe suggests that the energy barrier to the formation of the monoligated Pd(ITMe) species in the 1st step of Scheme 3.04 is close that for formation of Pd($\text{I}^{\text{t}}\text{Bu}$).^{24, 185}



Scheme 3.04: Dissociative mechanism for oxidative addition of aryl chlorides to $\text{Pd}(\text{NHC})_2$.

Ligand exchange reactions¹⁵ and theoretical calculation^{24, 186} suggest this is not, in fact, the case and that formation and solvation of $\text{Pd}(\text{ITMe})$ is a more energetically disfavoured than formation of solvated $\text{Pd}(\text{t}^t\text{Bu})$.²⁶

The other explanation is that the aryl species is coordinating directly to the bis-carbene species with no formation of a monoligated species i.e. an associative mechanism. Work by Juland *et al*¹⁸⁷ using IBn, 1,3-di-benzyl-4,5-di-*tert*-butylimidazolidin-2-ylidene found the oxidative addition of aryl halides was found to proceed via an associative mechanism (Scheme 3.05).



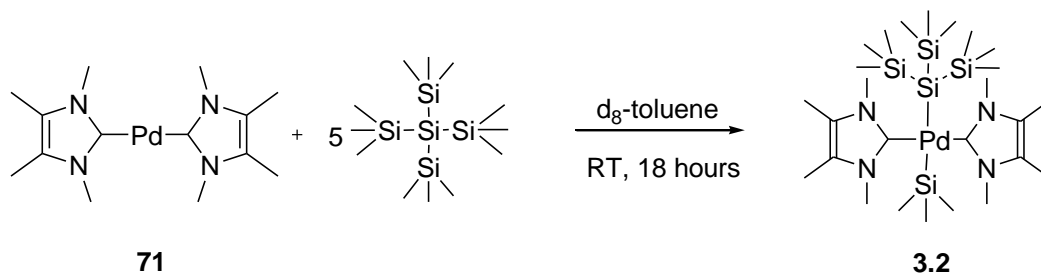
Scheme 3.05: Associative mechanism for oxidative addition of aryl chlorides to $\text{Pd}(\text{NHC})_2$.

The benzyl group at the 1 and 3 position are smaller than the tert-butyl groups of I^{tBu} ²³. In fact, the methyl groups of ITMe are even less bulky than the benzyl groups, so if it is steric factors that determine whether addition is associative or dissociative, then ITMe could adopt an associative mechanism¹⁸⁸.

The relatively fast formation is also of interest because it shows that, in this system, the formation of the oxidative addition product is not the rate-limiting step.

3.2.3 Unsuccessful kinetic studies of Pd(ITMe)₂

There have been two main difficulties that have prevented the elucidation of the mechanism of this reaction. The first problem to be overcome was the very low solubility of **71** in common solvents. However, when the solubility of the complex in *d*₈-toluene was being assessed, an unexpected complication occurred. Left overnight at ambient temperature in *d*₈-toluene, the complex reacted with the internal NMR standard, Si(SiMe₃)₄, used in kinetic studies to calculate changes in reactant concentration. This reaction produced the novel complex, **3.2** (Scheme 3.06).



Scheme 3.06: Unexpected reaction of **71** with NMR standard, Si(SiMe₃)₄

The carbon analogue of Si(SiMe₃)₄, C(SiMe₃)₄, was then synthesised¹⁸⁹ and, after initial tests, it was thought this a suitable alternative internal standard.

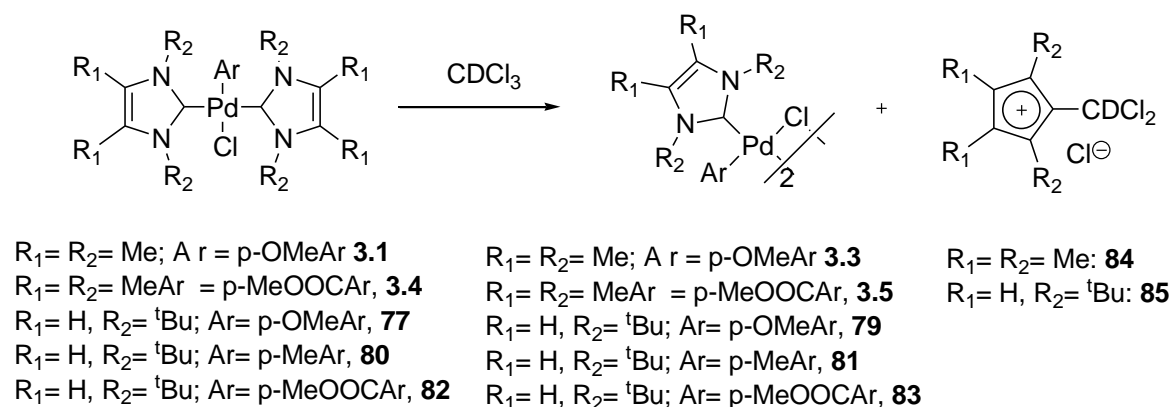
The poor solubility of **71** was still an issue and best solubility was found to be in *d*₈-thf. However, after stock solutions of 4-chloroanisole and C(SiMe₃)₄ in *d*₆-benzene were produced and the kinetics reaction attempted at 40°C, it became apparent that the C(SiMe₃)₄ was compromised as new peaks appeared in the -0.10 to 0.25 ppm range of the ¹H NMR. (*vide supra*, Section 3.2.5).

A reassessment of the suitability of using ¹H NMR data as the basis for obtaining meaningful kinetic information was made. It was apparent that, even with an inert internal standard, the poor solubility of **71** in all common NMR solvents (concentrations in the order of 10⁻⁶ mol dm⁻³ in 0.6ml volume) meant the error in the measurements of the concentration of any reaction species would be too large to be considered insignificant and render any calculations based on this data not sufficiently accurate.

3.2.4 Attempted isolation of the dimeric species, $[\text{Pd}(\text{ITMe})(\text{OMeAr})\text{Cl}]_2$

Previously within our group, we have isolated the dimeric species of the oxidative addition of $\text{Pd}(\text{tBu})_2$ and 4-chloroanisole.¹⁸

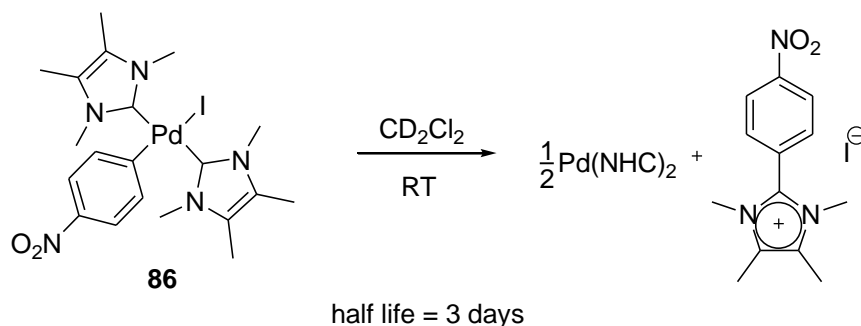
The second *NHC* reacts with chloroform to form imidazolium salt, **85**, thus rendering the reaction from monomer to dimer irreversible by effectively removing the second *NHC* from further reaction and preventing its re-coordination to the mono-ligated species (Scheme 3.07).



Scheme 3.07: Reaction of $[\text{Pd}(\text{NHC})_2(\text{Ar})\text{Cl}]$ in CHCl_3 ¹⁸

This reaction (Scheme 3.07) was undertaken with **3.1**. After 3 weeks at 40°C, in CDCl_3 , peaks in the ^1H NMR spectrum corresponding to the $[\text{Pd}(\text{ITMe})(\text{Ar})\text{Cl}]_2$ were observed at 2.38 ppm (12H, ITMe), 3.68 ppm (12H, ITMe) and 3.87 ppm (6H, ArOMe). There were also peaks for **84** and protonated imidazolium salt. However, attempts at isolation of **3.3** led to the isolation of the monomer, **3.1**, and imidazolium salts.

The complex did not appear to decompose *via* the generation of the aryl imidazolium salt as previously seen by Cavell and co-workers¹⁹⁰ during their studies with $[\text{Pd}(\text{ITMe})_2(\text{Ph})\text{I}]$, **86**, as shown in Scheme 3.08. There was no indication of palladium black or aryl imidazolium salt.



Scheme 3.08: Decomposition of $[\text{Pd}(\text{ITMe})_2(\text{NO}_2)\text{I}]$, **86**, found by Cavell *et al*.³

The generation of the dimer **3.3** takes considerably longer than for the $\text{Pd I}^t\text{Bu}$ analogue, **79**, which can be generated in 8 hours at 55°C to over 90% yield.¹⁸

This slow formation of **3.3** implies slow dissociation of ITMe from **3.1** and thus slow formation of the monoligated $\text{Pd}(\text{ITMe})(\text{anisole})\text{Cl}$ moiety considered as the active species for the next step in the catalytic cycle, *i.e.* the transamination. It is interesting that dissociation of ITMe from the oxidative addition product, **3.1**, is comparatively slow whereas **3.1** itself was formed at similar rate to **77**, especially as the dissociation from the bis carbene Pd complex is usually the slower step (dissociation from a 2 coordinate species is less favoured than from a 4 coordinate one).¹⁹¹ This could imply that the oxidative addition complex **3.1** forms *via* an associative mechanism.

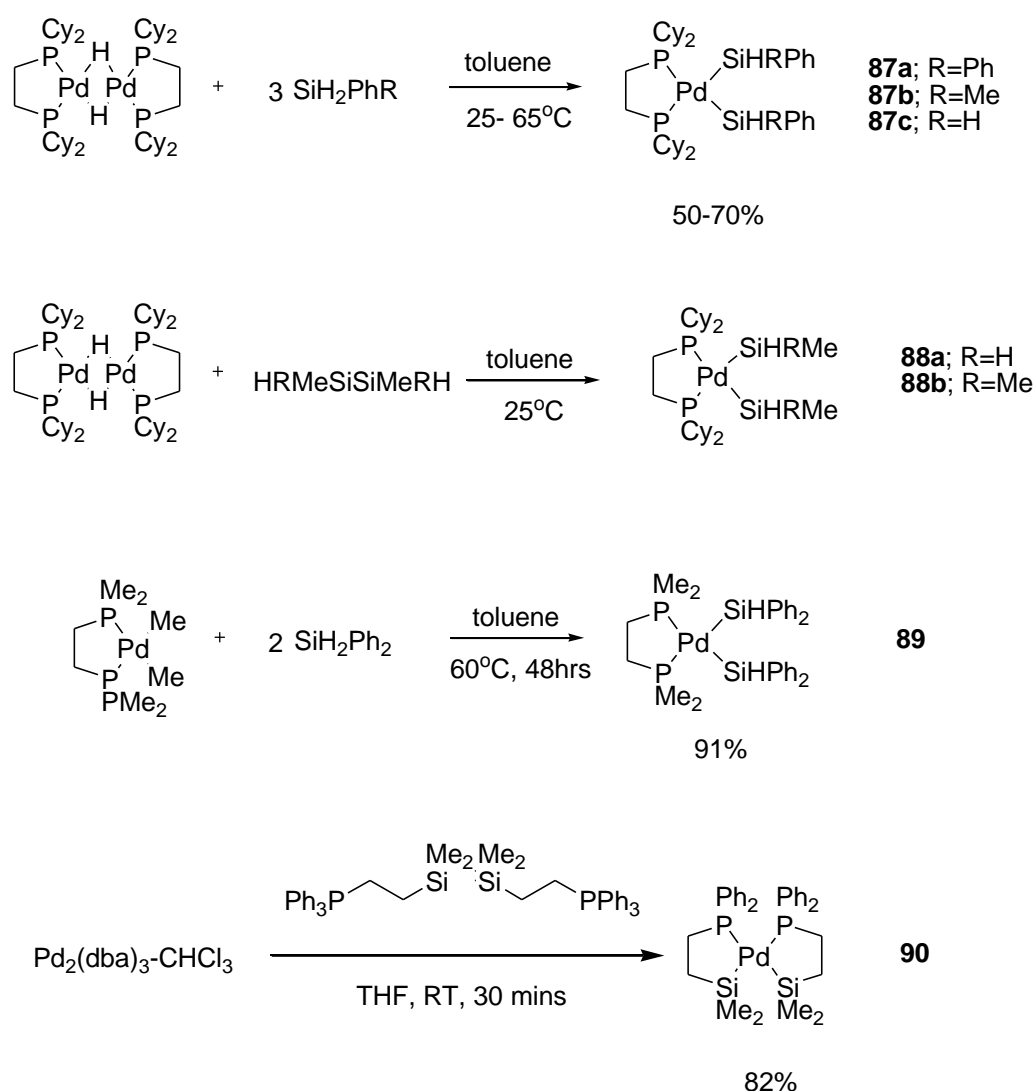
In an attempt to further elucidate the behaviour of ITMe aryl complexes in this catalytic system, $\text{Pd}(\text{ITMe})_2$ was reacted with the more activated aryl chloride, 4-chloromethyl benzoate. On addition of this aryl chloride to $\text{Pd}(\text{ITMe})_2$, palladium black almost immediately began to be deposited and 4-(1,2,3,4-tetramethyl imidazolium) methyl benzoate was also observed in ^1H NMR spectrum of the reaction mixture. $[\text{Pd}(\text{ITMe})_2(\text{methyl-benzoate})\text{Cl}]$, **3.4** formed in a reaction time comparable to its I^tBu analogue, **82**. However, the generation of the dimer, **3.5**, to a yield in excess of 50%, took weeks whereas the formation of **83** from **82** went to completion within 8 hours.

A threshold level of electronic density on a complex is required in order to achieve oxidative addition, but once the threshold is achieved, the sterics of the *NHC* become the more important consideration.²⁸ Here, it can be seen that $\text{Pd}(\text{ITMe})_2$ has readily formed an oxidative addition product on addition of the aryl chlorides, 4-chloroanisole and 4-methoxybenzene. It is the dissociation of ITMe from the $[\text{Pd}(\text{ITMe})_2(\text{aryl})\text{Cl}]$ complex that is the slower step. This may imply an associative mechanism for the

formation of **3.1** but kinetic studies performed to establish this were hampered by the poor solubility of both **72**, $\text{Pd}(\text{ITMe})_2$ and **3.1**, $[\text{Pd}(\text{ITMe})_2(\text{Ar})\text{Cl}]$.

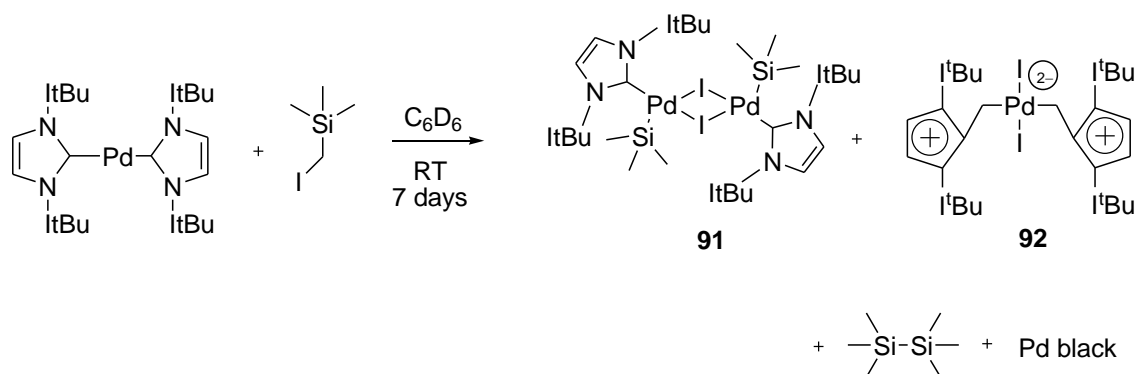
3.2.5 Silyl complexes of Pd-NHC complexes

Palladium catalysts have been used in a variety of important industrial processes such as hydrosilylation, bis-silylation, preparation of polysilanes and silylation of organic halides.^{192, 193} However, due to their high catalytic activity, isolation of the (silyl)palladium species has proved difficult with only a few stable complexes known³² and these have usually been stabilised by chelation, either of the ligand or the silane, or by very strong electron-withdrawing silyl groups such as SiCl_3 .³³ Some stable Pd-Si complexes and their synthesis are shown in Scheme 3.09.



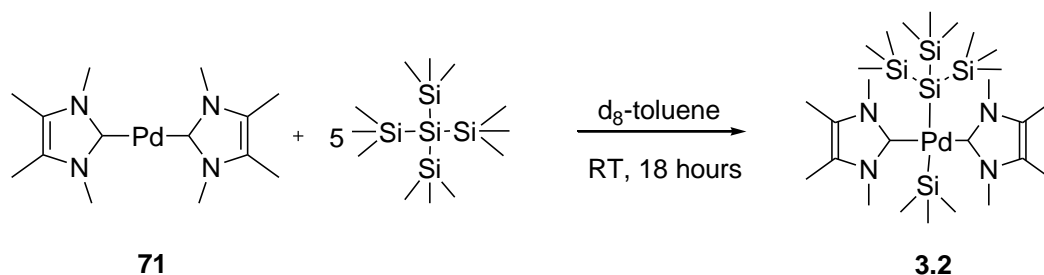
Scheme 3.09: Stable Palladium-silyl complexes^{194, 195, 196}

Recently in our group, we isolated two I^tBu silyl palladium iodide complexes from $\text{Pd}(\text{I}^t\text{Bu})_2$. This was done in anticipation of achieving the oxidative addition of silicon-halide bonds to the palladium centre. The result was carbon-silicon bond activation and insertion of CH_2 into the carbene-palladium bond³³ as depicted in Scheme 3.10.



Scheme 3.10: Reaction of $\text{Pd}(\text{I}^t\text{Bu})_2$ with (trimethylsilyl)methyl iodide³³

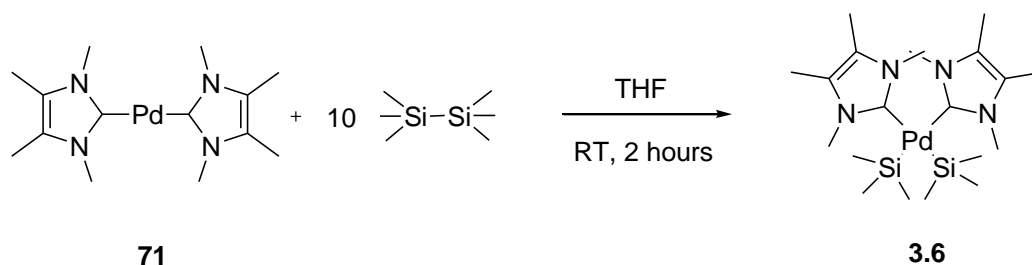
The analogous reaction with $\text{Pd}(\text{ITMe})_2$ would have been attempted but before this could be put into operation, the unexpected reaction between $\text{Pd}(\text{ITMe})_2$ and tetrakis(trimethylsilyl)silane, a compound often used in kinetics reactions as an internal standard was discovered. (*vide infra*, Section 2.2.2, Scheme 3.11).



Scheme 3.11: Reaction of $\text{Pd}(\text{ITMe})_2$ with $\text{Si}(\text{SiMe}_3)_4$
(also depicted above in Scheme 3.06 in section 3.2.2)

No other palladium bis-carbene complex used in our group has shown such reactivity with $\text{Si}(\text{SiMe}_3)_4$. $[\text{Pd}(\text{ITMe})_2(\text{Si}(\text{SiMe}_3)_3(\text{SiMe}_3))]$, **3.2**, could not be isolated in common solvents; it was generated using an large excess of $\text{Si}(\text{SiMe}_3)_4$ and these two species invariable precipitated from solution in tandem.

The reaction of HMDS (hexamethyldisilane) with $\text{Pd}(\text{ITMe})_2$ was undertaken to ascertain whether cleavage of the Si-Si bond would occur in this less sterically crowded disilane. The result was the formation of the novel palladium silyl complex, **3.6**, [*cis*- $\text{Pd}(\text{ITMe})_2(\text{SiMe}_3)_2$] depicted in Scheme 3.12.



Scheme 3.12: Reaction of $\text{Pd}(\text{ITMe})_2$ with HMDS: [*cis*- $\text{Pd}(\text{ITMe})_2(\text{SiMe}_3)_2$], **3.6**

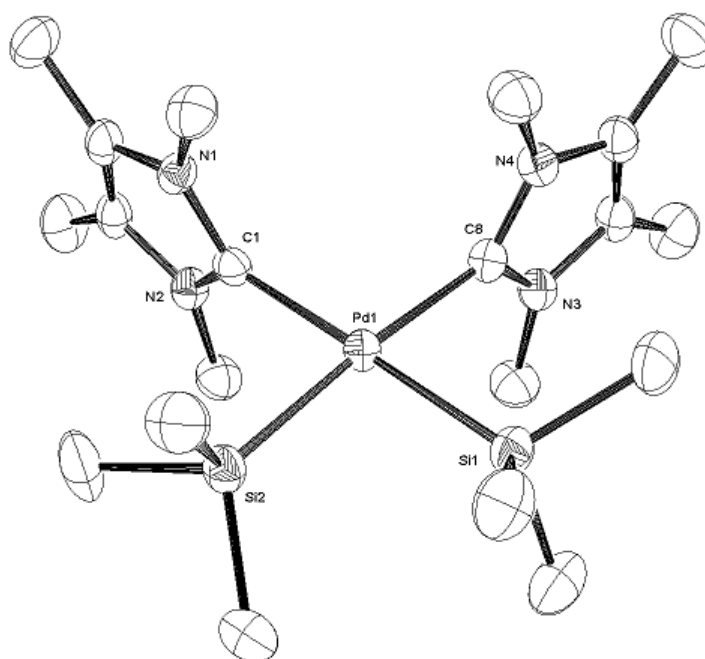


Figure 46: Ortep diagram of the molecular structure of *cis*-[[$\text{Pd}(\text{ITMe})_2(\text{TMS})_2$], **3.6**, showing 50% thermal ellipsoids. Hydrogens omitted for clarity.

Selected bond lengths (Å) and angles(°):

$\text{Pd}(1)\text{-C}(1)$ 2.109(3); $\text{Pd}(1)\text{-C}(8)$ 2.117(3); $\text{Pd}(1)\text{-Si}(2)$ 2.3556(8); $\text{Pd}(1)\text{-Si}(1)$ 2.3597(8);
 $\text{C}(1)\text{-Pd}(1)\text{-C}(8)$, 95.61(11); $\text{C}(1)\text{-Pd}(1)\text{-Si}(2)$, 88.99(8); $\text{C}(8)\text{-Pd}(1)\text{-Si}(1)$, 86.88(8);
 $\text{Si}(1)\text{-Pd}(1)\text{-Si}(2)$, 88.57(3); $\text{C}(8)\text{-Pd}(1)\text{-Si}(2)$; 175.25(8); $\text{C}(1)\text{-Pd}(1)\text{-Si}(1)$; 176.67(8)

Bond length (Å) or angle (°)	3.6	87a
Pd-L(1)	2.109(3)	2.3518(7)
Pd-L(2)	2.117(3)	2.3614(8)
Pd-Si(1)	2.3597(8)	2.3563(9)
Pd-Si(2)	2.3556(8)	2.359(1)
L(1)-Pd-Si(2)	88.99(8)	94.91(4)
L(2)-Pd-Si(1)	86.88(8)	95.75(3)
L-Pd-L	95.61(11)	85.70 (3)
Si(1)-Pd-Si(2)	88.57(3)	83.77 (4)

3.6; L(1)= NHC C(1), L(2)= NHC C(8); **87a** L(1)-L(2)= CyPCH₂CH₂PCy (dcpe);

Table 3.2: Selected bond lengths and angles of **3.6** and **87a** (Scheme 3.09)

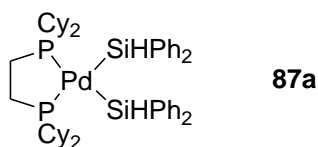


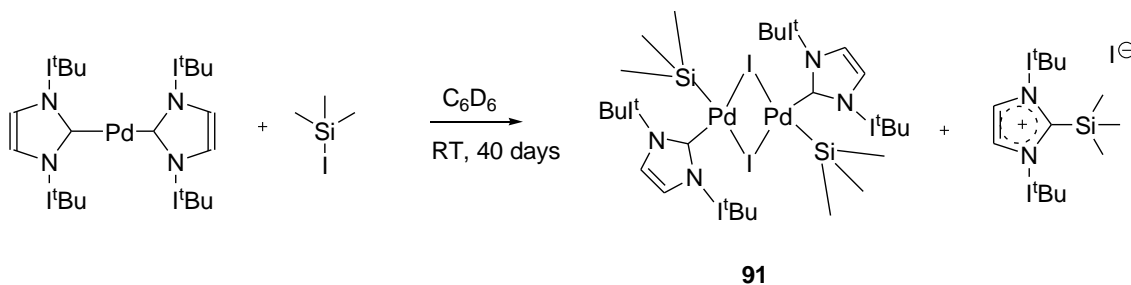
Figure 47: Pd(dcpe)(SiHPh)₂

(Formation shown in Scheme 3.09)

Crystals of **3.6** were grown in benzene at -50°C. The complex adopts the *cis* configuration. This is distinct from Pd(*NHC*)(Ar)X complexes such as [Pd(ITMe)₂(anisole)Cl], **3.1** as their crystal structures are almost invariably the *trans* configuration.¹⁷ Comparison of **3.6** with the bis-chelated complex, **87a**, (Figure 47) shows the Pd-L bond is shorter in **3.6**, whilst the Pd-Si bond lengths are comparable. The larger angle of **87a** is the L-Pd-Si angle, whereas **3.6** has the largest angle between the two ITMe ligands, L-Pd-L. This will be partially due to the difference in silyl groups of **87a** and **3.6**. The presence of hydrogen on the SiHPh₂ of **87a** will allow closer approach of the silyl groups. It is also a function of the bidentate ligand which is restricted in its ability to increase its internal angle. Larger monodentate ligands would necessitate a larger L-Pd-L angle and this would most likely cause a steric clash

between the trimethylsilyl groups as they were forced into closer proximity, preventing the complexes formation.

The dimer **91** has also been generated by the protocol described in Scheme 3.13; reaction of $\text{Pd}(\text{I}^t\text{Bu})_2$ with trimethylsilyl iodide.



Scheme 3.13: Reactivity of $\text{Pd}(\text{I}^t\text{Bu})_2$ towards Me_3SiI ³³

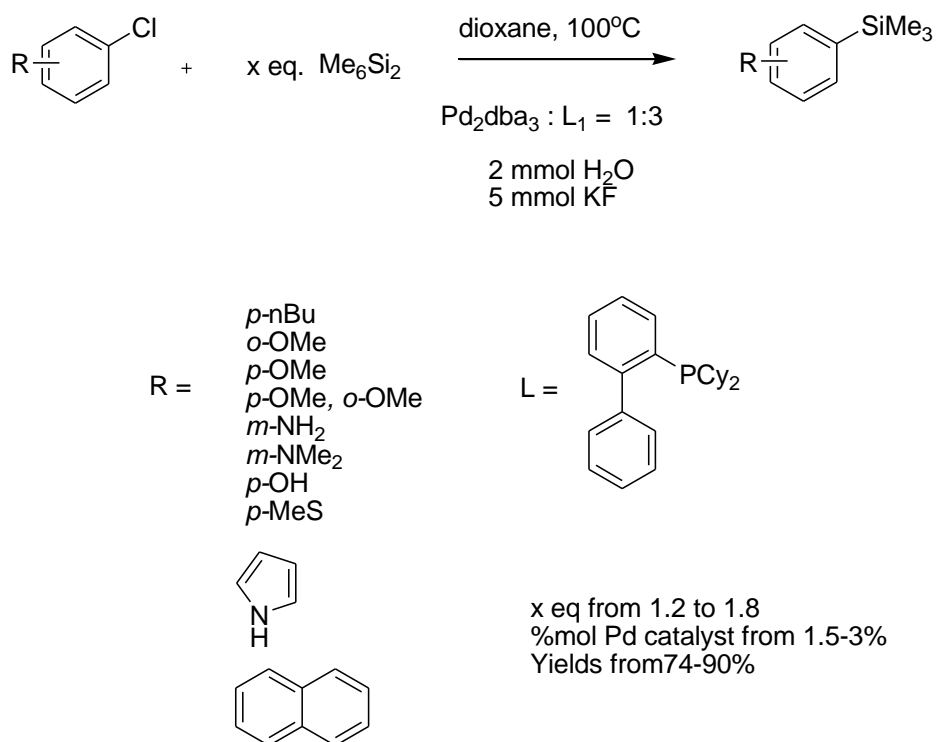
However, no reaction was observed when reaction of $\text{Pd}(\text{I}^t\text{Bu})_2$ with HMDS was attempted (Scheme 3.12) at RT nor at 60°C.

When the reaction of $\text{Pd}(\text{ITMe})_2$ and Me_3SiI was attempted on an NMR scale in d_6 -benzene, immediate generation of palladium black was observed. Within 2 hours of the reaction commencing, the solution had gone from a bright yellow to almost colourless. The ^1H NMR spectrum showed an intractable mixture.

It was hoped that thermolysis of **3.6** in CDCl_3 would abstract a *NHC* ligand and the dimer, $[\text{Pd}(\text{ITMe})(\text{TMS})(\text{Cl})]_2$ would form, a chloride/ITMe analogue of **91** shown in Scheme 3.13. However, this also led to palladium black and an intractable mixture of unknown products.

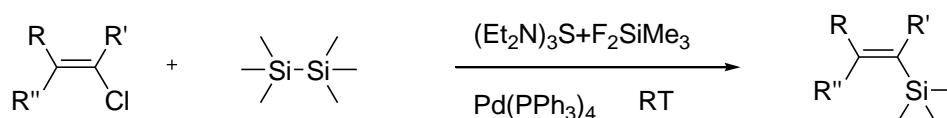
The different reactivity of the two bis-carbene complexes could be due to steric factors, specifically the interactions of the I^tBu CH_2 group with the palladium centre³³.

Whilst silyl chlorides are usually used to achieve silylation, the cleavage of the Si-Si bond in hexamethyldisilane by palladium (0) is known^{197, 36} and has been used to substitute halides for trimethylsilyl groups in aryl halides. Recently, Buchwald and co-workers developed a system for silylation of aryl chlorides using the protocol described in Scheme 3.14.¹⁹⁸



Scheme 3.14: Palladium catalysis to generate the trimethylsilylarene from the aryl chloride using HMDS as silylating agent

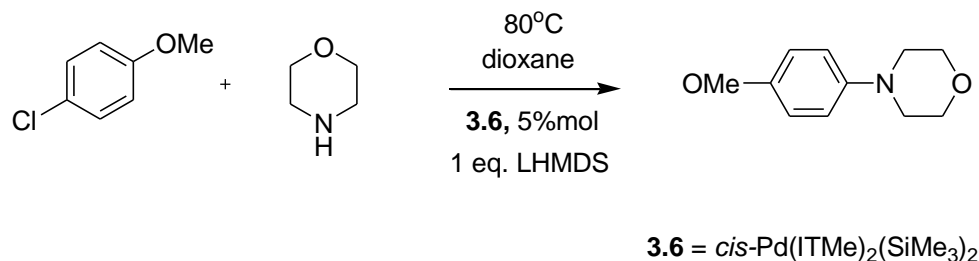
Palladium catalysts have been used with HMDS (hexamethyldisilane) for the silylation of vinyl chlorides³⁴ but in this case, tris(diethylamino)sulfonium difluoro(trimethyl)silicate (TASF) had to be used to induce cleavage of the Si-Si bond by the palladium catalyst (Scheme 3.15).



Scheme 3.15: Silylation of vinyl chloride using HMDS and Pd catalyst

3.2.6 Preliminary catalytic studies with and [Pd(ITMe)₂(anisole)Cl], **3.1** and [Pd(ITMe)₂(SiMe₃)₂], **3.6**.

The activity of **3.6** as a Buchwald-Hartwig amination catalyst has been assessed *via* GC-MS. Interestingly, despite the relatively low reaction temperature (80° C), the *meta* product, as well as the expected *para* product, have been produced (Scheme 3.16).



Scheme 3.16: Reaction of 4-chloroanisole and morpholine using **3.6** as catalyst and LHMDS as base.

The generation of an isomeric mixture of arylamines by the presence of LHMDS (Lithium hexamethyldisilylamine) is not unprecedented. Indeed, at high enough temperatures, the presence of LHMDS facilitates the generation of a benzyne species. It was thought, however, that the reaction was performed at a temperature low enough to prevent benzyne generation.^{199,200,201} No isomerisation occurred when [Pd(ITMe)₂(anisole)Cl], **3.1**, was used as catalyst for the same reaction on an NMR scale (Scheme 3.16) when no internal standard, Si(SiMe₃)₄ was present and the base was NaOC(Et)₃. However, as mentioned in section 2.2.6 of this thesis, [Pd(ITMe)(neopentyl)Cl]₂ does isomerise 4-chloroanisole to 3-chloroanisole (in 50% yield) in the presence of Si(SiMe₃)₄ using NaOCEt₃ as base.

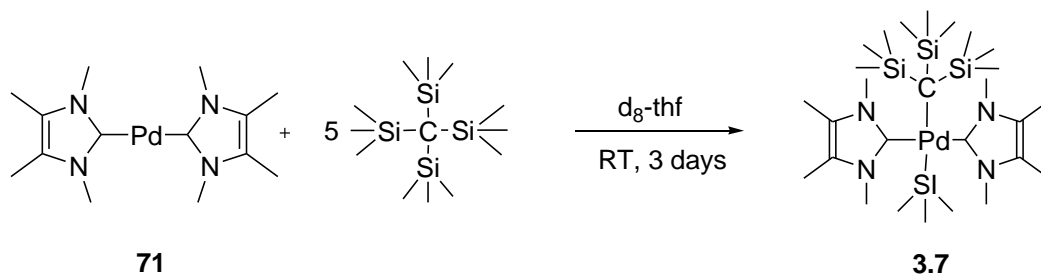
This would seem to suggest that the presence of the Si(SiMe₃)₄ substrate combined with a Pd(ITMe) species is inducing this isomerisation.

Beller and co-workers reported a similar mixture of *p* and *m* isomers formed when using the palladacycle, trans-di(μ-acetato)-bis[o-(di-*o*-tolylphosphino)benzyl]dipalladium(II). They hypothesised that after reduction of the palladacycle by base, two mechanisms could operate concurrently; a mechanism involving heterolytic cleavage of the Ar-X bond and a radical mechanism involving silyl radicals and aryne generation.²⁰²

In the reactions catalysed by **3.6**, the palladium species formed by reduction of **3.6**, $[\text{Pd}(\text{ITMe})_2(\text{SiMe}_2)_2]$ by base is not known but no evidence of hexamethyldisilane was seen in these reactions so it may not be a simple case of regeneration of $\text{Pd}(\text{ITMe})_2$.

3.2.7. C-Si bond cleavage

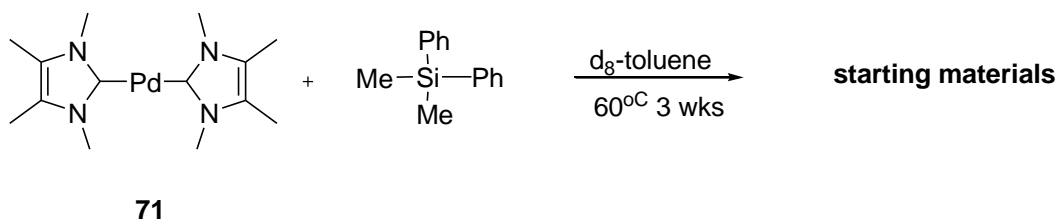
To replace the $\text{Si}(\text{SiMe}_3)_4$ as internal NMR integration standard, $\text{C}(\text{SiMe}_3)_4$ was made from literature procedures.²⁰⁴ The high dilution of **71**, $\text{Pd}(\text{ITMe})_2$ in the NMR solvents at first meant that $\text{C}(\text{SiMe}_3)_4$ loading was too high, masking any peaks from products of **71** that may have been seen around 0.00 ppm so initially $\text{C}(\text{SiMe}_3)_4$ did not appear to react with **71**. However, when a d_6 -benzene stock solution was made of $\text{C}(\text{SiMe}_3)_4$ to lower its concentration within the reaction, new peaks with a ratio 9:27 appeared at -0.03 ppm and 0.15 ppm and corresponding peaks, integrating to 12H, appeared at 1.95 ppm and 3.74 ppm. These peaks seem to indicate that the C-Si bond of between the quaternary carbon and one of the trimethylsilyl groups in $\text{C}(\text{SiMe}_3)_4$ has been cleaved (Scheme 3.17).



Scheme 3.17: ^1H NMR reaction of $\text{Pd}(\text{ITMe})_2$ with $\text{C}(\text{SiMe}_3)_4$

The reaction was scaled up and repeated in THF, however only unidentified ITMe species were recovered when isolation of **3.7** was attempted. Again, as with $[\text{Pd}(\text{ITMe})(\text{SiMe}_3)_3(\text{SiMe}_3)]$, **3.2**, the compound was very soluble in common solvents or could not be separated from the large amount of excess $\text{C}(\text{SiMe}_3)_4$ used in its synthesis.

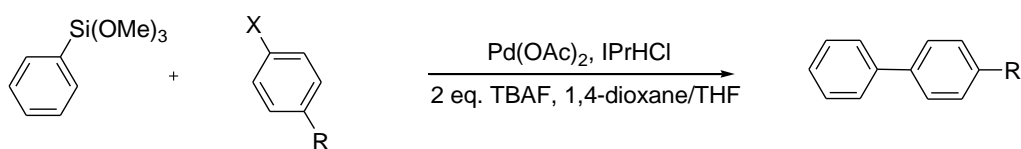
To determine whether $\text{Pd}(\text{ITMe})_2$, **71**, was capable of cleavage of less hindered C-Si bonds, the reaction in Scheme 3.18 was undertaken.



Scheme 3.18: Unsuccessful attempts to cleave the C-Si bond of diphenyl-dimethylsilane

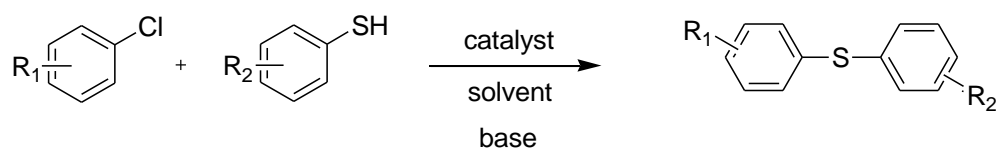
The reactant, diphenyl-dimethylsilane, has both aryl C-Si and alkyl C-Si bonds, of which the aryl C-Si bonds are generally the weaker. This lack of reactivity with diphenyl-dimethylmethane coupled with the fact that none of the C-Si bonds within the trimethylsilyl moiety in $\text{C}(\text{SiMe}_3)_3$ were cleaved, suggests that **71** is limited in its ability to cleave C-Si bonds

The Hiyama reaction involves cleavage of C-Si bonds, however they generally require activation before they can be cleaved as their more polar nature makes them stronger than Si-Si bonds. Electronegative substituents or fluorine anions are often capable of activating C-Si bonds. Nolan et al achieved coupling of aryl siloxanes and aryl halides (Scheme 3.19) where the C-Si bond is activated by the large fluorine anion, TBAF, $[\text{N}(n\text{-Bu})_4]^+\text{F}^-$.²⁰⁵



Scheme 3.19: Cross coupling protocol where a C-Si bond is activated by TBAF, $[\text{N}(n\text{-Bu})_4]^+\text{F}^-$

3.2.8 Use of Pd bis carbene complexes for aryl chloride-aryl thiol coupling



Scheme 3.20: General reaction for catalytic coupling of aryl thiols with aryl chlorides

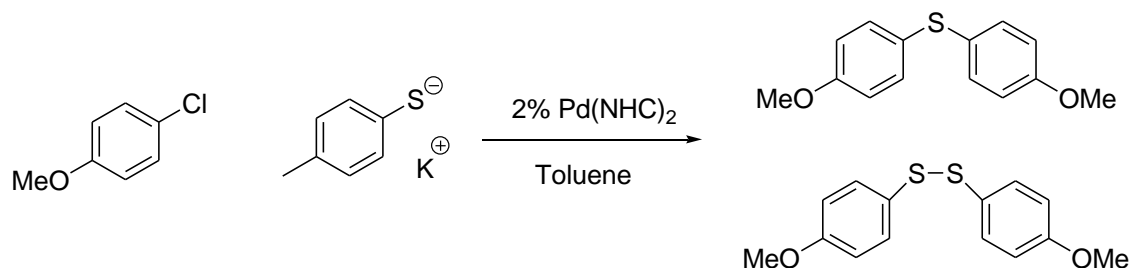
The general reaction protocol for coupling of aryl chlorides with aryl thiols to substitute chloride for sulphide and generate a new C-S bond is depicted in Scheme 3.20 above.

Palladium catalysed coupling of thiols with aryl chlorides has previously been reported by Hartwig *et al* using the CyPF-^tBu ligand, showing excellent yields with 2% catalyst loading at 110 °C in toluene.²⁰⁶

Work has also been reported by Zhang *et al*²⁰⁷ using Ni(NHC)₂ complexes with aryl bromides at 100 °C in DMF with 3% Ni(NHC)₂. This work showed that among the monochelating *NHC* ligands the best coupling was achieved by strong electron donating *NHC*s. However, overall the best coupling was achieved by bischelating *NHC*s which form more stable complexes to give longer catalytic lifetimes.

The reactions were followed by GC-MS with *n*-dodecane as internal standard.

Initial attempts at NMR reactions were hindered by the immediate formation of the potassium thiolate, which is sparingly soluble in d₈-toluene. A change of base was considered but it has previously been found that more soluble bases often give poorer results in these couplings.⁴⁷ After this, the potassium 4-methoxyphenyl thiolate was added preformed to the solution of 4-chloroanisole and 2% mol Pd(NHC)₂ and the reactions followed by GC-MS. The reaction is shown in Scheme 3.20 and the results tabulated in Table 3.3.



Scheme 3.20: Coupling reaction of aryl chloride with aryl thiol using Pd(NHC)₂ as catalyst

Catalyst 2% mol	Temp/ °C	Solvent	Reaction length	% Yield*
Pd(SIPr) ₂	110	Toluene	24hrs	10
Pd(SIPr) ₂	80	Toluene	7 days	18.1
Pd(I ^t Bu) ₂	80	Toluene	7 days	20.4

*Coupling product yield calculated by loss of 4-chloroanisole in rxn mixture by GC-MS

Table 3.3: Results of Pd(NHC)₂ complexes as pre-catalysts for the aryl thiol coupling

The reaction using the Pd(SIPr)₂ as catalyst was complicated by the considerable formation of the disulphide. There was no further catalytic activity observed in the 110 °C reaction after the first 24 hours, presumably caused by catalyst degradation. This cross coupling reaction is often found to have a low turnover number.⁴⁷

Using Pd(I^tBu)₂ as the catalyst achieved better results, with 20% coupling product after 7 days at 80 °C with negligible amounts of disulphide by-product formed.

This is one of the few reactions where I^tBu out-performs SIPr. This may well be due to the alkyl *NHC*, I^tBu, making the Pd centre more electron rich and echoes the result found by Zhang and co-workers⁴⁷ (*vide infra*) that the more electron rich, sterically hindered *NHCs* give better results. The steric hindrance is thought to prevent formation of the disulphide.⁴⁶

3.3 Conclusions

The oxidative addition product of $\text{Pd}(\text{ITMe})_2$ and 4-chloroanisole forms readily but conversion to a dimeric species is very slow, implying an associative mechanism for the formation of $[\text{Pd}(\text{ITMe})(\text{ArOMe})\text{Cl}]$. The same trend is observed *via* ^1H NMR for the reaction with 4-chloro-methylbenzoate.

Unsuccessful attempts to follow the oxidative addition reaction by NMR led to the unexpected reaction with the NMR standard, $\text{Si}(\text{SiMe}_3)_4$. This led to the synthesis and isolation of the complex **3.6** which shows comparatively good catalytic activity but generates both the *para* isomer and the *meta* isomer of the aryl amination product. $\text{Pd}(\text{ITMe})_2$ has limited ability to cleave C-Si bonds but is more reactive with Si-Si bonds, reflecting known trends in bond lengths.

Finally, $\text{Pd}(\text{t}^i\text{Bu})_2$ and $\text{Pd}(\text{SIPr})_2$ are poor catalysts for aryl-S bond formation. This is most likely due to the Pd-S bond being difficult to cleave.

3.4 Experimental Section

PdCl_2 was prepared from K_2PdCl_4 , supplied by Aldrich, using Amberlite© IR120 cation exchange resin in the H^+ form¹⁰. K_2PdCl_4 is dissolved in water and passed through the resin. The H_2PdCl_4 eluent had the solvent removed by rotor vaporator to leave the solid PdCl_2 .²⁰⁸

$[\text{Pd}(\eta^3\text{-methallyl})(\text{ITMe})\text{Cl}]$ and ITMe were synthesised according to literature procedures^{209,210}. 4-chloroanisole, 4-chlorotoluene, 4-methoxychlorobenzene, and morpholine, hexamethyldisilane, diphenyl-dimethylmethane and dodecane were purchased from Aldrich and dried over activated 3Å molecular sieves, degassed and vacuum transferred into ampoules equipped with greaseless stopcocks. $\text{C}(\text{TMS})_4$ and $\text{Si}(\text{TMS})_4$ were prepared from literature procedures²¹¹. For General Experimental, see Appendix I.

3.4.1. Synthesis of $\text{Pd}(\text{ITMe})_2$, 71.

In the glove box, $[\text{Pd}(\eta^3\text{-methallyl})(\text{ITMe})\text{Cl}]$ (0.058, 0.178mmol) was weighed out and placed in an ampoule. ITMe (0.049g, 2.2 eq.) was weighed into one Schlenk and KO^tBu (0.049g, 2.4eq) was weighed into a second Schlenk. 30ml of toluene was added to the $[\text{Pd}(\eta^3\text{-methallyl})(\text{ITMe})\text{Cl}]$, 10ml to the KO^tBu and 5ml to the ITMe. The ITMe was added *via* cannula to the suspension and stirred. Next, the KO^tBu was added *via* cannula to the reaction mixture. The suspension was vigorously stirred throughout this addition. The reaction mixture was heated to 60 °C for 48 hours. The dark orange reaction mixture was then filtered through flame-dried celite©. The orange toluene filtrate was concentrated then left in the -50°C freezer for 2 days. The bright yellow powder that precipitated was found to be the desired product. 66% yield.

$^1\text{H NMR}(d_5\text{-pyridine})$: 4.04 ppm (s; 6H); 1.84 ppm (s; 6H); $^1\text{H NMR}(d_6\text{-benzene})$: 3.92 ppm (s; 6H); 1.55 ppm (s; 6H);

Other data found to be in agreement Lit ref: Titcomb, L.; University of Sussex, Brighton, DPhil Thesis, **2001**

3.4.2. Synthesis of $[\text{Pd}(\text{ITMe})_2(\text{CH}_3\text{O}-4\text{-C}_6\text{H}_4)\text{Cl}]$, 3.1

In the dry glove box, $\text{Pd}(\text{ITMe})_2$ (12mg, 0.03mmol) was weighed out and placed in an ampoule. The ampoule was charged with 30ml of benzene and 2 eq. of 4-chloroanisole were added via syringe to the ampoule which was then heated at 60 °C under reduced pressure for 3 days. The solvent was then removed in *vacuo* and the resulting grey powder re-dissolved in toluene and filtered by cannula. The product was recovered after 2 days at -50 °C as white powder in 69% yield. Crystals suitable for x-ray crystallography were grown in d_8 -toluene.

^1H NMR(d_8 -toluene): 7.16 ppm (d; 2H); 6.47 ppm (d, 2H) 3.78 ppm (s; 12H); 3.20 ppm (s, 3H, OCH_3) 1.40 ppm (s; 12H); (CDCl_3): 6.94-6.92 ppm (2H, d, $J_{\text{H-H}} = 8.32\text{Hz}$); 6.46-6.44 ppm (2H, d, $J_{\text{H-H}} = 7.98\text{Hz}$); 3.98 ppm (s; 12H NCH_3 (NHC)); (s; 12H, CH_3 (NHC $\text{C}=\text{C}$)); 3.64 ppm (s, 3H); 2.00 ppm (s; 12H, CH_3 (NHC $\text{C}=\text{C}$)); ^{13}C { ^1H } NMR: sample not sufficiently concentrated. MS 391 m/z M^+ , 354 m/z $[\text{M}-\text{Cl}]^+$. **Elemental analysis:** Anal. Calc'd. for $\text{C}_{20}\text{H}_{31}\text{N}_4\text{OPdCl}$: C: 42.77, H: 6.99, N: 8.17. Found C: 42.79, H: 6.90, N: 8.19

Crystals suitable for X-ray crystallography were grown in d_8 -toluene.

3.4.3. $[\text{Pd}(\text{ITMe})(\text{CH}_3\text{O}-4\text{-C}_6\text{H}_4)\text{Cl}]_2$, 3.3 - observed by ^1H NMR:

In the dry glove box, $[\text{Pd}(\text{ITMe})_2(\text{CH}_3\text{O}-4\text{-C}_6\text{H}_4)\text{Cl}]$ (4mg, 0.01mmol) was dissolved in 0.6ml d_1 -chloroform. The NMR sample was heated to 50°C and after 3 weeks the NMR analysis revealed $[\text{Pd}(\text{ITMe})(\text{anisole})\text{Cl}]_2$ had been produced.

^1H NMR (CDCl_3): 7.68-7.66 ppm (d; 4H aryl CH); 7.12- 7.10 ppm (d, 4H, aryl CH) 3.87 ppm (s; 6H, OCH_3); 3.67 ppm (s; 12H NCH_3 (NHC)); 2.37 ppm (s; 12H, CH_3 (NHC $\text{C}=\text{C}$)); **.MS (ESI) of crude product:** 607 m/z $[\text{M}-\text{ITMe}-\text{CH}_3]^+$; 517 m/z $[\text{M}-\text{ITMe}-\text{CH}_3\text{OC}_6\text{H}_6]^+$; 481 m/z , $[\text{M}-\text{ITMe}-\text{CH}_3\text{OC}_6\text{H}_6-\text{OCH}_3]^+$

3.4.4. Synthesis of $[\text{Pd}(\text{ITMe})_2(\text{CH}_3\text{OOC-4-C}_6\text{H}_4)\text{Cl}]$, **3.4**

Procedure as with 3.1 but 4-chloromethoxybenzene is placed in a Schlenk in the dry glove box before a solution is made up of it which is transferred to the reaction vessel.

$^1\text{H NMR}$ (CDCl_3): 8.27-7.97 ppm (2H, d, $J_{\text{H-H}} = 7.96\text{Hz}$, aryl CH); 7.99-7.97 ppm ((2H, d, $J_{\text{H-H}} = 8.09\text{Hz}$, aryl CH); 3.84 ppm (s; 12H NCH_3 (NHC)); 3.70 ppm (s, 3H, COOCH_3) 2.05 ppm (s; 12H, CH_3 ($\text{NHC C}=\text{C}$)); ^{13}C { ^1H } **NMR**: sample not sufficiently concentrated. **MS** 525 m/z $[\text{M}]^+$ **Elemental analysis**: Anal. Calc'd. for $\text{C}_{21}\text{H}_{31}\text{N}_4\text{O}_2\text{PdCl}$: C: 50.29, H: 5.95, N: 10.66. Found C: 50.70, H: 6.71, N: 9.18, 9.21

Crystals grown in toluene were not suitable for X-ray crystallography.

3.4.5. $[\text{Pd}(\text{ITMe})(\text{CH}_3\text{OOC-4-C}_6\text{H}_4)\text{Cl}]_2$, **3.5** - observed by $^1\text{H NMR}$:

In the dry glove box, $[\text{Pd}(\text{ITMe})_2(\text{CH}_3\text{OOC-4-C}_6\text{H}_4)\text{Cl}]$ (4mg, 0.01mmol) was dissolved in 0.6ml d_1 -chloroform. The NMR sample was heated to 50°C and the NMR analysis revealed **3.5** after 4 weeks.

$^1\text{H NMR}$ (CDCl_3): 7.34-7.32 ppm (2H, d, $J_{\text{H-H}} = 7.85\text{Hz}$, aryl CH); 6.81-6.79 ppm ((2H, d, $J_{\text{H-H}} = 7.85\text{Hz}$, aryl CH); 3.52 ppm (s, 3H, COOCH_3); 3.36 ppm (s; 12H, NCH_3 (NHC)); 2.27 ppm (s; 12H, CH_3 ($\text{NHC C}=\text{C}$)).

3.4.6. Synthesis of $[\text{Pd}(\text{ITMe})_2(\text{Si}(\text{SiMe}_3)_3(\text{SiMe}_3)_2]$, **3.2**

In the glove box, $\text{Pd}(\text{ITMe})_2$ (4mg, 0.01mmol) was weighed out and placed in an ampoule. 5 eq. (1.8g) of tetrakis(trimethyl)silane were added to the ampoule and 0.9ml of d_8 -toluene was added to the solids. The ampoule was left for 2 days at RT. The reaction mixture was placed in a Young's tap NMR tube and ^1H -NMR analysis showed the product had formed in 99% yield.

$^1\text{H NMR}$ (d_1 -chloroform): 3.43 ppm (s, 1H, 3.22 ppm (s; 6H); 2.47 ppm (2, 6H) 2.45 ppm (s, 6H) 0.43 ppm (s; 27H);) 0.11 ppm (s; 9H); $^1\text{H NMR}$ (d_8 -toluene): 3.32 ppm (s; 12H); 1.45 ppm (s, 12H) 0.42 ppm (s; 27H); 0.10 ppm (s, 9H) **MS (ES)**: 427 m/z $[\text{M}-(\text{SiMe}_3)_3]^+$, 248 m/z $[(\text{SiMe}_3)_3]^+$

3.4.7. Synthesis of [Pd(ITMe)₂(SiMe₃)₂], 3.6

In the glove box, Pd(ITMe)₂ (12mg, 0.03mmol) was weighed out and placed in an ampoule and 30ml of THF added. 10 eq. of hexamethyldisilane were added *via* syringe to the ampoule which was then stirred at RT for 2 days. Volatiles were removed *in vacuo* and the resulting white powder was washed twice with cold pentane. The product was then re-dissolved in toluene and kept at -50 °C for 2 days whereupon crystals suitable for x-ray crystallography were grown.

¹H NMR(*d*₆-benzene): 3.30 ppm (s; 12H); 1.38 ppm (s, 12H) 0.49 ppm (s; 18H); ¹³C {¹H} NMR: sample not sufficiently concentrated. MS (ES): 427 *m/z* M-(SiMe₃)₃, 311 *m/z* [Pd(ITMe)₂]⁺. Crystals suitable for X-ray crystallography grown in toluene.

3.4.8. General procedure for the catalytic amination of aryl halides with any of the pre-catalysts: ¹H NMR

In a dry glove box, an NMR tube with a Young's tap was charged with a solution of 0.6ml of NMR solvent containing base, the internal standard, the pre-catalyst, and the reactants, morpholine and 4-chloroanisole. An initial NMR scan is taken. The NMR tube is then placed in a heating block at the designated reaction temperature and NMR scans are taken at appropriate times during the reaction length.

3.4.9. General procedure for observation of the reaction of aryl chlorides and aryl/alkyl thiols with any of the pre-catalysts: GC-MS

In a dry glove box, a Young's ampoule was charged with the pre-catalyst. The ampoule transferred to a Schlenk vacuum line and dry, deoxygenated solvent is added *via* cannula. The prescribed quantity of 4-chloroanisole is injected into the reaction ampoule. The procedure is repeated for the thiol and for the GC-MS internal standard (dodecane). After 5 minutes stirring, the first sample is transferred into a GC-MS vial. The reaction vessel is heated in an oil bath, preheated to the reaction temperature. Periodically, further samples are taken.

3.5 References

- ¹⁶¹ Herrmann, W. A.; Elison, M.; Fischer, J.; Kocher, C.; Artus, G. R. J., *Angew. Chem., Int. Ed. Engl.* **1995**, *34*, 2371.
- ¹⁶² Arduengo, A. J., III; Harlow, R. L.; Kline, M. *J. Am. Chem. Soc.* **1991**, *113*, 361
- ¹⁶³ McGuinness, D. S., Cavell, K. J., Skelton, B. W., White, A. H., *Organometallics*, **1999**, *18*, 1597.
- ¹⁶⁴ a) Green, M.J., Cavell, K.J., Skelton, B.W., White, A.H., *J. Organomet. Chem.*, **1998**, *554*, 175; b) McGuinness, D. S., Green, M. J., Cavell, K. J., Skelton, B. W., White, A. H., *J. Organomet. Chem.*, **1998**, *565*, 165; c) Magill, A. M., McGuinness, D. S., Cavell, K. J., Britovsek, G. J. P., Gibson, V. C., White, A. J. P., Williams, D. J., Yates, B. F., White, A. H., Skelton, B. W., *J. Organomet. Chem.*, **2001**, *617–618*, 546.
- ¹⁶⁵ a) Bohm, V.P.W., Gstottmayr, C.W.K., Weskamp, T., Herrmann, W.A., *Journal of Organometallic Chemistry*, **2000**, *595* 186; b) Weskamp, T., Bohm, V.P.W., Herrmann, W.A., *J. Organomet. Chem.*, **2000**, *600*, 12.
- ¹⁶⁶ Herrmann, W. A., Elison, M., Fischer, J., Kocher, C., Artus, G. R. J., *Chem. Eur. J.*, **1996**, *2*, 772.
- ¹⁶⁷ Tafipolsky, M., Scherer, W., Ofele, K., Artus, G., Pedersen, B., Herrmann, W. A., McGrady, G. S., *J. Am. Chem. Soc.*, **2002**, *124*, 5865
- ¹⁶⁸ Dorta, R., Stevens, E. D., Scott, N. M., Costabile, C., Cavallo, L., Hoff, C. D., Nolan, S. P., *J. Am. Chem. Soc.*, **2005**, *127*, 2485.
- ¹⁶⁹ Cavello, L., Correa, A., Costabile, C., Jacobsen, H., *J. Organomet. Chem.*, **2005**, *690*, 5407.
- ¹⁷⁰ Kelly III, R. A., Clavier, H., Giudice, S., Scott, N. M., Stevens, E. D., Bordner, J., Samardjiev, I., Hoff, C. D., Cavallo, L., Nolan, S. P., *Organometallics* **2008**, *27*, 202
- ¹⁷¹ Clavier, H., Nolan, S.P., *Chem. Commun.*, **2010**, *46*, 841.
- ¹⁷² Herrmann, W.A., Gooßen, L.J., Speigler, M., *J. Organomet. Chem.*, **1997**, *547*, 357.;
- ¹⁷³ Cazin, C. S. J., ed, Springer, London, **2010** and references therein
- ¹⁷⁴ Herrmann, W., Schwarz, J., *Organometallics*, **1999**, *18*, 4082.
- ¹⁷⁵ Titcomb, L, University of Sussex, Brighton, DPhil Thesis, **2002**
- ¹⁷⁶ Caddick, S., Cloke, F.G.N., Hitchcock, P.B., Leonard, J., de K. Lewis, A.K., McKerrecher, D., Titcomb. L.R., *Organometallics*, **2002**, *21*, 4318

-
- ¹⁷⁷ de K. Lewis, A. K., Caddick, S., Cloke, F. G. N., Billingham, N. C., Hitchcock, P. B., Leonard, J., *J. Am. Chem. Soc.*, **2003**, *125*, 10066.
- ¹⁷⁸ Lewis, A.K.de K., Caddick, S., Esposito, O., Cloke, F.G.N., Hitchcock, P.B., *Dalton Trans.*, **2009**, *35*, 7094
- ¹⁷⁹ Esposito, O., Hitchcock, P.B., Lewis, A.K.de K., Caddick, S., Cloke, F.G.N., *Organometallics*, **2008**, *27*, 6411
- ¹⁸⁰ Arentsen K., University of Sussex, Brighton, DPhil Thesis, **2006**; Esposito, O, University of Sussex, Brighton, DPhil Thesis, **2007**
- ¹⁸¹ Esposito, O, University of Sussex, Brighton, DPhil Thesis, **2007**
- ¹⁸² Dorta, R., Stevens, E. D., Scott, N. M., Costabile, C., Cavallo, L., Hoff, C. D., Nolan, S. P., *J. Am. Chem. Soc.*, **2005**, *127*, 2485
- ¹⁸³ Cavello, L., Correa, A., Costabile, C., Jacobsen, H., *J. Organomet. Chem.*, **2005**, *690*, 5407.
- ¹⁸⁴ Green, J. C., Benjamin, J. H., Lonsdale, R., *J. Organomet. Chem.*, **2005**, *690*, 6054.
- ¹⁸⁵ Stambuli, J. P.; Buhl, M.; Hartwig, J. F.; *J. Am. Chem. Soc.*, **2002**, *124*, 9346
- ¹⁸⁶ Ryan, C., Lewis, A., K. de K., Caddick, S., Kaltsoyannis, N., *Theor Chem Acc* , **2011**, *129*, 303
- ¹⁸⁷ Pytkowicz, J.; Roland, S.; Mangeney, P.; Jutand A. *J. Organomet. Chem.* **2003**, *678*, 166.
- ¹⁸⁸ Wurtz, S., Glorius, F., *Acc. Chem. Res.*, **2008**, *41*, 1523.
- ¹⁸⁹ Gilman, C.L. Smith H., *J. Organometal. Chem.*, **1967**, *8*, 98.
- ¹⁹⁰ Cavell, K. J., McGuinness, D., S., *Coord. Chem. Rev.*, **2004**, *248*, 671.
- ¹⁹¹ Crabtree, R., H., ed., Wiley, Hoboken, New Jersey, **2009**, and references therein
- ¹⁹² Shimada, S.; Tanaka, M. *Coord Chem Rev* **2006** *250* 991
- ¹⁹³ Esposito, O., Roberts, D. E., Cloke, F. G. N., Caddick, S., Green, J. C.. Hazari, N.; Hitchcock, P. B., *Eur J Inorg Chem*, **2009**, 1844.
- ¹⁹⁴ Hatanaka, Y, Hiyama, T, *Tetrahedron Lett.*, **1987**, *28*, 40, 4715
- ¹⁹⁵ Tanabe, M., Mawatari, A., Osakada, K., *Organometallics*, **2007**, *26*, 2937
- ¹⁹⁶ Murakami, M., Yoshida, T., Ito, Y., *Organometallics*, 1994, *13*, 2900.
- ¹⁹⁷ a)Matsumoto, H., Yoshihiro, K., Nagashima, S., Watanabe, H., Nagai, Y., *J. Organomet. Chem.*,**1977**, *128*, 409.b) Urata, H., Suzuki, H, Moro-oka, Y., Ikawa, T., *J. Organomet. Chem.*, **1982** *234* 367

-
- ¹⁹⁸ McNeill, E., Barder, T.E., Buchwald, S.L., *Org. Lett.*, **2007**, 9, 3785.
- ¹⁹⁹ Lee, S. Jørgensen, M., Hartwig, J. F., *Org. Lett.*, **2001**, 3, 17
- ²⁰⁰ Lermar, I.C., Cawley, M.J., Cloke, F.G.N., Arentsen, K., Scott, J.S., Pearson, S.E., Hayler J., Caddick, S., *J. Organomet. Chem.* **2005**, 690, 5841
- ²⁰¹ Harris, M. C., Huang, X., Buchwald, S. L., *Org. Lett.*, **2002**, 4, 3703
- ²⁰² Belier, M., Riermeier, T. H., Reisinger, C-P., Herrmann, W. A., *Tetrahedron Lett.*, **1997**, 38, 2073.
- ²⁰³ Tanabe, M., Mawatari, A., Osakada, K., *Organometallics*, **2007**, 26, 2937
- ²⁰⁴ H. Gilman, C.L. Smith H., *J. Organometal. Chem.*, **1967**, 8, 98.
- ²⁰⁵ Lee, H.M., Nolan, S. P., *Org Lett.*, **2000**, 2, 2053.
- ²⁰⁶ Fernandez-Rodriguez, M A, Shem, Q, Hartwig, J F, *J Am Chem Soc*, **2006**, 128, 7, 2180.
- ²⁰⁷ Zhang, Y, Ngeow, K C, Ying, J Y, *Org Lett*, **2007**, 9, 2495
- ²⁰⁸ Hartley, F., R., Jones, S. R., *J. Organomet. Chem.*, **1973**, 66, 465.
- ²⁰⁹ Kuhn, N., Kratz, T., *Synthesis*, **1993**, 561.
- ²¹⁰ Cawley, M.J., Cloke, F.G.N., Fitzmaurice, R.J., Pearson, S.E., Scott, J.S., Caddick, S., *Org. Biomol. Chem.*, **2008**, 6, 2820

Chapter Four:

Attempts to isolate an aryl palladium chloride complex of 2,6-diisopropylimidazolin-2-ylidene using aryl Grignards and [Pd(1,5-COD)Cl₂]

4.1 Introduction

The behaviour of many *NHC* palladium complexes has now been extensively researched; as has their ability as catalysts for many different cross-coupling reactions.¹ The general trend perceived is that, of the more commonly used, simple, mono-ligating *NHCs* (Figure 16, Chapter 1), SIPr and IPr form complexes that show excellent catalytic activity in cross-coupling reactions.¹

[Pd(I^tBu)₂(aryl)Cl] complexes have previously been isolated in our group *via* oxidative addition of aryl chloride (aryl= 4-chloroanisole, 4-chlorotoluene, and 4-methoxybenzene) to the zero-valent bis-ligated Pd(I^tBu)₂.² However, attempts to isolate the analogous SIPr complexes by reacting Pd(SIPr)₂ with these aryl halides have failed due to the reductive elimination of the arylimidazolinium compound.³

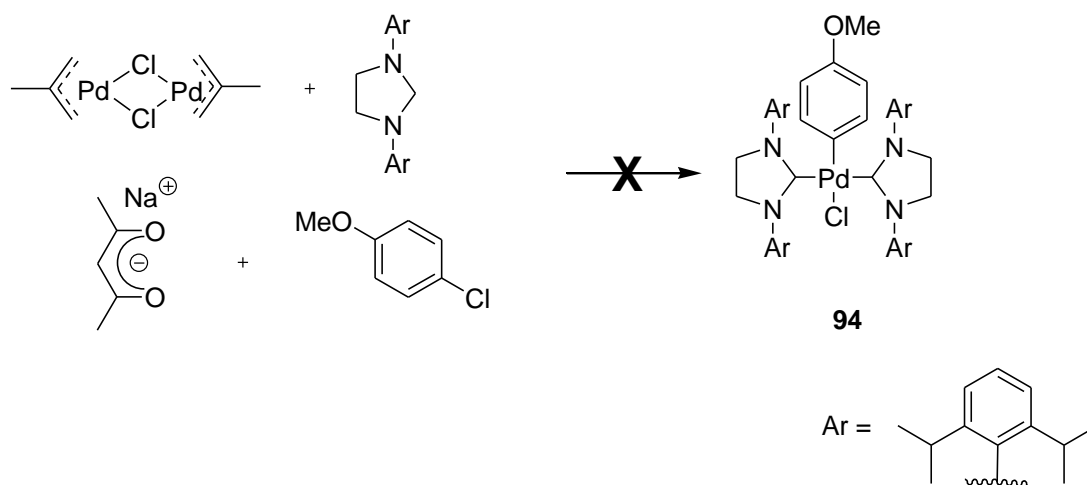
Thus, our interest in isolating [Pd(SIPr)₂(aryl)Cl] complexes is two-fold: generation of a potentially excellent new catalyst and the possibility that these complexes may further elucidate the mechanism of oxidative addition of aryl chlorides to Pd-*NHC* species.

4.2 Results and Discussion

4.2.1 Revisiting the attempts to form aryl oxidative addition product directly.

Initially, the approach taken was to generate the oxidative addition product of $\text{Pd}(\text{SIPr})_2$ and aryl chloride by a one pot synthesis where $\text{Pd}(\text{SIPr})_2$ was generated *in situ* (Scheme 4.01). 4-chloroanisole was chosen as the aryl chloride reactant because the presence of the electron-donating OMe group at the *para* position on the arene makes it one of the poorer coupling partners and thus it was reasoned that the rate of OA would be slower and thus increase our chances of isolating the desired product.

However the reaction, which is illustrated in Scheme 4.01, led to an intractable mixture of products and there were no conclusive evidence that the oxidative addition product had formed.



Reaction conditions: Temperatures: 40°C, 50°C, Solvents: benzene

Scheme 4.01: Unsuccessful attempt to form desired complex **94** from a one-pot procedure

The reaction of pre-formed $\text{Pd}(\text{SIPr})_2$ with 4-chloroanisole was also revisited (Scheme 4.02).⁴

The reaction undertaken in CHCl_3 at 50°C yielded colourless crystals. However, when these were resolved, they were found to be $[\text{Pd}(\text{SIPr})_2(\text{Cl})]_2$.

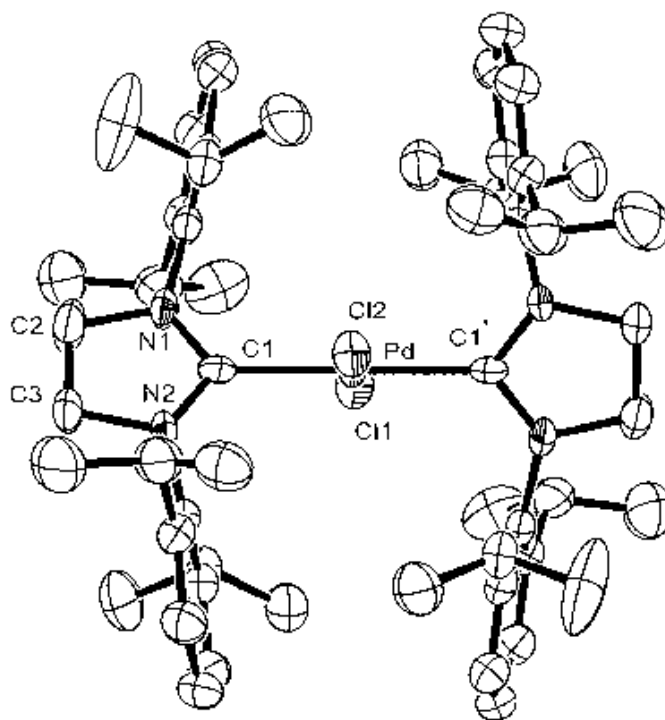
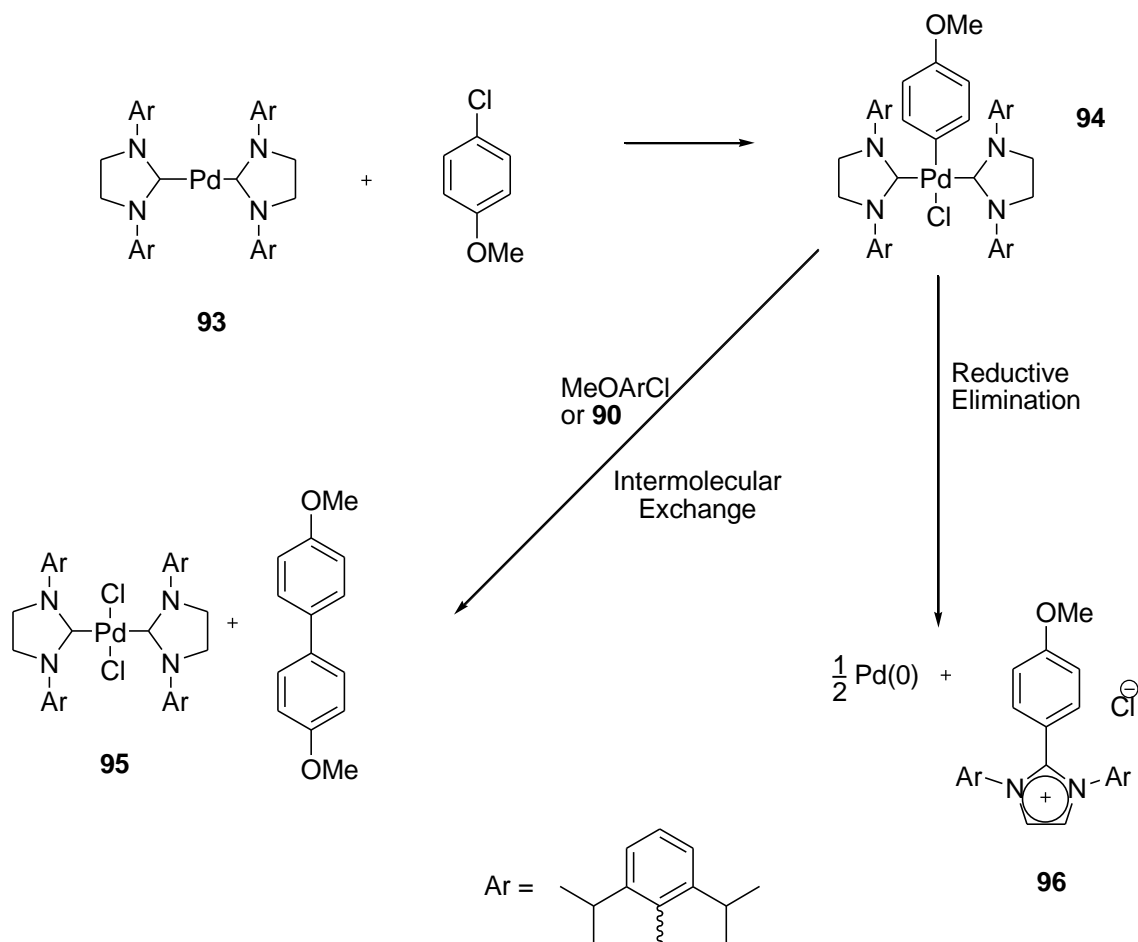


Figure 48: Ortep diagram of the molecular structure of $[\text{Pd}(\text{SIPr})_2\text{Cl}_2]$, **95**, showing 50% thermal ellipsoids. Hydrogens omitted for clarity. Selected bond lengths (Å) and angles($^\circ$): Pd-C(1) 2.049(5), Pd-Cl(2) 2.290(2) Pd-Cl(1) 2.305(2)
C(1)-Pd-C(1') 179.7(3), C(1)-Pd-Cl(2) 89.86(17)
C(1)-Pd-Cl(1) 90.14(17), C(2)-Pd-Cl(1) 180.0

No significant deviation in bond lengths from comparable complexes.

There is a well-known reductive elimination pathway from aryl *NHC* palladium complexes^{3,5} previously discussed in this thesis and shown again in Scheme 4.02.

However, the main identifiable product of these reactions was formation of methoxyphenyl 2,6- diisopropylimidazolinium chloride, the aryl imidazolinium salt, **96**. This is formed by the reductive elimination pathway in Scheme 4.02 whilst intermolecular exchange pathway shows the results in the formation of **95**.



Reaction conditions: Temperatures: 40°C, 50°C; Solvents: benzene, chloroform

Scheme 4.02: Reaction of Pd(SIPr)₂ with 4-chloroanisole

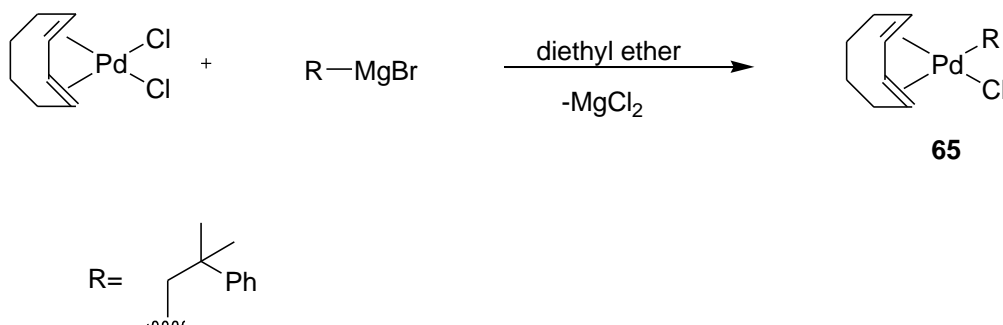
It was difficult to envisage that direct addition of the aryl chloride would yield the desired aryl *NHC* palladium complex. The aryl *NHC* palladium species is too transient at the elevated temperature required for its formation by direct oxidative addition, reacting before it can be isolated.⁶

Therefore, an indirect method to form the aryl SIPr palladium product, **94**, was sought.

4.2.2: Indirect formation of Pd *NHC* aryl halide complexes: Reactions using mesityl magnesium bromide.

Aryl Grignards were the later arylating agent of choice over aryl lithiums as they are less reactive than organolithium reagents. The milder nature of the aryl Grignard would hopefully prevent double addition of aryl substrate to palladium and thus hinder the formation of Pd(0).

Gutierrez *et al*⁷ has previously used Grignards to form aryl and alkyl palladium complexes from Pd(1, 4-COD)Cl₂ as illustrated in Scheme 4.03.*

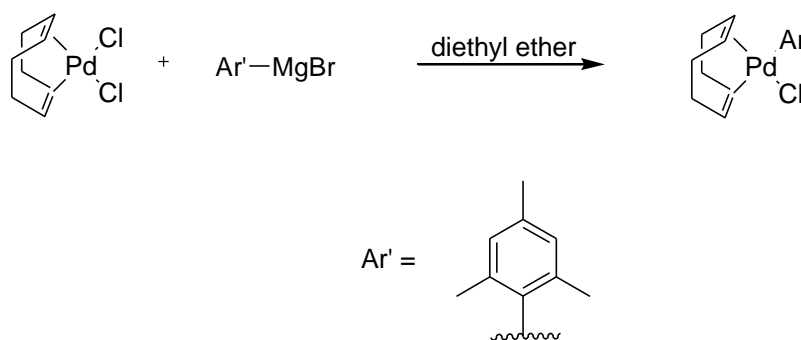


Scheme 4.03: [Pd(1, 4- COD)(CH₂(Me₂Ph))] to Pd(1, 4-COD)(Ph(C(CH₃)₃)]

Albeniz *et al*⁸ also produced Pd(COD)(aryl)X complexes but by transarylation between [Pd(C₆F₅)ether)] (ether = tetrahydrofuran or diethyl ether) and PdCl₂(NCPh)₂ followed by ligand exchange of NCPh with 1,5-cyclooctadiene.

The first Grignard used was mesityl magnesium bromide as it was readily available. It was reacted with Pd(1,5-COD)Cl₂ in an attempt to prepare [Pd(mesityl)(1,5-COD)Cl] (Scheme 4.04).

*The Scheme by Gutierrez *et al* was previously depicted in Scheme 2.3

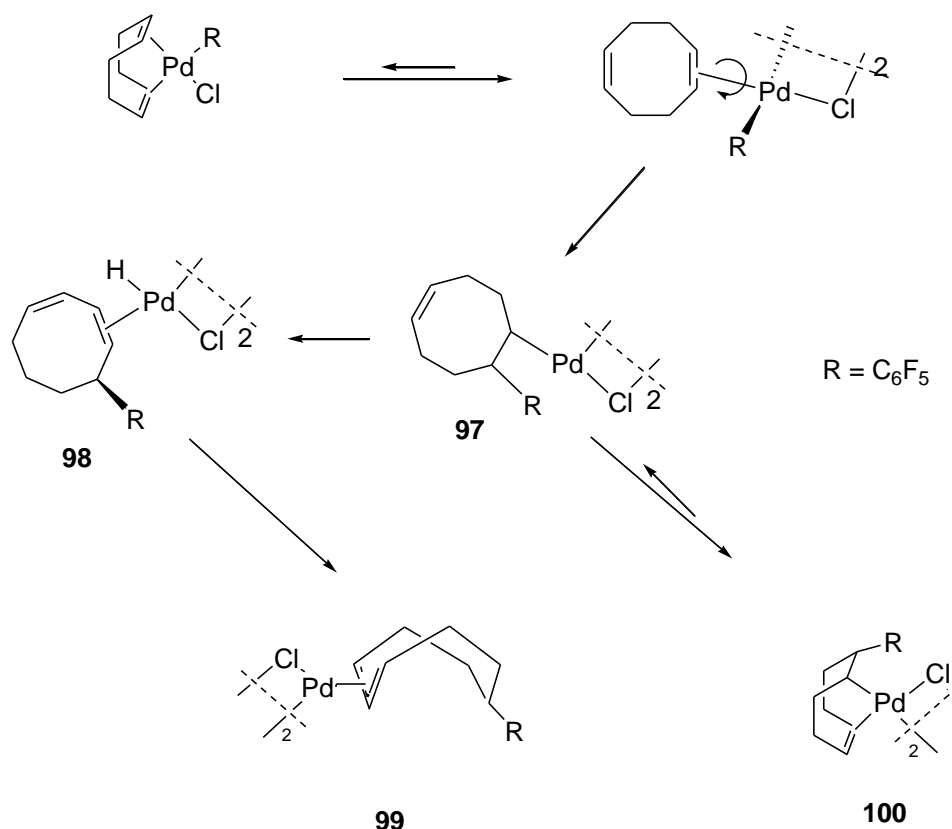


Reaction conditions: i) Addition of Ar'MgBr drop wise into Pd(1,5- COD)Cl₂ at -78°C
 ii) 3 hours, RT

Scheme 4.04: Desired reaction of Pd(1,5-COD)Cl₂ with mesityl magnesium bromide

The ¹H NMR spectrum indicates the formation of a mesityl 1,5-COD complex based on the integration of the peaks. The arrangement of the ligands, however, was unclear. Addition of mesitylene across one of the cyclooctadiene double bonds was suggested by the ¹H NMR data which showed seven peaks associated with the methylene and vinyl hydrogens of cyclooctadiene; significantly, peaks for the vinyl hydrogens were indicative of three different environments. The presence of the bromine peak in the mass spectrum also cast doubt on which halogen was present in the complex, particularly as a chloride adduct is easily abstracted and replaced by a bromide.^{9,10}

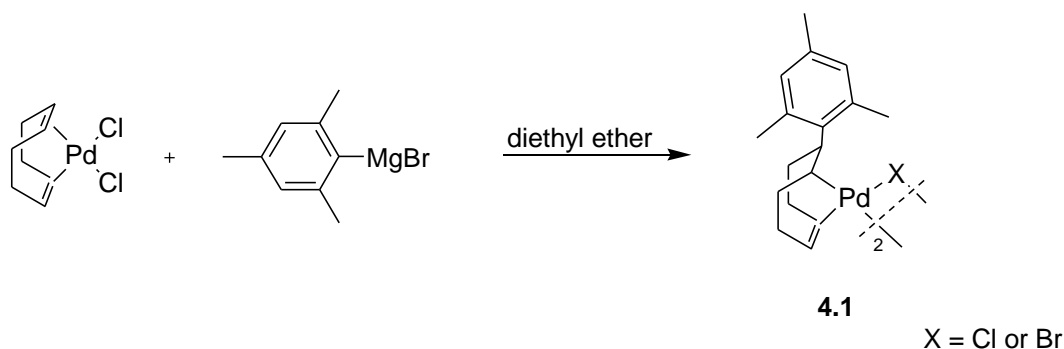
Activation of the alkene bonds in 1,5- cyclooctadiene is rare hence its ubiquitous use as a ligand in organometallic chemistry.¹¹ Albeniz *et al* found that [Pd(1,5-COD)(C₆F₅)Cl] slowly isomerised in solution at room temperature to the dimers, [Pd(8-C₆F₅-1:4-5-η³-cyclooctenyl)(μ-Cl)]₂, **100** and [Pd(6-C₆F₅-1-3-η³-cyclooctenyl)(μ-Cl)]₂, **99**. Scheme 4.06 summarises this reaction where the initiation step is partial dissociation of one of the COD alkenes from the palladium centre followed by the rotation by 90°C of η²-cyclooctenyl species to allow the R group to coordinate to the cyclooctadiene.



Scheme 4.05: The isomerisation of $[\text{Pd}(\text{COD})(\text{C}_6\text{F}_5)\text{Cl}]$ to both the allyl- cyclooctenyl species **99**, and the σ , π - cyclooctenyl species, **100**.

Formation of **99** is affected by the solvent properties; co-ordinating solvents can slow its formation by coordination to the vacant sites in a transitory mechanistic species, **97**, which has a detrimental effect on the formation of **98** and the subsequent palladium-hydride elimination from **98** needed to form **99**. Coordination of solvent to vacant sites on this transitory species does not have a significant effect on the coordination of the intramolecular double bond to palladium.⁸ Hence, in diethyl ether, the σ , π -cyclooctenyl species is the major product.

Stockland *et al* also saw this behaviour with $[\text{Pd}(1,5\text{-COD})(\text{ethyl})\text{Cl}]$ where, a d_6 -benzene ^1H NMR sample kept at ambient temperature transformed to a σ , π - complex, *via* ethene elimination, forming $[\text{Pd}(1,5\text{-COD})(\text{H})\text{Cl}]$ which then rearranged to the dimeric $[\text{Pd}(1-\eta^1, 4, 5-\eta^2-\text{C}_8\text{H}_{12})\text{Cl}]_2$.¹² Scheme 4.06 depicts this speculative reaction.

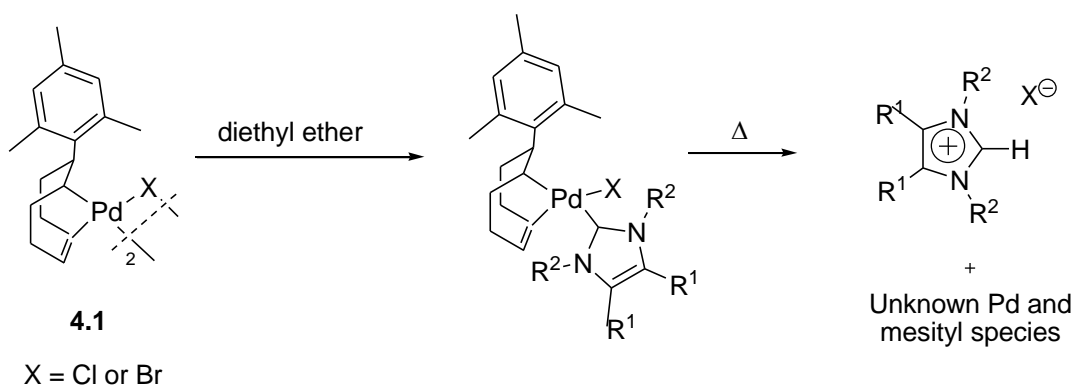


Reaction conditions: i) Addition of ArMgBr drop wise into Pd(COD)Cl₂ at -78°C
ii) 3 hours, RT

Scheme 4.06: Suggested reaction of Pd(1,5-COD)Cl₂ with mesityl magnesium bromide.

Speculative structure of **4.1** is [Pd(8-mesityl, 1-η¹, 4, 5-η²-C₈H₁₂))X]₂.

The crude product containing **4.1** was put into reaction with 3 different *NHCs*: SIPr, I^tBu and ITMe, depicted in Scheme 4.07.



4.2 R¹ = Me; R² = Me

4.3 R¹ = H; R² = Ar Ar = diisopropylphenyl

101 R¹ = H; R² = ^tBu

Scheme 4.07: Reaction of *NHCs* with crude **4.1**

The reaction of **4.1** with SIPr was undertaken initially at RT, where, after a short time (approx. 5 minutes), the precipitation of a white solid was observed. The ¹H NMR spectrum of this white solid exhibited the characteristic signals of SIPrH⁺, specifically the imidazolium hydrogen at *circa*.11 ppm. The reaction was then repeated at 0 °C for 3 hours, 3 times the length of the RT experiment to ensure ligand substitution fully occurred at this lower temperature.

The ^1H NMR data obtained from the white microcrystalline powder, formed as a precipitate, did appear to indicate from the integration of the H peaks that formation of $[\text{Pd}(\text{SIPr})(8\text{-mesityl}, 1\text{-}\eta^1, 4, 5\text{-}\eta^2\text{-C}_8\text{H}_{12})\text{X}]$, **4.3** had occurred. However, this complex was not isolated and only observed by ^1H NMR. Crystals grown in diethyl ether at -30°C were identified as $\text{SIPrH}^+\text{Br}^-$.

Reaction of **4.1** with I^tBu was attempted at 0°C but no complex was observed and formation of I^tBuH^+ was evidenced by the imidazolium H peak at 10.34 ppm in the ^1H NMR spectrum.

In the case where ITMe was used, the novel compound, **4.2**, was isolated in moderate yield (32%).

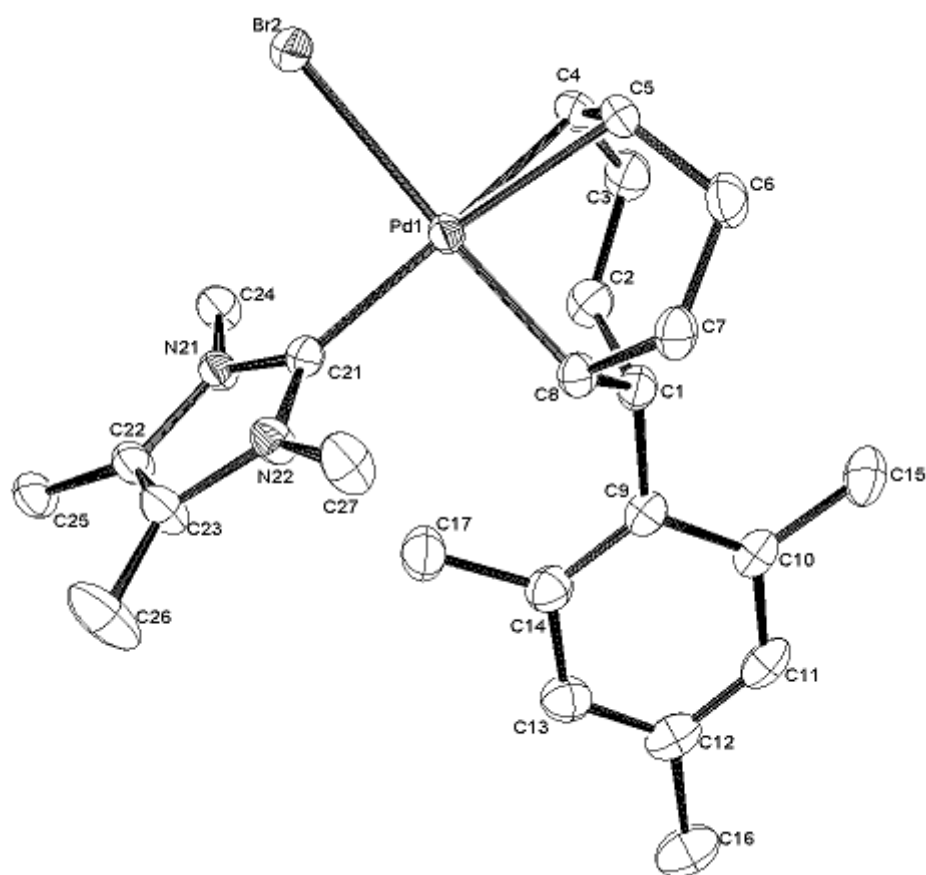


Figure 102: Ortep diagram of the mmolecular structure of [Pd(ITMe)(8-mesityl, 1- η^1 , 4, 5- η^2 -C₈H₁₂)Br], **4.2**, showing 50% thermal ellipsoids.

Hydrogens omitted for clarity. Selected bond lengths (Å) and angles (°):

Pd(1)-C(21) 2.015(3); Pd(1)-C(8) 2.075(3); Pd(1)-C(5) 2.248(3); Pd(1)-C(4) 2.262(3); Pd(1)-Br(2) 2.5671(4); C(21)-Pd(1)-C(8) 92.21(13); C(21)-Pd(1)-C(5) 166.38(13); C(8)-Pd(1)-C(5) 81.17(13); C(21)-Pd(1)-C(4) 157.46(13); C(8)-Pd(1)-C(4) 89.63(13); C(5)-Pd(1)-C(4) 35.31(13); C(21)-Pd(1)-Br(2) 90.00(9); C(8)-Pd(1)-Br(2) 174.49(9); C(5)-Pd(1)-Br(2) 95.61(9); C(4)-Pd(1)-Br(2) 90.26(9).

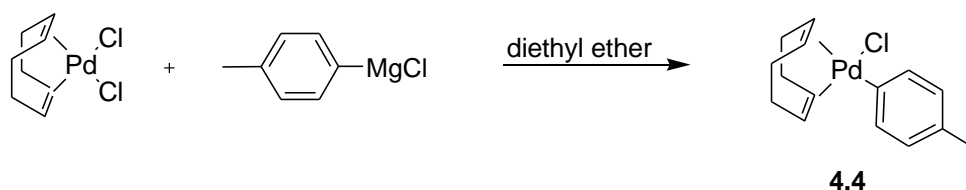
It would appear that ITMe has reacted with the σ , π -cyclooctenyl species, $[\text{Pd}(\text{8-mesityl}, 1-\eta^1, 4, 5-\eta^2 - \text{C}_8\text{H}_{12})\text{X}]_2$, **4.1**, formed by the isomerisation of $[\text{Pd}(1,5\text{-COD})(\text{mesityl})\text{Cl}]$ whilst the generation of the imidazolium salts by reaction of I^tBu and SIPr suggests that $\text{Pd}(1,5\text{-COD})(\text{mesityl})\text{X}$ ($\text{X}=\text{Br}, \text{Cl}$) is also present and formed by a pathway similar to the one which creates **99** in Scheme 4.05. This correlates with the results found by Albeniz *et al* shown in Scheme 4.07. The reason why the complex $\text{Pd}(1,5\text{-COD})(\text{mesityl})\text{BrCl}$ shows this behaviour is likely to be due to the presence of the *ortho* CH_3 groups causing steric crowding at the palladium centre¹³ whilst the palladium has activated the cyclooctadiene double bonds sufficiently to make addition of the mesityl substrate across the double bond favoured.^{8,9,13,14,15}

Another explanation is that the analogous complexes to **4.2** for I^tBu and SIPr, **101** and **4.3** undergo β hydrogen elimination. The larger steric bulk of these two *NHC*s compared to ITMe may necessitate rearrangement of $[\text{Pd}(\text{NHC})(\text{8-mesityl}, 1-\eta^1, 4, 5-\eta^2 - \text{C}_8\text{H}_{12})\text{Br}]$ to a geometry which will allow β hydrogen elimination and relieve steric strain. This would result in the formation of the observed imidazolium salt and a Pd complex, **99**, where the R group is mesityl. This is analogous to isomerisation between **100** and **99**, which has been observed, although in the case of $\text{R} = \text{C}_6\text{F}_5$, it did not occur until elevated temperatures⁸ but the activation energy may be lower for mesityl or be lowered by the introduction of a bulky ligand such as SIPr or I^tBu .

The complex, **4.2**, is analogous to the migratory insertion complex, $[\text{Pd}(\text{ITMe})(\text{8-mesityl}, 1-\eta^1, 4, 5-\eta^2 - \text{C}_8\text{H}_{12})\text{X}]$, for a Mizoroki-Heck reaction of 1,5-COD and aryl halide. Elimination of the Heck coupling product, $[(\text{Z})\text{-5-mesitylcyclooctadiene}]$, could be attempted with base. As a mono-ligated *NHC* complex, its ability as a pre-catalyst for the Heck reaction or, indeed, Buchwald-Hartwig aryl amination and other cross-couplings, could be evaluated. It is well-established that ratio of 1:1 of Pd to *NHC* is optimal for catalytic activity and thus well-defined, monodentate *NHC* complexes are generally better catalysts than the bidentate complexes of the same *NHC*.^{16,17}

4.2.3 Reactions using 4-tolylmagnesium chloride.

Previously within our group, $[\text{Pd}(\text{I}^t\text{Bu})_2(\text{Ar})\text{Cl}]$ complexes have been isolated and characterised¹⁸. Formation of one of these by an indirect route would be desirable so that an analogous $[\text{Pd}(\text{SIPr})_2(\text{Ar})\text{Cl}]$ might also be synthesised. To this end, 4-tolylmagnesium chloride in THF was prepared; the chloride being chosen to prevent an issue occurring with regards to the identity of the halide ligand; the 4-tolyl derivative chosen for its simplicity and lack of *ortho*-groups.⁸

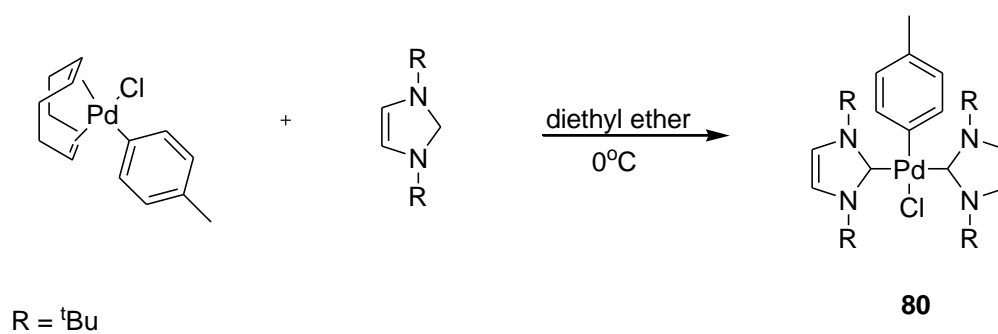


Reaction conditions: i) Addition of 4-tolylMgBr (THF) drop wise into $\text{Pd}(\text{COD})\text{Cl}_2$ at -78°C
 ii) 4 hours, RT

Scheme 4.08: Synthesis of $[\text{Pd}(1,5\text{-COD})(\text{tolyl})\text{Cl}]$, **4.4**

Scheme 4.08 depicts the reaction undertaken. ^1H NMR data of the crude product indicated that $[\text{Pd}(\text{tolyl})(1,5\text{-COD})\text{Cl}]$ has been successfully generated as the tolyl methyl peak at 2.37 ppm intergrated with 1,5-COD methylene peaks in ratio of 3:8. However, peaks from the homocoupling product, 4-(4-methylphenyl)toluene were also seen. Attempts to isolate the complex have failed, generally yielding 4-(4-methylphenyl)toluene even when recrystallisation was attempted from toluene.

The crude $[\text{Pd}(1,5\text{-COD})(\text{tolyl})\text{Cl}]$, **4.4** was then used in reaction with I^tBu . This successfully generated the $[\text{Pd}(\text{I}^t\text{Bu})_2(\text{tolyl})\text{Cl}]$, **80**, as observed by ^1H NMR¹⁹. Very little side product was observed (Scheme 4.09). The experiment was not attempted with SIPr at this time.



Reaction conditions: 0°C , 1 hour.

Scheme 4.09: The formation of $[\text{Pd}(\text{tBu})(\text{tolyl})\text{Cl}]$, **80**, by an indirect method using 4-tolylmagnesium chloride

4.3. Conclusions

Whilst an oxidative addition product complex of SIPr has not been generated, an indirect route to the oxidative addition product, $[\text{Pd}(\text{I}^t\text{Bu})_2(\text{tolyl})\text{Cl}]$, has been found. Other *NHCs* could be tried in this reaction at low temperatures to prevent reductive elimination of the 4-tolyl imidazolium salt.

There was non-innocent interaction of 1,5-cyclooctadiene in the $\text{Pd}(\text{1,5-COD})_2\text{Cl}_2$ /mesityl magnesium bromide / *NHC* system, where addition of the mesityl species across a cyclooctadiene double bond was observed. This system could be evaluated as a potential catalyst in Heck coupling; as could the novel complex, $[\text{Pd}(\text{ITMe})(8\text{-mesityl}, 1\text{-}\eta^1, 4, 5\text{-}\eta^2 - \text{C}_8\text{H}_{12})\text{Br}]$ which has been synthesised by the reaction of mesityl magnesium bromide with $\text{Pd}(\text{1,5-COD})\text{Cl}_2$ followed by addition of ITMe. As a monodentate *NHC* complex, its catalytic ability in other cross-couplings may also be worth assessing.

4.4 Experimental Section

PdCl_2 , $\text{Pd}(1,5\text{-COD})\text{Cl}_2$, SIPr, I^tBu , and ITMe were synthesised according to literature procedures given in previous chapters. 1,5 cyclooctadiene, 4-chloroanisole, 4-chlorotoluene were purchased from Aldrich and stored at room temperature over 3 Å molecular sieves. 4-tolyl magnesium chloride in THF was synthesised according to A Text book of Quantitative Inorganic Analysis by A. I. Vogel and kept at 4°C. Mesityl magnesium bromide was purchased from Aldrich, transferred to a Young's ampoule and kept at 4°C.

For General Experimental: See Appendix I

4.4.1. Synthesis of $\text{Pd}(\text{SIPr})_2\text{Cl}_2$, 95

$\text{Pd}(\text{SIPr})_2$ (0.058g, 0.058mmol) was weighed out in the dry glove box and placed in a Young's ampoule and 5ml of CHCl_3 was added. The reaction mixture was stirred for 30 mins at RT resulting in a pale yellow solution. A microlitre-syringe was flushed with argon and 4-chloroanisole (2 eq., 0.014ml, 0.117mmol) was injected into the reaction mixture through a subaseal. The reaction was heated at 50°C for 17 hours, let to equilibrate at RT and volatiles removed *in vacuo* and the resulting cream-coloured solid washed with hexane. Crystallisation was achieved after 3 days at -50 °C from slow diffusion of *n*-pentane into a THF solution of the reaction product. Yield: 22% yield.

^1H NMR Agrees with previously reported²⁰

MS (ES): m/z 496 (M- SIPr – 2Cl)+).

4.4.2. Synthesis of $[\text{Pd}(\text{8-mesityl}, 1\text{-}\eta^1, 4, 5\text{-}\eta^2\text{-C}_8\text{H}_{12}))\text{X}_2]$ (X=Cl, Br), 4.1

$\text{Pd}(1,5\text{-COD})\text{Cl}_2$ (0.198g, 0.7mmol) was weighed out and placed in a Young's ampoule and cycled on the Schlenk line and 15ml of THF was added. The Grignard reagent (1.022M diethyl ether solution, 0.4ml, 1eq) was measured with a syringe and injected into a small ampoule containing 5ml of THF. The $\text{Pd}(1,5\text{-COD})\text{Cl}_2$ suspension was cooled to -78°C using an acetone/dry ice bath. The diluted mesityl magnesium bromide

solution was slowly added dropwise to the cold Pd(1,5-COD)Cl₂ suspension via a thin cannula at a rate of aprox. 1 drop every 5 seconds. After the addition was completed, the reaction stirring was left for a further hour at -78°C. It was then left for a further 3 hours at RT. The dark reaction mixture was then filtered through Celite® and volatiles removed from the yellow filtrate *in vacuo* to furnish the title compound as The product was a yellow microcrystalline solid produced in 62% yield.

¹H {¹³C} NMR (*d*₆-benzene): 6.80, 6.72 ppm (m; 2H, aryl CH); 6.62 ppm (m, 1H, C=C (cycloocta-1-ene)); 6.12- 6.09 ppm (m, 2H, C=C (cycloocta-1-ene)); 4.18 ppm (m, 1H, CH (cycloocta-1-ene)) 2.86 ppm (CH₃ (mesityl)) 2.60-2.52 ppm (m, 1H, CH (cycloocta-1-ene)) 2.45-2.36 ppm (m, 1H, CH₂ (cycloocta-1-ene)); 2.13 ppm (s; 6H, (CH₃ (mesityl))); 1.84-.1.30 ppm (m, 6H, CH₂ (cycloocta-1-ene)) 0.86- 0.81 (m, 1H, CH₂ (cycloocta-1-ene)); **¹³C{¹H} NMR** (*d*₆-benzene): - 135.64 ppm (Ar); 134.82 ppm (Ar); 131.85 ppm (Ar); 129.37 ppm (C=C); 66.14.ppm (CH-Pd); 49.36 ppm (CH₂ (cycloocta-1-ene)); 42.98 ppm (CH₂ (cycloocta-1-ene)); 40.18 ppm (CH₂ (cycloocta-1-ene)); 28.10 ppm (CH₂ (cycloocta-1-ene)); 24.20 ppm (CH-Ar); 22.22 ppm (CH₃-Ar); 20.90 ppm (CH₃-Ar); Elemental analysis was not found. **MS (ES):** *m/z* 335 (M-CH₃- Cl/Br) +; 229 [(Z)-5-mesitylcyclooctadiene)]+

4.4.3. Synthesis of [Pd(ITMe)(8-mesityl, 1-η¹, 4, 5-η² – C₈H₁₂)Br], 4.2

In the dry glove box, a Schlenk tube is charged with 0.092g (0.259mmol) of [Pd(8-mesityl-1,4,5-η³ – C₈H₁₂)X₂] and an ampoule charged with ITMe (0.031g, 1 eq.). The two vessels were cycled 3 times onto the Schlenk vacuum line then dry diethyl ether was added to each (15 ml). The solution of [Pd(8-mesityl-1,4,5-η³ – C₈H₁₂)X₂] in diethyl ether was cooled in an ice bath. The yellow solution of ITMe was added by cannula to the yellow solution of [Pd(8-mesityl-1,4,5-η³ – C₈H₁₂)X₂] whereupon the solution became colourless almost immediately and a white precipitate formed. The reaction was run for an hour at RT. The ether was removed *in vacuo* and the pale yellow solid product was washed with pentane (2 x 10ml). The product was recrystallized from a diethyl ether solution kept at -30°C for 2 months.

¹H {¹³C} NMR(*d*₆-benzene): 6.71-6.63 ppm (d; 2H; CH (mesityl)); 3.72 ppm (s, 6H, CH₃ (NHC)); 3.32 ppm (m, 2H, C=C (cycloocta-1-ene)); 2.82 ppm (m, 1H, CH (cycloocta-1-ene)), 2.89

ppm (m, 3H, CH₃(mesityl)), 2.27 ppm (m, 3H, CH₃(mesityl)) 2.07 ppm (m, 3H, CH₃(mesityl)) 1.82 ppm (s, 6H, CH₃ (NHC)); 1.90-1.65 ppm(m, 4H, CH₂(cycloocta-1-ene)) 1.42- 1.27 ppm (m, 4H CH₂ (cycloocta-1-ene)) 0.97-0.90 ppm (m; 2H) CH₂ (cycloocta-1-ene); ¹³C{¹H} NMR sample not sufficiently concentrated. MS (ES): *m/z* 435 (M- Cl-CH₃); 514 (M- Br-CH₃). Elemental analysis was not found. Crystals suitable for X-ray crystallography grown in diethyl ether at -30°C for 2 months. (See Appendix II)

4.4.4. [Pd(SIPr) (8-mesityl, 1- η¹, 4, 5-η² – C₈H₁₂)Br], 4.3.

The procedure is the same as with Pd(ITMe) (8-mesityl 1,4,5-η³ – C₈H₁₂)Br except ITMe is substituted by SIPr.

¹H {¹³C} NMR (*d*₆-benzene): 7.73- 7.70 ppm (dd; 2H; J_(H-H)= 4 Hz CH (diisopropylphenyl)); 7.56-7.51 ppm (m; 2H; CH (mesityl)); 7.56- 7.51 ppm (dd; 2H; J_(H-H)= 4 Hz CH (diisopropylphenyl)); 4.24- 4.21 ppm (m, 1H, PdCH(cycloocta-1-ene), 3.93 ppm (b, s, 4H, CH (diisopropylphenyl)) 3.89 ppm (b, s, 4H, CH (diisopropylphenyl)) 3.80-3.75 (m, 1H, CH (cycloocta-1-ene)), 2.07 ppm (m, 9H, CH₃(mesityl)) 1.90-1.65 ppm(m, 4H, CH₂(cycloocta-1-ene)) 1.42- 1.27 ppm (m, 4H CH₂ (cycloocta-1-ene)) 0.97-0.90 ppm (m; 2H) CH₂ (cycloocta-1-ene); 0.84 ppm (m,12H, CH₂ (diisopropylphenyl));

4.4.5. Synthesis of [Pd(1,5-COD)(tolyl)Cl], 4.4.

The reaction is the same as performed in 4.4.2 expect for the use of 4-tolyl magnesium chloride solution (1.64M THF solution, 0.4ml, 1eq) and Pd(1,5-COD)Cl₂ (0.198g, 0.7mmol). The product was a yellow microcrystalline solid.

¹H {¹³C} NMR (*d*₁-chloroform): 7.97 ppm (m; 2H, aryl CH); 7.40 ppm (m, 2H, aryl CH) 7.00 ppm (m, 2H vinyl CH (cycloocta-1-ene); 4.43 ppm (m, 2H, vinyl CH (cycloocta-1-ene); 2.06 ppm (s; 3H, tolyl-CH₃); 1.67-1.48 ppm (m,8H, CH₂ (cycloocta-1-ene)) ¹³C{¹H} NMR sample not sufficiently concentrated. MS (ES): *m/z* 182 [4,4'-dimethylbiphenyl]+

4.5 References

- ¹ Cazin, C. S. J., ed, Springer, London, **2010** and references therein.
- ² de K. Lewis, A. K., Caddick, S., Cloke, F. G. N., Billingham, N. C., Hitchcock, P. B., Leonard, J., *J. Am. Chem. Soc.*, **2003**, *125*, 10066.
- ³ Titcomb, L, University of Sussex, Brighton, DPhil Thesis, **2002**
- ⁴ Lewis, A. K. de Kirian, D.Phil Thesis, University of Sussex, September **2004**
- ⁵ McGuinness, D.S., Cavell, K.J., Skelton, B. W., White, A. H , *Organometallics*, **1999**, *18*, 1596; Cavell, K.J., McGuinness, D.S., *Coord. Chem. Rev.*, **2004**, *248*, 671.
- ⁶ Marshall W., J., Grushin, V. V., *Organomet.*, **2003**, *22*, 1591
- ⁷ Gutierrez, E., Nicasio, M.C., Paneque, M., Ruiz, C., Salazar, V., *J. Organomet. Chem.*, **1997**, *549*, 167.
- ⁸ Albiniz, A.C., Espinet, P., Jeannin, Y., Philoche-Levisalles, M., Mann, B.E., *J. Am. Chem. Soc.*, **1990**, *112* 6594
- ⁹ March, J. “Advanced Organic Chemistry”, 4th ed, John Wiley and Sons, Inc., New York, **1992**.
- ¹⁰ Fallis, K. A., Anderson, G. K., Rath, N. P, *Organometallics* **1993**,*12*, 2435
- ¹¹ S. M. Wahidur Rahaman, Shrabani Dinda, Arup Sinha, and Jitendra K. Bera, *Organometallics*, Advanced copy received online October 19, 2012.
- ¹² Stockland, Jr., R. A., Anderson, G. K., Rath, N. P., Braddock-Wilking, J., Ellegood, J. C., *Can. J. Chem.*, **1996**, *74*, 1990 and references therein.
- ¹³ Hillier, A. C., Grasa, G. A., Viciu, M. S., Lee, H. M., Yang, C., Nolan, S.P., *J. Organomet. Chem.*, **2002**, *653*, 69
- ¹⁴ Trost, B. M., Semmelhack, M. F., Fleming, I., Elsevier, Oxford, 1991,
- ¹⁵ Beletskaya, I. P., Cheprakov, A. V., *Chem. Rev.* **2000**, *100*, 30093066
- ¹⁶ Marion, N., Nolan, S. P., *Acc. Chem. Res.*, **2008**, *41*, 1440.
- ¹⁷ See Chapter One, section on cross-coupling reactions
- ¹⁸ Caddick, S., Cloke, F.G.N., Hitchcock, P.B., Leonard, J., de K. Lewis, A.K., McKerrecher, D., Titcomb, L.R., *Organometallics*, **2002**, *21*, 4318
- ¹⁹ de K. Lewis, A. K., Caddick, S., Cloke, F. G. N., Billingham, N. C., Hitchcock, P. B., Leonard, J., *J. Am. Chem. Soc.*, **2003**, *125*, 10066.
- ²⁰ Arentsen, K., D.Phil Thesis, University of Sussex, April **2006**

Appendix I: Experimental details

General Experimental

All manipulations were carried out using standard Schlenk techniques under Ar (BOC Pureshield) or in a MBraun glovebox (N_2 , <1 ppm O_2 and <1 ppm H_2O) unless otherwise stated. All glassware were dried at 140 °C for a minimum of 1 hour. Diatomaceous earth (filter agent Celite[®] 545) was dried overnight in a 200 °C oven and flame dried under dynamic vacuum prior to use. Filtrations by cannula were performed using Whatman[®] 25 mm glass microfibre filters that had been dried at 140 °C for at least 48 hours prior to use.

Solvents were purchased from Fischer unless otherwise stated and were pre-dried over sodium wire for a minimum 72 hours (except $CHCl_3$ and CH_2Cl_2). They were then refluxed over the appropriate drying agent (Table A1) under an atmosphere of N_2 . They were stored in ampoules equipped with greaseless stopcocks (Youngs or ROTAFLO) over a potassium mirror or activated 4 Å molecular sieves (Table A1-1) under an atmosphere of argon. Once collected the dried solvent was transferred into an ampoule, degassed, and stored under argon.

Table A1-1: Drying agents and storage conditions of solvents

Solvent	Drying agent	Stored over
Toluene	Sodium	Potassium mirror
Diethyl ether	Sodium/potassium alloy	Potassium mirror
Pentane	Sodium/potassium alloy	Potassium mirror
Petroleum ether	Sodium/potassium alloy	Potassium mirror
Benzene	Potassium	Potassium mirror
Hexane	Potassium	Potassium mirror
THF	Potassium	4 Å Molecular sieves
CH_2Cl_2	Calcium hydride	4 Å Molecular sieves
Chloroform	Calcium hydride	4 Å Molecular sieves

Deuterated solvents (99%) were dried by refluxing over a suitable drying agent (Table A1-2) in Youngs ampoules, then vacuum transferred and degassed by three freeze-thaw cycles, prior to storage under dinitrogen in a MBraun glove box (<1 ppm O₂/ <1 ppm H₂O) in Youngs ampoules.

Table A1-2: Drying agents used for deuterated solvents

Solvent	Drying Agent
<i>d</i> ₈ -Toluene	Potassium
<i>d</i> ₆ -Benzene	Potassium
<i>d</i> ₅ -Pyridine	Potassium
<i>d</i> ₈ -THF	Potassium
Chloroform- <i>d</i>	Calcium Hydride

Instrumental Details

NMR data were acquired using a Bruker Avance DPX-300 or Varian Direct Drive S400 S500 spectrometers operating at 300, 400 and 500 MHz respectively (¹H). All NMR data is reported in accordance with the chemical shift convention outlined by IUPAC *ie.* a positive chemical shift denotes a positive frequency and *vice versa* with respect to the designated reference substance. ¹H and ¹³C nmr spectra were referenced internally either using the residual protio solvent (¹H) or the carbon signals of the deuterated solvent (¹³C). Unless otherwise stated all spectra were recorded at 303K. Coupling constants are reported in hertz.

Mass spectra (EI, FAB, and GC-MS) were recorded by Dr. A. Abdul-Sada at the University of Sussex on a VG autospec Fisons instrument (electron ionisation at 70 eV) or a Kratos MS25 mass spectrometer.

Elemental analyses were performed by Steven Boyer at the Elemental Analysis Service, London Metropolitan University, or by the Mikroanalytisches Labor GmbH, Remagen, Germany.

X-ray structural analyses and data refinements were carried out by Dr. P. B. Hitchcock, Dr. Martin Coles, Dr. Nikolaos Tsoureas and Dr. Mark Roe at the University of Sussex:

Single crystal X-ray diffraction analysis and data collection for compounds (ADD) were performed at 173 K on a Enraf-Nonius KappaCCD diffractometer equipped with an Oxford Cryosystems low temperature device with graphite-monochromated Mo K α radiation ($\lambda = 0.71073 \text{ \AA}$). The programs used for control and integration were Collect, Scalepack, and Denzo. The crystals were mounted on a glass fiber with silicon grease, from vacuum oil. All solutions and refinements were performed using the WinGX package² and all software packages within. All non-hydrogen atoms were refined using anisotropic thermal parameters, and hydrogens were added using a riding model. .

Data for compound ADD were collected at the National Crystallography Service at the University of Southampton using an Enraf-Nonius FR-591 rotating anode equipped with an APEX II CCD detector at 100K using an Oxford Cryostream low temperature device. The software packages used for data collection, cell refinement, data reduction, structure solution and refinement were the same as above.

Crystallographic data and refinement details for the molecular structures discussed in this thesis are presented in Appendix II and in more detail in electronic format as cif files in the CD-ROM disk appended in this thesis.

Appendix II: Crystallographic Data:

CIF files available on CD-ROM

A2.1: Crystal data for cis-Pd(ITMe) ₂ (Cl) ₂ , 67	A2-2
A2.2: Crystal data for trans-Pd(ICy) ₂ (Cl) ₂ , 2.3	A2-7
A2.3 Crystal data for trans-Pd(ICy) ₂ (neopentyl)Cl, 2.5	A2-13
A2.4 Crystal data for [Pd(I ^t Bu)Cl ₃] ⁻ [I ^t BuH] ⁺ , 2.9	A2-20
A2.5 Crystal data for trans-[Pd(ITMe) ₂ (<i>p</i> -anisole)(Cl)] 3.1	A2-29
A2.6: Crystal data for cis-[Pd(ITMe) ₂ (SiMe ₃) ₂], 3.6	A2-35
A2.7: Crystal data for trans-Pd(SIPr) ₂ (Cl) ₂ , 95	A2-42
A2.8: Crystal data for [Pd(ITMe)(8-mesityl (η ¹ (4, 5-η ²) – C ₈ H ₁₂)Br], 2.2	A2-48

A2.1: Crystal data for *cis*-Pd(ITMe)₂(Cl)₂Table 1. Crystal data and structure refinement for *cis*-Pd(ICy)₂(Cl)₂

Identification code	der14
Empirical formula	C17 H30 Cl2 N4 Pd
Formula weight	467.75
Temperature	293(2) K
Wavelength	0.71073 Å
Crystal system, space group	monoclinic, P21/c
Unit cell dimensions	a = 10.7309(4) Å alpha = 90 deg. b = 17.0824(7) Å beta = 130.383(2) deg. c = 14.2560(4) Å gamma = 90 deg.
Volume	1990.60(12) Å ³
Z, Calculated density	4, 1.561 Mg/m ³
Absorption coefficient	1.207 mm ⁻¹
F(000)	960
Crystal size	0.1 x 0.04 x 0.04 mm
Theta range for data collection	3.45 to 27.43 deg.
Limiting indices	-13 ≤ h ≤ 13, -22 ≤ k ≤ 22, -17 ≤ l ≤ 18
Reflections collected / unique	26050 / 4510 [R(int) = 0.0868]
Completeness to theta = 27.43	99.4 %
Refinement method	Full-matrix least-squares on F ²
Data / restraints / parameters	4510 / 0 / 225
Goodness-of-fit on F ²	0.934
Final R indices [I > 2σ(I)]	R1 = 0.0428, wR2 = 0.0800
R indices (all data)	R1 = 0.0802, wR2 = 0.0942
Largest diff. peak and hole	0.777 and -0.649 e.Å ⁻³

Table 2. Atomic coordinates ($\times 10^4$) and equivalent isotropic displacement parameters ($\text{\AA}^2 \times 10^3$) for *cis*-Pd(ITMe)₂(Cl)₂.

U(eq) is defined as one third of the trace of the orthogonalized U_{ij} tensor.

x	y	z	U(eq)	
Pd(1)	1910(1)	114(1)	2704(1)	20(1)
Cl(2)	677(1)	1243(1)	2763(1)	30(1)
Cl(3)	3093(1)	850(1)	2032(1)	29(1)
N(1)	-57(4)	-1076(2)	2828(3)	28(1)
N(2)	1569(4)	-434(2)	4519(3)	23(1)
N(11)	2647(4)	-1169(2)	1687(3)	23(1)
N(12)	4037(4)	-1323(2)	3622(3)	22(1)
C(1)	1075(5)	-502(2)	3371(4)	21(1)
C(2)	-277(6)	-1376(3)	3632(5)	33(1)
C(3)	755(6)	-975(3)	4686(4)	30(1)
C(4)	-924(6)	-1363(3)	1571(4)	41(1)
C(5)	-1489(7)	-2002(3)	3257(6)	55(2)
C(6)	1170(7)	-1063(3)	5903(5)	44(1)
C(7)	2772(5)	124(3)	5455(4)	29(1)
C(11)	2901(5)	-856(2)	2666(3)	19(1)
C(12)	3631(5)	-1827(2)	2027(4)	25(1)
C(13)	4514(5)	-1926(2)	3251(4)	25(1)
C(14)	1458(6)	-887(3)	419(4)	34(1)
C(15)	3623(6)	-2282(3)	1139(4)	33(1)
C(16)	5781(6)	-2510(3)	4129(4)	36(1)
C(17)	4656(5)	-1236(3)	4879(3)	26(1)
C(21)	-4513(11)	-173(5)	1020(8)	85(2)
C(22)	-5026(10)	-789(5)	342(8)	91(2)
C(23)	-4031(11)	483(5)	742(7)	103(3)

Table 3. Bond lengths [Å] and angles [deg] for *cis*-Pd(ITMe)₂(Cl)₂

Pd(1)-C(1)	1.978(4)
Pd(1)-C(11)	1.989(4)
Pd(1)-Cl(2)	2.3714(11)
Pd(1)-Cl(3)	2.3855(11)
N(1)-C(1)	1.348(5)
N(1)-C(2)	1.409(6)
N(1)-C(4)	1.468(6)
N(2)-C(1)	1.360(5)
N(2)-C(3)	1.394(5)
N(2)-C(7)	1.458(5)
N(11)-C(11)	1.347(5)
N(11)-C(12)	1.397(5)
N(11)-C(14)	1.463(5)
N(12)-C(11)	1.351(5)
N(12)-C(13)	1.398(5)
N(12)-C(17)	1.460(5)
C(2)-C(3)	1.340(6)
C(2)-C(5)	1.489(7)
C(3)-C(6)	1.494(6)
C(12)-C(13)	1.353(6)
C(12)-C(15)	1.480(6)
C(13)-C(16)	1.485(6)
C(21)-C(22)	1.286(9)
C(21)-C(23)	1.395(10)
C(21)-C(23)#1	1.986(11)
C(22)-C(23)#1	1.288(9)
C(23)-C(22)#1	1.288(9)
C(23)-C(21)#1	1.986(11)
C(1)-Pd(1)-C(11)	89.25(16)
C(1)-Pd(1)-Cl(2)	88.79(12)
C(11)-Pd(1)-Cl(2)	178.00(12)
C(1)-Pd(1)-Cl(3)	176.20(12)

C(11)-Pd(1)-Cl(3)	89.71(11)
Cl(2)-Pd(1)-Cl(3)	92.27(4)
C(1)-N(1)-C(2)	111.2(4)
C(1)-N(1)-C(4)	124.5(4)
C(2)-N(1)-C(4)	124.3(4)
C(1)-N(2)-C(3)	110.5(3)
C(1)-N(2)-C(7)	125.5(3)
C(3)-N(2)-C(7)	124.0(3)
C(11)-N(11)-C(12)	111.1(3)
C(11)-N(11)-C(14)	125.4(3)
C(12)-N(11)-C(14)	123.5(3)
C(11)-N(12)-C(13)	111.5(3)
C(11)-N(12)-C(17)	125.0(3)
C(13)-N(12)-C(17)	123.5(3)
N(1)-C(1)-N(2)	104.8(3)
N(1)-C(1)-Pd(1)	129.1(3)
N(2)-C(1)-Pd(1)	126.0(3)
C(3)-C(2)-N(1)	105.9(4)
C(3)-C(2)-C(5)	131.7(5)
N(1)-C(2)-C(5)	122.5(4)
C(2)-C(3)-N(2)	107.6(4)
C(2)-C(3)-C(6)	131.2(5)
N(2)-C(3)-C(6)	121.1(4)
N(11)-C(11)-N(12)	104.8(3)
N(11)-C(11)-Pd(1)	127.3(3)
N(12)-C(11)-Pd(1)	127.8(3)
C(13)-C(12)-N(11)	106.7(4)
C(13)-C(12)-C(15)	130.5(4)
N(11)-C(12)-C(15)	122.8(4)
C(12)-C(13)-N(12)	105.9(4)
C(12)-C(13)-C(16)	131.7(4)
N(12)-C(13)-C(16)	122.4(4)
C(22)-C(21)-C(23)	120.0(8)
C(22)-C(21)-C(23)#1	39.5(5)
C(23)-C(21)-C(23)#1	89.3(6)
C(21)-C(22)-C(23)#1	101.0(9)
C(22)#1-C(23)-C(21)	121.3(8)

C(22)#1-C(23)-C(21)#1	39.5(5)
C(21)-C(23)-C(21)#1	90.7(6)

Symmetry transformations used to generate equivalent atoms:

#1 -x-1,-y,-z

A2.2: Crystal data for *trans*-Pd(ICy)₂(Cl)₂

Table 1. Crystal data and structure refinement for may509_b.

Identification code	may509_b	
Empirical formula	C ₃₀ H ₄₈ Cl ₂ N ₄ Pd	
Formula weight	642.02	
Temperature	173(2) K	
Wavelength	0.710703 Å	
Crystal system	Triclinic	
Space group	P $\bar{1}$ (No.2)	
Unit cell dimensions	a = 11.1258(2) Å	α = 84.345(1)°.
	b = 11.1408(1) Å	β = 89.265(1)°.
	c = 12.9012(2) Å	γ = 76.170(1)°.
Volume	1545.10(4) Å ³	
Z	2	
Density (calculated)	1.38 Mg/m ³	
Absorption coefficient	0.80 mm ⁻¹	
F(000)	672	
Crystal size	0.36 x 0.12 x 0.06 mm ³	
Theta range for data collection	3.47 to 27.52°.	
Index ranges	-14 ≤ h ≤ 14, -14 ≤ k ≤ 14, -16 ≤ l ≤ 16	
Reflections collected	29431	
Independent reflections	7058 [R(int) = 0.051]	
Reflections with I > 2σ(I)	5705	
Completeness to theta = 27.52°	99.2 %	
Absorption correction	Semi-empirical from equivalents	
Tmax. and Tmin.	0.7130 and 0.6451	
Refinement method	Full-matrix least-squares on F ²	
Data / restraints / parameters	7058 / 66 / 362	
Goodness-of-fit on F ²	0.948	
Final R indices [I > 2σ(I)]	R1 = 0.036, wR2 = 0.083	
R indices (all data)	R1 = 0.050, wR2 = 0.090	
Largest diff. peak and hole	1.03 and -1.03 e.Å ⁻³	

One of the cyclohexyl substituents was disordered over two positions; the lower occupancy carbon atoms were isotropic

Data collection KappaCCD , Program package WinGX , Abs correction MULTISCAN

Refinement using SHELXL-97 , Drawing using ORTEP-3 for Windows

Table 2. Atomic coordinates ($\times 10^4$) and equivalent isotropic displacement parameters ($\text{\AA}^2 \times 10^3$) for may509_b. $U(\text{eq})$ is defined as one third of the trace of the orthogonalized U^{ij} tensor.

	x	y	z	$U(\text{eq})$
Pd(1)	5000	0	0	19(1)
Pd(2)	10000	0	5000	26(1)
Cl(1)	5048(1)	-1698(1)	1193(1)	43(1)
Cl(2)	9128(1)	1680(1)	3827(1)	40(1)
N(1)	7784(2)	-940(2)	237(2)	42(1)
N(2)	7154(2)	724(2)	996(3)	46(1)
N(3)	12322(2)	1013(2)	4666(2)	37(1)
N(4)	12449(2)	-622(2)	3880(2)	33(1)
C(1)	6758(2)	-55(2)	412(2)	31(1)
C(2)	8808(3)	-717(4)	716(4)	73(2)
C(3)	8408(3)	309(4)	1200(4)	76(2)
C(4)	7813(2)	-1952(2)	-423(2)	28(1)
C(5)	8366(3)	-3204(3)	155(2)	36(1)
C(6)	8397(3)	-4237(3)	-548(2)	39(1)
C(7)	9103(3)	-4058(3)	-1522(3)	44(1)
C(8)	8540(4)	-2819(4)	-2111(2)	51(1)
C(9)	8490(4)	-1761(3)	-1428(3)	49(1)
C(10)	6356(3)	1870(3)	1349(3)	37(1)
C(11)	6166(3)	1711(3)	2511(3)	43(1)
C(12)	5420(3)	2919(3)	2906(3)	40(1)
C(13)	6024(3)	3982(3)	2591(3)	42(1)
C(14)	6136(4)	4156(3)	1425(3)	51(1)
C(15)	6905(4)	2974(3)	1021(3)	58(1)
C(16)	11702(3)	137(2)	4504(2)	30(1)
C(17)	13441(3)	799(3)	4144(3)	45(1)
C(18)	13517(3)	-221(3)	3648(3)	44(1)
C(25)	12196(3)	-1770(2)	3551(2)	30(1)
C(26)	11971(3)	-1662(2)	2380(2)	32(1)
C(27)	11791(3)	-2875(3)	2031(3)	37(1)
C(28)	12871(3)	-3957(3)	2396(3)	39(1)
C(29)	13010(3)	-4069(3)	3569(3)	40(1)

C(30)	13243(3)	-2876(3)	3927(3)	39(1)
C(19)	11785(7)	1978(6)	5479(6)	20(2) ^a
C(20)	11440(6)	3261(5)	4871(4)	35(2) ^a
C(21)	10971(6)	4253(5)	5615(5)	40(2) ^a
C(22)	11901(6)	4226(6)	6450(6)	44(2) ^a
C(23)	12304(8)	2985(9)	7032(5)	54(2) ^a
C(24)	12765(6)	1951(7)	6313(5)	46(2) ^a
C(19A)	11998(8)	2000(8)	5251(6)	22(2) ^b
C(20A)	12590(7)	3086(6)	5035(6)	49(2) ^b
C(21A)	12126(8)	4069(7)	5791(6)	50(2) ^b
C(22A)	12351(10)	3535(9)	6888(7)	41(2) ^b
C(23A)	11877(9)	2379(8)	7144(7)	60(2) ^b
C(24A)	12296(7)	1444(7)	6366(5)	40(2) ^b

^a 51.7 %, 48.3 %

Table 3. Bond lengths [Å] and angles [°] for may5t

Pd(1)-C(1)	2.019(3)	C(28)-C(29)	1.513(5)
Pd(1)-Cl(1)	2.3084(7)	C(29)-C(30)	1.528(4)
Pd(2)-C(16)	2.027(3)	C(19)-C(20)	1.527(8)
Pd(2)-Cl(2)	2.3125(7)	C(19)-C(24)	1.534(8)
N(1)-C(1)	1.352(3)	C(20)-C(21)	1.529(7)
N(1)-C(2)	1.387(4)	C(21)-C(22)	1.497(8)
N(1)-C(4)	1.472(3)	C(22)-C(23)	1.477(9)
N(2)-C(1)	1.354(3)	C(23)-C(24)	1.538(8)
N(2)-C(3)	1.381(4)	C(1)-Pd(1)-C(1)'	180.0
N(2)-C(10)	1.479(3)	C(1)-Pd(1)-Cl(1)	88.97(9)
N(3)-C(16)	1.356(3)	C(1)''-Pd(1)-Cl(1)	91.03(9)
N(3)-C(17)	1.388(4)	C(1)-Pd(1)-Cl(1)'	91.03(9)
N(3)-C(19)	1.585(8)	C(1)''-Pd(1)-Cl(1)'	88.97(9)
N(4)-C(16)	1.355(4)	Cl(1)-Pd(1)-Cl(1)'	180.00(5)
N(4)-C(18)	1.385(4)	C(16)''-Pd(2)-C(16)	180.00(18)
N(4)-C(25)	1.476(3)	C(16)''-Pd(2)-Cl(2)	90.74(8)
C(2)-C(3)	1.336(5)	C(16)-Pd(2)-Cl(2)	89.26(8)
C(4)-C(5)	1.509(4)	C(16)''-Pd(2)-Cl(2)''	89.26(8)
C(4)-C(9)	1.514(4)	C(16)-Pd(2)-Cl(2)''	90.74(8)
C(5)-C(6)	1.528(4)	Cl(2)-Pd(2)-Cl(2)''	180.0
C(6)-C(7)	1.495(5)	C(1)-N(1)-C(2)	110.4(2)
C(7)-C(8)	1.506(5)	C(1)-N(1)-C(4)	124.3(2)
C(8)-C(9)	1.530(5)	C(2)-N(1)-C(4)	125.1(2)
C(10)-C(11)	1.510(5)	C(1)-N(2)-C(3)	110.5(2)
C(10)-C(15)	1.521(5)	C(1)-N(2)-C(10)	124.6(2)
C(11)-C(12)	1.533(4)	C(3)-N(2)-C(10)	124.9(2)
C(12)-C(13)	1.515(4)	C(16)-N(3)-C(17)	110.6(2)
C(13)-C(14)	1.505(5)	C(19A)-N(3)-C(17)	119.9(4)
C(14)-C(15)	1.524(4)	C(16)-N(3)-C(19)	118.5(4)
C(17)-C(18)	1.343(4)	C(19A)-N(3)-C(19)	12.1(4)
C(25)-C(26)	1.522(4)	C(17)-N(3)-C(19)	130.5(3)
C(25)-C(30)	1.523(4)	C(16)-N(4)-C(18)	111.0(2)
C(26)-C(27)	1.523(4)	C(16)-N(4)-C(25)	124.3(2)
C(27)-C(28)	1.526(4)	C(18)-N(4)-C(25)	124.6(2)
		N(1)-C(1)-N(2)	105.0(2)

N(1)-C(1)-Pd(1)	127.13(19)
N(2)-C(1)-Pd(1)	127.69(19)
C(3)-C(2)-N(1)	106.9(3)
C(2)-C(3)-N(2)	107.1(3)
N(1)-C(4)-C(5)	111.4(2)
N(1)-C(4)-C(9)	111.2(2)
C(5)-C(4)-C(9)	111.3(2)
C(4)-C(5)-C(6)	110.4(2)
C(7)-C(6)-C(5)	111.6(3)
C(6)-C(7)-C(8)	110.4(3)
C(7)-C(8)-C(9)	110.9(3)
C(4)-C(9)-C(8)	111.5(2)
N(2)-C(10)-C(11)	110.4(3)
N(2)-C(10)-C(15)	110.1(3)
C(11)-C(10)-C(15)	112.2(3)
C(10)-C(11)-C(12)	111.3(3)
C(13)-C(12)-C(11)	110.8(3)
C(14)-C(13)-C(12)	110.4(3)
C(13)-C(14)-C(15)	110.5(3)
C(10)-C(15)-C(14)	111.1(3)
N(4)-C(16)-N(3)	104.7(3)
N(4)-C(16)-Pd(2)	126.20(19)
N(3)-C(16)-Pd(2)	129.0(2)
C(18)-C(17)-N(3)	107.0(3)
C(17)-C(18)-N(4)	106.7(3)
N(4)-C(25)-C(26)	111.4(2)
N(4)-C(25)-C(30)	109.5(2)
C(26)-C(25)-C(30)	112.9(2)
C(25)-C(26)-C(27)	111.3(2)
C(26)-C(27)-C(28)	110.9(2)
C(29)-C(28)-C(27)	110.4(2)
C(28)-C(29)-C(30)	110.6(3)
C(25)-C(30)-C(29)	110.1(3)
C(20)-C(19)-C(24)	109.8(5)
C(20)-C(19)-N(3)	106.9(5)
C(24)-C(19)-N(3)	110.4(5)

C(19)-C(20)-C(21)	110.0(5)
C(22)-C(21)-C(20)	112.0(5)
C(23)-C(22)-C(21)	112.2(5)
C(22)-C(23)-C(24)	112.7(6)
C(19)-C(24)-C(23)	110.7(5)

Symmetry transformations used to generate equivalent atoms:

' -x+1,-y,-z " -x+2,-y,-z+1

A2.3 Crystal data for *trans*-Pd(ICy)₂(neopentyl)Cl.Table 1. Crystal data and structure refinement for *trans*-Pd(ICy)₂(neopentyl)Cl

Identification code	der23	
Empirical formula	C ₃₅ H ₅₉ Cl N ₄ Pd	
Formula weight	677.71	
Temperature	173(2) K	
Wavelength	0.71073 Å	
Crystal system	Monoclinic	
Space group	P2 ₁ /c	
Unit cell dimensions	a = 17.562(4) Å	α = 90°.
	b = 10.597(2) Å	β = 105.62(3)°.
	c = 21.809(4) Å	γ = 90°.
Volume	3909.0(14) Å ³	
Z	4	
Density (calculated)	1.152 Mg/m ³	
Absorption coefficient	0.568 mm ⁻¹	
F(000)	1440	
Crystal size	0.10 x 0.08 x 0.04 mm ³	
Theta range for data collection	3.42 to 27.50°.	
Index ranges	-22 ≤ h ≤ 22, -13 ≤ k ≤ 13, -28 ≤ l ≤ 28	
Reflections collected	49715	
Independent reflections	8799 [R(int) = 0.1324]	
Completeness to theta = 27.50°	97.9 %	
Absorption correction	Semi-empirical from equivalents	
Max. and min. transmission	0.9776 and 0.9453	
Refinement method	Full-matrix least-squares on F ²	
Data / restraints / parameters	8799 / 6 / 374	
Goodness-of-fit on F ²	1.093	
Final R indices [I > 2σ(I)]	R1 = 0.0785, wR2 = 0.1762	
R indices (all data)	R1 = 0.1386, wR2 = 0.2048	
Largest diff. peak and hole	1.648 and -0.561 e.Å ⁻³	

Table 2. Atomic coordinates ($\times 10^4$) and equivalent isotropic displacement parameters ($\text{\AA}^2 \times 10^3$) *trans*-Pd(ICy)₂(neopentyl)Cl. U(eq) is defined as one third of the trace of the orthogonalized U^{ij} tensor.

	x	y	z	U(eq)
C(028)	2292(4)	9610(6)	1124(3)	35(2)
C(029)	4078(4)	12050(6)	920(3)	36(2)
C(030)	1551(4)	10437(8)	986(4)	49(2)
C(031)	1110(5)	10323(8)	271(4)	62(2)
C(032)	1776(6)	11858(8)	1097(5)	78(3)
C(33A)	1025(10)	10130(50)	1406(13)	82(9)
C(33B)	1000(50)	9530(150)	1280(60)	82(9)
C(001)	5105(4)	10733(6)	1680(3)	32(1)
C(1)	2535(4)	7417(6)	1920(3)	31(1)
C(2)	3385(4)	10993(5)	2218(3)	28(1)
C(002)	4197(4)	12688(6)	2296(3)	32(1)
C(003)	2745(4)	11623(6)	3077(3)	30(1)
C(004)	4226(4)	11083(6)	1451(3)	29(1)
C(005)	2119(4)	12655(7)	2943(3)	46(2)
C(006)	5244(4)	11298(7)	586(3)	38(2)
C(007)	3296(4)	6717(6)	1165(3)	30(1)
C(008)	2619(5)	11422(8)	4189(3)	49(2)
C(009)	3780(4)	12841(6)	2721(3)	37(2)
C(010)	2932(4)	6323(7)	472(3)	38(2)
C(011)	1725(4)	7335(7)	2713(3)	44(2)
C(012)	1953(5)	5556(6)	2026(4)	45(2)
C(013)	2377(5)	5382(6)	1607(4)	45(2)
C(014)	3184(4)	11555(7)	3772(3)	39(2)
C(015)	3523(5)	6562(8)	82(4)	53(2)
C(016)	4062(4)	6038(7)	1453(4)	47(2)
C(017)	4371(4)	11603(7)	362(3)	43(2)
C(018)	4289(5)	5881(8)	361(4)	56(2)
C(019)	827(5)	7209(9)	2543(4)	59(2)
C(020)	2109(5)	6715(8)	3349(3)	53(2)
C(021)	1783(5)	7249(10)	3879(4)	66(3)
C(022)	884(6)	7108(12)	3702(5)	90(4)
C(023)	4638(4)	6244(8)	1055(4)	59(2)

A2-15

C(024)	510(6)	7757(12)	3072(5)	87(3)
C(025)	1560(5)	12520(9)	3362(4)	59(2)
C(026)	5407(4)	10299(7)	1113(3)	40(2)
C(027)	2014(5)	12490(9)	4069(4)	59(2)
N(1)	2045(3)	6792(5)	2216(3)	37(1)
N(2)	2722(3)	6517(5)	1543(2)	32(1)
N(3)	3290(3)	11803(5)	2679(2)	28(1)
N(4)	3946(3)	11564(4)	1985(2)	27(1)
Cl(1)	3763(1)	8669(2)	3107(1)	40(1)
Pd(1)	2937(1)	9219(1)	2051(1)	25(1)

Table 3. Bond lengths [\AA] and angles [$^\circ$] for *trans*-Pd(ICy)₂(neopentyl)Cl

C(028)-C(030)	1.531(9)
C(028)-Pd(1)	2.075(6)
C(029)-C(004)	1.516(8)
C(029)-C(017)	1.519(9)
C(030)-C(33A)	1.500(18)
C(030)-C(031)	1.548(11)
C(030)-C(032)	1.559(11)
C(030)-C(33B)	1.62(10)
C(001)-C(004)	1.535(9)
C(001)-C(026)	1.540(9)
C(1)-N(2)	1.357(8)
C(1)-N(1)	1.376(8)
C(1)-Pd(1)	2.029(6)
C(2)-N(3)	1.366(7)
C(2)-N(4)	1.366(8)
C(2)-Pd(1)	2.033(6)
C(002)-C(009)	1.336(9)
C(002)-N(4)	1.383(7)
C(003)-N(3)	1.468(7)
C(003)-C(014)	1.506(9)
C(003)-C(005)	1.523(9)
C(004)-N(4)	1.471(7)
C(005)-C(025)	1.517(10)
C(006)-C(017)	1.514(10)
C(006)-C(026)	1.531(9)
C(007)-N(2)	1.479(8)
C(007)-C(016)	1.507(9)
C(007)-C(010)	1.531(9)
C(008)-C(014)	1.523(9)
C(008)-C(027)	1.527(11)
C(009)-N(3)	1.385(8)
C(010)-C(015)	1.531(9)
C(011)-N(1)	1.466(8)
C(011)-C(020)	1.519(10)
C(011)-C(019)	1.525(10)

C(012)-C(013)	1.337(10)
C(012)-N(1)	1.370(8)
C(013)-N(2)	1.371(8)
C(015)-C(018)	1.503(11)
C(016)-C(023)	1.515(11)
C(018)-C(023)	1.523(12)
C(019)-C(024)	1.527(12)
C(020)-C(021)	1.530(11)
C(021)-C(022)	1.529(12)
C(022)-C(024)	1.519(14)
C(025)-C(027)	1.534(11)
Cl(1)-Pd(1)	2.4397(18)

C(030)-C(028)-Pd(1)	121.2(5)
C(004)-C(029)-C(017)	112.1(5)
C(33A)-C(030)-C(028)	112.7(13)
C(33A)-C(030)-C(031)	112.1(13)
C(028)-C(030)-C(031)	108.7(6)
C(33A)-C(030)-C(032)	107(2)
C(028)-C(030)-C(032)	110.8(6)
C(031)-C(030)-C(032)	105.6(7)
C(33A)-C(030)-C(33B)	25(4)
C(028)-C(030)-C(33B)	99(4)
C(031)-C(030)-C(33B)	99(5)
C(032)-C(030)-C(33B)	132(6)
C(004)-C(001)-C(026)	110.1(5)
N(2)-C(1)-N(1)	103.3(5)
N(2)-C(1)-Pd(1)	128.0(4)
N(1)-C(1)-Pd(1)	128.7(5)
N(3)-C(2)-N(4)	103.8(5)
N(3)-C(2)-Pd(1)	126.5(4)
N(4)-C(2)-Pd(1)	128.8(4)
C(009)-C(002)-N(4)	106.5(5)
N(3)-C(003)-C(014)	111.3(5)
N(3)-C(003)-C(005)	110.2(5)
C(014)-C(003)-C(005)	112.0(5)
N(4)-C(004)-C(029)	110.2(5)

N(4)-C(004)-C(001)	110.4(5)
C(029)-C(004)-C(001)	111.3(5)
C(025)-C(005)-C(003)	111.6(6)
C(017)-C(006)-C(026)	111.0(6)
N(2)-C(007)-C(016)	111.4(5)
N(2)-C(007)-C(010)	110.2(5)
C(016)-C(007)-C(010)	111.7(6)
C(014)-C(008)-C(027)	111.4(6)
C(002)-C(009)-N(3)	107.7(6)
C(007)-C(010)-C(015)	109.8(6)
N(1)-C(011)-C(020)	109.9(6)
N(1)-C(011)-C(019)	111.2(6)
C(020)-C(011)-C(019)	111.1(6)
C(013)-C(012)-N(1)	107.2(6)
C(012)-C(013)-N(2)	107.0(6)
C(003)-C(014)-C(008)	111.5(6)
C(018)-C(015)-C(010)	111.2(6)
C(007)-C(016)-C(023)	110.6(6)
C(006)-C(017)-C(029)	109.9(6)
C(015)-C(018)-C(023)	111.0(6)
C(011)-C(019)-C(024)	110.3(7)
C(011)-C(020)-C(021)	111.4(7)
C(022)-C(021)-C(020)	110.2(7)
C(024)-C(022)-C(021)	110.5(8)
C(016)-C(023)-C(018)	112.4(7)
C(022)-C(024)-C(019)	110.8(9)
C(005)-C(025)-C(027)	111.2(6)
C(006)-C(026)-C(001)	111.2(6)
C(008)-C(027)-C(025)	109.7(6)
C(012)-N(1)-C(1)	110.9(6)
C(012)-N(1)-C(011)	124.1(6)
C(1)-N(1)-C(011)	124.7(6)
C(1)-N(2)-C(013)	111.6(5)
C(1)-N(2)-C(007)	123.4(5)
C(013)-N(2)-C(007)	124.7(5)
C(2)-N(3)-C(009)	110.5(5)
C(2)-N(3)-C(003)	125.6(5)

C(009)-N(3)-C(003)	123.9(5)
C(2)-N(4)-C(002)	111.4(5)
C(2)-N(4)-C(004)	124.8(5)
C(002)-N(4)-C(004)	123.8(5)
C(1)-Pd(1)-C(2)	177.1(3)
C(1)-Pd(1)-C(028)	88.5(3)
C(2)-Pd(1)-C(028)	94.2(3)
C(1)-Pd(1)-Cl(1)	90.20(18)
C(2)-Pd(1)-Cl(1)	87.04(17)
C(028)-Pd(1)-Cl(1)	175.67(19)

A2.4 Crystal data for $[\text{Pd}(\text{I}^t\text{Bu})\text{Cl}_3][\text{I}^t\text{BuH}]^+$

Table 1. Crystal data and structure refinement details.

Identification code	src0211a		
Empirical formula	$\text{C}_{50}\text{H}_{88}\text{Cl}_6\text{N}_8\text{Pd}_2$		
Formula weight	1226.78		
Temperature	120(2) K		
Wavelength	0.71073 Å		
Crystal system	Monoclinic		
Space group	$P21/c$		
Unit cell dimensions	$a = 20.0126(4)$ Å	$\alpha = 90^\circ$	
	$b = 19.9149(4)$ Å	$\beta = 103.8880(10)^\circ$	
	$c = 15.8077(3)$ Å	$\gamma = 90^\circ$	
Volume	6116.0(2) Å ³		
Z	4		
Density (calculated)	1.332 Mg / m ³		
Absorption coefficient	0.888 mm ⁻¹		
$F(000)$	2552		
Crystal	Block; yellow		
Crystal size	0.22 × 0.20 × 0.18 mm ³		
θ range for data collection	4.06 – 27.49°		
Index ranges	$-25 \leq h \leq 25, -25 \leq k \leq 25, -20 \leq l \leq 20$		
Reflections collected	78748		
Independent reflections	13905 [$R_{\text{int}} = 0.0480$]		
Completeness to $\theta = 27.49^\circ$	99.1 %		
Absorption correction	Semi-empirical from equivalents		
Max. and min. transmission	0.8565 and 0.8286		
Refinement method	Full-matrix least-squares on F^2		
Data / restraints / parameters	13905 / 0 / 619		
Goodness-of-fit on F^2	1.046		
Final R indices [$F^2 > 2\sigma(F^2)$]	$R1 = 0.0370, wR2 = 0.0820$		
R indices (all data)	$R1 = 0.0479, wR2 = 0.0873$		
Largest diff. peak and hole	0.588 and -1.054 e Å ⁻³		

Table 2. Atomic coordinates [$\times 10^4$], equivalent isotropic displacement parameters [$\text{\AA}^2 \times 10^3$] and site occupancy factors. U_{eq} is defined as one third of the trace of the orthogonalized U^{ij} tensor.

Atom	x	y	z	U_{eq}	$S.o.f.$
C1	8287(1)	8152(1)	1213(2)	22(1)	1
C2	8391(1)	7559(1)	2454(2)	28(1)	1
C3	7881(1)	7997(1)	2412(2)	26(1)	1
C4	7253(1)	8880(1)	1349(2)	23(1)	1
C5	7537(1)	9512(1)	1008(2)	28(1)	1
C6	6687(1)	8558(1)	647(2)	29(1)	1
C7	6967(2)	9088(2)	2128(2)	32(1)	1
C8	9240(1)	7238(1)	1585(2)	28(1)	1
C9	9432(2)	7367(2)	733(2)	56(1)	1
C10	9844(2)	7400(3)	2341(3)	87(2)	1
C11	9032(2)	6507(2)	1599(3)	68(1)	1
C12	6278(1)	2722(1)	8925(2)	23(1)	1
C13	6463(1)	2394(1)	7638(2)	30(1)	1
C14	6070(1)	1931(2)	7881(2)	31(1)	1
C15	7004(2)	3499(2)	8170(2)	35(1)	1
C16	7211(2)	3923(2)	8990(2)	58(1)	1
C17	6567(3)	3891(2)	7417(3)	90(2)	1
C18	7670(2)	3259(2)	7942(3)	58(1)	1
C19	5569(1)	1684(1)	9164(2)	31(1)	1
C20	6065(2)	1127(2)	9579(2)	40(1)	1
C21	4944(2)	1396(2)	8501(2)	43(1)	1
C22	5302(2)	2057(2)	9861(2)	44(1)	1
C23	6204(1)	9251(1)	6276(2)	21(1)	1
C24	6934(1)	8428(1)	6238(2)	27(1)	1
C25	6897(1)	8509(1)	7071(2)	25(1)	1
C26	6360(1)	8978(1)	4769(2)	26(1)	1
C27	5849(2)	9548(2)	4486(2)	36(1)	1
C28	6060(2)	8315(1)	4358(2)	34(1)	1
C29	7050(2)	9138(2)	4562(2)	36(1)	1
C30	6196(1)	9237(1)	7878(2)	22(1)	1
C31	6821(1)	9499(2)	8548(2)	31(1)	1
C32	5883(1)	8619(1)	8209(2)	30(1)	1

C33	5654(1)	9785(1)	7622(2)	26(1)	1
C34	1167(1)	9101(1)	1216(2)	24(1)	1
C35	2110(1)	8569(1)	1137(2)	29(1)	1
C36	2195(1)	8791(1)	1963(2)	29(1)	1
C37	1151(1)	8597(1)	−265(2)	24(1)	1
C38	447(1)	8931(2)	−543(2)	33(1)	1
C39	1629(1)	8871(2)	−808(2)	33(1)	1
C40	1089(1)	7835(1)	−330(2)	32(1)	1
C41	1465(1)	9430(1)	2818(2)	24(1)	1
C42	2027(1)	9950(2)	3149(2)	32(1)	1
C43	759(1)	9764(1)	2591(2)	28(1)	1
C44	1490(2)	8864(2)	3467(2)	43(1)	1
C45	795(2)	5566(2)	1396(3)	54(1)	1
C46	873(2)	5431(2)	571(3)	73(1)	1
C47	1032(2)	4787(3)	359(3)	71(1)	1
C48	1094(2)	4276(2)	965(2)	54(1)	1
C49	1003(2)	4419(2)	1783(2)	43(1)	1
C50	860(2)	5060(2)	1995(2)	40(1)	1
N1	8644(1)	7653(1)	1714(1)	24(1)	1
N2	7814(1)	8369(1)	1646(1)	21(1)	1
N3	6600(1)	2887(1)	8285(1)	26(1)	1
N4	5950(1)	2134(1)	8677(1)	26(1)	1
N5	6496(1)	8901(1)	5742(1)	23(1)	1
N6	6432(1)	9024(1)	7089(1)	21(1)	1
N7	1463(1)	8766(1)	673(1)	22(1)	1
N8	1597(1)	9125(1)	2001(1)	23(1)	1
Pd1	8438(1)	8500(1)	108(1)	18(1)	1
Pd2	6273(1)	3255(1)	9960(1)	20(1)	1
Cl1	9255(1)	9219(1)	936(1)	29(1)	1
Cl2	8620(1)	8941(1)	−1211(1)	26(1)	1
Cl3	7668(1)	7694(1)	−635(1)	27(1)	1
Cl4	5306(1)	3768(1)	9113(1)	36(1)	1
Cl5	6283(1)	3976(1)	11173(1)	24(1)	1
Cl6	7189(1)	2597(1)	10708(1)	28(1)	1

Table 3. Bond lengths [\AA] and angles [$^\circ$].

C1–N1	1.362(3)
C1–N2	1.365(3)
C1–Pd1	1.967(2)
C2–C3	1.331(4)
C2–N1	1.395(3)
C3–N2	1.399(3)
C4–N2	1.503(3)
C4–C6	1.524(4)
C4–C5	1.532(4)
C4–C7	1.534(3)
C8–N1	1.504(3)
C8–C9	1.508(4)
C8–C11	1.516(4)
C8–C10	1.517(5)
C12–N4	1.353(3)
C12–N3	1.363(3)
C12–Pd2	1.952(3)
C13–C14	1.326(4)
C13–N3	1.396(3)
C14–N4	1.397(3)
C15–N3	1.499(3)
C15–C17	1.513(5)
C15–C16	1.519(4)
C15–C18	1.538(5)
C19–N4	1.503(3)
C19–C22	1.527(4)
C19–C20	1.529(4)
C19–C21	1.537(4)
C23–N5	1.334(3)
C23–N6	1.336(3)
C24–C25	1.347(4)
C24–N5	1.391(3)
C25–N6	1.388(3)
C26–N5	1.504(3)
C26–C27	1.523(4)
C26–C29	1.526(4)
C26–C28	1.528(4)
C30–N6	1.497(3)

C30–C33	1.523(3)
C30–C31	1.525(4)
C30–C32	1.530(4)
C34–N8	1.330(3)
C34–N7	1.334(3)
C35–C36	1.351(4)
C35–N7	1.384(3)
C36–N8	1.384(3)
C37–N7	1.502(3)
C37–C38	1.524(4)
C37–C40	1.524(4)
C37–C39	1.530(3)
C41–N8	1.506(3)
C41–C44	1.518(4)
C41–C43	1.526(3)
C41–C42	1.526(4)
C45–C50	1.368(5)
C45–C46	1.377(6)
C46–C47	1.381(6)
C47–C48	1.383(6)
C48–C49	1.378(5)
C49–C50	1.367(5)
Pd1–Cl1	2.3258(6)
Pd1–Cl3	2.3362(6)
Pd1–Cl2	2.3696(6)
Pd2–Cl4	2.3108(7)
Pd2–Cl6	2.3317(6)
Pd2–Cl5	2.3927(6)
N1–C1–N2	105.6(2)
N1–C1–Pd1	127.06(18)
N2–C1–Pd1	127.30(18)
C3–C2–N1	107.4(2)
C2–C3–N2	107.7(2)
N2–C4–C6	108.2(2)
N2–C4–C5	110.76(19)
C6–C4–C5	111.2(2)
N2–C4–C7	109.1(2)

C6–C4–C7	110.0(2)
C5–C4–C7	107.6(2)
N1–C8–C9	114.0(2)
N1–C8–C11	107.2(2)
C9–C8–C11	107.8(3)
N1–C8–C10	106.6(2)
C9–C8–C10	110.0(3)
C11–C8–C10	111.2(4)
N4–C12–N3	106.0(2)
N4–C12–Pd2	127.80(18)
N3–C12–Pd2	126.12(19)
C14–C13–N3	107.6(2)
C13–C14–N4	107.5(2)
N3–C15–C17	106.7(3)
N3–C15–C16	113.1(2)
C17–C15–C16	111.9(3)
N3–C15–C18	107.4(2)
C17–C15–C18	110.3(3)
C16–C15–C18	107.3(3)
N4–C19–C22	112.8(2)
N4–C19–C20	107.2(2)
C22–C19–C20	110.3(3)
N4–C19–C21	107.7(2)
C22–C19–C21	107.8(2)
C20–C19–C21	111.0(2)
N5–C23–N6	109.3(2)
C25–C24–N5	107.2(2)
C24–C25–N6	107.6(2)
N5–C26–C27	108.7(2)
N5–C26–C29	106.8(2)
C27–C26–C29	111.1(2)
N5–C26–C28	107.6(2)
C27–C26–C28	110.5(2)
C29–C26–C28	111.9(2)
N6–C30–C33	109.22(19)
N6–C30–C31	107.82(19)
C33–C30–C31	110.6(2)
N6–C30–C32	107.2(2)

C33–C30–C32	110.1(2)
C31–C30–C32	111.9(2)
N8–C34–N7	109.3(2)
C36–C35–N7	107.7(2)
C35–C36–N8	106.8(2)
N7–C37–C38	108.9(2)
N7–C37–C40	107.3(2)
C38–C37–C40	111.2(2)
N7–C37–C39	107.8(2)
C38–C37–C39	110.0(2)
C40–C37–C39	111.6(2)
N8–C41–C44	107.2(2)
N8–C41–C43	108.5(2)
C44–C41–C43	111.1(2)
N8–C41–C42	107.6(2)
C44–C41–C42	111.7(2)
C43–C41–C42	110.5(2)
C50–C45–C46	119.8(4)
C45–C46–C47	119.8(4)
C46–C47–C48	120.2(4)
C49–C48–C47	119.2(4)
C50–C49–C48	120.4(3)
C49–C50–C45	120.6(3)
C1–N1–C2	109.9(2)
C1–N1–C8	130.1(2)
C2–N1–C8	120.0(2)
C1–N2–C3	109.4(2)
C1–N2–C4	127.9(2)
C3–N2–C4	122.5(2)
C12–N3–C13	109.2(2)
C12–N3–C15	130.6(2)
C13–N3–C15	120.0(2)
C12–N4–C14	109.6(2)
C12–N4–C19	129.7(2)
C14–N4–C19	120.4(2)
C23–N5–C24	108.0(2)
C23–N5–C26	126.5(2)
C24–N5–C26	125.5(2)

C23–N6–C25	107.9(2)
C23–N6–C30	127.0(2)
C25–N6–C30	125.0(2)
C34–N7–C35	107.8(2)
C34–N7–C37	127.1(2)
C35–N7–C37	125.0(2)
C34–N8–C36	108.4(2)
C34–N8–C41	127.3(2)
C36–N8–C41	124.2(2)
C1–Pd1–Cl1	87.41(7)
C1–Pd1–Cl3	88.96(7)
Cl1–Pd1–Cl3	174.51(3)
C1–Pd1–Cl2	178.86(7)
Cl1–Pd1–Cl2	91.77(2)
Cl3–Pd1–Cl2	91.92(2)
C12–Pd2–Cl4	85.83(7)
C12–Pd2–Cl6	87.60(7)
Cl4–Pd2–Cl6	171.83(3)
C12–Pd2–Cl5	175.95(8)
Cl4–Pd2–Cl5	92.47(2)
Cl6–Pd2–Cl5	94.39(2)

Symmetry transformations used to generate

A2.5 Crystal data for *trans*-[Pd(ITMe)₂(p-anisole)(Cl)]Table 1. Crystal data and structure refinement for [PdCl(carbene)₂(C₆H₄OMe)] . (toluene-d₆).

Identification code	jun508	
Empirical formula	C ₂₁ H ₃₁ Cl N ₄ O Pd . (C ₇ D ₈)	
Formula weight	597.53	
Temperature	173(2) K	
Wavelength	0.71073 Å	
Crystal system	Triclinic	
Space group	P $\bar{1}$ (No.2)	
Unit cell dimensions	a = 8.6374(2) Å	α = 74.536(1)°.
	b = 12.1483(3) Å	β = 75.117(1)°.
	c = 14.8770(3) Å	γ = 76.245(1)°.
Volume	1429.84(6) Å ³	
Z	2	
Density (calculated)	1.39 Mg/m ³	
Absorption coefficient	0.77 mm ⁻¹	
F(000)	612	
Crystal size	0.20 x 0.15 x 0.10 mm ³	
Theta range for data collection	3.41 to 26.00°.	
Index ranges	-10 ≤ h ≤ 10, -14 ≤ k ≤ 14, -17 ≤ l ≤ 18	
Reflections collected	21774	
Independent reflections	5589 [R(int) = 0.038]	
Reflections with I > 2σ(I)	5159	
Completeness to theta = 26.00°	99.3 %	
Tmax. and Tmin.	0.927 and 0.861	
Refinement method	Full-matrix least-squares on F ²	
Data / restraints / parameters	5589 / 0 / 298	
Goodness-of-fit on F ²	1.026	
Final R indices [I > 2σ(I)]	R1 = 0.038, wR2 = 0.094	
R indices (all data)	R1 = 0.041, wR2 = 0.096	
Largest diff. peak and hole	1.81 and -0.79 e.Å ⁻³ (near disordered solvate)	
The solvate molecules are disordered about inversion centres and were included with isotropic C atoms and with hydrogens omitted.		

Data collection KappaCCD , Program package WinGX , Abs correction MULTISCAN

Refinement using SHELXL-97 , Drawing using ORTEP-3 for Windows

Table 2. Atomic coordinates ($\times 10^4$) and equivalent isotropic displacement parameters ($\text{\AA}^2 \times 10^3$) for jun508. $U(\text{eq})$ is defined as one third of the trace of the orthogonalized U^{ij} tensor.

	x	y	z	$U(\text{eq})$
Pd	2900(1)	2719(1)	2329(1)	21(1)
Cl	3769(1)	4562(1)	1945(1)	39(1)
O(1)	932(3)	-2126(2)	3274(2)	37(1)
N(1)	723(3)	3264(2)	867(2)	25(1)
N(2)	3233(3)	3138(2)	181(2)	25(1)
N(3)	2765(3)	2656(2)	4420(2)	24(1)
N(4)	4978(3)	1648(2)	3829(2)	23(1)
C(1)	2233(4)	3059(3)	1049(2)	23(1)
C(2)	776(4)	3484(3)	-112(2)	30(1)
C(3)	2357(4)	3401(3)	-544(2)	29(1)
C(4)	-768(4)	3275(3)	1591(3)	38(1)
C(5)	-728(5)	3717(4)	-502(3)	42(1)
C(6)	3175(5)	3520(4)	-1570(2)	41(1)
C(7)	5004(4)	2978(3)	21(2)	35(1)
C(8)	3574(4)	2311(3)	3608(2)	22(1)
C(9)	3650(4)	2224(3)	5143(2)	25(1)
C(10)	5051(4)	1587(3)	4767(2)	24(1)
C(11)	1186(4)	3435(3)	4505(3)	34(1)
C(12)	3070(4)	2514(3)	6101(2)	34(1)
C(13)	6494(4)	937(3)	5183(2)	33(1)
C(14)	6250(4)	1075(3)	3163(2)	32(1)
C(15)	2277(4)	1150(3)	2634(2)	22(1)
C(16)	3156(4)	308(3)	2131(2)	29(1)
C(17)	2770(4)	-799(3)	2323(2)	30(1)
C(18)	1443(4)	-1075(3)	3034(2)	26(1)
C(19)	544(4)	-257(3)	3554(2)	26(1)
C(20)	969(4)	823(3)	3364(2)	25(1)
C(21)	1673(6)	-2909(3)	2658(3)	49(1)
C(1S)	3960(7)	5622(5)	5629(4)	66(1)
C(2S)	3566(7)	5679(5)	4749(4)	71(1)
C(3S)	5424(7)	4932(5)	5848(4)	65(1)
C(4S)	2959(9)	6129(7)	6249(6)	40(2)a
C(5S)	9472(10)	-211(7)	420(6)	44(2)
C(6S)	9461(6)	-342(4)	-514(4)	59(1)a
C(7S)	8049(13)	-583(9)	202(8)	64(2)

A2.31

C(8S)	8020(8)	-462(6)	1163(5)	83(2)a
C(9S)	9187(13)	102(9)	1227(7)	62(2)a

a	occupancy			0.5
---	-----------	--	--	-----

Table 3. Bond lengths [\AA] and angles [$^\circ$] for jun508.

Pd-C(15)	2.007(3)
Pd-C(8)	2.033(3)
Pd-C(1)	2.040(3)
Pd-Cl	2.4078(8)
O(1)-C(18)	1.377(4)
O(1)-C(21)	1.424(4)
N(1)-C(1)	1.352(4)
N(1)-C(2)	1.399(4)
N(1)-C(4)	1.451(4)
N(2)-C(1)	1.349(4)
N(2)-C(3)	1.400(4)
N(2)-C(7)	1.460(4)
N(3)-C(8)	1.349(4)
N(3)-C(9)	1.396(4)
N(3)-C(11)	1.460(4)
N(4)-C(8)	1.351(4)
N(4)-C(10)	1.394(4)
N(4)-C(14)	1.456(4)
C(2)-C(3)	1.344(5)
C(2)-C(5)	1.492(4)
C(3)-C(6)	1.492(5)
C(9)-C(10)	1.347(5)
C(9)-C(12)	1.490(4)
C(10)-C(13)	1.492(4)
C(15)-C(16)	1.390(4)
C(15)-C(20)	1.402(4)
C(16)-C(17)	1.400(5)
C(17)-C(18)	1.384(5)
C(18)-C(19)	1.387(5)
C(19)-C(20)	1.384(4)
C(1S)-C(4S)	1.273(9)
C(15)-Pd-C(8)	88.99(11)
C(15)-Pd-C(1)	88.87(11)
C(8)-Pd-C(1)	177.70(12)
C(15)-Pd-Cl	177.51(9)
C(8)-Pd-Cl	90.53(8)
C(1)-Pd-Cl	91.57(9)

C(18)-O(1)-C(21)	117.1(3)
C(1)-N(1)-C(2)	111.4(3)
C(1)-N(1)-C(4)	124.5(3)
C(2)-N(1)-C(4)	124.1(3)
C(1)-N(2)-C(3)	111.5(3)
C(1)-N(2)-C(7)	124.1(3)
C(3)-N(2)-C(7)	124.3(3)
C(8)-N(3)-C(9)	112.0(3)
C(8)-N(3)-C(11)	123.4(3)
C(9)-N(3)-C(11)	124.6(3)
C(8)-N(4)-C(10)	111.7(3)
C(8)-N(4)-C(14)	123.7(3)
C(10)-N(4)-C(14)	124.6(3)
N(2)-C(1)-N(1)	104.3(2)
N(2)-C(1)-Pd	126.8(2)
N(1)-C(1)-Pd	128.8(2)
C(3)-C(2)-N(1)	106.4(3)
C(3)-C(2)-C(5)	131.5(3)
N(1)-C(2)-C(5)	122.1(3)
C(2)-C(3)-N(2)	106.3(3)
C(2)-C(3)-C(6)	131.4(3)
N(2)-C(3)-C(6)	122.3(3)
N(3)-C(8)-N(4)	103.9(2)
N(3)-C(8)-Pd	128.7(2)
N(4)-C(8)-Pd	127.3(2)
C(10)-C(9)-N(3)	106.0(3)
C(10)-C(9)-C(12)	130.9(3)
N(3)-C(9)-C(12)	123.1(3)
C(9)-C(10)-N(4)	106.5(3)
C(9)-C(10)-C(13)	131.0(3)
N(4)-C(10)-C(13)	122.5(3)
C(16)-C(15)-C(20)	115.8(3)
C(16)-C(15)-Pd	121.0(2)
C(20)-C(15)-Pd	123.2(2)
C(15)-C(16)-C(17)	122.9(3)
C(18)-C(17)-C(16)	119.3(3)
O(1)-C(18)-C(17)	124.4(3)
O(1)-C(18)-C(19)	116.3(3)
C(17)-C(18)-C(19)	119.3(3)
C(20)-C(19)-C(18)	120.3(3)

C(19)-C(20)-C(15)

122.3(3)

A2.6: Crystal data for *cis*-[Pd(ITMe)₂(SiMe₃)₂]Table 1. Crystal data and structure refinement for Pd(SiMe₃)₂(C₃N₂Me₄)₂ · 1.5 C₆D₆

Identification code	oct609	
Empirical formula	2(C ₂₀ H ₄₂ N ₂ Pd Si ₂), 3(C ₆ D ₆)	
Formula weight	1236.64	
Temperature	173(2) K	
Wavelength	0.71073 Å	
Crystal system	Monoclinic	
Space group	<i>P</i> 2/ <i>c</i>	
Unit cell dimensions	<i>a</i> = 22.7672(3) Å	∠ = 90°.
<i>b</i> = 11.3252(1) Å	∠ = 119.569(1)°.	
<i>c</i> = 30.1701(5) Å	∠ = 90°.	
Volume	6766.01(16) Å ³	
<i>Z</i>	4	
Density (calculated)	1.21 Mg/m ³	
Absorption coefficient	0.64 mm ⁻¹	
<i>F</i> (000)	2616	
Crystal size	0.19 x 0.18 x 0.13 mm ³	
Theta range for data collection	3.48 to 27.11°.	
Index ranges	-29 ≤ <i>h</i> ≤ 29, -14 ≤ <i>k</i> ≤ 14, -38 ≤ <i>l</i> ≤ 38	
Reflections collected	101713	
Independent reflections	14919 [<i>R</i> (int) = 0.093]	
Reflections with <i>I</i> > 2σ(<i>I</i>)	9997	
Completeness to theta = 27.11°	99.7 %	
Absorption correction	Semi-empirical from equivalents	
<i>T</i> _{max} . and <i>T</i> _{min} .	0.9272 0.8550	
Refinement method	Full-matrix least-squares on <i>F</i> ²	
Data / restraints / parameters	14919 / 0 / 665	
Goodness-of-fit on <i>F</i> ²	1.017	
Final <i>R</i> indices [<i>I</i> > 2σ(<i>I</i>)]	<i>R</i> 1 = 0.041 <i>wR</i> 2 = 0.074	
<i>R</i> indices (all data)	<i>R</i> 1 = 0.082, <i>wR</i> 2 = 0.085	
Largest diff. peak and hole	0.42 and -0.78 e.Å ⁻³	

There are two independent molecules in the unit cell and three benzene solvate molecules

Data collection KappaCCD , Program package WinGX , Abs correction MULTISCAN

Refinement using SHELXL-97 , Drawing using ORTEP-3 for Windows

Table 2. Atomic coordinates ($\times 10^4$) and equivalent isotropic displacement parameters ($\text{\AA}^2 \times 10^3$) for oct609. $U(\text{eq})$ is defined as one third of the trace of the orthogonalized U^{ij} tensor.

x	y	z	U(eq)	
Pd(1)	-1219(1)	7165(1)	584(1)	23(1)
Pd(2)	6102(1)	7800(1)	6532(1)	23(1)
Si(1)	-1780(1)	8710(1)	0(1)	30(1)
Si(2)	-1684(1)	7869(1)	1079(1)	29(1)
Si(3)	6687(1)	6175(1)	6454(1)	32(1)
Si(4)	6481(1)	7201(1)	7378(1)	32(1)
N(1)	-1035(1)	4685(2)	1092(1)	25(1)
N(2)	-148(1)	5705(2)	1526(1)	26(1)
N(3)	-254(1)	7081(2)	119(1)	28(1)
N(4)	-1092(1)	5933(2)	-298(1)	27(1)
N(5)	5134(1)	7578(2)	5359(1)	28(1)
N(6)	5906(1)	8827(2)	5504(1)	25(1)
N(7)	5977(1)	10350(2)	6868(1)	28(1)
N(8)	5048(1)	9436(2)	6609(1)	25(1)
C(1)	-769(1)	5769(2)	1107(1)	25(1)
C(2)	-585(2)	3958(3)	1490(1)	31(1)
C(3)	-25(2)	4598(3)	1766(1)	30(1)
C(4)	-1715(2)	4340(3)	713(1)	37(1)
C(5)	-752(2)	2709(3)	1554(1)	45(1)
C(6)	628(2)	4309(3)	2230(1)	47(1)
C(7)	320(2)	6689(3)	1713(1)	36(1)
C(8)	-821(2)	6670(3)	107(1)	27(1)
C(9)	-178(2)	6615(3)	-281(1)	31(1)
C(10)	-708(2)	5897(3)	-543(1)	32(1)
C(11)	193(2)	7948(3)	482(1)	40(1)
C(12)	404(2)	6904(3)	-355(1)	48(1)
C(13)	-906(2)	5181(3)	-1010(1)	48(1)
C(14)	-1736(2)	5332(3)	-480(1)	41(1)
C(15)	-2672(2)	9182(3)	-173(1)	49(1)
C(16)	-1290(2)	10142(3)	166(1)	51(1)
C(17)	-1923(2)	8398(3)	-667(1)	55(1)
C(18)	-2589(2)	7380(3)	840(2)	49(1)
C(19)	-1686(2)	9516(3)	1207(1)	42(1)
C(20)	-1239(2)	7288(4)	1762(1)	55(1)
C(21)	5683(1)	8105(2)	5747(1)	24(1)

A2.37

C(22)	5022(2)	7964(3)	4883(1)	31(1)
C(23)	5503(2)	8751(3)	4974(1)	31(1)
C(24)	4729(2)	6695(3)	5435(1)	48(1)
C(25)	4469(2)	7475(4)	4392(1)	53(1)
C(26)	5639(2)	9471(3)	4618(1)	49(1)
C(27)	6514(2)	9534(3)	5769(1)	51(1)
C(28)	5676(2)	9296(3)	6673(1)	26(1)
C(29)	5546(2)	11131(3)	6931(1)	31(1)
C(30)	4957(2)	10550(3)	6765(1)	30(1)
C(31)	6679(2)	10602(3)	7023(1)	43(1)
C(32)	5772(2)	12324(3)	7165(1)	44(1)
C(33)	4306(2)	10928(3)	6727(1)	43(1)
C(34)	4543(2)	8504(3)	6417(1)	36(1)
C(35)	7626(2)	6456(4)	6737(2)	58(1)
C(36)	6441(2)	5805(3)	5768(1)	59(1)
C(37)	6608(2)	4659(3)	6688(1)	52(1)
C(38)	7354(2)	6584(3)	7818(1)	42(1)
C(39)	5876(2)	6048(4)	7383(1)	59(1)
C(40)	6451(2)	8398(4)	7807(1)	67(1)
C(41)	3899(2)	3973(4)	5579(1)	55(1)
C(42)	3457(2)	4870(4)	5366(2)	59(1)
C(43)	3380(2)	5695(4)	5665(2)	64(1)
C(44)	3758(3)	5592(4)	6189(2)	75(2)
C(45)	4203(2)	4675(5)	6397(2)	76(1)
C(46)	4274(2)	3876(4)	6091(2)	65(1)
C(47)	1007(3)	10452(4)	2360(2)	77(1)
C(48)	426(2)	9886(4)	2016(2)	64(1)
C(49)	198(2)	9959(3)	1509(2)	51(1)
C(50)	550(2)	10601(3)	1337(2)	56(1)
C(51)	1134(2)	11172(4)	1670(2)	73(1)
C(52)	1369(3)	11093(4)	2187(2)	84(2)
C(53)	-2641(2)	3482(4)	-1735(2)	77(2)
C(54)	-2727(2)	2862(4)	-1380(2)	71(1)
C(55)	-2416(2)	1793(4)	-1219(2)	77(1)
C(56)	-2027(2)	1350(4)	-1405(2)	73(1)
C(57)	-1940(2)	1960(4)	-1757(2)	66(1)
C(58)	-2252(2)	3036(4)	-1922(2)	75(1)

Table 3. Bond lengths [\AA] and angles [$^\circ$] for oct609.

Pd(1)-C(1)	2.109(3)
Pd(1)-C(8)	2.117(3)
Pd(1)-Si(2)	2.3556(8)
Pd(1)-Si(1)	2.3597(8)
Pd(2)-C(28)	2.099(3)
Pd(2)-C(21)	2.099(3)
Pd(2)-Si(3)	2.3497(9)
Pd(2)-Si(4)	2.3544(8)
Si(1)-C(16)	1.890(3)
Si(1)-C(15)	1.907(3)
Si(1)-C(17)	1.908(3)
Si(2)-C(18)	1.900(3)
Si(2)-C(19)	1.905(3)
Si(2)-C(20)	1.908(3)
Si(3)-C(35)	1.898(4)
Si(3)-C(37)	1.899(3)
Si(3)-C(36)	1.904(3)
Si(4)-C(38)	1.897(3)
Si(4)-C(40)	1.900(4)
Si(4)-C(39)	1.903(4)
N(1)-C(1)	1.360(3)
N(1)-C(2)	1.400(4)
N(1)-C(4)	1.452(4)
N(2)-C(1)	1.356(4)
N(2)-C(3)	1.404(4)
N(2)-C(7)	1.450(4)
N(3)-C(8)	1.357(4)
N(3)-C(9)	1.402(4)
N(3)-C(11)	1.450(4)
N(4)-C(8)	1.352(4)
N(4)-C(10)	1.397(4)
N(4)-C(14)	1.455(4)
N(5)-C(21)	1.359(4)
N(5)-C(22)	1.398(4)
N(5)-C(24)	1.452(4)
N(6)-C(21)	1.353(3)
N(6)-C(23)	1.399(4)
N(6)-C(27)	1.451(4)

N(7)-C(28)	1.357(4)
N(7)-C(29)	1.401(4)
N(7)-C(31)	1.456(4)
N(8)-C(28)	1.354(4)
N(8)-C(30)	1.396(4)
N(8)-C(34)	1.454(4)
C(2)-C(3)	1.341(4)
C(2)-C(5)	1.500(4)
C(3)-C(6)	1.491(4)
C(9)-C(10)	1.342(4)
C(9)-C(12)	1.487(4)
C(10)-C(13)	1.490(4)
C(22)-C(23)	1.332(4)
C(22)-C(25)	1.499(4)
C(23)-C(26)	1.498(4)
C(29)-C(30)	1.349(4)
C(29)-C(32)	1.493(4)
C(30)-C(33)	1.491(4)

C(1)-Pd(1)-C(8)	95.61(11)
C(1)-Pd(1)-Si(2)	88.99(8)
C(8)-Pd(1)-Si(2)	175.25(8)
C(1)-Pd(1)-Si(1)	176.67(8)
C(8)-Pd(1)-Si(1)	86.88(8)
Si(2)-Pd(1)-Si(1)	88.57(3)
C(28)-Pd(2)-C(21)	95.59(10)
C(28)-Pd(2)-Si(3)	173.88(8)
C(21)-Pd(2)-Si(3)	88.89(8)
C(28)-Pd(2)-Si(4)	88.37(8)
C(21)-Pd(2)-Si(4)	171.64(8)
Si(3)-Pd(2)-Si(4)	87.74(3)
C(16)-Si(1)-C(15)	104.02(17)
C(16)-Si(1)-C(17)	102.03(17)
C(15)-Si(1)-C(17)	99.11(17)
C(16)-Si(1)-Pd(1)	114.05(11)
C(15)-Si(1)-Pd(1)	121.56(11)
C(17)-Si(1)-Pd(1)	113.42(11)
C(18)-Si(2)-C(19)	104.55(15)
C(18)-Si(2)-C(20)	101.99(17)
C(19)-Si(2)-C(20)	99.88(16)

C(18)-Si(2)-Pd(1)	113.81(11)
C(19)-Si(2)-Pd(1)	120.44(11)
C(20)-Si(2)-Pd(1)	113.77(11)
C(35)-Si(3)-C(37)	106.06(18)
C(35)-Si(3)-C(36)	100.82(18)
C(37)-Si(3)-C(36)	100.05(17)
C(35)-Si(3)-Pd(2)	113.08(13)
C(37)-Si(3)-Pd(2)	120.54(13)
C(36)-Si(3)-Pd(2)	113.82(12)
C(38)-Si(4)-C(40)	99.37(17)
C(38)-Si(4)-C(39)	104.76(17)
C(40)-Si(4)-C(39)	102.4(2)
C(38)-Si(4)-Pd(2)	124.16(11)
C(40)-Si(4)-Pd(2)	114.60(12)
C(39)-Si(4)-Pd(2)	109.10(11)
C(1)-N(1)-C(2)	112.2(2)
C(1)-N(1)-C(4)	123.6(2)
C(2)-N(1)-C(4)	124.1(2)
C(1)-N(2)-C(3)	112.3(2)
C(1)-N(2)-C(7)	123.3(2)
C(3)-N(2)-C(7)	124.3(3)
C(8)-N(3)-C(9)	111.7(2)
C(8)-N(3)-C(11)	123.7(2)
C(9)-N(3)-C(11)	124.5(2)
C(8)-N(4)-C(10)	111.8(2)
C(8)-N(4)-C(14)	123.7(2)
C(10)-N(4)-C(14)	124.3(3)
C(21)-N(5)-C(22)	111.8(2)
C(21)-N(5)-C(24)	123.5(2)
C(22)-N(5)-C(24)	124.7(3)
C(21)-N(6)-C(23)	111.9(2)
C(21)-N(6)-C(27)	123.1(2)
C(23)-N(6)-C(27)	124.9(3)
C(28)-N(7)-C(29)	112.2(2)
C(28)-N(7)-C(31)	123.4(3)
C(29)-N(7)-C(31)	124.3(3)
C(28)-N(8)-C(30)	112.3(2)
C(28)-N(8)-C(34)	122.9(2)
C(30)-N(8)-C(34)	124.8(3)
N(2)-C(1)-N(1)	103.0(2)

N(2)-C(1)-Pd(1)	129.5(2)
N(1)-C(1)-Pd(1)	127.5(2)
C(3)-C(2)-N(1)	106.4(3)
C(3)-C(2)-C(5)	130.9(3)
N(1)-C(2)-C(5)	122.7(3)
C(2)-C(3)-N(2)	106.0(3)
C(2)-C(3)-C(6)	131.7(3)
N(2)-C(3)-C(6)	122.2(3)
N(4)-C(8)-N(3)	103.8(2)
N(4)-C(8)-Pd(1)	128.3(2)
N(3)-C(8)-Pd(1)	127.8(2)
C(10)-C(9)-N(3)	106.2(3)
C(10)-C(9)-C(12)	130.9(3)
N(3)-C(9)-C(12)	122.9(3)
C(9)-C(10)-N(4)	106.6(3)
C(9)-C(10)-C(13)	130.7(3)
N(4)-C(10)-C(13)	122.7(3)
N(6)-C(21)-N(5)	103.3(2)
N(6)-C(21)-Pd(2)	128.9(2)
N(5)-C(21)-Pd(2)	127.81(19)
C(23)-C(22)-N(5)	106.5(3)
C(23)-C(22)-C(25)	130.9(3)
N(5)-C(22)-C(25)	122.6(3)
C(22)-C(23)-N(6)	106.5(3)
C(22)-C(23)-C(26)	131.1(3)
N(6)-C(23)-C(26)	122.4(3)
N(8)-C(28)-N(7)	103.3(2)
N(8)-C(28)-Pd(2)	128.8(2)
N(7)-C(28)-Pd(2)	127.9(2)
C(30)-C(29)-N(7)	106.0(3)
C(30)-C(29)-C(32)	131.7(3)
N(7)-C(29)-C(32)	122.3(3)
C(29)-C(30)-N(8)	106.3(3)
C(29)-C(30)-C(33)	131.0(3)
N(8)-C(30)-C(33)	122.7(3)

A2.7: Crystal data for *trans*-Pd(SIPr)₂Cl₂Table 1. Crystal data and structure refinement for [PdCl₂(Ar)₂] . pentane

Identification code	aug20	
Empirical formula	C ₅₄ H ₇₆ Cl ₂ N ₄ Pd . (C ₅ H ₁₂)	
Formula weight	1030.63	
Temperature	173(2) K	
Wavelength	0.71073 Å	
Crystal system	Orthorhombic	
Space group	P2 ₁ 2 ₁ 2 (No.18)	
Unit cell dimensions	a = 13.0164(15) Å	α = 90°.
	b = 20.450(2) Å	β = 90°.
	c = 10.6415(13) Å	γ = 90°.
Volume	2832.6(6) Å ³	
Z	2	
Density (calculated)	1.21 Mg/m ³	
Absorption coefficient	0.46 mm ⁻¹	
F(000)	1100	
Crystal size	0.4 x 0.2 x 0.1 mm ³	
Theta range for data collection	3.55 to 25.89°.	
Index ranges	-13 ≤ h ≤ 15, -19 ≤ k ≤ 25, -13 ≤ l ≤ 11	
Reflections collected	12156	
Independent reflections	4893 [R(int) = 0.081]	
Reflections with I > 2σ(I)	4055	
Completeness to theta = 25.89°	94.4 %	
Tmax. and Tmin.	0.9529 and 0.6114	
Refinement method	Full-matrix least-squares on F ²	
Data / restraints / parameters	4893 / 0 / 308	
Goodness-of-fit on F ²	1.060	
Final R indices [I > 2σ(I)]	R1 = 0.057, wR2 = 0.128	
R indices (all data)	R1 = 0.075, wR2 = 0.137	
Absolute structure parameter	0.52(5)	
Largest diff. peak and hole	0.61 and -0.91 e.Å ⁻³	
The complex lies on a crystallographic 2-fold rotation axis.		

Data collection KappaCCD , Program package WinGX , Abs correction MULTISCAN

Refinement using SHELXL-97 , Drawing using ORTEP-3 for Windows

Table 2. Atomic coordinates ($\times 10^4$) and equivalent isotropic displacement parameters ($\text{\AA}^2 \times 10^3$) for aug207. $U(\text{eq})$ is defined as one third of the trace of the orthogonalized U_{ij} tensor.

	x	y	z	$U(\text{eq})$
Pd	0	0	979(1)	32(1)
Cl(1)	0	0	-1187(2)	46(1)
Cl(2)	0	0	3131(2)	46(1)
N(1)	421(3)	1449(2)	598(5)	40(1)
N(2)	-1058(4)	1296(2)	1463(5)	43(1)
C(1)	-232(3)	991(2)	984(6)	32(1)
C(2)	35(7)	2115(2)	804(9)	80(3)
C(3)	-991(5)	2016(3)	1333(8)	63(2)
C(4)	1477(4)	1385(3)	189(6)	40(2)
C(5)	1707(4)	1468(2)	-1075(7)	41(1)
C(6)	2746(5)	1470(3)	-1418(8)	49(2)
C(7)	3513(5)	1393(3)	-500(8)	55(2)
C(8)	3255(5)	1318(3)	736(7)	49(2)
C(9)	2235(5)	1311(3)	1123(7)	44(2)
C(10)	910(5)	1579(3)	-2093(7)	58(2)
C(11)	864(7)	2312(4)	-2470(9)	83(3)
C(12)	1104(7)	1169(4)	-3250(7)	77(2)
C(13)	1995(5)	1273(3)	2526(7)	49(2)
C(14)	2256(11)	1918(4)	3166(9)	117(4)
C(15)	2559(6)	724(4)	3147(8)	66(2)
C(16)	-2055(4)	1045(3)	1813(7)	41(2)
C(17)	-2348(5)	1060(3)	3071(7)	42(2)
C(18)	-3354(5)	902(3)	3343(7)	51(2)
C(19)	-4041(5)	731(3)	2416(7)	52(2)
C(20)	-3734(5)	710(3)	1186(7)	48(2)
C(21)	-2725(4)	870(2)	831(6)	40(1)
C(22)	-1618(5)	1244(3)	4137(7)	56(2)
C(23)	-1865(7)	1937(4)	4617(9)	87(3)
C(24)	-1654(6)	753(4)	5219(7)	63(2)
C(25)	-2441(5)	888(3)	-535(7)	45(2)
C(26)	-2933(7)	1476(4)	-1190(9)	67(2)

C(27)	-2719(6)	254(3)	-1198(7)	60(2)
C(1S)	-5000	0	-4100(13)	138(6)
C(2S)	-4834(16)	-636(7)	-3528(12)	176(7)
C(3S)	-4666(11)	-1271(11)	-4111(14)	220(10)



Table 3. Bond lengths [Å] and angles [°] for aug20

Pd-C(1)	2.049(5)
Pd-Cl(2)	2.290(2)
Pd-Cl(1)	2.305(2)
N(1)-C(1)	1.330(6)
N(1)-C(4)	1.448(7)
N(1)-C(2)	1.467(6)
N(2)-C(1)	1.344(6)
N(2)-C(16)	1.445(7)
N(2)-C(3)	1.480(7)
C(2)-C(3)	1.464(10)
C(4)-C(5)	1.388(9)
C(4)-C(9)	1.409(9)
C(5)-C(6)	1.400(9)
C(5)-C(10)	1.518(9)
C(6)-C(7)	1.406(10)
C(7)-C(8)	1.366(10)
C(8)-C(9)	1.391(9)
C(9)-C(13)	1.527(10)
C(10)-C(12)	1.511(11)
C(10)-C(11)	1.552(9)
C(13)-C(15)	1.495(9)
C(13)-C(14)	1.522(10)
C(16)-C(17)	1.392(10)
C(16)-C(21)	1.407(9)
C(17)-C(18)	1.379(9)
C(17)-C(22)	1.527(9)
C(18)-C(19)	1.377(10)
C(19)-C(20)	1.369(10)
C(20)-C(21)	1.405(8)
C(21)-C(25)	1.501(9)
C(22)-C(24)	1.530(10)
C(22)-C(23)	1.539(9)
C(25)-C(27)	1.519(8)
C(25)-C(26)	1.531(9)

C(1)-Pd-C(1)'	179.7(3)
C(1)-Pd-Cl(2)	89.86(17)
C(1)-Pd-Cl(1)	90.14(17)
Cl(2)-Pd-Cl(1)	180.0
C(1)-N(1)-C(4)	129.5(4)
C(1)-N(1)-C(2)	112.9(5)
C(4)-N(1)-C(2)	116.9(5)
C(1)-N(2)-C(16)	130.6(4)
C(1)-N(2)-C(3)	112.3(5)
C(16)-N(2)-C(3)	115.5(4)
N(1)-C(1)-N(2)	107.5(4)
N(1)-C(1)-Pd	127.0(3)
N(2)-C(1)-Pd	125.4(4)
C(3)-C(2)-N(1)	104.0(4)
C(2)-C(3)-N(2)	103.1(5)
C(5)-C(4)-C(9)	123.1(5)
C(5)-C(4)-N(1)	119.0(6)
C(9)-C(4)-N(1)	117.6(6)
C(4)-C(5)-C(6)	117.5(6)
C(4)-C(5)-C(10)	124.2(5)
C(6)-C(5)-C(10)	118.3(7)
C(5)-C(6)-C(7)	120.3(7)
C(8)-C(7)-C(6)	120.5(6)
C(7)-C(8)-C(9)	121.4(7)
C(8)-C(9)-C(4)	117.3(7)
C(8)-C(9)-C(13)	119.0(6)
C(4)-C(9)-C(13)	123.5(5)
C(12)-C(10)-C(5)	112.5(6)
C(12)-C(10)-C(11)	109.4(7)
C(5)-C(10)-C(11)	110.8(6)
C(15)-C(13)-C(14)	110.0(8)
C(15)-C(13)-C(9)	111.8(6)
C(14)-C(13)-C(9)	110.3(6)
C(17)-C(16)-C(21)	123.3(6)
C(17)-C(16)-N(2)	119.1(6)

C(21)-C(16)-N(2)	117.1(6)
C(18)-C(17)-C(16)	117.2(6)
C(18)-C(17)-C(22)	119.5(7)
C(16)-C(17)-C(22)	123.3(6)
C(19)-C(18)-C(17)	121.7(7)
C(20)-C(19)-C(18)	120.2(6)
C(19)-C(20)-C(21)	121.5(6)
C(20)-C(21)-C(16)	116.0(6)
C(20)-C(21)-C(25)	119.8(6)
C(16)-C(21)-C(25)	124.1(5)
C(17)-C(22)-C(24)	112.2(6)
C(17)-C(22)-C(23)	110.1(6)
C(24)-C(22)-C(23)	110.3(7)
C(21)-C(25)-C(27)	111.7(5)
C(21)-C(25)-C(26)	110.9(6)
C(27)-C(25)-C(26)	111.1(6)

Symmetry transformations used to generate equivalent atoms:

^a -x,-y,z

A2.8: Crystal data for [Pd(ITMe)(8-mesityl ($\eta^1(4, 5-\eta^2) - C_8H_{12}$))Br]

Table 1. Crystal data and structure refinement for src0207.

Identification code	shelxl
Empirical formula	C ₂₄ H ₃₅ Br N ₂ Pd
Formula weight	537.85
Temperature	293(2) K
Wavelength	0.71073 Å
Crystal system, space group	monoclinic, P21/c
Unit cell dimensions	a = 14.1843(5) Å alpha = 90 deg. b = 10.7510(3) Å beta = 121.942(2) deg. c = 18.5780(6) Å gamma = 90 deg.
Volume	2404.09(13) Å ³
Z, Calculated density	4, 1.486 Mg/m ³
Absorption coefficient	2.445 mm ⁻¹
F(000)	1096
Crystal size	0.26 x 0.21 x 0.02 mm
Theta range for data collection	3.20 to 27.57 deg.
Limiting indices	-18<=h<=15, -13<=k<=13, -23<=l<=24
Reflections collected / unique	22087 / 5459 [R(int) = 0.0475]
Completeness to theta =	27.57 98.3 %
Refinement method	Full-matrix least-squares on F ²
Data / restraints / parameters	5459 / 0 / 260
Goodness-of-fit on F ²	1.114
Final R indices [I>2sigma(I)]	R1 = 0.0362, wR2 = 0.0726
R indices (all data)	R1 = 0.0476, wR2 = 0.0784
Largest diff. peak and hole	

Table 2. Atomic coordinates ($\times 10^4$) and equivalent isotropic displacement parameters ($\text{\AA}^2 \times 10^3$) for 2011src0207.

$U(\text{eq})$ is defined as one third of the trace of the orthogonalized U_{ij} tensor.

	x	y	z	$U(\text{eq})$
Pd(1)	-2786(1)	-2280(1)	-4872(1)	18(1)
Br(2)	-4650(1)	-3094(1)	-6103(1)	25(1)
N(21)	-3782(2)	-2984(2)	-3862(2)	20(1)
N(22)	-3725(2)	-1003(2)	-3901(2)	23(1)
C(1)	-286(3)	-2372(3)	-3514(2)	25(1)
C(2)	-540(3)	-3744(3)	-3806(2)	29(1)
C(3)	-824(3)	-3896(3)	-4722(2)	32(1)
C(4)	-1880(3)	-3273(3)	-5405(2)	27(1)
C(5)	-1993(3)	-2049(3)	-5638(2)	28(1)
C(6)	-1105(3)	-1070(3)	-5210(2)	30(1)
C(7)	-1140(3)	-485(3)	-4468(2)	27(1)
C(8)	-1300(3)	-1475(3)	-3950(2)	22(1)
C(9)	432(3)	-2254(3)	-2553(2)	25(1)
C(10)	1583(3)	-2051(3)	-2178(2)	27(1)
C(11)	2268(3)	-1950(3)	-1302(2)	30(1)
C(12)	1866(3)	-2033(3)	-769(2)	32(1)
C(13)	744(3)	-2252(4)	-1136(2)	32(1)
C(14)	27(3)	-2384(3)	-2011(2)	30(1)
C(15)	2115(3)	-1971(4)	-2705(3)	39(1)
C(16)	2631(4)	-1913(4)	181(3)	45(1)
C(17)	-1175(3)	-2684(5)	-2333(2)	41(1)
C(21)	-3469(3)	-2043(3)	-4167(2)	20()
C(22)	-4213(3)	-2544(3)	-3384(2)	24(1)
C(23)	-4186(3)	-1291(3)	-3416(2)	28(1)
C(24)	-3620(3)	-4299(3)	-3956(2)	25(1)
C(25)	-4592(3)	-3410(3)	-2960(2)	27(1)
C(26)	-4533(4)	-317(4)	-3033(3)	48(1)
C(27)	-3527(3)	261(3)	-4077(3)	33(1)

Table 3. Bond lengths [Å] and angles [deg] for 2011src0207.

Pd(1)-C(21)	2.015(3)
Pd(1)-C(8)	2.075(3)
Pd(1)-C(5)	2.248(3)
Pd(1)-C(4)	2.262(3)
Pd(1)-Br(2)	2.5671(4)
N(21)-C(21)	1.344(4)
N(21)-C(22)	1.400(4)
N(21)-C(24)	1.458(4)
N(22)-C(21)	1.348(4)
N(22)-C(23)	1.399(4)
N(22)-C(27)	1.459(4)
C(1)-C(9)	1.521(5)
C(1)-C(2)	1.548(5)
C(1)-C(8)	1.556(5)
C(2)-C(3)	1.537(5)
C(3)-C(4)	1.514(5)
C(4)-C(5)	1.368(5)
C(5)-C(6)	1.506(5)
C(6)-C(7)	1.541(5)
C(7)-C(8)	1.530(4)
C(9)-C(14)	1.406(5)
C(9)-C(10)	1.412(5)
C(10)-C(11)	1.390(5)
C(10)-C(15)	1.523(5)
C(11)-C(12)	1.382(6)
C(12)-C(13)	1.380(5)
C(12)-C(16)	1.511(5)
C(13)-C(14)	1.395(5)
C(14)-C(17)	1.514(5)
C(22)-C(23)	1.350(5)
C(22)-C(25)	1.491(4)
C(23)-C(26)	1.489(5)
C(21)-Pd(1)-C(8)	92.21(13)
C(21)-Pd(1)-C(5)	166.38(13)
C(8)-Pd(1)-C(5)	81.17(13)
C(21)-Pd(1)-C(4)	157.46(13)
C(8)-Pd(1)-C(4)	89.63(13)

C(5)-Pd(1)-C(4)	35.31(13)
C(21)-Pd(1)-Br(2)	90.00(9)
C(8)-Pd(1)-Br(2)	174.49(9)
C(5)-Pd(1)-Br(2)	95.61(9)
C(4)-Pd(1)-Br(2)	90.26(9)
C(21)-N(21)-C(22)	111.5(3)
C(21)-N(21)-C(24)	124.8(3)
C(22)-N(21)-C(24)	123.6(3)
C(21)-N(22)-C(23)	111.2(3)
C(21)-N(22)-C(27)	124.7(3)
C(23)-N(22)-C(27)	124.2(3)
C(9)-C(1)-C(2)	112.2(3)
C(9)-C(1)-C(8)	114.8(3)
C(2)-C(1)-C(8)	115.4(3)
C(3)-C(2)-C(1)	111.4(3)
C(4)-C(3)-C(2)	116.4(3)
C(5)-C(4)-C(3)	126.1(3)
C(5)-C(4)-Pd(1)	71.8(2)
C(3)-C(4)-Pd(1)	112.5(2)
C(4)-C(5)-C(6)	125.5(3)
C(4)-C(5)-Pd(1)	72.91(19)
C(6)-C(5)-Pd(1)	107.6(2)
C(5)-C(6)-C(7)	110.1(3)
C(8)-C(7)-C(6)	111.4(3)
C(7)-C(8)-C(1)	110.8(3)
C(7)-C(8)-Pd(1)	101.2(2)
C(1)-C(8)-Pd(1)	115.3(2)
C(14)-C(9)-C(10)	117.7(3)
C(14)-C(9)-C(1)	124.0(3)
C(10)-C(9)-C(1)	118.2(3)
C(11)-C(10)-C(9)	120.0(3)
C(11)-C(10)-C(15)	118.1(3)
C(9)-C(10)-C(15)	121.9(3)
C(12)-C(11)-C(10)	122.4(3)
C(11)-C(12)-C(13)	117.5(3)
C(11)-C(12)-C(16)	121.1(4)
C(13)-C(12)-C(16)	121.3(4)
C(12)-C(13)-C(14)	122.1(4)
C(13)-C(14)-C(9)	120.2(3)
C(13)-C(14)-C(17)	117.1(3)

C(9)-C(14)-C(17)	122.7(3)
N(21)-C(21)-N(22)	104.8(3)
N(21)-C(21)-Pd(1)	124.0(2)
N(22)-C(21)-Pd(1)	131.2(2)
C(23)-C(22)-N(21)	106.1(3)
C(23)-C(22)-C(25)	132.3(3)
N(21)-C(22)-C(25)	121.6(3)
C(22)-C(23)-N(22)	106.4(3)
C(22)-C(23)-C(26)	131.0(3)
N(22)-C(23)-C(26)	122.5(3)

Symmetry transformations used to generate equivalent atoms: